



**HAL**  
open science

# Studies of interaction of selenoprotein P and selenized vasopressin in presence of auranofin and cisplatin

Jérémy Lamarche

► **To cite this version:**

Jérémy Lamarche. Studies of interaction of selenoprotein P and selenized vasopressin in presence of auranofin and cisplatin. Inorganic chemistry. Université de Pau et des Pays de l'Adour, 2021. English. NNT : 2021PAUU3050 . tel-03664077

**HAL Id: tel-03664077**

**<https://theses.hal.science/tel-03664077>**

Submitted on 10 May 2022

**HAL** is a multi-disciplinary open access archive for the deposit and dissemination of scientific research documents, whether they are published or not. The documents may come from teaching and research institutions in France or abroad, or from public or private research centers.

L'archive ouverte pluridisciplinaire **HAL**, est destinée au dépôt et à la diffusion de documents scientifiques de niveau recherche, publiés ou non, émanant des établissements d'enseignement et de recherche français ou étrangers, des laboratoires publics ou privés.

# THÈSE

UNIVERSITE DE PAU ET DES PAYS DE L'ADOUR  
École doctorale sciences exactes et leurs applications ED 211

Présentée et soutenue le 16 décembre 2021

par **Jérémy LAMARCHE**

Pour obtenir le grade de docteur  
de l'Université de Pau et des Pays de l'Adour  
Spécialité : Chimie bioinorganique et analytique

## Etude des interactions de la sélénoprotéine P et de la vasopressine diséléniée en présence d'auranofine et de cisplatine

Studies of interaction of selenoprotein P and selenized vasopressin in presence of auranofin and cisplatin

### MEMBRES DU JURY

#### RAPPORTEURS

- Ewa BULSKA
- Jorge RUIZ-ENCINAR

Professeur / Université de Varsovie Faculté de Chimie- Pologne  
Maître de conférences / Université de Oviedo Faculté de chimie Analytique- Espagne

#### EXAMINATEURS

- Jose Luis GOMEZ-ARIZA
- Katarzyna BIERLA

Directeur de Recherche / Université de Huelva Faculté de sciences expérimentales- Espagne  
Ingénieur de Recherche CNRS / Université de Pau et des Pays de l'Adour, IPREM- Pau

#### DIRECTEURS

- Ryszard LOBINSKI

Directeur de Recherche CNRS / Université de Pau et des Pays de l'Adour, IPREM- Pau

- Luisa RONGA

Maître de conférences / Université de Pau et des Pays de l'Adour, IPREM- Pau





*Do anything, even the impossible; it may only take a little longer when a miracle is required.*

*Faites n'importe quoi, même l'impossible ; cela peut ne prendre qu'un peu plus de temps lorsqu'un miracle est requis.*





## Table of content

|   |           |
|---|-----------|
| <b>ACKNOWLEDGEMENT</b>  | <b>9</b>  |
| <b>ABSTRACT</b>   | <b>13</b> |
| <b>RESUME</b>   | <b>15</b> |
| <b>LIST OF ABBREVIATIONS</b>  | <b>19</b> |
| <b>LITTERATURE SECTION</b>  | <b>23</b> |
| <b>1. SELENIUM : ELEMENT 34 IN THE PERIODIC TABLE</b>                                       | <b>25</b> |
| <b>2. SELENIUM SPECIES IN BIOLOGY</b>   | <b>29</b> |
| <b>2.1. Selenium vs. sulfur metabolite pathways</b>   | <b>29</b> |
| <b>2.2. Selenocysteine: the 21st proteogenic amino acid</b>                                 | <b>30</b> |
| 2.2.1. Reactivity of selenocysteine vs. cysteine  | 31        |
| 2.2.2. Rate advantage versus redox advantage  | 32        |
| <b>2.3. Selenoproteins</b>  | <b>33</b> |
| 2.3.1. Mechanisms of SeCys insertion in selenoproteins                                      | 33        |
| 2.3.2. Human selenoproteome   | 35        |
| 2.3.3. Selenoproteomes of other organisms   | 37        |
| <b>2.4. Thioredoxin reductases</b>  | <b>37</b> |
| <b>2.5. Selenoprotein P</b>   | <b>38</b> |
| 2.5.1. Discovery and importance   | 38        |
| 2.5.2. Structure  | 39        |
| <b>3. SELENOLS AS TARGETS FOR METALLODRUGS</b>  | <b>43</b> |
| <b>3.1. Metallo drugs</b>   | <b>43</b> |
| 3.1.1. Platinum compounds   | 43        |
| 3.1.2. Gold compounds   | 44        |
| 3.1.3. Other metals compounds   | 45        |
| <b>3.2. Reactivity of selenium with metal ions</b>  | <b>45</b> |
| <b>3.3. Thioredoxin reductase and its mimics as target for metallo drugs</b>                | <b>47</b> |
| 3.3.1. Interactions of thioredoxin reductase with gold and other metals compounds           | 47        |
| 3.3.2. Thioredoxin reductase proxies and their interaction with gold and platinum compounds | 49        |
| <b>3.4. Interaction of metallo drug with other selenoproteins</b>                           | <b>50</b> |
| <b>3.5. Interactions of others selenocompounds with metallo drugs</b>                       | <b>51</b> |

|  |           |
|--|-----------|
| <b>4. ANALYTICAL TECHNIQUES FOR SELENIUM SPECIATION AND STUDIES OF SE-METAL INTERACTIONS</b>   | <b>53</b> |
| <b>4.1. Separation of biological selenium species</b>  | <b>53</b> |
| 4.1.1. Affinity chromatography   | 53        |
| 4.1.2. Size exclusion chromatography   | 54        |
| 4.1.3. Reversed phase chromatography   | 54        |
| <b>4.2. Detection of selenium by inductively coupled plasma mass spectrometry</b>  | <b>55</b> |
| 4.2.1. Principle of inductively coupled plasma mass spectrometry   | 55        |
| 4.2.2. Spectral interferences in selenium inductively coupled plasma mass spectrometry detection and their removal                                 | 57        |
| 4.2.3. Quantification of selenium  | 58        |
| <b>4.3. Detection of selenopeptides, and their adducts with metals by soft-ionization mass spectrometry</b>  | <b>59</b> |
| 4.3.1. Electrospray ionization   | 59        |
| 4.3.2. Matrix assisted laser desorption/ionisation – Time-of flight mass spectrometry  | 61        |
| 4.3.3. Tandem mass spectrometry  | 62        |
| 4.3.4. Hyphenated techniques with dual inductively coupled plasma mass spectrometry and electrospray ionisation tandem mass spectrometry detection | 64        |
| 4.3.5. Mass spectrometry techniques in proteomics  | 64        |
| <b>5. ANALYTICAL CHEMISTRY OF SELENOPROTEIN P</b>  | <b>69</b> |
| <b>5.1. Isolation and purification of selenoprotein P</b>  | <b>69</b> |
| 5.1.1. Immunoaffinity precipitation and chromatography   | 69        |
| 5.1.2. Heparin affinity methods  | 70        |
| 5.1.3. Immobilized metal affinity methods  | 70        |
| 5.1.4. Sequential purifications  | 70        |
| <b>5.2. Detection of selenoprotein P</b>   | <b>71</b> |
| <b>5.3. Characterization of selenoprotein P</b>  | <b>73</b> |
| 5.3.1. Matrix assisted laser desorption/ionisation mass spectrometry   | 73        |
| 5.3.2. Electrospray mass spectrometry  | 74        |
| <b>5.4. Quantification of selenoprotein P</b>  | <b>75</b> |
| 5.4.1. Immunoassays  | 75        |
| 5.4.2. Inductively coupled plasma mass spectrometry-based methods  | 76        |
| 5.4.3. Gel-electrophoresis-based methods   | 77        |
| 5.4.4. Isobaric tagging for relative and absolute quantification   | 78        |

|  |            |
|--|------------|
| The use of LC-MS/MS as a way to quantify SELENOP was developed with the advent of new techniques such as label-free quantification (LFQ), and tandem mass tag (328).     | 78         |
| <b>6. MASS SPECTROMETRY APPROACHES TO STUDY SELENIUM INTERACTIONS WITH METALLODRUGS</b>  | <b>81</b>  |
| <i>6.1. Matrix assisted laser desorption/ionisation mass spectrometry and electrospray ionisation mass spectrometry studies of selenoprotein-metalloodrugs adducts</i>   | 81         |
| <i>6.2. Probing the molecular co-occurrence of selenium and gold by high pressure liquid chromatography hyphenated with inductively coupled plasma mass spectrometry</i> | 83         |
| <i>6.3. Probing selenoprotein-metalloodrugs binding by enzymatic digestion of the adduct</i>   | 83         |
| <i>6.4. Studies of model selenopeptides and other species</i>  | 85         |
| <b>EXPERIMENTAL SECTION</b>  | <b>95</b>  |
| <b>8. MATERIALS AND METHODS</b>  | <b>97</b>  |
| <i>8.1. Samples</i>  | 97         |
| <i>8.2. Metalloodrugs and model compounds</i>  | 97         |
| <i>8.3. Chemicals</i>  | 97         |
| <i>8.4. Buffers</i>  | 97         |
| <i>8.5. Instrumentation and materials</i>  | 100        |
| <i>8.5.1. Sample preparation equipment</i>   | 100        |
| <i>8.5.2. High pressure liquid chromatography and columns</i>  | 100        |
| <i>8.5.3. Inductively coupled plasma mass spectrometry</i>   | 101        |
| <i>8.5.4. Electrospray mass spectrometry</i>   | 101        |
| <i>8.6. Methods</i>  | 104        |
| <i>8.6.1. Purification of selenoprotein P</i>  | 104        |
| <i>8.6.2. Quantification of selenoprotein P</i>  | 107        |
| <i>8.6.3. Characterisation of selenoproteinP</i>   | 108        |
| <i>8.6.4. Studies of interaction between selenoprotein P and metalloodrugs (auranofin and cisplatin)</i>   | 109        |
| <i>8.6.5. Studies of interactions between vasopressin, diselenovasopressin and auranofin</i>   | 110        |
| <b>RESULTS AND DISCUSSION SECTION</b>  | <b>111</b> |
| <b>9. ISOLATION AND PURIFICATION OF SELENOPROTEIN P</b>  | <b>113</b> |
| <i>9.1. Purification of selenoprotein P from serum</i>   | 113        |
| <i>9.1.1. Optimisation of immobilized metal affinity chromatography</i>  | 113        |
| <i>9.1.2. Optimized selenoprotein P purification using immobilized metal affinity chromatography</i>   | 116        |

|              |  |            |
|--------------|--|------------|
| 9.1.3.       | <i>Repurification of selenoprotein P using heparin affinity</i>  | 116        |
| 9.1.4.       | <i>Concentration of selenoprotein P after heparin separation</i>   | 119        |
| <b>10.1.</b> | <b><i>Size exclusion chromatography</i></b>  | <b>123</b> |
| <b>10.2.</b> | <b><i>Sodium dodecylsulfate-polyacrylamide gel electrophoresis</i></b>   | <b>123</b> |
| <b>10.3.</b> | <b><i>Electrospray ionisation mass spectrometry analysis</i></b>   | <b>126</b> |
| <b>10.4.</b> | <b><i>Quantification</i></b>   | <b>133</b> |
| <b>11.</b>   | <b>STUDIES OF INTERACTION OF SELENOPROTEIN P WITH METALLODRUGS</b>   | <b>135</b> |
| <b>11.1.</b> | <b><i>Interaction of auranofin and cisplatin with full-length selenoprotein P</i></b>  | <b>135</b> |
| <b>11.2.</b> | <b><i>Identification of the interaction between selenoprotein P and metallodrugs on the peptide level</i></b>                | <b>136</b> |
| 11.2.1.      | <i>Auranofin</i>   | 136        |
| 11.2.2.      | <i>Cisplatin</i>   | 142        |
| <b>12.</b>   | <b>COMPARATIVE REACTIVITY OF MEDICINAL GOLD(I) COMPOUNDS WITH THE CYCLIC PEPTIDE VASOPRESSIN AND ITS DISELENIDE ANALOGUE</b> | <b>147</b> |
| <b>12.1.</b> | <b><i>Unreacted peptides characterization</i></b>  | <b>147</b> |
| <b>12.2.</b> | <b><i>Disulfide and diselenide reduction</i></b>   | <b>147</b> |
| <b>12.3.</b> | <b><i>Effect of temperature on the reduction of the diselenide peptide</i></b>   | <b>147</b> |
| <b>12.4.</b> | <b><i>Reaction of auranofin with reduced peptides (thiol or selenol)</i></b>   | <b>150</b> |
| <b>12.5.</b> | <b><i>Reaction of gold(I) compounds with the oxidized peptide (S-S and Se-Se)</i></b>  | <b>150</b> |
| 12.5.1.      | <i>Comparison of reactivity at 37°C and at 70°C</i>  | 159        |
| 12.5.2.      | <i>Comparison of reactivity between auranofin analogues</i>  | 159        |
| 12.5.3.      | <i>Comparison of reactivity of the S-S and Se-Se bridges</i>   | 159        |
| <b>13.</b>   | <b>CONCLUSION</b>  | <b>164</b> |
|              | <b>REFERENCE</b>   | <b>166</b> |
|              | <b>LIST OF FIGURES</b>   | <b>192</b> |
|              | <b>LIST OF TABLE</b>   | <b>196</b> |
|              | <b>ANNEXES</b>   | <b>201</b> |
|              | <b>LIST OF ANNEXES</b>   | <b>202</b> |
|              | <b>LIST FIGURES OF ANNEXE 1</b>  | <b>205</b> |

## *Acknowledgement*

This thesis is the culmination of a work carried out at the Institute of Analytical Sciences and Physico-Chemistry for the Environment and Materials (IPREM), under the direction of Professor Ryszard LOBINSKI, director of IPREM and the co-direction of Luisa RONGA, who shared their experience with me and supported me during the preparation of my defence.

I would like to express my gratitude to Ryszard LOBINSKI, Director of IPREM, for allowing me to carry out this work within the team of analytical chemistry and for the confidence he placed in an organic chemist willing to pursue a thesis in analytical chemistry and for being the chairman of the jury assisting to my PhD defence.

I would like to thank Professor Ewa BULSKA from the University of Warsaw and Dr Jorge RUIZ-ENCINAR from University of Oviedo for having accepted to be the reviewers of this work as well as Research director José Luis GOMEZ-ARIZA from the University of Huelva for taking part of the jury.

This work was initiated as a regional project between the University of Pau (IPREM lab) and the region Nouvelle Aquitaine. So, I would like to thank the funder to have made this project possible.

Many thanks to Katarzyna BIERLA, research engineer at CNRS, who helped greatly to advance the work of this thesis and to help me understand where the initial problems were. I would also like to thank her for the expertise she transmitted all over the thesis on the instrument, and her patience and answer to the thousands of questions that I have asked during this thesis.

I would like to thank Simon GODIN, research engineer at IPREM, who helped me for the ESI-MS and nanoHPLC part of this thesis, for his time and expertise on these sensitive techniques.

I would also like to thank the team of Jean GUILLON in Bordeaux, who has welcomed me during 3 months to work on peptide synthesis. I personally thank Jean for the answer and expertise on organic chemistry that has helped me to overcome some problems during my time there. A really special thanks to Sandra RUBIO, that take the time to explain to me the key to peptide synthesis and the functioning of the automat as well as the transmission of her knowledge on this field. I also thank Solène SAVRIMOUTOU, Stéphane MOREAU for the coffee break and lunch times moments.

A really special thanks to Sandrine Veloso, that took time to help me remake some of this thesis figure, thanks to her tremendous expertise of R, thank you also for the great time we spend together and the enriching discussion that we had together.

My thanks also to my colleagues and friends for the time we spent in the lab joking, and working. Special thanks to my favourite lab partner Izabela, Lucile and my thesis clone Maroussia. All my gratitude to my PhD friends, Cloé, Aurore, Asmodée and Laurie, and my office comrades Bastien, Robin, Javier and Océane that have greatly improved my stay here with unforgivable moments.

I would like to thank the person that has changed forever the experience of my thesis, my Tiago that has been supporting me in my up and down, during these 3 years and have been by my side all along in the shadow.

I would like to thank Dominique VERVANDIER-FASSEUR, David MONCHAUD that have believed in me and have contributed to the obtention of this thesis.

I would like to thank my friends, Coraline, Elodie, Maryne, Aymeric and Pauline for the moment we shared during these 3 years and before, my friends from Lyon, Sophie, Maïly, Jonathan and the others for the quality time, I had when I was coming back home, my friend from Dijon Farah and Hicheme for the nice moment we shared during and after the master that started this thesis.

Finally, I would like to thank my family that supported me since the beginning of my studies and made it possible for me to be here today writing the manuscript that would put an end to this formidable adventure that started 9 years ago after obtaining my scientific high school diploma in France.







## *Abstract*

Selenium is known to be an essential trace element with antioxidant activities. Its physiological role is mainly due to its co-translational incorporation into selenoproteins as selenocysteine (SeCys), referred to as the 21<sup>st</sup> amino acid. selenoprotein P (SELENOP) is the major selenoprotein in plasma with up to 10 SeCys in its sequence. Because of the chemical complexity of the serum matrix, the low abundance of selenoprotein P, and the occurrence of its putative multiple isoforms and post-translational modifications (e.g., glycosylation, Se-S and Se-Se bridges), the characterization of selenoprotein P requires the protein selective pre-concentration and custom-designed optimization of analytical methodology.

Containing 10 SeCys residues, SELENOP is a potential preferential target for metallodrugs such as auranofin and cisplatin. The interactions have not been studied yet at the molecular level, despite considerable evidence that free selenols are binding sites for auranofin in another selenoprotein, thioredoxin reductase. The lack of studies of selenoprotein P is likely due to the fact that the protein cannot be heterologously expressed and needs to be purified from serum where it is present at ng/g concentration (as Se).

This thesis presents the development of the method of purification of SELENOP from human serum using two-dimensional affinity chromatography. The two chromatographic steps using immobilized metal (cobalt) affinity and heparin affinity chromatography allowed the purification of SELENOP with excellent selectivity. The subsequent characterization of the purified SELENOP by nanoHPLC - electrospray ESI MS/MS allowed accounting for almost all selenocysteine-containing tryptic SELENOP peptides and the elucidation of some glycosylation sites. In addition, the recovery of selenium incorporated in SELENOP was quantitatively monitored, for the first time, at each step of the purification procedure. The recovery of SELENOP was 14% after all the purification steps. Selenium present in SELENOP was found to account for 35% of total selenium in serum.

The purification of SELENOP allowed the first study of its interactions with auranofin and cisplatin containing, Au(I) and Pt(II), respectively. The protein metalation was observed after incubation of SELENOP with both metallodrugs. After digestion with trypsin, Au and Pt modifications were observed on the resulting peptides. Either in the case of auranofin and cisplatin, two SELENOP peptides were found to form Au or Pt adducts by Cys and SeCys binding (MS/MS characterization). These four peptides, specific to SELENOP, displayed different sequences.

Moreover, to comparatively study the interactions of the Se-Se and S-S bridges with metallodrugs, vasopressin and its di-selenide analogues were used as model peptides. Their reactivity with auranofin and its strict analogues was investigated by LC-electrospray MS/MS. Evidence was obtained of the possible cleavage of the S-S and Se-Se bridges induced by Au(I) in the absence of reducing agents, in contrast to the previous studies requiring a prior reduction of the Se-Se bond to make it react with Au(I) compounds. In addition, we found that at high temperatures (70 °C), the sulfur and selenium atoms were metallated with the preferential binding of gold to selenium, the reaction not taking place under physiological conditions (37 °C).



## Résumé

### Introduction

Le sélénium est connu pour être un oligo-élément essentiel aux activités antioxydantes. Son rôle physiologique est principalement dû à son incorporation co-translationnelle dans les sélénoprotéines comme la sélénocystéine (SeCys), appelée 21<sup>e</sup> acide aminé. La sélénoprotéine P (SELENOP) est la principale sélénoprotéine plasmatique avec jusqu'à 10 SeCys dans sa séquence. En raison de la complexité chimique de la matrice sérique, de la faible abondance de la sélénoprotéine P et de l'apparition de ses isoformes multiples putatives et des modifications post-translationnelles (par exemple, glycosylation, pont Se-S et Se-Se), la caractérisation de la sélénoprotéine P nécessite sa préconcentration et l'optimisation sur mesure de la méthodologie analytique.

Contenant 10 résidus SeCys, SELENOP est une cible potentielle pour les métallo-drogues (auranofine, cisplatine). Les interactions n'ont pas encore été étudiées au niveau moléculaire, malgré des preuves considérables que les sélénoles libres sont des sites d'interaction pour l'auranofine dans une autre sélénoprotéine, la thiorédoxine réductase. Le manque d'études sur la sélénoprotéine P est probablement dû au fait que la protéine ne peut pas être exprimée de manière hétérologue et doit être purifiée à partir du sérum où elle est présente à une concentration de ng/g (sous forme de Se).

Alors que les effets de détoxification du sélénium par son action sur les métaux, tels que par ex. Hg et les effets inhibiteurs des sélénoenzymes ont été largement démontrés, les preuves moléculaires de ces liaisons ont été relativement rares. Les études visant à sonder la liaison du sélénium par des techniques moléculaires, telles que la spectrométrie de masse ou, par des techniques spécifiques aux liaisons chimiques, telles que la spectroscopie à structure fine d'absorption étendue des rayons X (EXAFS), ont été largement limitées à la thiorédoxine réductase. Par conséquent, le développement de méthodes permettant d'avoir un aperçu du site de liaison aux métaux et du type de liaison induite par une telle liaison est d'un intérêt considérable pour étudier plus avant les mécanismes liant le sélénium à la détoxification des métaux lourds ou à l'action thérapeutique des métallomédicaments.

La question la plus importante est que le sélénium se présente en biologie sous plusieurs formes, telles que les sélénoles (SeH), les diséléniures (-Se-Se-) et les ponts -Se-S- chacun en compétition potentielle avec les analogues soufrés, tels que les thiols (-SH) et des disulfures (-SS-). La situation est compliquée par le rôle joué par la disponibilité stérique des sites contenant Se ou S et la présence d'autres motifs de liaison (Lys, His, Met) au sein de la structure protéique qui peuvent lier le métal et entrer en compétition avec les sites contenant Se.

Le sélénium dans le sang et les tissus humains est présent à des niveaux inférieurs au nM. Ce fait ainsi que la complexité de la matrice font que les études moléculaires *in vivo* ne peuvent être menées avec succès que par un petit nombre de techniques instrumentales avancées, et notamment par spectrométrie de masse. Les développements récents de la sensibilité de la chromatographie avec détection spécifique du sélénium (ICP MS) et de la résolution et de la sensibilité de l'électrospray MS offre un certain nombre d'outils intéressants pour sonder les interactions sélénium métal. Même ainsi, les études de composés modèles, soit isolés du sérum, soit synthétisés ont leur place dans les études moléculaires des interactions Se-métal.

Les métallomédicaments, tels que les composés Pt et Au, ont récemment suscité un intérêt considérable en tant que ligands du sélénium. Comme indiqué ci-dessus, les études se sont presque tous limités à une enzyme, la thiorédoxine réductase et à ses proxies. Un facteur important facilitant ces études, outre

l'intérêt indéniable de la démonstration de l'inhibition de TrxR par des métallomédicaments, a été la possibilité d'expression de la protéine et donc, sa disponibilité sous forme pure. Cependant, TrxR n'est pas la protéine la plus abondante dans le sérum humain. Plusieurs autres existent, toutes contenant au moins un résidu de sélénocystéine, libre ou oxydé pour former un pont Se-S ou Se-Se. Parmi ces protéines, la plus abondante est la sélénoprotéine P qui contient jusqu'à 10 résidus de sélénocystéine. Bien qu'il existe des preuves de la formation de complexes covalents stables de SELENOP avec des métaux lourds, il n'y a pratiquement pas eu d'études sondant la spécificité de la liaison au sélénium et la nature du site de liaison. Une des raisons à cela était l'impossibilité de l'expression hétérogène de SELENOP. Par conséquent, la protéine pour les études d'interaction avec les métaux doit être isolée et purifiée à partir de sérum naturel, ce qui peut être tout un défi sachant que la concentration totale de Se dans le sérum est d'environ 100 ng/ml et SELENOP ne représente que 1/3 à 1/2 de celui-ci.

## Résumé des travaux

L'un des objectifs de cette thèse a donc été de revisiter les schémas d'isolement de SELENOP rapportés ailleurs afin de développer une méthode capable de produire des quantités suffisantes de SELENOP pour produire des signaux spécifiques aux espèces de Se mesurables pour des études par spectrométrie de masse des interactions de SELENOP avec des composés à base de Au et Pt. Pour cela, différents types de chromatographie d'affinité, tels que l'IMAC ou l'héparine, seuls ou en séquence, ont été revisités. L'accent a été mis sur l'optimisation des étapes de concentration inter-chromatographie et le suivi de la récupération de SELENOP. Différentes conditions chromatographiques ont été testées pour obtenir la meilleure résolution et séparation à chaque étape et augmenter le recouvrement à chaque étape de la purification.

Un élément inhérent à la thèse a été une caractérisation approfondie de la sélénoprotéine isolée par spectrométrie de masse haute résolution et haute précision. Aussi étrange que cela puisse paraître, très peu de preuves de spectrométrie de masse pour les données de séquence d'acides aminés de SELENOP existent dans la littérature. Par conséquent, une méthode basée sur la digestion trypsique et la spectrométrie HPLC MS/MS a dû être développée afin de démontrer l'identité chimique de la protéine isolée et purifiée et d'acquérir un support de bases pour l'interprétation des données sur les interactions de SELENOP avec les composés à base de Pt et d'Au.

L'objectif ultime relatif à SELENOP a été d'étudier sa liaison avec l'auranofine et le cisplatine, en sondant la formation des composés métalliques SELENOP et en acquérant des preuves moléculaires sur les sites de liaison avec l'Au et le Pt.

La propension des résidus de SeCys à s'oxyder pour former des liaisons Se-Se ou Se-S soulève une question importante sur leur réactivité avec les métallomédicaments. Alors qu'il est maintenant bien documenté que l'auranofine et ses analogues se lient rapidement et étroitement aux protéines portant des cystéines ou des sélénocystéines libres, la capacité de ces composés à base d'or d'interagir directement avec les ponts disulfure et diséléniure et à les cliver est beaucoup moins comprise. Cela nous a incité à étudier en détail les réactions de l'auranofine et de ses analogues avec des molécules modèles contenant des motifs disulfures et diséléniure.

Pour cela, nous avons décidé d'utiliser, en tant que peptides modèles, l'hormone vasopressine (AVP), connue pour son action antidiurétique et vasopressive, et son analogue séléniée, la selenovasopressine ([Se-Se]-AVP), dans lequel le pont disulfure a été remplacé par un pont diselenide tout en gardant l'affinité de AVP envers le récepteur de la vasopressine.

## Conclusion

Cette thèse présente donc le développement de la méthode de purification de SELENOP à partir de sérum humain en utilisant la chromatographie d'affinité bidimensionnelle. La méthode de purification du SELENOP développée a permis d'obtenir de la SELENOP relativement pur pour l'étude de ses interactions avec les métallomédicaments. La séparation de SELENOP des autres sélénoprotéines a été réalisée à l'aide de la colonne IMAC-Héparine à double affinité. Le SELENOP a pu être facilement séparé des autres protéines présentes dans le sérum comme observé par SDS-PAGE. Les améliorations méthodologiques obtenues offrent une méthode viable pour purifier SELENOP du sérum en quantités suffisantes pour étudier ses interactions avec les métaux.

Les récupérations de 14% mesurées peuvent sembler faibles mais elles sont impossibles à comparer avec les études de la littérature car c'est à notre connaissance la première fois où de telles récupérations ont été systématiquement mesurées à chaque étape de la procédure. La principale source de pertes est l'étape de concentration après purification par affinité à l'héparine générant un volume important de solution diluée. L'affinité non spécifique à la filtration SPE utilisée peut être une des raisons mais la présence de  $\alpha$ -2-macroglobuline dans l'éluât ouvre la possibilité de la formation d'adduits SELENOP- $\alpha$ -2-macroglobuline. Cela peut également être la raison de l'absence de pic de la SELENOP au volume d'élution en chromatographie d'exclusion stérique. Une autre question ouverte est de savoir pourquoi la quantité de SELENOP mesurée avec le kit de protéines est légèrement différente de celle obtenue par d'autres techniques telles que la quantification du sélénium total.

En termes de quantification de SELENOP dans le sérum, nos résultats sont similaires à ceux rapportés dans la littérature, ce qui signifie que l'effet matriciel du sérum n'est pas si important et ne nécessite pas nécessairement l'utilisation de techniques de quantification plus sophistiquées telles que la dilution isotopique ICP MS.

La caractérisation de la SELENOP purifiée nous a permis de détecter de nouveaux sélénopeptides qui n'étaient pas détectés jusqu'à présent dans la littérature. Sur les quatre peptides présentés dans la littérature, nous en avons identifié trois par caractérisation MS et 2 nouveaux peptides non publiés ont également été détectés. L'un de ces peptides présentait une O-glycosylation qui a été élucidée grâce aux données MS/MS. Le total des SeCys qui ont été identifiés (six des dix total) grâce aux 5 peptides que nous avons identifiés, est à notre connaissance le nombre de SeCys le plus élevé détecté à ce jour pour SELENOP, ce qui signifie que seules les 4 derniers SeCys situées à l'extrémité N-terminale de SELENOP ont encore besoin d'être formellement identifiées.

La disponibilité de la SELENOP purifiée, a permis d'observer, pour la première fois, la formation d'adduits avec l'auranofine et le cisplatine. Le site de métallation a été conservé après digestion tryptique. Plusieurs peptides qui présentaient des interactions entre Cys, SeCys et des métallomédicaments ont pu être observés. Ces résultats corroborent l'hypothèse selon laquelle la SELENOP peut interagir avec les métallomédicaments via les résidus SeCys et Cys. Après incubation de la SELENOP avec l'auranofine, deux peptides ont été obtenus avec un adduit  $\text{AuPEt}_3^+$  sur les acides aminés Cy et SeCys, et, après incubation avec le cisplatine, deux peptides ont été obtenus avec un adduit  $\text{Pt}(\text{NH}_3)_2\text{Cl}^+$  également sur Cys et SeCys, le site de liaison a été déterminé en utilisant les données de fragmentation obtenues par MS/MS. Les quatre peptides obtenus sont spécifiques de SELENOP, tous les peptides présentent des séquences différentes. Ces observations ont été possibles grâce à l'excellente sensibilité du spectromètre de masse de pointe, cependant plus de peptides ont été identifiés malheureusement, l'identification formelle du site de liaison n'a pas été possible à cause d'une concentration insuffisante pour obtenir des

data en MS/MS validant le site de liaison. Le cisplatine et l'auranofine interagissent avec un site actif similaire (Cys, SeCys), cependant, leur mécanisme de liaison devrait être différent en raison de leur propre chimie.

Pour l'instant, les études des interactions des sélénoles et diséléniures avec les métaux et les métallocomposés sont encore largement dépendantes de la disponibilité de composés modèles. Les études sur la sélénovasopressine offrent un aperçu clair de la réactivité comparative des composés d'or médicaux avec des biomolécules contenant des liaisons disulfures ou diséléniure. Nous avons observé que les composés d'or(I) sont capables de réagir avec S-S ou Se-Se à haute température (70°C) en formant des adduits où le ligand Et<sub>3</sub>PAu est directement lié au S ou au Se. En revanche, aucune réaction ne se produit entre les composés d'or étudiés et les vasopressines S-S ou Se-Se oxydées dans des conditions physiologiques (37°C) en l'absence d'agents réducteurs.

Le pont disulfure, à 37 °C, est plus sujet à la réduction que le pont diséléniure. Par conséquent, lors de l'ajout d'un agent réducteur, la liaison S-S peut être clivée et peut former des adduits avec les composés Au(I). En revanche, la réduction de la liaison Se-Se est plus difficile à obtenir et n'a lieu qu'à haute température. A 70°C, les composés d'or sont capables de cliver à la fois le pont disulfure et diséléniure et de former les adduits correspondants. La réaction se produit préférentiellement pour le Se-Se sur la liaison S-S probablement en raison du caractère plus doux du groupe sélénoate.

Nos résultats appuient davantage l'opinion selon laquelle les protéines contenant SeCys (25 chez l'homme) sont des cibles préférentielles et probables des électrophiles mous de Lewis, tels que les métaux lourds, par ex. Hg, Pb, As, Cd impliqués dans la toxicologie environnementale et humaine, et composés métalliques (contenant Au, Ag, Pt, etc.) employés comme agents thérapeutiques. Cependant, les réactions rapides et faciles des composés métalliques avec le groupe sélénocystéine n'ont lieu que lorsque le SeCys est présent sous sa forme sélénoles ou sélénoate (réduite). En revanche, lorsque SeCys a formé un pont Se-Se, ces réactions n'ont lieu qu'à des températures bien supérieures aux températures physiologiques. Ces résultats offrent une perspective intéressante à l'axe de recherche sur l'interaction des métallomédicaments et des protéines plasmatiques.

## *List of abbreviations*

[Se-Se]-AVP: Selenovasopressin  
AC: Alternative Current  
ACN: Acetonitrile  
Ala: Alanine  
Alb: Albumin  
Arg: Arginine  
ATP: Adenosine Triphosphate  
AVP: Vasopressin  
BEH: Bridged Ethylene Hybrid  
CAM: CarbAmidoMethylation  
COVID: Coronavirus disease  
Cys: Cysteine  
DC: Direct Current  
DIO: Iodothyronine deiodinase  
DNA: DeoxyriboNucleic Acid  
DTT: DiThioThreitol  
EDTA: EthyleneDiamineTetraAcetic acid  
EF: Elongation Factor  
ELISA: Enzyme-Linked ImmunoSorbent Assay  
ESI: ElectroSpray Ionization  
FDA: Food and Drug Administration  
Gal: Galactose  
GE: Gel Electrophoresis  
Gpx: Glutathione peroxidase  
GSH: Glutathione  
Hep62: Hepatoma cell line 62  
His: Histidine  
HNO<sub>3</sub>: Acide nitrique  
HPLC: High Pressure Liquid Chromatography  
HRMS: High Resolution Mass Spectrometry  
HSAB: Hard and Soft Acids and Bases  
IAM: IodoAcetaMide  
ICP: Inductively Coupled Plasma  
IDA: Isotopic Dilution Analysis



IE: Affinity Chromatography

IEF: IsoElectric Focusing

Ile: Isoleucine

IMAC: Immobilized Metal Affinity Chromatography

IT: Ion Trap

iTRAQ: Isobaric Tag for Relative and Absolute Quantification

LA: Laser Ablation

LC: Liquid Chromatography

LD: Limit of Detection

Leu: Leucine

LQ: Limit of Quantification

Lys: Lysine

MALDI: Matrix-Assisted Laser Desorption/Ionization

Me: Methyl

Met: Methionine

MQ: Milli-Q Water

mRNA: Messenger RNA

MS: Mass Spectrometry

MS/MS: Tandem Mass Spectrometry

MsrB: Methionine-R-sulfoxide or Selenoprotein X

NAcGal: N-acetylgalactosamine

NADPH: Nicotinamide Adenine Dinucleotide Phosphate Oxidase

NeuNAC: N-acetylneuraminic acid

NHC: N-heterocyclic carbene

O-Gly: O-Glycosylation

PAGE: PolyAcrylamide Gel Electrophoresis

Path-P: Thiophosphate ligand

Path-S: thioglucose ligand

Ph: Phenyl

PTM: Post Translational Modification

PVDF: PolyVinylidene Fluoride

Q: Quadrupole

qO: Collision Cell

RNA: RiboNucleic Acid

RP: Reversed Phase Chromatography

RSD: Relative Standard Deviation

SDS: Sodium Dodecyl Sulfate

SeAlb: SelenoAlbumin

SEC: Size Exclusion Chromatography

SECIS: SElenoCysteine Insertion Sequence

SeCys: Selenocysteine

SeIB: Elongation factor (mSeIB or eEFSec)

SELENOP: Selenoprotein P

SPE: Solid Phase Extraction

TATG: TetraAcetylThioGlucose

TCEP: Tris(2-carboxyethyl)phosphine

TGX: Tris-Glycine eXtended

TOF: Time Of Flight

tRNA: Transfer RNA

Trx: Thioredoxin

TrxR: Thioredoxin Reductase

UFH: UnFractionated Heparin

UPLC: Ultra Performance Liquid Chromatography

UV: UltraViolet

Val: Valine

VICAT: Visible Isotope-Coded Affinity Tags

WHO: World Health Organisation

ETUDE DES INTERACTIONS DE LA SELENOPROTEINE P ET DE LA VASSOPRESSINE DISSELENIEE EN  
PRESENCE D'AURANOFINE ET DE CISPLATINE

Jérémy LAMARCHE – 16 décembre 2021

---

## ***LITTERATURE SECTION***



## 1. Selenium : element 34 in the periodic table

Selenium was discovered in 1817 by the Swedish chemist Jöns Jacob Berzelius who investigated a reddish sludge responsible for a strange disease among his factory workers. The element was named selenium, in link with the Greek Moon Goddess "*Seléné*" by analogy with "*Tellu*", the Roman goddess of the Earth, due to the significant similarities between selenium and the earlier discovered tellurium (1).

For a long time selenium was considered uniquely as a toxic element (2–4). However, starting from the mid-50ties (5–7), its essential character has become known. In the 1970s, the World Health Organisation (WHO) recognised selenium as an essential trace element (8). This dual character: essential or toxic as a function of concentration and species makes selenium a fascinating element to study.

Selenium belongs to the chalcogen family, it is located in column 16, line 4 of the periodic table at number 34. It is considered a metalloid, which means that physical and chemical properties are intermediates between those of a metal and a non-metal, similarly to tellurium, bismuth or arsenic. Its atomic weight is 78.96 g.mol<sup>-1</sup>. Its melting point is 217 °C, and its boiling point is 685 °C. It exists in organic and inorganic forms, and has five degrees of oxidation: + VI (selenate, SeO<sub>4</sub><sup>2-</sup>), + IV (selenite, SeO<sub>3</sub><sup>2-</sup>), -II (selenide, H<sub>2</sub>Se), -I (diselenide, H<sub>2</sub>Se<sub>2</sub>) and 0 (elemental Se) (**Table 1**) (9–11). It has six stable natural isotopes (**Table 2**), and two radioactive isotopes produced by nuclear fission, the long-lived <sup>79</sup>Se β emitter (2.8x10<sup>5</sup> years) present in spent nuclear fuel and the shorter-lived <sup>75</sup>Se (119.8 days), widely used as a radiotracer or as an imaging agent in iron and steel welding.

Table 1 Chemical and physical properties of selenium.

| Property  | Value   |
|---|---|
| Relative atomic mass  | 78.96   |
| Atomic number   | 34  |
| Atomic radius (in pm, emp.)                                 | 115   |
| Covalent radius (in pm, emp.)                               | 116   |
| Van der Waals radius (in pm)                                | 190   |
| Ion radius (Pauling) ox state (VI), (-II) (in pm)           | 42, 198   |
| Bond length of selenide (in pm)                             | 232   |
| Bond length of carbon-selenium (in pm)                      | 196   |
| Molecular volume (in cm <sup>3</sup> )                      | 16.42   |
| Diatomic bond energies (in kJ.mol <sup>-1</sup> )           | 332.6 (Se-Se), 314.5 (Se-H), 590.4 (Se-C)   |
| Homolytic bond cleavage energies (in kJ.mol <sup>-1</sup> ) | 334.9 (H-Se-H), 234 (CH <sub>3</sub> -Se-CH <sub>3</sub> ), 197.6 (CH <sub>3</sub> -Se-Se-CH <sub>3</sub> ) |
| Electron affinity (in kJ.mol <sup>-1</sup> )                | 195   |
| Ionization energies (in kJ.mol <sup>-1</sup> )              | 914 (1 <sup>st</sup> ), 2045 (2 <sup>nd</sup> ), 2973.7 (3 <sup>rd</sup> )                                  |
| Polarizability (in Å)                                       | 3.8   |
| Pauling electronegativity                                   | 2.55  |
| pK <sub>a</sub>   | 5.24  |
| Melting point   | 217 °C  |
| Boiling point   | 684.8 °C  |
| Electronegativity   | 2.48  |
| Electronic structure  | [Ar]3d <sup>10</sup> 4s <sup>2</sup> 4p <sup>4</sup>  |
| Oxidation state   | -2, 0, +2, +4, +6   |

Selenium chemical properties are often compared to those of sulfur (9). Selenides and sulfides are alike in terms of appearance, composition and properties. Several chemical species contain a C-Se bond, for example, selenols (RSeH), selenoethers (R<sub>2</sub>Se; R<sub>2</sub>Se<sub>2</sub>), mixed Se-S compounds (e.g., RSSeH) and selenoamino acids, selenosugars and selenoproteins. Selenium can also form halides (RSeX), where X denotes fluor, chlorine, bromine and iodine (10). Selenium is also known to reduce several metals' toxicity, such as mercury, cadmium, silver, copper, arsenic by forming selenides (10, 12).

Table 2 Isotopic abundance of selenium

| Isotope          | Atomic mass | Natural abundance (%) | Relative abundance (compared to <sup>80</sup> Se) |
|------------------|-------------|-----------------------|---|
| <sup>74</sup> Se | 73.92247    | 0.89                  | 1.8   |
| <sup>76</sup> Se | 75.91921    | 9.4                   | 19  |
| <sup>77</sup> Se | 76.91991    | 7.6                   | 15  |
| <sup>78</sup> Se | 77.91731    | 24                    | 48  |
| <sup>80</sup> Se | 79.91651    | 50                    | 100   |
| <sup>82</sup> Se | 81.91669    | 8.7                   | 18  |

Se and S have the same oxidation states and the same functional groups (*Figure 1*) and their structures are often very similar, promoting co-crystallization of analogous compounds.

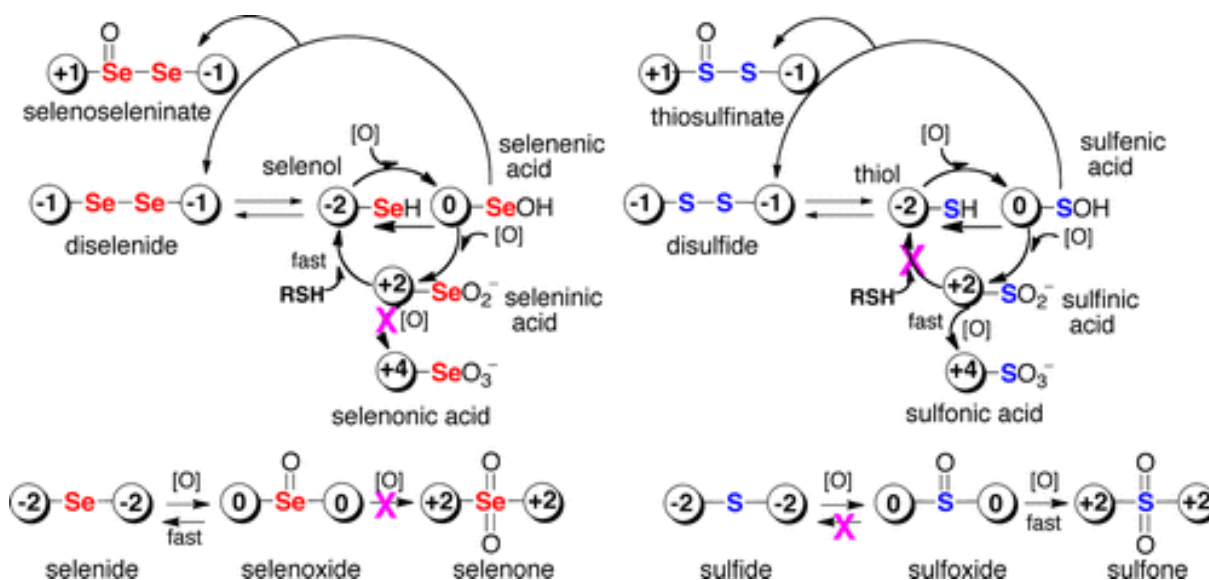


Figure 1 Structures and oxidation numbers of sulfur and selenium compounds resulting from the two electron oxidation reaction (9)

The significant differences between the two chalcogens reflect those between light and heavy elements. Since heavy elements are more "softer" (easier polarizable) than light elements, this generally leads to faster nucleophilic and electrophilic substitutions. Most selenium bonds are weaker than sulfur ones; this results in a much faster-breaking reaction of this bond. Its "weaker" bonds result in an  $\sigma^*$  orbital of the Se-X bond of energy lower than that of an S-X bond, and therefore more reactive owing to an acceptor electron. Thus, all the oxidation states of selenium are much more electrophilic than those of its sulfur analogues. The higher these oxidation states, the less stable the species compared to those of sulfur. Besides, like all heavy elements, selenium is also more tolerant to hypervalent binding (11). In terms of acidity, the weaker hydrogen bond and an increase in size and polarizability of Se are reflected

by the low basicity of selenolates. The pK<sub>a</sub> of seleno-species (**Figure 2**) ranges from 3 to 6 pK<sub>a</sub> units (13).

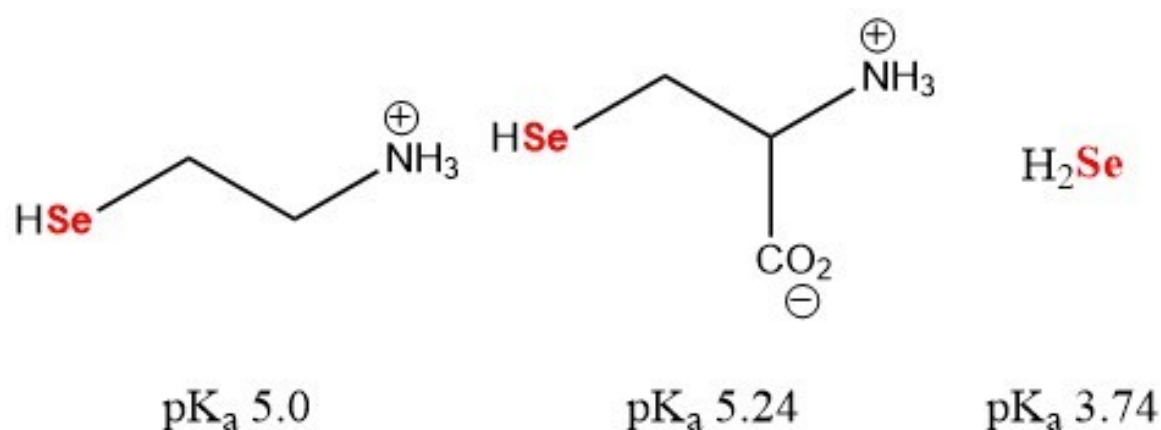


Figure 2 pK<sub>a</sub> values of selenols

Despite the lower basicity, selenolate ion is considered as a good nucleophile, a likely consequence of selenium's high polarizability. This observation is valid for S<sub>N</sub>2 substitutions as well as aromatic substitutions. In protic solvents, the weaker hydrogen bond acceptor properties of selenolates contribute to the high nucleophilicity (9). At physiological pH, selenols are entirely converted into selenolates which are active nucleophiles, and more reactive than their sulfur analogues (9). Since selenolates have low basicity, in general, they are good leaving groups.

One of the rare cases where the Se-X bond is strong, in the case of hypervalent compounds, where the number of bonds plus the pairs of free electrons is greater than that allowed by Lewis's byte rule. The calculation of the association energy ( $\text{Me}_2\text{Y} + \text{Me}^- \rightarrow \text{Me}_3\text{Y}^-$ ) is -13.1kcal for Y = Se (14). This effect has complex origins, but the contributing factors are the weaker steric effects of selenium due to its longer bonds and lower LUMO  $\sigma^*$  orbital which more favourably leads to a three-centre hypervalent binding situation and four electrons. This greater tolerance to hypervalent (also shared by neighbouring element pairs such as Cl/Br and P/As and heavier elements like Te, I, Sb) can be seen in many contexts. Another case in which Se-X bonds are strong is the case of binding to metals (15).

Nucleophilic attacks on selenium (which generally passes through hypervalent intermediates such as R<sub>4</sub>Se or R<sub>3</sub>Se<sup>-</sup>) generally occur more rapidly than for sulfur, because the intermediate compounds selenates have a lower energy formation (16).

The difference in selenium's size compared to sulfur (atomic radius of 115 ppm versus 110 ppm) results in larger hybridized orbitals, the longer the bond length, the weaker the  $\pi$  orbital overlap. One consequence of this is the lack of stability of selenoesters compared to thioesters by resonance with carbonyl groups (17). Chemists and nature have thus taken advantage of this significant reactivity, using selenoesters as acyl transfer reagents. They are used to catalyse native chemical ligation reactions (18–20) and selenoprotein K which uses its SeCys residue to form a selenoester catalyzing the reaction of acyl transfer from a palmitoyl group to calcium channel (21).





## 2. Selenium species in biology

Usually present in surface waters and soils as  $\text{HSeO}_3^- / \text{SeO}_3^{2-}$  (selenite) and  $\text{SeO}_4^{2-}$  selenate (22), selenium can be biologically methylated (dimethylselenide, dimethyldiselenide, etc.) or assimilated in biomass (selenized amino acids, metabolites) (23) following the sulfur metabolic pathways. The main seleno amino acids are analogues of methionine and cysteine (**Figure 3**).

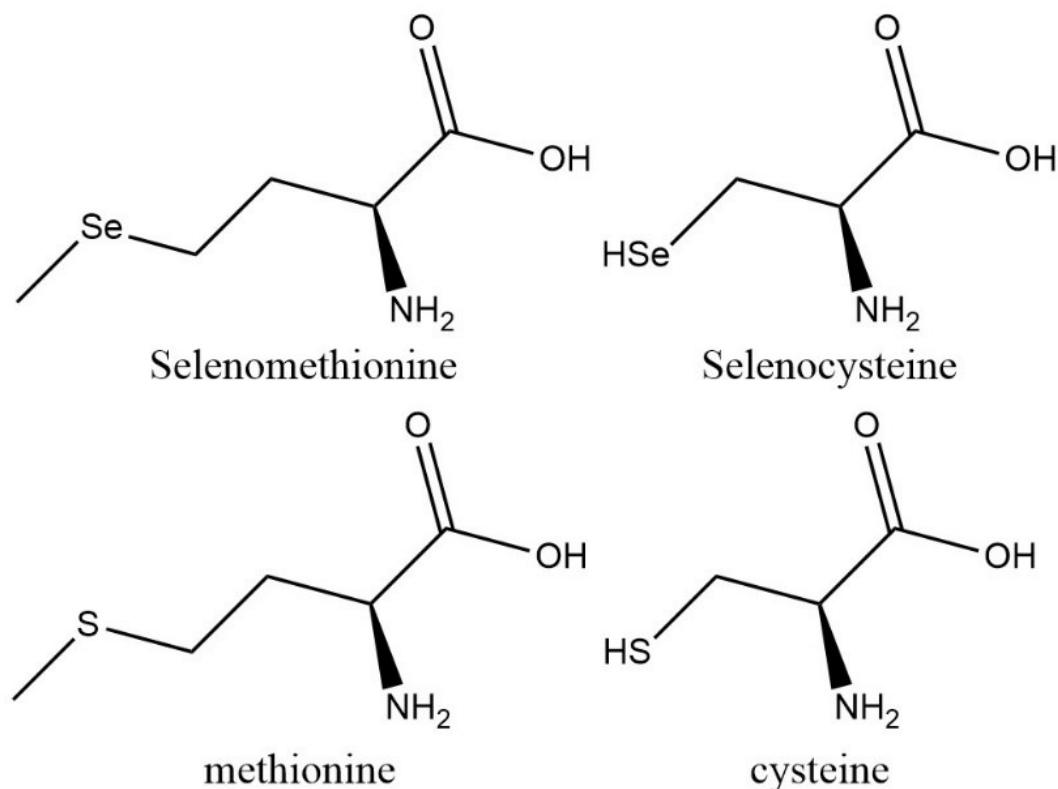


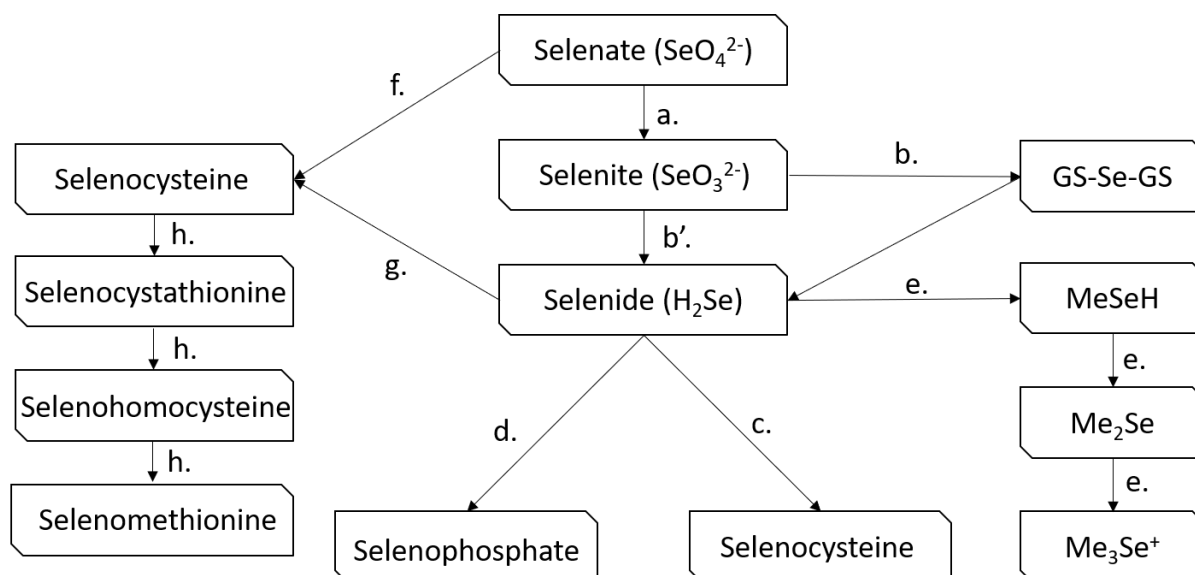
Figure 3 Chemical structures of methionine and cysteine and their Se counterparts: selenocysteine and selenomethionine

### 2.1. Selenium vs. sulfur metabolite pathways

Se and S often share a common metabolic pathway owing their chemical and physical resemblance. In other words, Se can act as a substitute for S in physiological and metabolic processes. In plants, several integration pathways for the integration of Se into proteins or smaller molecules are following those of sulfur (**Figure 4**)(24).

The primary uptake source of selenium of mammals is from the diet, mainly as selenomethionine (25). Like SeMet, SeCys and Se-methylselenocysteine from cereal grains, plants and animal proteins, in which the Se content depends on the area of growth, more precisely from soil and fodder (26). Even if selenium uptake also encompasses selenite and selenate, the uptake of selenopeptides is privileged in mammals' biology. Mammals are using selenium for protein synthesis and reproduction purposes (spermatogenesis) (27). Selenium is used as a sulfur counterpart in several protein families for its capacity to resist extensive oxidation and can be found in several species of animals, mammals include.

During the assimilation of sulfur and selenium, a selenium atom can randomly replace a sulfur atom. The frequency of the phenomenon is directly proportional to the concentration of selenium in the cell during protein synthesis. The random replacement leads to a myriad of species, eg. in Se-rich yeast (**Figure 5**). More than 60 Se species have been reported, often chaotically, with some data interpretation errors. The metabolism of selenite leads to the formation of a covalent bond between Se and carbon, producing many organoselenium compounds. The most straightforward building unit is a selenol R1–CH<sub>2</sub>–Se–H, which is the Se equivalent of alcohol and thiol.



*Figure 4 Assimilation of inorganic selenium. The letters correspond to the metabolic pathways involved. a) Reduction of selenates similarly to a pathway known for sulphate using ATP sulfurylase (28). In some bacteria (*Thauera selenatis*), it is a selenate reductase that replaces the ATP sulfurylase (29); b) Non enzymatic reaction of selenites with glutathione, followed by a reduction, which lead to selenide catalysed by glutathione or thioredoxin reductase (30). There is also a pathway b') in mammals, consisting of a direct reduction by thioredoxin reductase(31); c) Nonspecific formation of selenocysteine by cysteine synthase; d) Formation of selenophosphate by a selenophosphate synthetase (in connection with the specific synthesis of selenocysteine), and e) Methylation reactions by S-adenosyl-methionine transferase; these methylated compounds are excreted by organisms to eliminate excess selenium (32), f.) enzymatic reaction leading to the transformation of serine into selenocysteine with of ATP reacting with selenate leading to adenosylselenate which react with serine to give selenocysteine , g.) Non enzymatic reaction leading to the transformation of serine into selenocysteine with GSH reacting with Selenite leading to GS-SE-GS followed by a reduction into selenide which react with serine to give selenocysteine, h.) Biosynthesis of selenomethionine with the reaction of homoserine on selenocysteine followed by reduction and akylation.*

The most widely represented selenol motifs present in yeast metabolites are shown in **Figure 5**, including methylselenol, SeCys, selenohomocysteine and selenoadenosine (33).

## 2.2. Selenocysteine: the 21st proteogenic amino acid

Selenocysteine, an analogue of cysteine (**Figure 3**), is a cysteine in which the sulfur atom of the thiol group has been replaced by selenium, thus forming a selenol. Selenocysteine is considered the 21st proteogenic amino acid because it has a specific and non-random mechanism of incorporation, unlike selenomethionine (34).

### 2.2.1. Reactivity of selenocysteine vs. cysteine

Selenocysteine (SeCys) has characteristics similar to cysteine (Cys), its sulfur counterpart, particularly in terms of electronegativity, ionic radius, and oxidation state. On the other hand, SeCys is a more potent nucleophile than cysteine under neutral and acidic conditions. This property is explained by the fact that SeCys has a lower pKa (5.24) compared to Cys (8.25) and therefore it is deprotonated at biological pH while Cys is in the thiol state. This makes SeCys a considerably more potent nucleophile under neutral and acidic conditions.

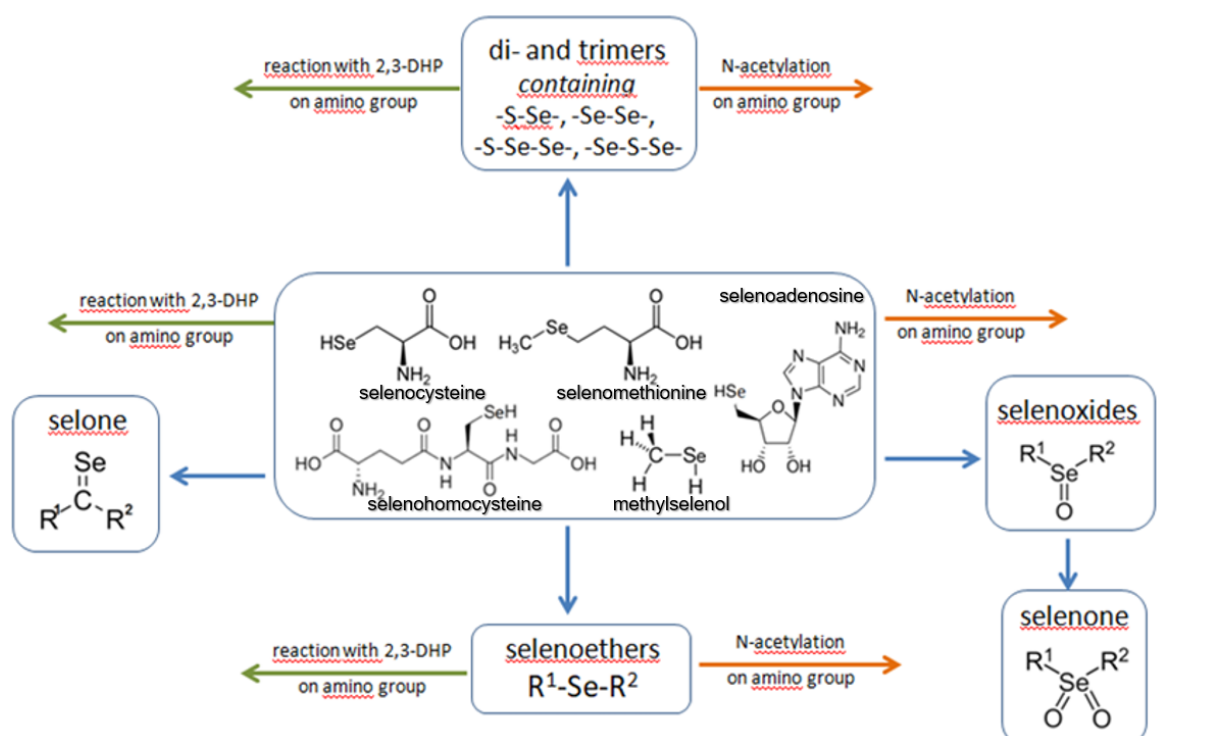


Figure 5 Main selenometabolites in Se-rich yeast (courtesy of Joanna Szpunar)

Nature may be able to increase the nucleophilicity of sulfur at physiological pH. the pKa values of cysteines in the protein microenvironment can be strongly disturbed, as evidenced by the pKa values of the Cys residues of the active site of papain, caricain and ficin respectively 3.3, 2.9, and 2.5 (35).

Moreover, selenium is softer than sulfur, with a polarizable volume of 3.8 Å in comparison with the 2.9 Å of sulfur (36). The Hard and Soft Acids and Bases (HSAB) theory suggests that many non-physiological soft-type metal compounds (Pt, Au, Hg, As, etc.) can strongly interact with the selenium (soft) present in selenoproteins (37).

The reactivity of proteins containing selenocysteine is often much stronger than of those containing cysteine. The energy cost of the synthesis of selenocysteine is quite high; selenocysteine is readily oxidized and reduced back to its original form (9).

The weaker hydrogen bond and the increase in size and polarizability of the heavier atom are reflected by a significantly lower basicity of selenolates compared to thiolates ranging from 3 to 4 pKa units (Figure 6) (13). Thus, most cysteine is in the thiol state at neutral pH, while selenocysteine is almost entirely ionized to selenolate at the same pH.

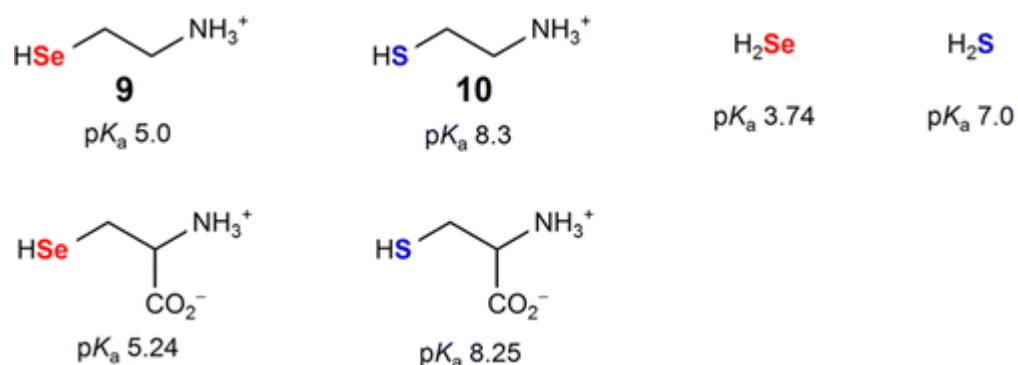


Figure 6 : Comparison of pK<sub>a</sub> values of thiols and selenols

Despite their lower basicity, selenolate ions are ca. one order of magnitude more nucleophilic than thiolates due to the acceptor properties of the weaker hydrogen bond. Selenides are also more nucleophilic than sulfides (9).

Furthermore, its redox potential ( $E_0 = -388$  mV) being much lower than that of Cys ( $E_0 = -220$  mV), SeCys is easily oxidized under normal pressures and temperatures thus promoting the formation of diselenide bridges (38).

The different oxidation and reduction rates observed in chalcogen oxides resides in the difference of their electronic structures. The first oxidation of sulfides/selenides to sulfoxides/selenoxides is comparable, with the selenium being slightly more reactive. Yet, the second oxidation is more difficult for selenoxides. That consequence results from a much higher dipolar character of the Se-O bond, resulting in lower nucleophilicity of the lone pair on Se (9).

Compared to the dithiol/disulfide pair, in which the equilibrium constant is 600-fold lower for the same conditions and will favours the dithiol, the equilibrium constant for oxidation of diselenol to a diselenide greatly favours the diselenide.

Moreover, the selenol form of the SeCys is highly unstable and easily converted to dehydroalanine with the loss Se by  $\beta$ -elimination. This elimination can be catalysed either by temperature, alkaline conditions or the used of reducing agents such as DTT or TCEP (39). This  $\beta$ -elimination is based on the high propensity of selenols to be selectively reduced in presence of thiols to form radicals, and was chemically describe in the case of sulfide/selenide bridge (40). The deselenization of SeCys is employed as an extension to native chemical ligation at selenocysteine and can be accomplished in one minute under anaerobic conditions to give alanine. Under aerobic conditions (oxygen saturation), selenocysteine is converted into serine (39).

The conversion of Cys into dehydroalanine via beta elimination is also described and, in the case of the bioactive peptide Oxytocin peptide, it undergoes hydrolysis leading to the formation of a pyruvoyl group at the N-terminus (41).

### 2.2.2. Rate advantage versus redox advantage

Research trying to explain why sulfur is replaced by selenium in certain enzymes were based on experiments with the replacement of catalytic SeCys residue with Cys in several SeCys-containing enzymes (42–45). The replacement of Se with S resulted in mutant enzymes with greatly impaired catalytic activity. On the contrary, the replacement of S with Se in Cys-containing enzymes resulted in enhanced catalytic activity (46–49). However, Lacourciere and Stadtma *et al.* found that the catalytic

activity of the Cys-containing selenophosphate synthetase from *E. coli* had higher specific activity when compared to the SeCys one from *H. influenzae* (50), meaning that the selenocysteine role is not to enhanced catalytic activities in the case of *H. influenzae*. This conclusion was later reinforced by Kanzok *et al.* that showed that selenium was not required in the active site of TrxR because a Cys-ortholog enzyme had comparable activity (51). That conclusion shows that SeCys and other forms of selenium are not entirely related to enhanced catalytic function compared to sulfur.

Other studies have shown another additional gain of Se upon S substitution in the enzyme is a better peroxidase activity (52–58). This function's gain correlated well with its superior redox properties relative to sulfur. Selenium confers peroxidase activity to an enzyme because it is both a good nucleophile and a good electrophile. This property allows selenium to cycle between reduced and oxidized state without permanently becoming oxidized. From this perspective, selenium redox properties resemble more to a transition metal (9).

The work of Rocher *et al.* was the first to mention that SeCys may have evolved in an enzyme to prevent "**self-inactivation**" (44). This hypothesis was formed by studying the Cys-mutant of Gpx1, which had lower activity than the SeCYS-containing Gpx1 but was readily inactivated in the presence of its substrate, H<sub>2</sub>O<sub>2</sub>, and organic hydroperoxides. They hypothesized that the Cys-mutant Gpx1 inactivation resulted from the oxidation of the peroxidatic Cys residue to Cys-SO<sub>2</sub>- with a possible β-elimination to form a dehydroalanine. In the following decade, Dimastrogiovanni *et al.* (59), crystallized the Cys-mutant of the SeCys-containing Gpx4 from *Schistosoma mansoni*, which perhaps could confirm the hypothesis of Rocher *et al.* (44). That work showed the presence of a sulfonic acid residue on the X-ray structure of the Gpx4 mutant. The mutant of Gpx4 was inactive during purification, even in the presence of reducing agents. An interpretation of this phenomenon that matches Rocher *et al.* observation is that the mutant enzyme was able to react with the oxidant. Still, the S-oxide that formed was not electrophilic enough to resolve back to the active form of the enzyme, which results in the overoxidation and inactivation of the mutant enzyme.

## 2.3. Selenoproteins

Selenoproteins are a class of proteins having one to more selenocysteine residues in their peptide sequence. Its incorporation into the sequence is linked to the presence of a UGA codon which is not recognized as a stop codon. This observation was made following a selenocysteine residue in the genes of bovine glutathione peroxidase and eubacterial formate dehydrogenase (60, 61). Selenocysteine is an amino acid that does not exist in free form. Its synthesis is carried out in two steps, directly on the tRNA<sup>Sec</sup>, from serine.

### 2.3.1. Mechanisms of SeCys insertion in selenoproteins

Selenocysteine transfer RNA is an RNA strand characterized by its UCA anticodon capable of recognizing the UGA codon, and they are distinguished from conventional RNAs in many points. Their large size, around 100 base pairs, makes them one of the largest known tRNAs. In addition, it is characterized by a rod of the D arm six base pairs long against only 3 or 4 for a classic tRNA (**Figure 7**). This feature is a major identity determinant for an intermediate step of serine phosphorylation in eukaryotes (62). The acceptor's arm is also longer than on conventional tRNAs (63). This size is also essential for recognition by the specific elongation factor SelB, which is required to convert serine to

selenocysteine (64). Finally, its variable arm is also longer than in any other conventional tRNA and determines its serylation (65).

The original and complex nature of tRNA<sup>Sec</sup> can be explained as follows: it must be aminoacylated by a canonical tRNA. This is not the primary function and then be recognized by a non-conventional elongation factor. It must be recognized by the ribosome, and therefore present specific determinants of a classic tRNA (66); all of these characteristics make it unique in the world of transfer RNAs.

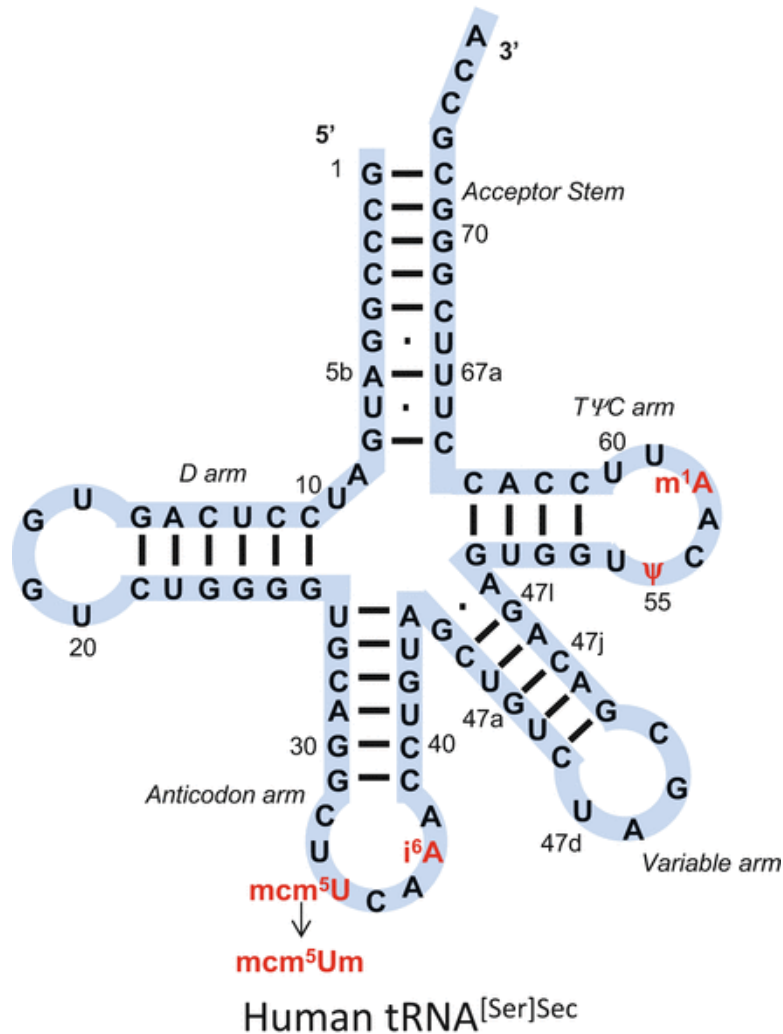


Figure 7 Human selenocysteine transfer RNA (67)

This process involves the initial aminoacylation of tRNA<sup>[Ser]Sec</sup> with serine by Ser-tRNA synthase, followed by phosphorylation of serine by phosphoseryl-tRNA kinase to give phosphoseryl-tRNA<sup>[Ser]Sec</sup>. The phosphoseryl-tRNA bound residue is then converted to SeCys by the enzyme selenocysteine synthase (Sec synthase), a reaction in which selenium, in the form of monoselenophosphate, is transferred to the tRNA<sup>[Ser]Sec</sup> to produce Sec-tRNA<sup>[Ser]Sec</sup> (68). The selenoprotein SPS2 is also essential in this process, which generates the monoselenophosphate necessary to synthesise SeCys. Another factor contributing to selenium metabolism is the enzyme selenocysteine lyase, which breaks down SeCys into L-alanine and selenide, allowing selenium to be recycled for further SeCys biosynthesis (69)(Figure 8).



Beside tRNA<sup>[Ser]Sec</sup>, several additional factors are necessary for the successful incorporation of SeCys at UGA codons rather than termination of protein synthesis. For eukaryotic selenoproteins, SeCys incorporation is directed by a specific stem-loop structural element, called the selenocysteine insertion sequence (SECIS), which is located in the 3'-untranslated region of selenoprotein mRNAs (43). The SECIS element forms the structural backbone for assembling several factors into an RNA-protein complex that directs the insertion of SeCys (70). Critical components of this complex in eukaryotic organisms include the SeCys-specific elongation factor (EFSec) and the SECIS 2 binding protein (SBP2) (71). EFSec is a GTP-dependent elongation factor that interacts exclusively with SeCys-tRNA<sup>[Ser]Sec</sup>, while SBP2 is a trans-acting factor that coordinates the insertion of SeCys by binding to SECIS elements located in selenoprotein mRNAs—and recruiting EFSec. The mechanism of selenoprotein synthesis has been the subject of several excellent review articles examined in much more detail (72, 73).

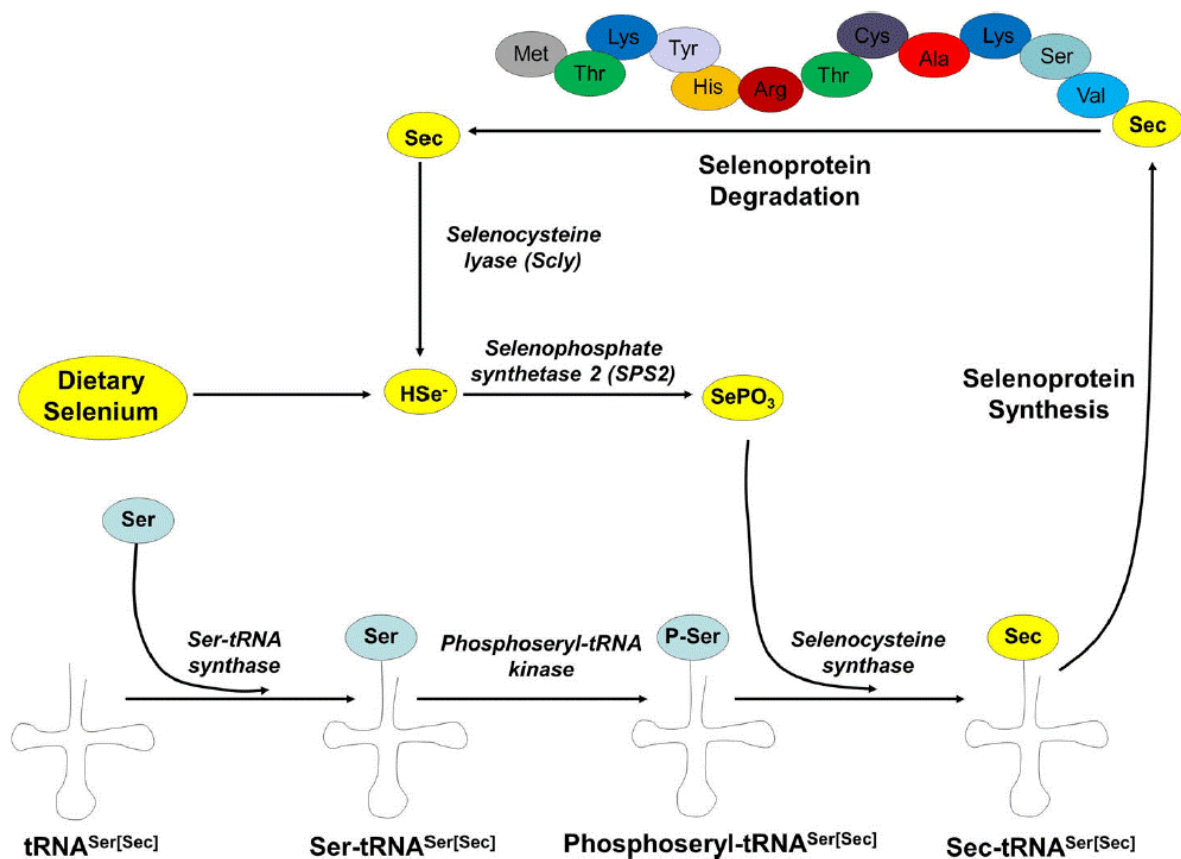


Figure 8 Overview of selenocysteine biosynthesis and degradation (74)

### 2.3.2. Human selenoproteome

In humans, 25 selenoproteins were identified up to date (75). The first selenoproteins were identified in the 1970s in mammals with the proteins of the glutathione peroxidase family. Since then, thanks to *in silico* approaches, the almost exhaustive repertoire of human selenoproteins has been determined (76).

Selenoproteins share few sequence similarities, and their great diversity reflects their involvement in various biological functions that do not have still been determined for some of them. Selenoproteins are not a family of proteins in the strict term since they do not derive from a common ancestor; however,



they share common physicochemical properties. In **Table 3**, they are presented according to an alphabetical order. One major similarity of selenoprotein is the presence of at least one SeCys residue in the amino acids sequence.

In this family of proteins, three groups of selenoenzymes can be distinguished. This group are thioredoxin reductases, iodothyronine deiodinases and glutathione peroxidases.

*Thioredoxin reductase* enzymes belong to the pyridine nucleotide-disulfide oxidoreductase family. TrxR catalyses the reduction of thioredoxins (Trx) by NADPH (27). These enzymes are considered to be the major protein disulfide reductases in cells, being potentially the physiological equivalent of reducing agents, such as dithiothreitol (77). These proteins also play a role in the protection against the oxidative stress of the cells and are considered as one of the guarantors of homeostasis (78). The family contains three proteins containing a SeCys residue that have similar reactivity domain, TrxR1, TrxR2 and TrxR3.

*Table 3 Humans selenoproteins*

| Selenoprotein    | Number of amino acids | SeCys residue position                          |
|------------------|-----------------------|---|
| <b>15kDA</b>     | 162                   | 93  |
| <b>DIO1</b>      | 249                   | 126   |
| <b>DIO2</b>      | 265                   | 133   |
| <b>DIO3</b>      | 278                   | 144   |
| <b>GPx1</b>      | 201                   | 47  |
| <b>GPx2</b>      | 190                   | 40  |
| <b>GPx3</b>      | 226                   | 73  |
| <b>GPx4</b>      | 197                   | 73  |
| <b>GPx6</b>      | 221                   | 73  |
| <b>SELENOH</b>   | 122                   | 44  |
| <b>SELENOI</b>   | 397                   | 387   |
| <b>SELENOK</b>   | 94                    | 92  |
| <b>SELENOM</b>   | 145                   | 48  |
| <b>SELENON</b>   | 556                   | 428   |
| <b>SELENOO</b>   | 669                   | 667   |
| <b>SELENOP</b>   | 381                   | 59, 300, 318, 330, 345, 352, 367, 369, 376, 378 |
| <b>SELENOS</b>   | 189                   | 188   |
| <b>SPS2</b>      | 448                   | 60  |
| <b>SELENOT</b>   | 182                   | 36  |
| <b>TrxR1</b>     | 499                   | 498   |
| <b>TrxR2</b>     | 655                   | 656   |
| <b>TrxR3</b>     | 523                   | 522   |
| <b>SELENOV</b>   | 346                   | 273   |
| <b>SELENOW</b>   | 87                    | 13  |
| <b>MsrB(X/R)</b> | 116                   | 95  |

(TrxR : thioredoxine reductase, DIO : Iodothyronine deiodinase, Gpx :glutathione peroxydase MsrB (X/R) : Selenoprotein X ou methionine-R-sulfoxyde reductase)

*Iodothyronine deiodinases* is a protein family implicated in the regulation process of the thyroids hormone production and circulation, more precisely the 3,5,3'-triiodothyronine (T3) levels. They also

seem to be implicated in the deiodation of the tyrosine T4 leading to the T3 active form from the outer and inner ring of the hormone (79). This family includes three proteins containing a SeCys residue that have closed reactivity domain, DIO1, DIO2 and DIO3.

*Glutathione peroxidase* is a family of selenoproteins with 5 SeCys containing proteins (GPx1, GPx2, GPx3, GPx4 and GPx6). GPx1 is the most abundant selenoprotein, in mammals being mostly expressed in liver and kidneys. The GPx are antioxidant selenoenzymes protecting organisms from oxidative stresses by catalysing the reduction of hydroperoxides at the expense of GSH (27). Like others selenoproteins their main action is to maintain a low cellular and blood oxide level to avoid any damage by the oxidative stress (80).

### 2.3.3. Selenoproteomes of other organisms

Selenoproteins are present in all living organism domains: bacteria, archaea and eukaryote. However, SeCys is not used by all organisms, in yeast and higher plants, the SeCys insertion machinery is not present and therefore they do not possess natural selenoproteins expression. The number of selenoproteins that can be expressed in different organisms varies, ranging from one in certain insects, to 9 in the common spider, 25 in humans, 32 in oysters (81) and even 37 in fishes (82). All mammals display a similar selenoproteome and the fish selenoproteome is known as the largest among the selenoproteomes (82). Even if species are displaying similar selenoproteome, each protein is specific to the species, only the active domains of those proteins are similar.

## 2.4. Thioredoxin reductases

The cytosolic and mitochondrial thioredoxin reductase (TrxR) and thioredoxins (Trx1 and Trx2) are critical components of the mammalian thioredoxin system (83). In addition, Trx and TrxR provide a coupled redox system required for redox reactions in biosynthetic pathways that control redox homeostasis in cells (84–86).

TrxRs are FAD-containing pyridine nucleotide disulfide oxidoreductases that utilize NADPH to reduce the active-site disulfide of Trxs. Thus, TrxR is necessary for all biochemical pathways in which Trx is a reducing substrate (86, 87) (**Figure 9**).

The thioredoxin system is mediated by crucial redox-sensitive biological processes, including cell survival, growth, migration, and inhibition of apoptosis. Moreover, TrxR plays also an important role in diverse physiological and pathological conditions such as parasitoses, chronic inflammatory, autoimmune diseases, and neurodegenerative disorders (88–96).

Considerable interest has been focused on thioredoxin reductase (TrxR) because its role as a regulator of homeostasis and various cellular signalling pathways essential for the functioning of cells. On the other hand, if it is defective, thioredoxin reductase is considered an attractive target for the development of anticancer agents as it is frequently overexpressed in cancer cells (97, 98). In addition, its interaction with several metallodrugs has been described as responsible for the inhibition of its enzymatic activity. This protein is involved in the defence and repair damage mechanisms due to oxidative stress. Considering its role in these mechanisms, this protein's-controlled activity and expression appear to be essential in research towards cancer prevention (99).

TrxRs are large homodimeric flavoproteins, and three isozymes, a cytosolic (TrxR1) and a mitochondrial (TrxR2) form, have been identified, the third one was only detected in testis and in

spermatids cytoplasm. TrxR has a peculiar structure: one part of the molecule is a flavoprotein very similar to GR, while the other is a flexible arm, not found in GR, and containing at its C-terminus an accessible cysteinyl group and a selenocysteine group in vicinal positions (86, 100). TrxRs also possess an N-terminal redox centre characterized by a dithiol motif (Cys-XXXX-Cys). These groups allow the enzyme to form chelate complexes with heavy metals, where the metal ion is simultaneously coordinated to a selenol group (–SeH) and a thiol group (–SH), and these interactions cause inhibition of its activity.

## 2.5. Selenoprotein P

### 2.5.1. Discovery and importance

Selenoprotein P is unique amongst all the characterized selenoproteins in that it contains multiple SeCys residues, whereas all other selenoproteins contain only one SeCys. The number of SeCys residues in SELENOP from different organisms varies, amounting to 10 for humans, 46 in oysters (101) and 132 in one-species bivalves (102) (Figure 10).

SELENOP was first reported in 1973 by Burk *et al.* (103) and Rotruck *et al.* (104). McConnell *et al.* (105) and Motsenbocker *et al.* (106) found that SELENOP was synthesized in the liver of rats and secreted into the plasma. A few years later, the existence of SELENOP was confirmed in humans, where it is considered a valuable marker for nutritional selenium status (107). In 2016, Gladyshev *et al.* proposed a non-ambiguous notation for all selenoproteins using the root symbol SELENO followed by a letter, leading to the creation of the abbreviation SELENOP for selenoprotein P, replacing the previously used abbreviations such as SeP, SEEP1, SelP (108). Expression, functions and role of SELENOP in mammals are known (109). It is considered as a transporter and playing a role in the storage of selenium in the brain, testis (110, 111) and kidney (112), more recent studies show a function in the regulation of heavy metals concentration (113, 114) and a role as an antioxidant in plasma (106).

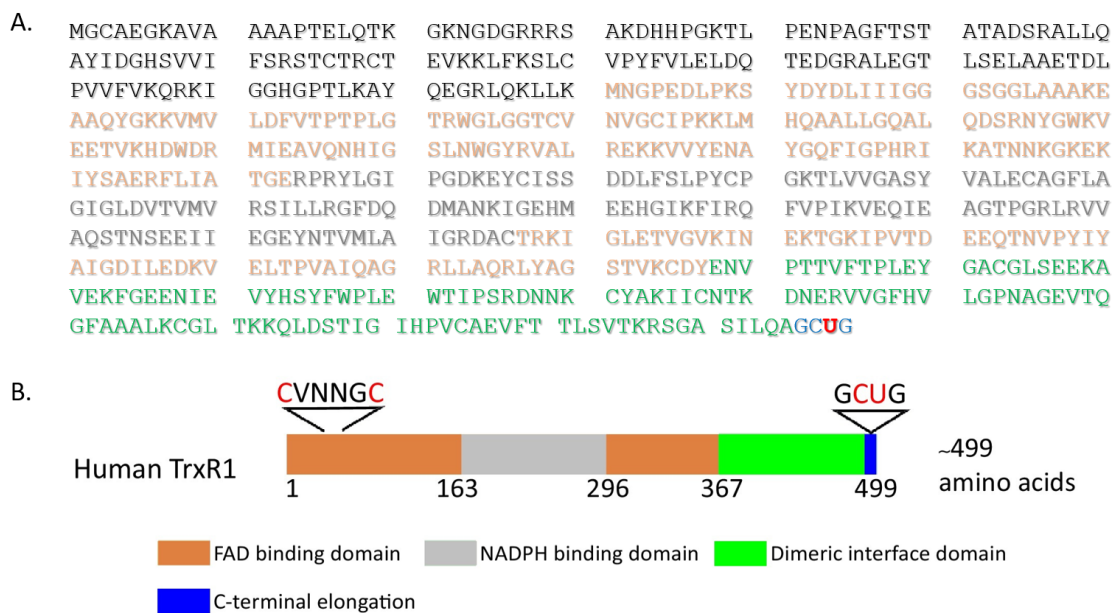


Figure 9 Sequence of human TrxR1 A.) Canonical form of TrxR1 (non-major form in cells); B.) Major form of TrxR1 (isoform 5)

As a biomarker, SELENOP can discriminate between the specific and nonspecific (and therefore non-significant) incorporation of Se in proteins (110, 115). It responds to Se supplementation over a wider range of intakes than GPx3 (116).

In marginally supplied individuals, low serum Se was found to be mirrored by the circulating SELENOP concentration, but not by the GPx3 activity (117). In studies of populations with relatively low selenium intakes, SELENOP was found to respond to different dietary selenium forms (118). Serum SELENOP concentration can be more than a biomarker of Se status: it was proposed to be used for the diagnosis and assessment of treatment efficacy and long-term prognosis in patients with pulmonary arterial hypertension (119) and hypertension (120). Recently, the mortality risk from COVID-19 was shown to be associated with selenium deficiency, and more specifically with SELENOP deficiency, causing a dysregulation of the redox homeostasis in pathological conditions which resulted in an excessive reactive oxygen species (ROS) generation (121, 122).

During the last 40 years, many functions have been attributed to SELENOP including its involvement in the storage of selenium in the brain, testis (110, 111) and kidney (112), defence against oxidative stress (123), loss of fertility (110), polycystic ovary syndrome (124) or regulation of heavy metals concentration (113, 114). SELENOP was reported to play a role in the potential development of various forms of cancer (125–128) and to be associated with neurodegenerative diseases such as Alzheimer's (126, 129–131). SELENOP was evoked as a therapeutic target for type 2 diabetes (129, 132–134) because of its role in the regulation of glucose metabolism and insulin sensitivity.

### 2.5.2. Structure

To date, the three-dimensional structure of SELENOP has not been solved. A possible reason for this is the difficulty in the exogenous over-expression of SELENOP in bacteria or in cultured cells, because of the presence of multiple SeCys residues in the polypeptide (135). Studies using recombinant SELENOP have been rare (71). Consequently, the SELENOP characterization was carried out on protein expressed endogenously by cell lines or purified from plasma and serum.

The matured predominant isoform of human SELENOP consists of 359 amino acids (AA) after cleavage of the predicted signal peptide (AA 1–21) (135) (**Figure 11a**). The selenium content (as SeCys) of SELENOP is distributed into two parts (109, 135). The N-terminal domain contains one selenocysteine at the 40th amino-acid in a U-x-x-C redox motif. The shorter C-terminal domain contains multiples selenocysteine, up to 9 in total for rats, mice, and humans (136, 137). The N-terminal domain is responsible for the enzymatic activity of this protein, while the C-terminal domain acts as the Se supplier (138) (**Figure 11b**).

SELENOP is not a homogenous protein. As a consequence of the SeCys gene expression by stop codon recoding, multiple forms of the SELENOP of different molecular weight exist in terms of relation to genotype, differential splicing, premature interrupted translation at one of the UGA codons, limited post-translational proteolysis or partial replacement of SeCys by Cys (135, 139–142). To date, four isoforms have been identified in rat plasma. Beside the full-length isoform with 10 selenocysteine residues, shorter isoforms terminating at the 2<sup>nd</sup>, 3<sup>rd</sup>, and 7<sup>th</sup> selenocysteine (141), with 1, 2 and 6 selenocysteines, respectively, were reported (143). Interestingly, in a study involving ca. 2000 subjects, the average determined number of Se atoms per SELENOP molecule (5.4) was considerably below the predicted number of 10 Se atoms (144).

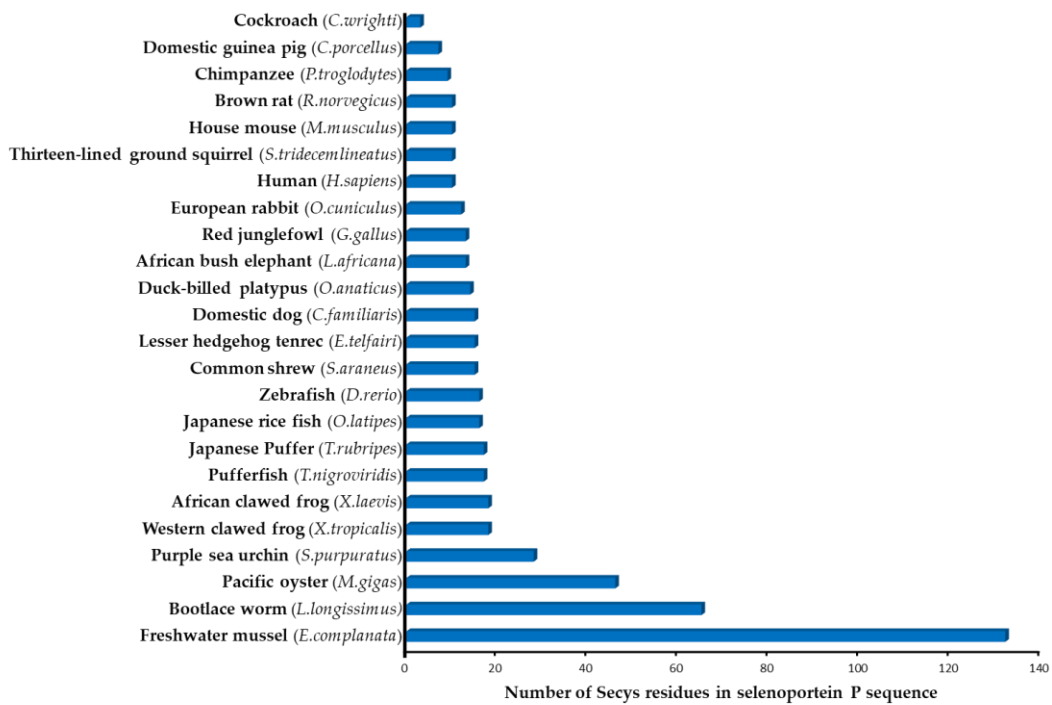


Figure 10 Putative number of SeCys residues in SeP in different organisms (81)

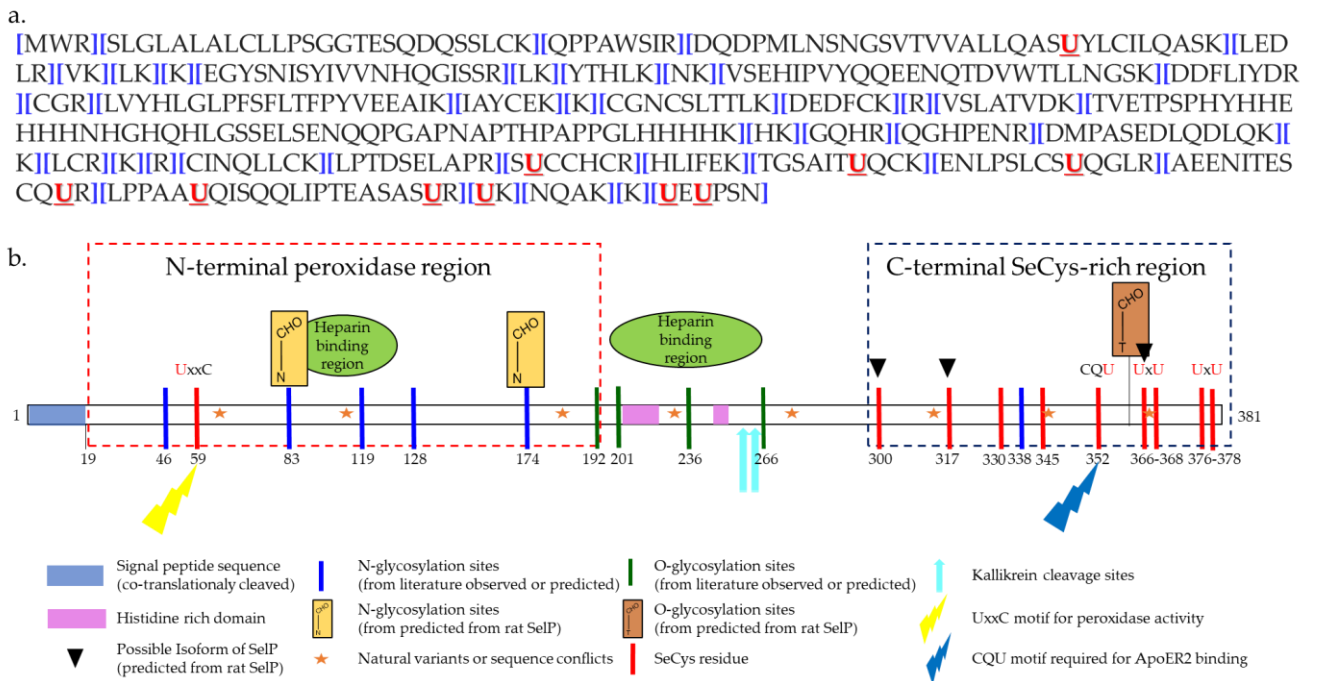


Figure 11 Sequence of human SELENOP (a) Amino-acid sequence of human SELENOP (138); (b) schematic representation of human SELENOP (on the basis of (135, 138) and Uniprot database).

In the native form, SELENOP contains selenenylsulfide and disulfide bridges. It possesses three N-glycosylation sites at the N-terminus and one O-glycosylation site at the C-terminus (145) and thus, can be referred to as glycoprotein. One highly glycosylated form is secreted by the liver (146). Selenium-supplemented HepG2 hepatoma cells secrete N-glycosylated SELENOP as well (147). The post-translational modifications are thought to confer a particular structural behaviour to SELENOP and to protect selenium by reducing its reactivity (148).



## 3.1. Metallodrugs

### 3.1.1. Platinum compounds

In mid-1960, an accidental discovery of anticancer properties of inorganic coordination compounds containing platinum revolutionized the chemotherapy cancer treatment (149). The six-coordinate octahedral *cis*-[PtCl<sub>4</sub>(NH<sub>3</sub>)<sub>2</sub>], with Pt<sup>4+</sup> ion and *cis*-[PtCl<sub>2</sub>(NH<sub>3</sub>)<sub>2</sub>], with Pt<sup>2+</sup> ion that was effective in arresting the cell division (150). Later known as “cisplatin” it turned out very effective on sarcoma and leukaemia cells while *trans* isomer exhibited little antitumor activity (150). This discovery triggered off research on Pt compounds as metallodrugs for cancer therapy and led to the approval of the other two compounds, referred to carboplatin and oxaliplatin, shown in **Figure 12**.

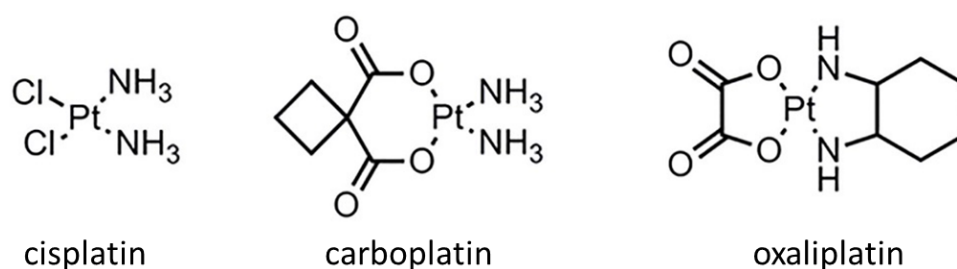


Figure 12 Chemical structure of cisplatin and the most common cisplatin derivatives

Major obstacles to the clinical use of platinum drugs include their toxicity and the development of cell resistance. To reduce these effects, it is crucial to understand the chemical properties, transport, metabolic pathways and mechanism of action of these compounds. There has been considerable evidence that the therapeutic and toxic effects of platinum drugs on cells are due to the formation of covalent bonds between platinum complexes and DNA, RNA and many proteins, such as, e.g., human albumin.

The chemistry of cisplatin has been extensively studied. In blood, the concentration of the chloride ion is about 105 mM and, according to Le Chatelier's principle (151), the loss of the chloride ion from cisplatin is suppressed by the chloride ion in solution. The reaction shown in **Figure 13** does not progress very far to the right (from **1** to **2**). According to the first-order kinetics for conversion from **1** to **2**, the half-life for cisplatin at 35.5 °C is 1.05 h. The binding of a water molecule to the Pt<sup>2+</sup> ion makes the water very acidic, and mono aqua species **3** is dissociated in the monohydroxo complex **4**. So, in an aqueous solution with a high chloride concentration, forms **1**, **2** and **4** predominate. In the cytoplasm, where chloride ion concentration is only 4 mM, the equilibria shift to the right and form **3**, **5** and **6** predominate.

A standard route of cisplatin administration is the infusion of the solutions, such as Platinol® and Plationol®AQ, containing 3.3 mM cisplatin (1 mg/ml) and 154 mM sodium chloride, NaCl (standard saline solution). Since the pH is adjusted to pH about 4, the solution in Platinol contains mainly (95%) of species **1** and only smaller amounts of **3** and **4** (149).

Recent studies have increased knowledge on cisplatin target, the initial target of cisplatin was the DNA (152, 153). The DNA platination is lethal to the cell, because the repair mechanisms are not able to remove the ligand from the DNA strand. Cisplatin is known to target membrane-bound Na<sup>+</sup>/H<sup>+</sup> exchanger proteins. When cisplatin binds to the protein in human colon cancer cells, it causes





167). A similar action of gold (III) complex was observed on human ovarian cancer stem lines, and in one study, it was compared with cisplatin and oxaliplatin. Antiproliferative and pro-apoptotic actions of gold complexes were more robust than those of platinum derivatives (166, 167). In another study, gold complexes were assessed for their antiproliferative potential in ovarian cancer cell lines and embryonic cell lines – it was found that they selectively inhibit thioredoxin reductase in cancer cells (167, 169).

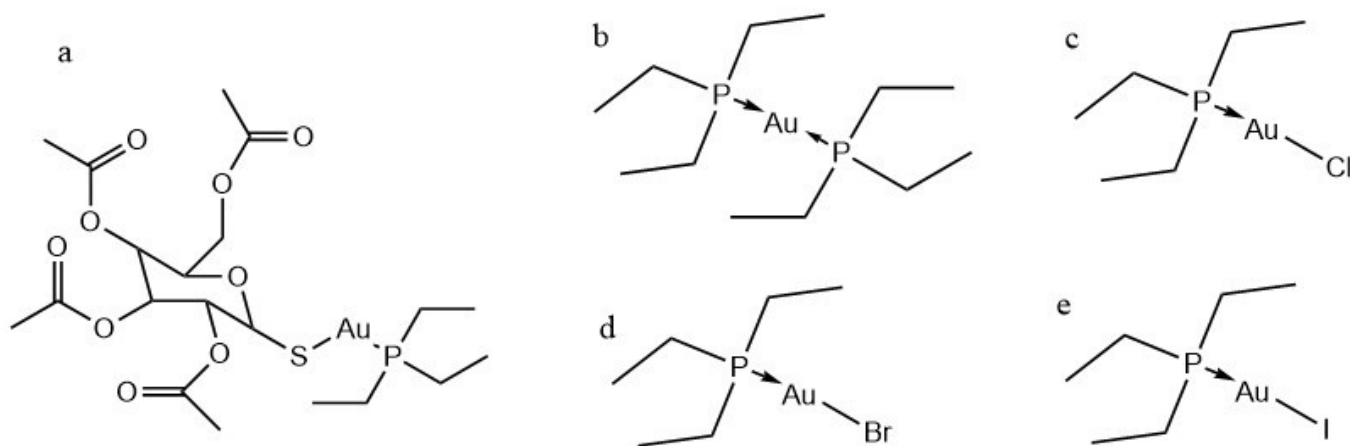


Figure 14 Auranofin and derivatives (a) Auranofin, (b)  $Au(Pt_3)_2$ , (c)  $Au(Pt_3)Cl$ , (d)  $Au(Pt_3)Br$ , (e)  $Au(Pt_3)I$

This interest in new metal compounds with different mechanisms of action than  $Pt^{2+}$  is driven by a wish to decrease the toxic side effect common with a platinum drug.

### 3.1.3. Other metals compounds

Intense works on other metallodrugs are pursued to find metallodrugs that can induce apoptosis of cancer cells without damaging healthy cells and provoking toxic side effects. Non-platinum metal anti-cancer complexes are currently not employed in the clinic. Nevertheless, complexes of ruthenium (e.g. NAMI-A and KP1019) **Figure 15** (172–174)), titanium (e.g. budotitane and titanocene dichloride) **Figure 15** (175, 176), or gallium (e.g. gallium nitrate, gallium chloride and gallium malonate) (177, 178) were already tested in clinical trials and complexes with e.g. silver, copper, iron, palladium, osmium, iridium or rhodium as central atom showed promising results in preclinical studies (179–191).

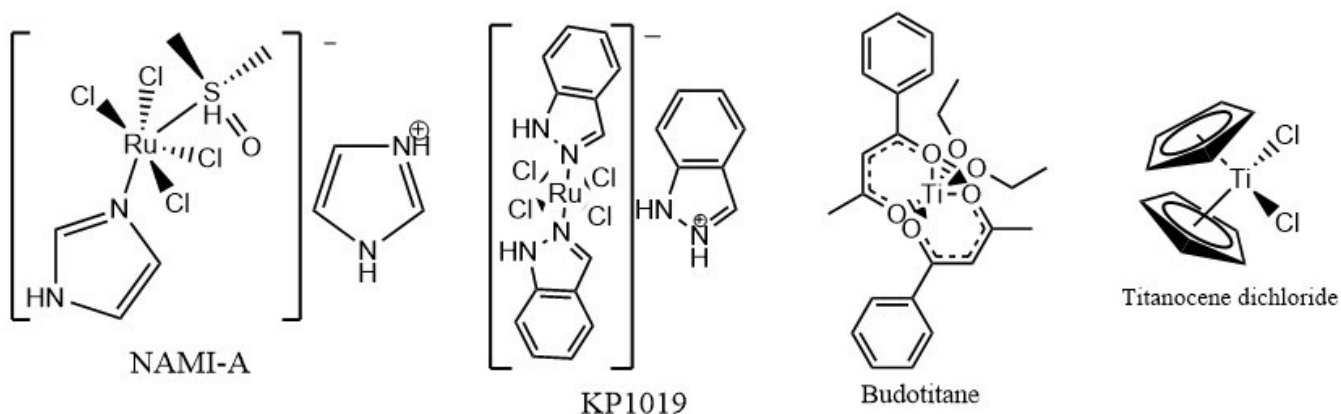


Figure 15 Chemical structure of non-platinum metal anti-cancer complexes

## 3.2. Reactivity of selenium with metal ions

The growing interest in selenium's role in biology has been focused on its ability to bind to other elements and, more specifically, to certain metalloids and metals. Selenium has been assumed to modify the toxicity of many heavy metals because of the chemical properties of their selenides by interacting with them. The group of Naganuma *et al.*, (192) is among the first to have studied the ability of selenium to interact *in vitro* and *in vivo* with a wide variety (more than 20) of metal ions. In more detail, they were able to observe that the behaviour of selenium in biological systems was influenced by many metals *in vitro* and *in vivo*. This observation is important in contemplating the biological roles of selenium as an essential element or as modifying factor for the toxicity of metal compounds. Significant change in tissue distribution of  $^{75}\text{Se}$  was observed when  $\text{Na}_2^{75}\text{SeO}_3$  was co-administered with  $\text{Hg}^{2+}$ ,  $\text{Pb}^{2+}$ ,  $\text{As}^{3+}$ ,  $\text{Cd}^{2+}$ ,  $\text{Ag}^+$ ,  $\text{Cu}^+$ ,  $\text{Zn}^{2+}$ ,  $\text{Cr}^{3+}$ ,  $\text{Cr}^{6+}$ ,  $\text{Pt}^{2+}$ ,  $\text{Au}^{3+}$ ,  $\text{Bi}^{3+}$  or  $\text{Pd}^{2+}$ .  $\text{Hg}^{2+}$  was the most effective and significantly altering the concentration of  $^{75}\text{Se}$  in all the tissues subjected to the measurement; and effects of  $\text{Pb}^{2+}$ ,  $\text{Cd}^{2+}$ ,  $\text{Ag}^+$  and  $\text{Cr}^{3+}$  were also meaningful (192). However, this pioneering study did not take into account the fact that the biological role of selenium is mainly accomplished via selenoproteins, a particular group of proteins containing in their structure selenocysteine (34).

According to the hard and soft acids and bases (HSAB) theory (37), selenium-containing compounds are soft Lewis's base. Therefore, selenium of selenoproteins can represent the preferential and likely target of soft Lewis's electrophiles, such as heavy metals, e.g., Hg, Pb, As, Cd involved in environmental and human toxicology, and noble metal compounds containing Au, Ag, Pt, etc..., employed as therapeutic agents.

The work of Di Sarra *et al.* (193) shows that auranofin in the presence of Ph-SH or Ph-SeH will react differently. As shown in **Figure 16**, the incoming SH or SeH nucleophile rapidly displaces the tetraacetylthioglucose (TATG) ligand (193). Both processes are reversible. Widely different equilibrium constants characterize them. The formation of the Se adduct displays an equilibrium that favours its formation, meaning that the reaction will be faster between Se and Au than S and Au.

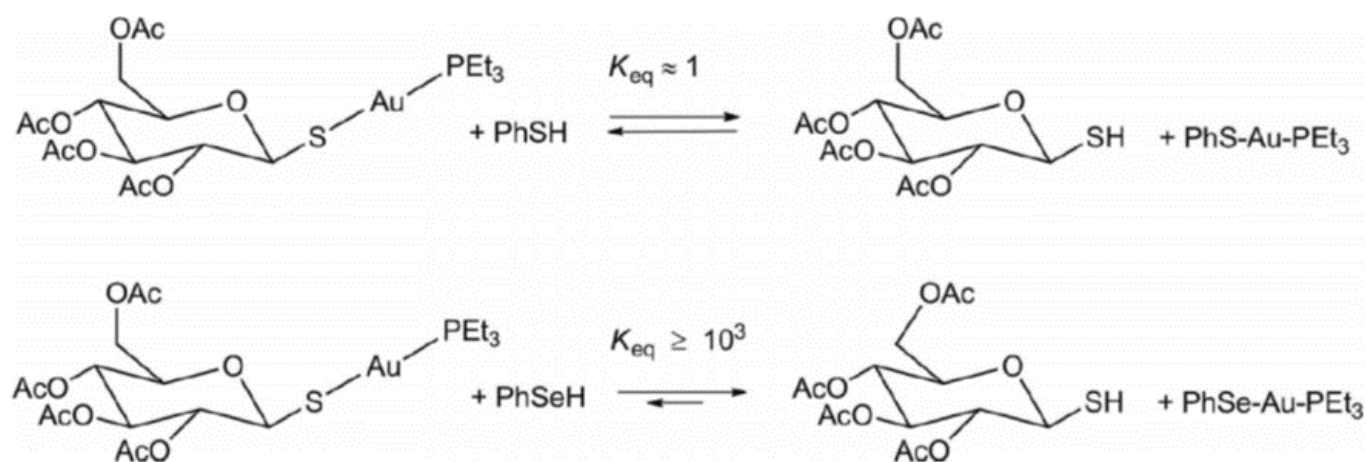


Figure 16 Ligand-exchange equilibria of auranofin in chloroform (239)

The reaction of auranofin with a thiol or selenol can be described like in **Figure 17**. In chloroform, the reaction leads to clean substitution of TATG thiolate moiety by  $\text{PhX}^-$  ( $\text{X} = \text{S}, \text{Se}$ ) to form a  $\text{Et}_3\text{P-Au-XPh}$  adduct. The reaction is reversible and characterize by a higher affinity of Au for Se rather than S by a factor of  $10^3$ . In pore polar solvent, like methanol, the reaction with S and Se is basically similar even if Se reaction is more complex. The initial adducts, in equilibrium with the reactant, eventually yield

$\text{Ph}_2\text{Se}_2$  through the facile oxidation of the selenol and the  $\text{PhSeH}$  oxidized can also react in excess with  $\text{Et}_3\text{PAuSePh}$  to form another adduct  $\text{PhSeAu}$  with a naked gold moiety (193).

### 3.3. Thioredoxin reductase and its mimics as target for metallodrugs

The crucial role of the interactions of metallodrugs with protein targets in determining the compounds' pharmacological action, uptake and biodistribution, and their overall toxicity profile, has been recognized and the number of studies has been increasing exponentially (194–196).

The two major serum proteins, albumin and transferrin, involved in the transport of metals and metallodrug in the bloodstream and metallothioneins, small, cysteine-rich intracellular proteins involved in the storage and detoxification of soft metal ions have been the most investigated proteins as metallodrug targets (189).

Thioredoxin reductase (TrxR) has attracted a lot of interest because of the reactivity of the selenocysteine residue at its *C-terminus* (156).

The inhibition effect of metallodrugs on TrxR is attributed to the binding of  $\text{Au}^{\text{I}}$  (from auranofin) binds to the C-terminal redox-active motif -GCUG- of thioredoxin reductase.

It is evident that SeCys moiety, together with sulfur, oxygen or nitrogen donors' groups, is a potential binding site for metals. However, even if this simplified vision seems to be logical and plausible, the experimental evidence is necessary to validate it. Also, besides selenol residues, selenoproteins contain sulfur, oxygen or nitrogen donor groups which can (and most probably do) represent competitive binding sites to SeCys. Work on inhibition by auranofin of TrxR was extensively pursued (197–199), but few publications present the structural detail of the interaction of gold compounds with TrxR. For that the development of MS techniques has increased insight on a comprehensive vision of this reaction.

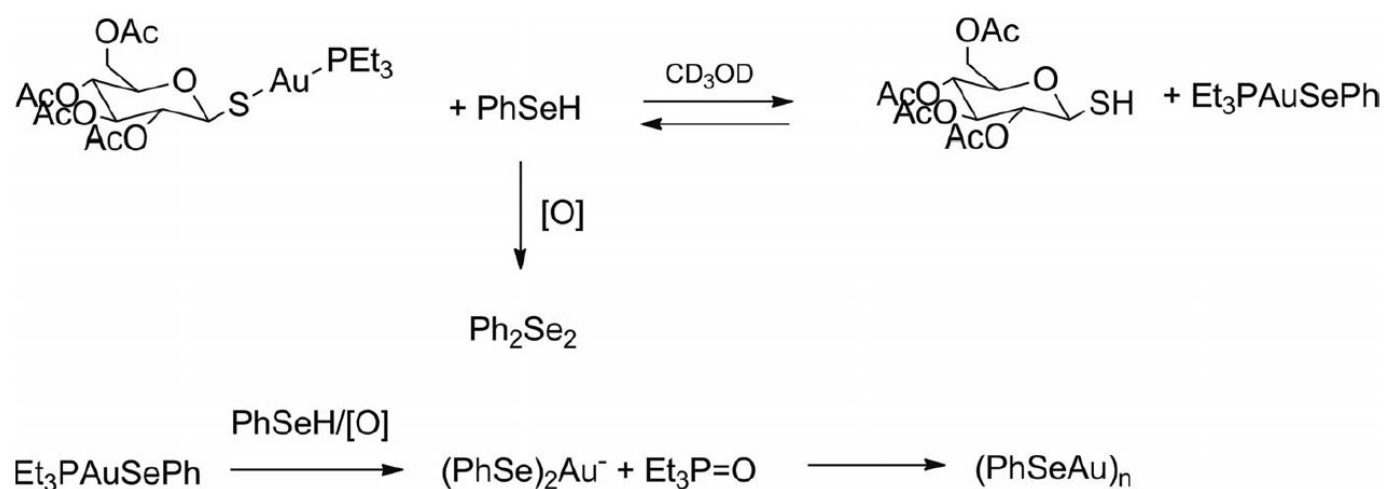


Figure 17 Nucleophilic substitution of a sulfur ligand by selenium ligand in auranofin and further reactions of  $\text{Et}_3\text{P-Au-SePh}$  (193)

#### 3.3.1. Interactions of thioredoxin reductase with gold and other metals compounds

Gold complexes, mainly those with the metal in the oxidation state +1 (soft Lewis acids), are able to irreversibly bind to the active site of mammalian TrxR through coordination to the selenocysteine residue (SeCys-498) at the C-terminal domain (200). In this way they exert antitumor effects through the inhibition of thioredoxin reductase (TrxR) and the respiratory chain complex I (201, 202).

**Table 4** summarizes studies of the interaction between thioredoxin reductase and Au-based drug candidates over the past 20 years (198, 201, 203–206) having provided molecular information by mass spectrometry. However, older studies have not investigated the type of interaction between the protein and Au complexes and the mode of action of thioredoxin reductase inhibition.

Au is not the only metal that has been studied. Other publications report interactions between thioredoxin reductase and potential metallodrugs based on other metals.

Works on compounds with Fe moiety were displaying a significant inhibitory effect on TrxR1 (207, 208), by the formation of a quinone methide after oxidation of the compounds that could react with SeCys of the TrxR. However, no MS data have confirmed the localisation of the compound along TrxR.

Osmium-based compounds were also investigated by Scalcon *et al.* (209, 210). They were also displaying inhibition of TrxR1 after oxidation. That similarity in terms of reactivity is due to the structural resemblance of osmocenyl-tamoxifene and ferrocifene which are both analogues of the Tamoxifen a commercial drug used as a selective oestrogen receptor modulator.

Mura *et al.* were the first to show that ruthenium-based compounds were acting as an inhibitor of TrxR1 in rat (211). This observation was later confirmed by Scalcon *et al.* where their analogue of tamoxifen with ruthenium was also displaying this inhibitory effect of TrxR1 (209).

Another metal-drug compound known for its toxicity was explored, arsenic. Arsenic-based compound like arsenic trioxide which is used in leukaemia, were investigated as a potential target for TrxR1 inhibition. The first studies from Talbot *et al.* observed that arsenic trioxide was decreasing selenoproteins synthesis of the studied cells line (198). Other studies from Lu *et al.* determine that arsenic trioxide was reacting with the SeCys active site of TrxR by mass spectrometry, they have considered that the blocking of SeCys results in the inhibition of TrxR (212).

The action of platinum-based drugs was also explored by Arnér *et al.* (213) and Prast-Nielsen *et al.* (214). Arnér *et al.* showed that their platinum compound binds the TrxR and then inhibits significantly its activity (213). Prast-Nielsen *et al.* showed a similar result concerning the inhibition of TrxR1 by Pt, however, the inhibition was less potent than the one induced by other metals such as Au and Pd salts (214).

A comparative investigation on the inhibition of the human TrxR and a hTrxR mutant (where Cys substituted SeCys) induced by selected Pt(II) and Au(I) compounds are also described. These studies showed that Pt(II) and Au(I) compounds are two to four orders of magnitude less effective in the inhibition of the mutant compared with the wild type hTrxR (204, 215).

Finally, gadolinium was also described as potential TrxR inhibitor. Hashemy *et al.* have showed that motexafin gadolinium is a non-competitive inhibitor of TrxR, not suppressing the protein activity, but increasing the production of the enzyme to counteract the inhibition (216).

*Table 4 Summary of studies on the interactions between full length thioredoxin reductase and (potential) gold-based metallodrugs*



| Gold based metallodrug   | Type of binding              | Main findings  | Ref   |
|--|------------------------------|--|-------|
| Auranofin,<br>Chloro(triethylphosphine)gold,<br>[N-(N',N'-dimethylaminoethyl)-1,8-<br>naphthalimide-4-<br>sulfide](triethylphosphine)gold(I) | Cys-Au                       | Mechanistic experiments indicates that inhibition of thioredoxin reductase is based on the covalent binding of gold triethylphosphine fragment Au (I)-thiourea complexes form strong bonds which inhibit TrxR activity with one of the highest reported capacities and show suppression of cellular reductase activity.  | (217) |
| Au(I)-thiourea   | SeCys-Au,<br>SeCys-Cys       | Different Au (I) and Au(III) compounds are found to be potent TrxR inhibitor. Multiple metallation sites were observed on TrxR.  | (218) |
| Auranofin, Au(III) and Au(I) complexes   | His-Au<br>SeCys-Au           | Auranofin reacts with the active selenol functions of reduced TrxR. They were able to quantify the total enzyme concentration and the active concentration using auranofin inhibition of TrxR1. Mass spectrometry is a useful tool to link molecular reactivity and target preference of metal-based drug candidate with their biological effect. It is also important to consider the antiproliferative activity of the ligands released when considering the cytotoxic effects of metal complexes. | (219) |
| Auranofin  | SeCys-Au                     |  | (220) |
| Au(III) complex (drug candidate)   | His-Au<br>Cys-Au<br>SeCys-Au |  | (221) |

### 3.3.2. Thioredoxin reductase proxies and their interaction with gold and platinum compounds

Ott *et al.* (217) used a cysteine-containing peptide as a model to investigate the binding of cysteine with a gold compound in TrxR. This synthetic peptide is constituted of 10 amino-acids and contains one cysteine. The GCVG moiety was created to look like the *C-terminus* of TrxR where Val replaced SeCys. After reduction, they were able to detect an AuPEt<sub>3</sub> fragment covalently bind to the Cys. This confirmed what they observed on TrxR, that one of the binding sites of gold compounds could be either Cys or SeCys peptide of *C-terminus* of TrxR.

Pratesi *et al.* (222) used a short peptide model of the C-terminal motif of human TrxR containing SeCys to study its interactions with Auranofin and other di-nuclear cytotoxic complexes of Au (III) using ESI mass spectrometry. In this study, the tetra-peptide Gly- [Cys-SeCys] -Gly (with an S-Se bridge) (**Figure 18**) derived from the C-terminal part of the protein did not show any reactivity towards the Au complexes in the absence of reducing agents. In contrast, after pre-reduction with dithiothreitol (DTT), binding

between the peptide and auranofin gold was detected with loss of its ligand tetraacetatethiogluucose and retention of the  $PEt_3$  ligand. They also demonstrated the presence of a second coordination site at the Cys residue.

Another longer peptide model of 12 amino acids corresponding to the C-terminal fragment of human hTrxR(488-499), corresponding to the sequence Ac-SGGDILQSGCUG-NH<sub>2</sub> (**Figure 18**) has been described by the same authors (223). They studied its reactivity towards a series of Au N-heterocyclic carbenes (NHC) and auranofin by ESI-MS.

**Table 5** summarizes studies of the interaction between proxies of thioredoxin reductase and Au-based drug candidates over the past 20 years (217, 222, 223) having provided molecular information by mass spectrometry.

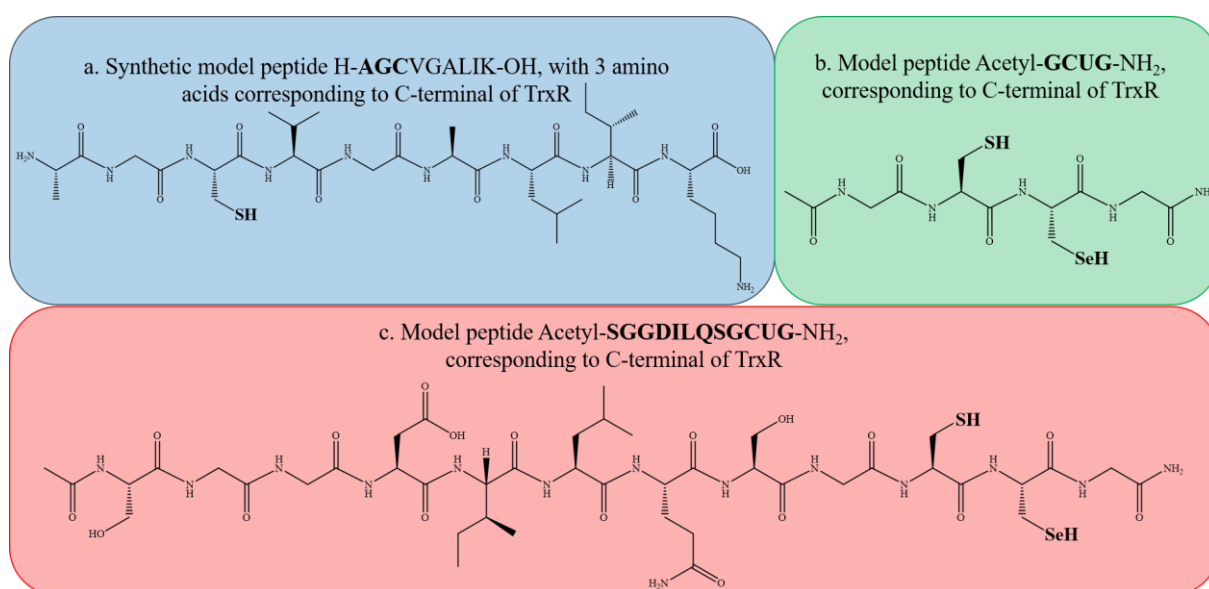


Figure 18 Model peptide used as proxies of TrxR (a. Ott et al. (217), b. Pratesi et al. (222), c. Pratesi et al. (223))

Table 5 Summary of studies on the interactions between thioredoxin reductase proxies and (potential) gold-based metallodrugs

| Gold based metallodrug   | Peptide sequence                    | Type of binding    | Main findings  | Ref   |
|--|-------------------------------------|--------------------|--|-------|
| Auranofin, Chloro(triethylphosphine)gold, [N-(N',N'-dimethylaminoethyl)-1,8-naphthalimide-4-sulfide](triethylphosphine)gold(I) | H-AGCVGALIK-OH                      | Au-Cys             | Au(I) binding with Cys moiety of the model peptide was reported.   | (217) |
| Auranofin, AuOXO <sub>6</sub> complex, Sodium tetrachloroaurate (NaAuCl <sub>4</sub> )   | Acetyl-GCUG-NH <sub>2</sub>         | Au-SeCys<br>Au-Cys | Au(I) binding between SeCys and Cys moiety of the C-terminal peptide of Thioredoxine reductase was reported.   | (222) |
| Gold N-heterocyclic carbene, Auranofin   | Acetyl-SGGDILQSGCUG-NH <sub>2</sub> | Au-SeCys<br>Au-Cys | Au(I) binding between SeCys and Cys moiety with the 12peptide model was reported with similar result than the one with reported with the tetrapeptide. | (223) |

### 3.4. Interaction of metallodrug with other selenoproteins

Like thioredoxin reductase, glutathione peroxidase is also a tetrameric selenoenzyme containing a selenocysteine in each subunit. Differently from TrxR which is largely described as a target for metallodrugs

action, for GPx only a few old articles report about its interaction with gold drugs but the structural interaction details are not reported and the Se-Au binding is only speculated (224–226).

### 3.5. Interactions of others selenocompounds with metallo drugs

Meier *et al.* (221) studied the interaction of Au (III) complexes with a mixture of amino acids (L-histidine, L-methionine, L-cysteine, L-glutamic acid, methyl seleno-L-cysteine (SeMe-Cys) and seleno-L-cysteine generated in situ). Gold compounds were displaying different reactivities with amino acids. Depending on the compounds the binding preference varies but SeCys, Cys and SeMe-Cys are the main targeted amino acids for gold compounds binding. The binding mechanism of the Au(III) compounds with the amino acids is preceded by a reduction or a loss of ligand of the Au(III) to form Au(I), the Au(I) being the reactive species that bind to the amino acids.

Model investigations were used to understand binding consisting of ferrocenyl quinone methide with glutathione reductase, a competitive reaction of equimolar amounts of reduced cystamine and selenocystamine with ferrocenyl quinone methides were conducted, cystamine and selenocystamine were used as a model to mimic Cys and SeCys. This experiment bring the evidence that the selective alkylation of selenol appears at neutral pH (207).

The competitive reactivity of gold species with disulfide and diselenide bridges and its consequences are poorly understood, and the studies have been scarce and limited to simple amino acids, selenocystein and selenocystamine (221, 227). The Se-Se bond and S-S bonds were found (by  $^{31}\text{P}$  NMR) to be broken with bis(trialkylphosphine) gold(I) bromide, resulting in the formation of  $\text{R}_3\text{PAu}^+$ ,  $\text{R}'\text{SeH}$ ,  $\text{R}'\text{Se-Au-PR}_3$ ,  $\text{R}_3\text{PO}$  and  $(\text{AuSeR}')_n$  (227). Selenocystamine was found to react with  $(\text{Et}_3\text{P})_2\text{AuBr}$  about 100 times faster than its corresponding disulfide. However, cystamine reacts twice as fast with  $(\text{Me}_3\text{P})_2\text{AuBr}$  compared to its corresponding diselenide. Meier *et al.* reacted  $(\text{SeCys})_2$  with gold(III) compounds by mass spectrometry but  $(\text{SeCys})_2$  were reduced before interaction with Au (221).





## 4.1. Separation of biological selenium species

Different chromatographic techniques are used to separate the selenoproteins present in complex mediums prior to their qualitative and quantitative detection. Selecting a suitable chromatographic technique depends on physical and chemical properties, such as polarity and charge of analytes of interest. The techniques used to separate selenoproteins from serum samples are liquid chromatography (LC) and gel electrophoresis (GE). The choice of a proper mobile phase, its pH and ionic strength, elution gradient, and time of analysis are critical to obtain a good separation and preserve the chemical forms of the protein of interest in case they were unstable, or prone to precipitate (228).

Affinity chromatography has been the main technique to isolate selenoproteins from serum. The main HPLC separation mechanisms used in the separation of selenocompounds and their metal adducts have been size-exclusion (SEC) and reversed-phase HPLC. Gel electrophoresis (SDS-PAGE) has been mostly used to confirm the selenoprotein expression and its purity.

### 4.1.1. Affinity chromatography

Affinity chromatography takes advantage of specific binding interactions between the analyte of interest (typically dissolved in the mobile phase), and a binding partner or ligand (immobilized on the stationary phase). In a typical affinity chromatography experiment, the ligand is attached to a solid, insoluble matrix usually, a polymer such as agarose or polyacrylamide, which is chemically modified to introduce reactive functional groups with which the ligand can react, forming stable covalent bonds (229). The stationary phase is first loaded into a column to which the mobile phase is introduced. Molecules that bind to the ligand will remain associated with the stationary phase. A buffer is then applied to remove non-target biomolecules by disrupting their weaker interactions with the stationary phase, while the biomolecules of interest will remain bound. Target biomolecules may then be removed by applying a so-called elution buffer, which disrupts interactions between the bound target biomolecules and the ligand. The target molecule is thus recovered in the eluting solution (230).

Affinity chromatography does not require the molecular weight, charge, hydrophobicity, or other physical properties of the analyte of interest to be known. However, knowledge of its binding properties is helpful in the design of a separation protocol (230).

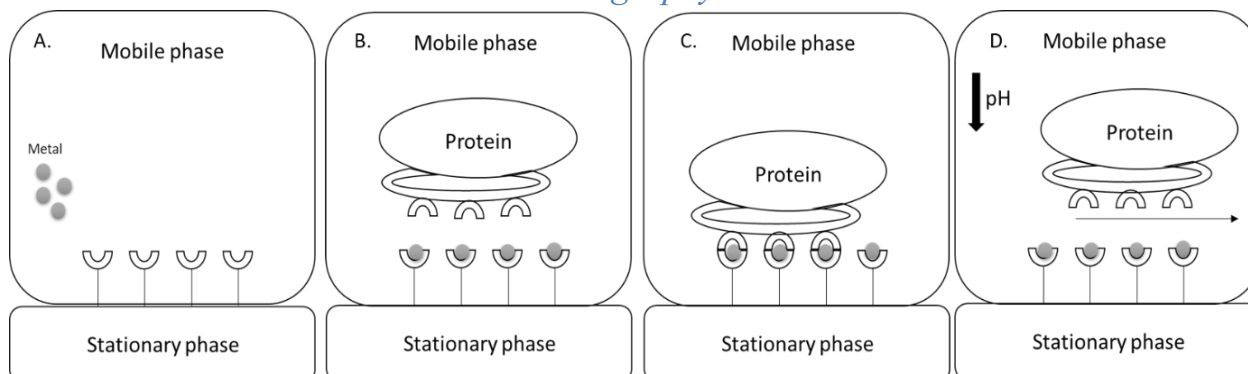
*Immobilized Metal Affinity Chromatography (IMAC)* is affinity chromatography whose mechanism is based on the chelation of immobilized metals. It aims to study complex samples such as biological samples. *Chelation* is a process in which a complex is formed between a metal cation and a ligand. In immobilized metal chelation, we initially have a metal ion immobilized in a column, into which we will flow the mixture under study. Bonds between the metal and the ligands will form at a pH between 7-8, obtained with a buffer solution introduced into the column. IMAC is used to separate proteins that naturally have histidine groups exposed on their surface (231) (**Figure 19**).

**Heparin**, also known as **unfractionated heparin (UFH)**, is a naturally occurring glycosaminoglycan. Specific binding of SELENOP and Heparin was described by Arteel *et al.* (231). Heparin columns are prepacked with Heparin Sepharose for high-resolution purification of proteins with affinity for heparin, such as DNA-binding proteins, coagulation factors, lipoproteins, and protein synthesis factors. Immobilized heparin has two main modes of interaction with proteins. First, it can operate as an affinity ligand for a wide range of biomolecules, including coagulation factors and other plasma proteins, lipoproteins, protein synthesis factors, enzymes that act on nucleic acids, and steroid receptors. Second,

Heparin also functions as a high-capacity cation exchanger due to its anionic sulphate groups. Gradient elution with salt is most commonly used in both cases.

*Figure 19 Immobilized metal affinity chromatography principle A. Metal ion are introduced to bind to the stationary phase, B. The protein of interest is introduced into the column, C. Protein histidine and metal chelate will interact forming a bond and retaining the protein on the column stationary phase, D. Using a pH gradient, the protein will be removed of the column*

#### 4.1.2. Size exclusion chromatography



The separation principle is based on the difference in the size and shape of molecules present in the sample. Smaller molecules are retained longer in the pores of the stationary phase, which is usually built of densely crosslinked polymers. The species of the largest size are washed out the fastest from the column because they do not penetrate into the pores of the stationary phase; **Figure 20** shows an example of separation of compounds by SEC columns showing the elution of high molecular weight compounds at first followed by intermediate and finally low molecular weight compounds. The degree of crosslinking and pore size of the bed are selected according to the mass range to protect the column from destruction or obstruction. There are two types of packing used in SEC, polymeric gels or modified silica particles.

In SEC columns, the number of theoretical plates is relatively small, and the separation efficiency is measured as the number of theoretical plates, which can be improved by using a stationary phase with a smaller particle size and adapting the chromatographic conditions.

Moreover, the success of SEC depends primarily on choosing conditions that give sufficient selectivity and counteract peak broadening effects during the separation; so, the selectivity of an SEC medium depends on its pore size distribution (232).

#### 4.1.3. Reversed phase chromatography

Reversed-phase chromatography RP-LC is the most commonly used type of liquid chromatography. It is based on the distribution of the solute between the two phases according to the binding properties of the medium, the hydrophobicity of the solute and the composition of the mobile phase: this technique uses gradient elution, so initially, experimental conditions are optimized to favour adsorption of the solute from the mobile phase to the stationary phase then, the mobile phase composition is modified to favour desorption of the solute from the stationary phase back into the mobile phase for elution (233). However, it is often impossible to achieve their complete separation in the case of strongly hydrophilic and high-polar compounds - analytes do not interact with the column bed and are not eluted selectively. This method is commonly used in the selenoprotein speciation for the separation of peptide and seleno-

species, but it was not described as the primary separation method. After tryptic digestion, it is usually chosen to separate selenopeptides prior to their analysis by ICP-MS or ESI-MS analysis.

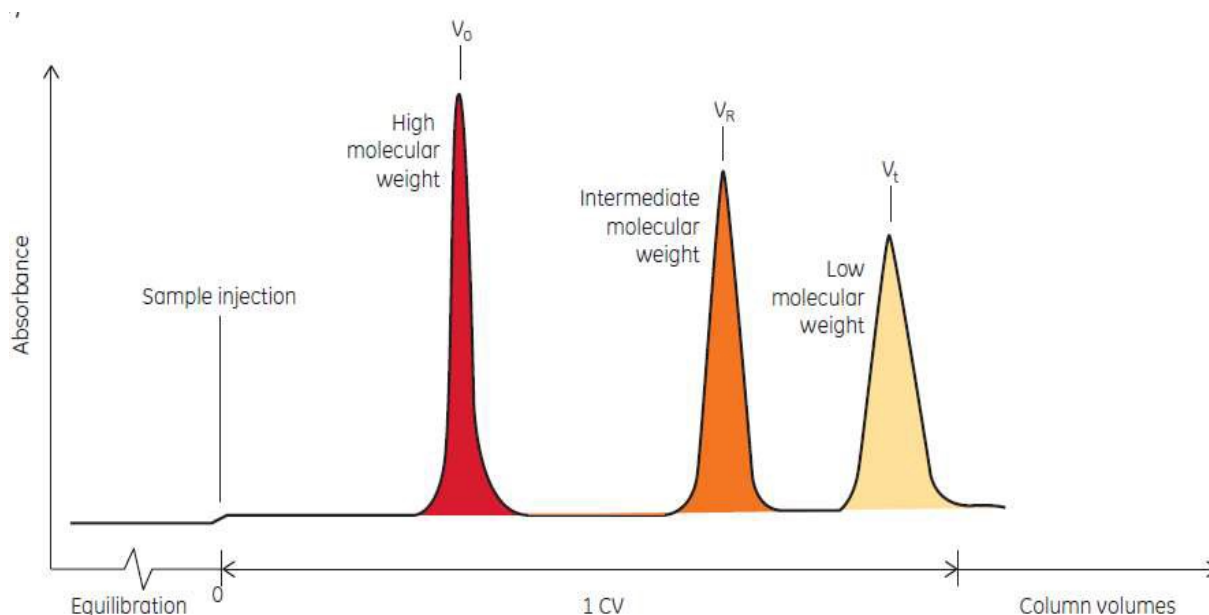


Figure 20 Separation mechanism by SEC columns (234)

## 4.2. Detection of selenium by inductively coupled plasma mass spectrometry

### 4.2.1. Principle of inductively coupled plasma mass spectrometry

ICP-MS is a reference technique used for trace elemental and isotopic analysis (235). ICP MS gives information about the total metal content of a sample but not about the oxidation state of the metal and its interaction with molecules present in the sample. Argon plasma used in ICP MS has a very high ionisation power which makes possible the analysis of a vast number of elements; 90% of the elements from the periodic table are ionised as monocharged positive ions by this technique. In a standard configuration, liquid samples are delivered to the nebuliser by a peristaltic pump, where they are converted into aerosols in the presence of a carrier argon gas; then, fine droplets of aerosols are separated from the large ones in a spray chamber. Concerning solid samples, laser ablation coupled to ICP MS is used to determine elements directly with minimal sample preparation.

The principle of ICP MS is consist of sample ionisation by plasma flame (**Figure 21**):

- The droplets are transported into the horizontal plasma torch consisting of three concentric tubes: outer tube, middle tube and sample injector.
- The outer tube and the middle tube are responsible for plasma cooling and adjusting its position, while the sample injector is responsible for the transport of the aerosol into the plasma.
- Argon flow is supplied to the internal tube at the stage of nebulisation of the sample. It acts as a carrier gas and transports the sample inside the injector.
- Argon flowing through the central tube - the auxiliary gas - separates the sample stream leaving the injector from the plasma flame, and prevents extinction of the plasma.

- Plasma is formed by RF oscillation of the current applied to the load coil creates an electromagnetic field at the top of the torch and the high-voltage spark applied to argon gas causes a loss of electrons for some argon atoms that are caught and accelerated in the magnetic field.
- Collisions of argon atoms with electrons lead to the formation of high-temperature plasma discharge at around 10000 K. The aerosols entering the plasma pass in different heating zones cause solvent vaporisation and the creation of tiny particles that are changed into charged atoms then into ions due to the collision with energetic argon electrons.
- Once monocharged positive ions are formed in the plasma, they are moved to the mass spectrometer via the interface region consisting of two metallic cones called sampler and skimmer, helping transition between the ICP ionisation chamber atmospheric pressure and the analysers under high vacuum.
- Finally, the ion passes through the cones and the optics to reach the analyser.

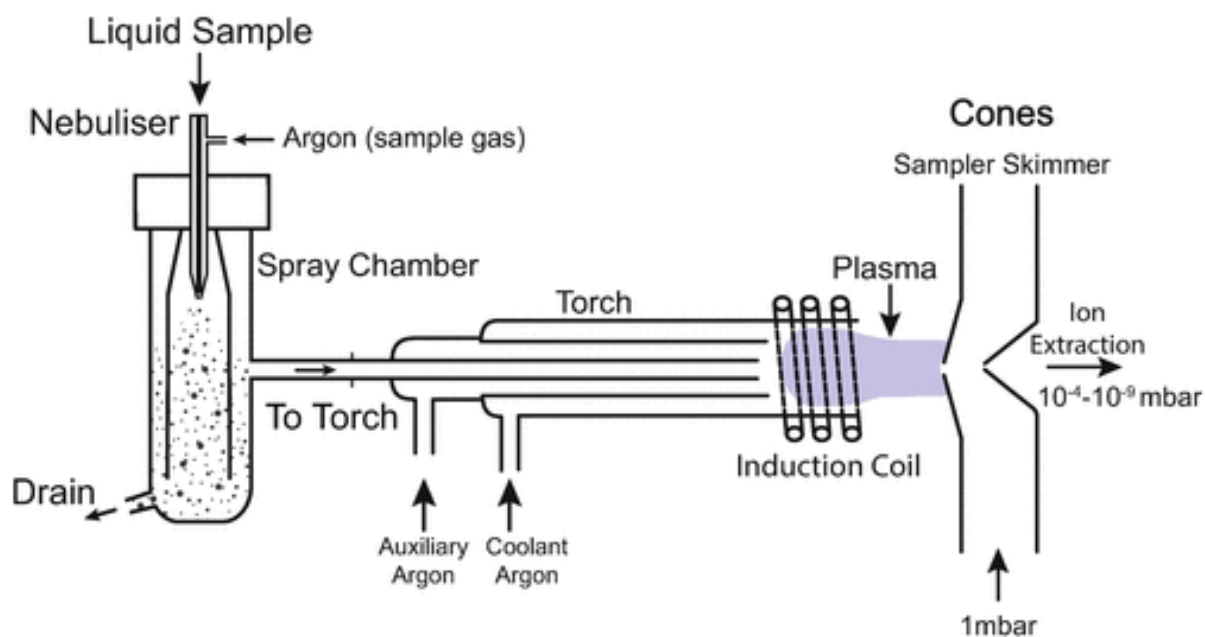


Figure 21 Principle of ICP-MS (185)

The most common analyser is quadrupole (Q) mass analyser is widely used as detectors in ICP and molecular ESI mass spectrometers (85% of all ICP mass spectrometers used for trace element analysis) because it is cheap, light-weight, use low ion acceleration and has absolute detection limits in sub-picogram range (236). Quadrupole mass analyser consists of four cylindrical or hyperbolic rods made of metal (stainless steel or molybdenum) that have the same length and diameter: these rods are set in parallel to each other and arranged in the way that the direct current (DC) field and alternating current (AC) of radiofrequency are placed on opposite pairs of rods. When a particular potential is applied to the rods, the analyte ion of interest oscillates down the middle of the four rods to the end, where it will emerge and be converted to an electrical pulse by the detector. The other ions of different mass to charge will be unstable, pass through the spaces between the rods, and be ejected from the quadrupole (237).

Even if quadrupole is currently the most used mass analyser some are also used with ICP, it is the case of the magnetic sector, time-of-flight (**Table 6**).

The ICP-MS technique is characterised by high selectivity. However, it suffers from some interference. Two main groups of interference can be distinguished:

- Matrix interferences - suppression or increase of the analyte signal, which leads to an incorrect determination result. They are related to differences in the physical properties of the matrix components.
- Spectral interferences - they can mask the presence of a peak or, on the contrary, increase its height. They may originate from the ions of other elements (isobaric interferences) that are part of the matrix, formed due to the combination of atoms (polyatomic interferences) or multiple ionisations.

Table 6 Advantages and limitation of the various mass analysers ([https://www.shimadzu.com/an/service-support/technical-support/analysis-basics/fundamental/mass\\_analyzers.html](https://www.shimadzu.com/an/service-support/technical-support/analysis-basics/fundamental/mass_analyzers.html))

| Mass Analyzer          | Description                     | Advantages  | Limitations  |
|------------------------|---------------------------------|---|--|
| <i>Magnetic Sector</i> | Scanning continuous             | High resolution<br>High dynamic range<br>High reproducibility<br>High sensitivity   | Expensive and bulky<br>Slow scan speed<br>High vacuum required<br>Difficult to couple with pulsed ionization techniques and LC |
| <i>Quadrupole</i>      | Scanning Mass Filter Continuous | Compact and simple<br>Relatively cheap<br>Good selectivity<br>Moderate vacuum required<br>Well suited for coupling to LC<br>High sensitivity and ion transmission | Limited mass range<br>Low resolution<br>Little qualitative information   |
| <i>Time-of-flight</i>  | Non-scanning Pulsed             | High resolution<br>Excellent mass range<br>Fast scan speed  | Required pulsed introduction to Ms<br>Requires fast data acquisition   |

#### 4.2.2. Spectral interferences in selenium inductively coupled plasma mass spectrometry detection and their removal

ICP-MS allows a specific detection of the individual selenium isotopes. Selenoprotein P can be therefore quantified via its selenium content once it has been separated from the other selenium-containing species. Even if the sensitivity of ICP-MS for selenium is inferior to that for most metals because of its higher first ionization potential (9.75 eV), higher proneness to matrix suppression, and the split of ions available among six isotopes, it is fully compatible with the requirements for SELENOP detection in HPLC.

The main problem is the choice of the least interfered isotope as all the Se isotopes can be interfered by polyatomic ions: Ar<sub>2</sub> dimers or Ar combinations with Br, S, or Cl. A possible interference is <sup>156</sup>Gd in serum of patients having received Gd contrast agents were also evoked (238). The interfering elements can be separated by HPLC (239) and are usually not a problem which favours the choice of <sup>77</sup>Se (7.63% abundance) or <sup>82</sup>Se (8.73%). However, spectral interferences are not removed by HPLC techniques, so a different technique is used to remove them, all Se spectral interferences with each Se isotope are summarized in **Table 7**.

Table 7 Spectral interferences and detection limit of Se

| Element | Number of isotopes | Polyatomic interferences   |
|---------|--------------------|--|
| Se      | <sup>74</sup> Se   | <sup>38</sup> Ar <sup>36</sup> Ar <sup>+</sup> , <sup>37</sup> Cl <sub>2</sub> <sup>+</sup> , <sup>40</sup> Ar <sup>34</sup> S <sup>+</sup>  |
|         | <sup>76</sup> Se   | <sup>40</sup> Ar <sup>36</sup> Ar <sup>+</sup> , <sup>40</sup> Ar <sup>36</sup> S <sup>+</sup> , <sup>31</sup> P <sub>2</sub> <sup>14</sup> N <sup>+</sup>   |
|         | <sup>77</sup> Se   | <sup>40</sup> Ar <sup>36</sup> ArH <sup>+</sup> , <sup>38</sup> Ar <sub>2</sub> H <sup>+</sup> , <sup>40</sup> Ar <sup>37</sup> Cl <sup>+</sup>  |
|         | <sup>78</sup> Se   | <sup>40</sup> Ar <sup>38</sup> Ar <sup>+</sup> , <sup>31</sup> P <sub>2</sub> <sup>16</sup> O <sup>+</sup>   |
|         | <sup>80</sup> Se   | <sup>40</sup> Ar <sub>2</sub> <sup>+</sup> , <sup>79</sup> BrH <sup>+</sup>  |
|         | <sup>82</sup> Se   | <sup>40</sup> Ar <sub>2</sub> H <sub>2</sub> <sup>+</sup> , <sup>12</sup> C <sup>35</sup> Cl <sub>2</sub> <sup>+</sup> , <sup>34</sup> S <sup>16</sup> O <sub>3</sub> <sup>+</sup> , <sup>81</sup> Br <sup>+</sup> |

The resolution power necessary to resolve these interferences exceeds that of sector-files and time-of-flight instruments. The interferences are dealt with by collisions generating either naked Se isotope (qQ) or shifting its m/z to higher mass by the formation of an oxide in the collision cell (QqQ)

#### Collision cell instruments (qQ)

The analytical quadrupole is preceded by another multipole acting as a collision/reaction cell. The cells are pressurized with a gas or a mixture of gases to reduce or eliminate the interfering polyatomic species by collision dissociation and/or gas-phase chemical reaction (186). The list of gases that can be used in collision/reaction cell ICP-MS is given below with the most often used reagent gases written in bold:

- Collision gasses: **He**, Ar, Ne, Xe
- Charge exchange gases: **H<sub>2</sub>**, **NH<sub>3</sub>**, Xe, CH<sub>4</sub>, N<sub>2</sub>
- Oxidation reagent gases: **O<sub>2</sub>**, **N<sub>2</sub>O**, NO, CO<sub>2</sub>
- Reduction reagent gases: H<sub>2</sub>, CO
- Other reaction (adduction) gases: **CH<sub>4</sub>**, C<sub>2</sub>H<sub>6</sub>, C<sub>2</sub>H<sub>4</sub>, CH<sub>3</sub>F, SF<sub>6</sub>, CH<sub>3</sub>OH

In case of selenium the most commonly used gases are hydrogen or mixture of hydrogen and helium, (240, 241). Significant (2-3 times) detection limit improvement is observed when monitoring <sup>80</sup>Se, for both total selenium determination and speciation analysis, comparing to <sup>82</sup>Se monitoring in standard mode. The detection limits of Se reach with this method is around 10-100 ppt.

#### Tandem MS/MS instruments

An additional analytical quadrupole is introduced in front of the collision/reaction cell. It operates as a mass filter, allowing ions with one m/z-ratio to enter the cell. This leads to better control over the reactions in the qQ cell and more insight into the reaction mechanisms and the origin of the reaction product ions observed (242).

### 4.2.3. Quantification of selenium

Two main techniques are used to quantify protein using ICP, the standard curve method and isotopic dilution (243, 244).

#### Standard curve methods

In ICP-MS, any compound of the determined element can be used as a standard because the response in ICP-MS is independent of its molecular environment (245). Therefore, protein selenium can be



quantified using selenite as standard by an external or standard addition calibration curve. The applications have been reviewed in the literatures (246). Note that an element standard can be used for protein quantification only when the analyte has been identified or the structure and stoichiometry of the analyte have been known. In this case, the matrix interference from the proteins can be negligible, and the element standard can be used for protein quantification with an accuracy of 10% or better, as long as the protein concentration is sufficiently low.

#### *Isotopic dilution*

The most effective method to correct for both matrix effects and instrument drift in ICP-MS is isotope dilution. A known amount of an isotopically-enriched isotope of the analyte is added to the sample, and measured. The change in the isotope ratio is used to calculate the original composition of the sample. Thus, the enriched isotope acts as both a calibration standard and an internal standard.

Different isotopes may exhibit differential transmission in the ICP (partly due to the space-charge effect). Therefore the measured isotope ratio must be corrected for mass bias (247, 248). This technique has been successfully applied to the analysis of analytes in urine, blood and plasma (249, 250). A caveat here is that isotope dilution requires the analyte to have at least two isotopes that are free of spectroscopic interference.

Therefore, the method does not apply to monoisotopic elements such as, e.g. gold. Although these methods are highly accurate and robust, they are also both laborious and expensive. For these reasons, isotope dilution methods are rarely used in routine measurements.

### **4.3. Detection of selenopeptides, and their adducts with metals by soft-ionization mass spectrometry**

In contrast to ICP MS in which the analyte molecule is atomized and the atoms (isotopes) are ionized, soft ionization techniques preserve the integrity of the molecule, producing ions by the addition or loss of one or several protons. The most common soft ionisation modes used in mass spectrometry of selenocompounds are electrospray ionisation (ESI), Matrix-Assisted Laser Desorption Ionisation (MALDI).

#### *4.3.1. Electrospray ionization*

Electrospray MS is one of the most popular ionization methods used to study peptides, proteins and their covalent and non-covalent complexes. Electrospray ionization can preserve the integrity of species without fragmenting them; it can be used for both low- and high-mass compounds. ESI MS can give information about relatively stable metalo-species that metal forms with amino acids, peptides, proteins and carbohydrates: there is a possibility to work in positive or negative ion mode since ESI provides protonated apparent molecular ions  $[M + zH]^{z+}$  with a charge of  $\geq 1$  (positive ion mode) and deprotonated ones  $[M-zH]^{z-}$  (negative ion mode) that enables to find the ideal conditions to ionize different types of charged species (251). The electrospray ionization consists of several stages: ion formation, nebulization and desolvation, which transfer ions from the liquid to the gas phase and their introduction into the MS vacuum. These stages are discussed below, illustrated in **Figure 22**, showing processes taking place from the ion formation until the mass analyser:



- The aqueous analytes are passing through the electrospray needle, which causes the generation of the spray of small, highly charged droplets as a result of contact of the sample stream with a high-value electric field.
- From the droplets, the neutral solvent molecules are evaporated, leading to a decrease in the droplet size and, in the end, to the formation of molecular ions. When the charge exceeds the Rayleigh limit, the droplet explosively dissociates, leaving a stream of charged ions.
- The molecular ions are often multiply charged, and in the next step, they are transported from the atmospheric pressure to the high vacuum area where they explode, generating the analyte ions.
- In the mass analyser, the ions are separated according to their mass-to-charge ratio.

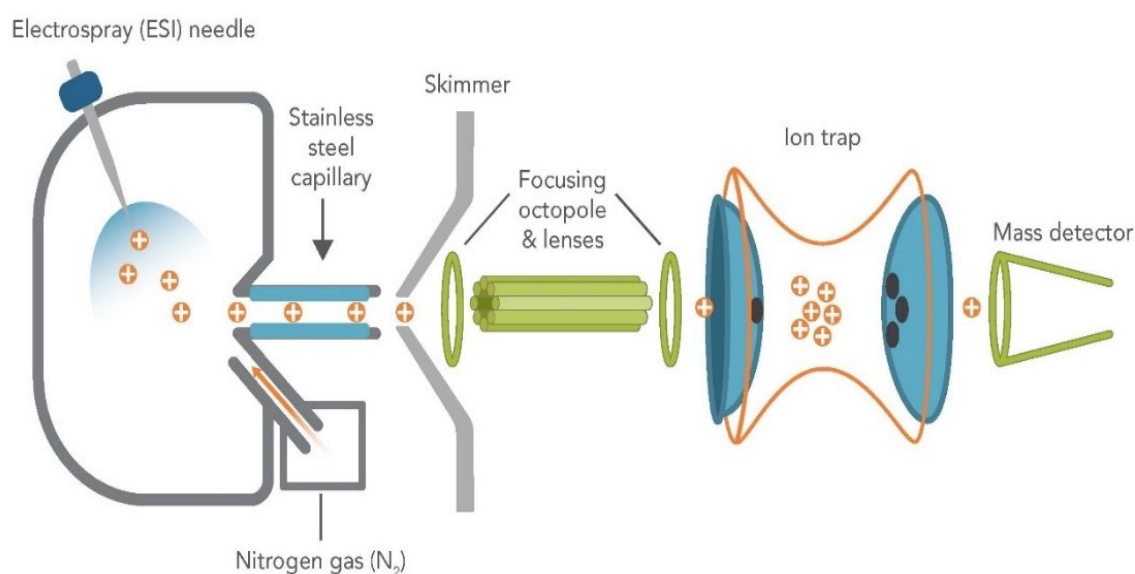


Figure 22 Principle of electrospray ionization (from eu.idtdna.com)

The ESI-MS mass spectrometry can be used independently or in combination with various separation techniques, such as LC chromatography: volatile solvents should be used to avoid source contamination. The presence of salts should be limited as much as possible to avoid crystallisation inside the system. If the salts are non-volatile, they may deposit on lens elements, leading to ionisation suppression and coating of the ion optics, leading to a significant sensitivity reduction.

The parameters to be optimised (236) in order to obtain optimal detection conditions such as high sensitivity and signal stability are:

- position of the probe: to maximise the introduction of analytes into the analyser
- drying gas flow and auxiliary: to optimise desolvation (vaporisation temperature can be used to facilitate desolvation) and to focus the spray better
- capillary tension applied to ionise the analytes: to maximise the generation of ions through the spray

- temperature of transfer through capillary: to complete desolvation and help transport of ions to the analyser
- voltage applied to the different poles of ions optics: to focus the ions towards the analyser

In addition to quadrupole, electrospray ionization is used in combination with different types of high-resolution mass analysers, such as time-of-flight (TOF), Orbitrap, or ion cyclotron resonance of which the features are summarized in **Figure 23** (252).

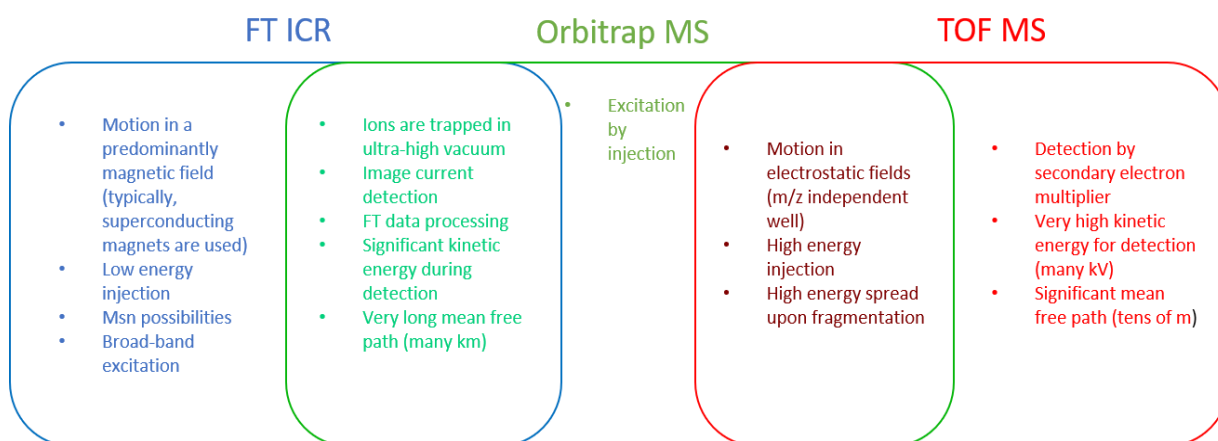


Figure 23 Comparison of physical and analytical features for high-resolution, full mass range techniques in mass spectrometry

The mass analyser used throughout this thesis has mostly been Orbitrap. The principle of operation of Orbitrap (**Figure 24**) is based on the confinement of ions in an electrostatic potential well created between carefully shaped coaxial central and outer electrodes. Ions are pulsed into the device to rotate around the central electrode and oscillate along with it. The outer electrode is split into two halves to allow differential image-current detection. Ion excitation is not necessary to induce large amplitude and coherent oscillations. Instead, ions are injected with the requisite coherent motion -by using a C trap- to accumulate, store, and thermalize the ions by a low nitrogen pressure before injection (236). Detection immediately occurs after all ions have been injected into the trap and after the voltage on the central electrode has stabilized (253). The image current from the trapped ions is detected and converted to a mass spectrum using the Fourier transform of the frequency signal.

#### 4.3.2. Matrix assisted laser desorption/ionisation – Time-of flight mass spectrometry

**Matrix-assisted laser desorption/ionisation (MALDI)** is an ionisation technique that uses a laser energy absorbing matrix to create ions from large molecules with minimal fragmentation (254). It has been applied to analyse biomolecules (biopolymers such as DNA, proteins, peptides and carbohydrates) and various organic molecules (such as polymers, dendrimers and other macromolecules), which tend to be fragile and fragment when ionised by more conventional ionisation methods.

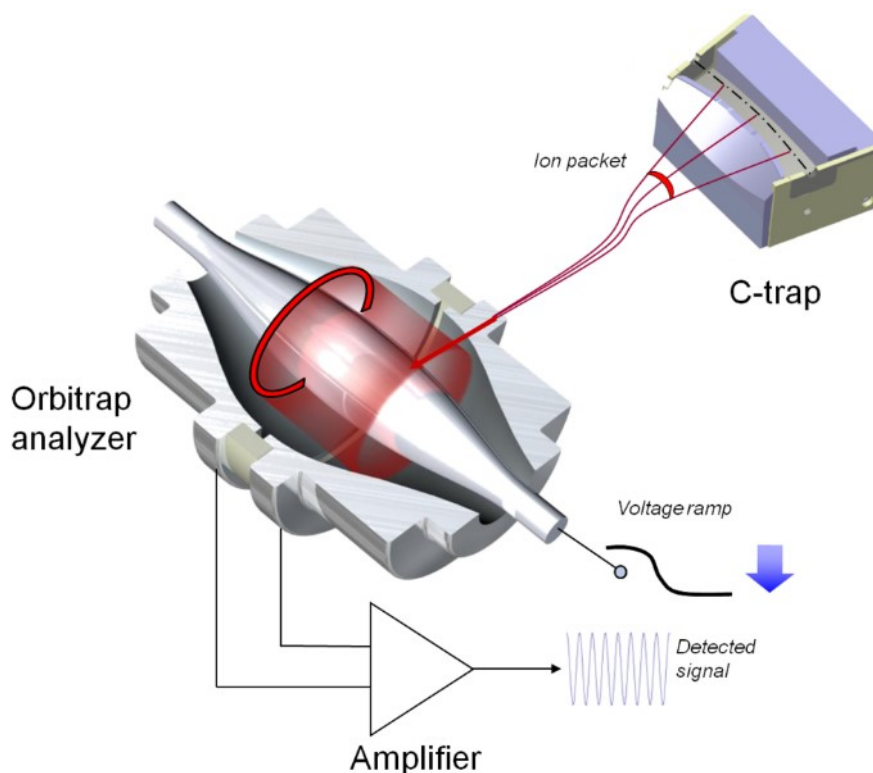


Figure 24 Principle of Orbitrap (from Thermo Fisher Scientific)

MALDI methodology is a three-step process. First, the sample is mixed with a suitable matrix material and applied to a metal plate. Second, a pulsed laser irradiates the sample, triggering ablation and desorption of the sample and matrix material. Finally, the analyte molecules are ionised by being protonated or deprotonated in the hot plume of ablated gases, and then they can be accelerated into whichever mass spectrometer is used to analyse them (**Figure 25**)(255).

MALDI is usually used in combination with a **Time-of-flight (TOF)** mass analyser (236). The main advantage of the TOF mass analyser is its speed and high mass range up to 100,000 Da.

#### 4.3.3. Tandem mass spectrometry

The Principle of Tandem Mass Spectrometry Tandem mass spectrometry is based on coupling mass spectrometers together in a series to analyse complex mixtures (**Figure 26**). The method uses two mass filters arranged sequentially with a collision cell between them. The filters can be used in static or scanning mode to select a particular mass-to-charge ( $m/z$ ) ratio or  $m/z$  range. The precursor ions collide with gas molecules in the collision cell and are fragmented into smaller ions referred to as product ions.

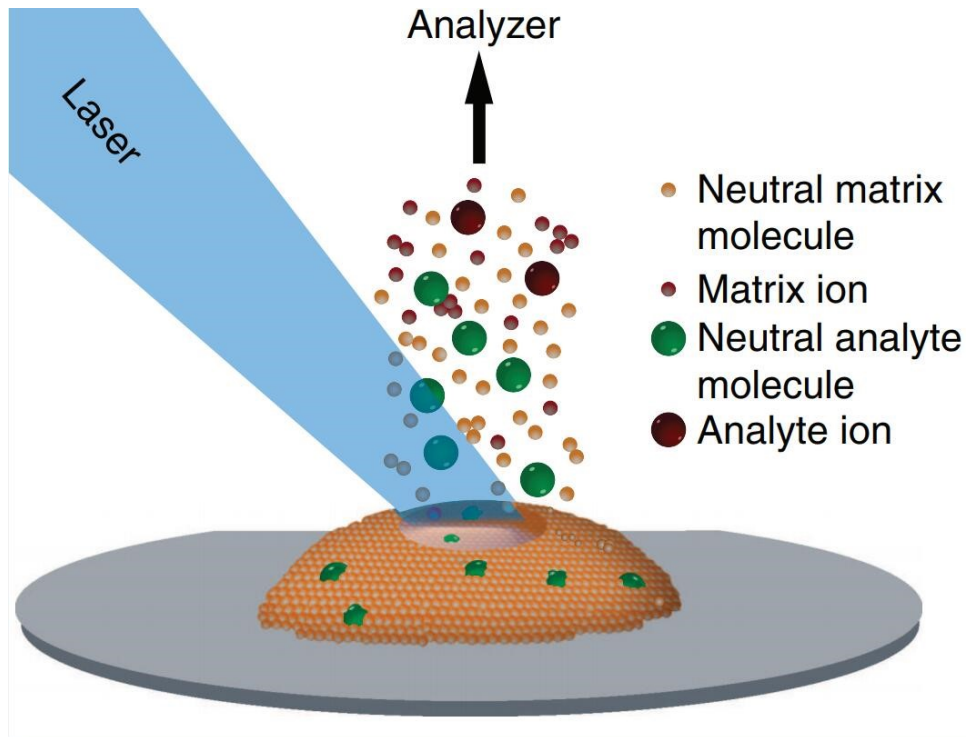


Figure 25 Principle of matrix-assisted laser desorption ionisation (from creative-proteomics.com)

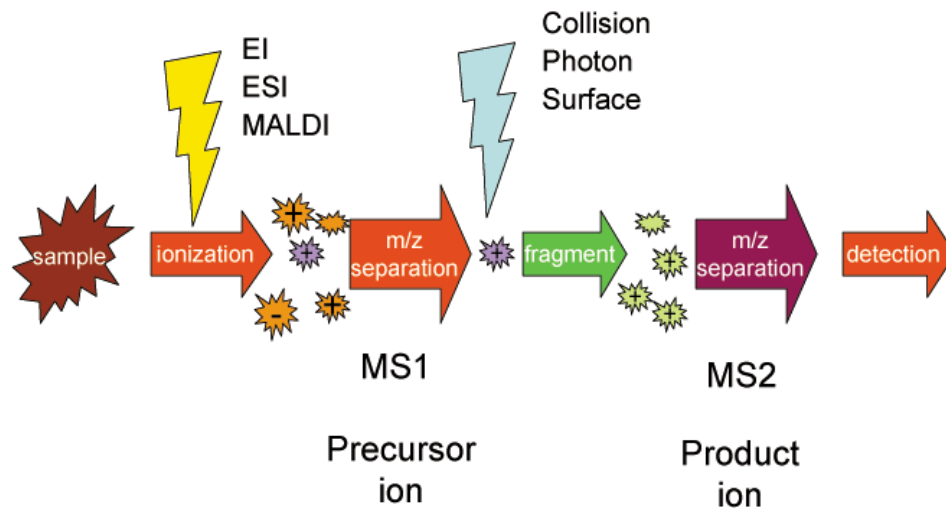


Figure 26 Principle of tandem mass spectrometry (from K.Murray)

Tandem mass spectrometers are versatile in that they can be operated using a variety of different scan modes depending on the clinical application. This method is used in peptide and amino acid sequencing, also called **De novo peptide sequencing**. It enables gas-phase isolation of individual peptide ion species followed by collision-induced dissociation and detection of the resultant amino-acid sequence-specific fragment ions (256). De novo peptide sequencing is a very sensitive, accurate, and efficient method for sequencing peptides via the generation of these fragment ions. In addition to providing means to identify proteins, tandem mass spectrometry also offers tools to interrogate proteins for post-translational modifications.

#### *4.3.4. Hyphenated techniques with dual inductively coupled plasma mass spectrometry and electrospray ionisation tandem mass spectrometry detection*

Hyphenated techniques based on the coupling chromatographic separation techniques with dual ICP-MS and ESI MS detection have become a gold standard for selenium speciation analysis and the analysis of selenium metal covalent modifications. Both detection techniques provide complementary information as detailed in **Figure 27**. ESI-MS is used for molecular and structural identification using ionised proteins fragments or peptides at low energy. On the contrary, ICP-MS, is an elemental technique which allows the detection of Se and its isotopes in precision without any info of the structure of the peptide nor the proteins.

These two techniques are used in coupling with HPLC systems for species separation before identification and detection and together are efficient in quantification and identification of species of interest based on the isotopic signal in ICP MS and complementarity of information provided by ESI MS.

ICP-MS is usually coupled to size exclusion (SEC), affinity chromatography (IE), reverse phase chromatography (RP) and other chromatographic separation (257). The hyphenation requires an acceptance by the plasma of the sample transmitted from the separation system. The parameters to be taken into account include the eluent flow rate and its composition. The key to a successful HPLC and ICP-MS coupling is the interface, so the column flow should be matched with the optimum nebulizer flow in the aim to get an effective separation, so typically the nebulizer selected is the one that assures the presence of the highest proportion of fine droplets in the aerosol (258).

The coupling of ESI-MS to liquid chromatography allows the separation of sample components and reduces matrix complexity which facilitates the analysis. The parameters to be adjusted include capillary temperature, carrier gas temperature, and spray voltage. At present, the methodologies used in proteomics are based mainly on liquid chromatographic methods combined with mass spectrometric (MS) detection(258).

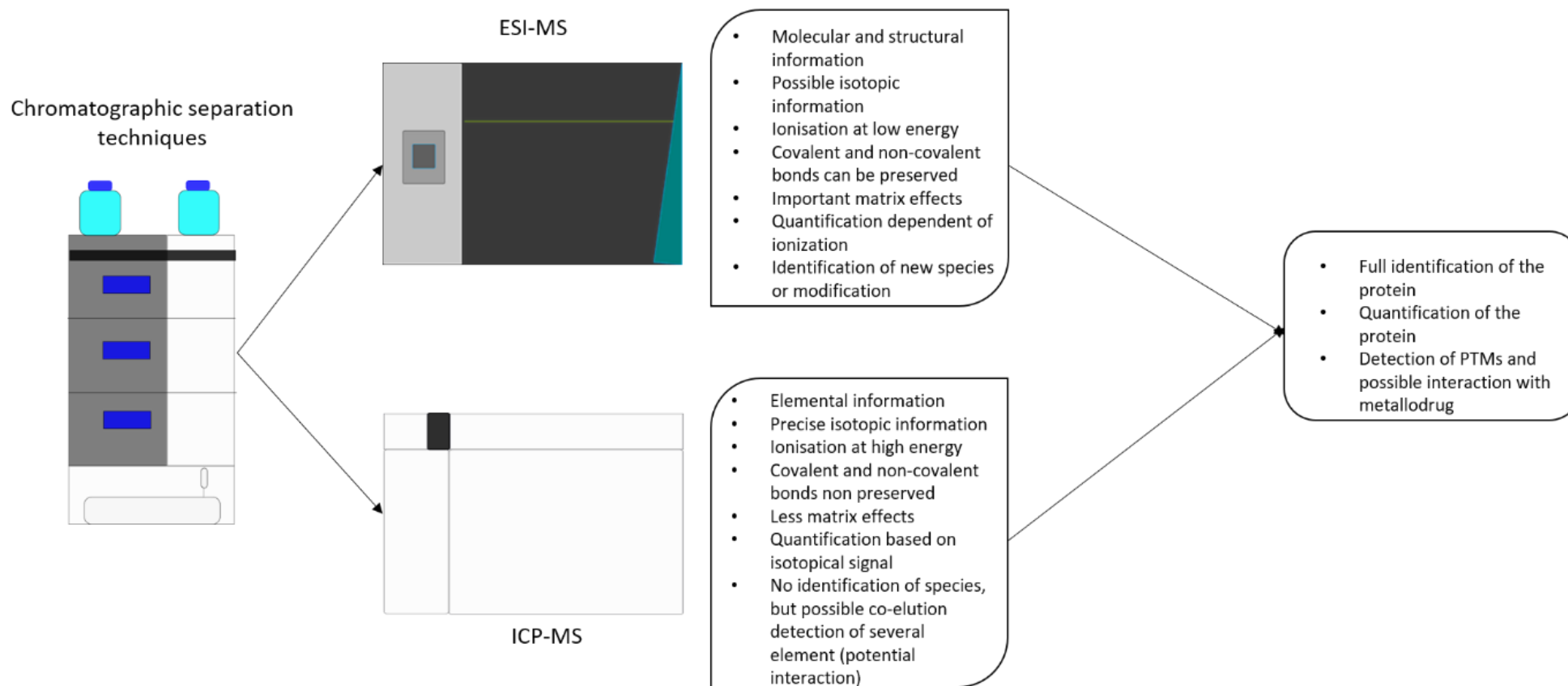
LC-MS-based methodologies have been used for the analysis of proteins for both target analysis and non-target profiling. Ultra-high performance liquid chromatography (UHPLC) presents an interest since it allows an increase in chromatographic resolution via capillary LC applications, enabling a reduction of sample consumption, especially when available sample volume is low. Results have shown further advantages such as detecting higher numbers of ions and an increase in sensitivity compared to ordinary LC-MS analysis (259). In more recent advancement, the development of nanoUPLC is also opening a new field of possibility in proteomics with the use of an ultralow amount of protein (260–262).

#### *4.3.5. Mass spectrometry techniques in proteomics*

Proteomics is the large-scale study of proteomes (**Figure 28**). Proteomics is used to investigate:

- proteins sequences and post-translational modification
- when and where proteins are expressed
- rates of proteins production, degradation; and steady state abundance
- the movement of proteins between subcellular compartments

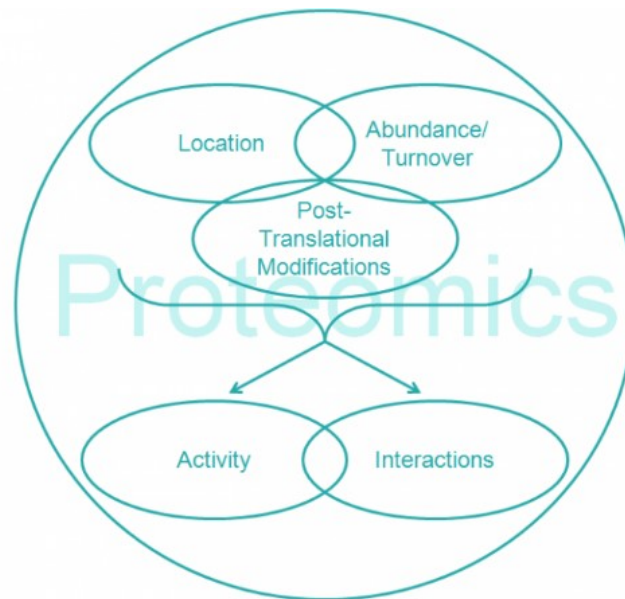
1  
2



3

Figure 27 Hyphenated techniques ICP-MS et ESI-MS specific information

- 4 • the involvement of proteins in metabolic pathways
- 5 • how proteins interact with one another



6  
7 *Figure 28 Areas of proteomics*

8 Proteomic experiments generally collect data on several properties of proteins in a sample. The use of  
9 mass spectrometry is predominant in proteomics domains.

10 The two principal approaches to identifying and characterizing proteins using MS are the “bottom-up”,  
11 which analyses peptides produced by proteolytic digestion, usually with trypsin, and “top-down”, which  
12 analyse intact proteins.

13 **Bottom-up proteomics** involves the proteolytic digestion of proteins before analysis by mass  
14 spectrometry. The term bottom-up implies that information about the constituent proteins is  
15 reconstructed from individually identified fragment peptides. The flowchart of bottom-up proteomics is  
16 illustrated in *Figure 29*.

17 The proteins purified by multidimensional chromatography or gel electrophoresis are digested with  
18 trypsin that cuts peptide bonds on Lys and Arg. The resulting mixture of peptides is reversed-phase  
19 chromatography and analysed by mass spectrometry. Finally, proteins are reconstructed from the  
20 information obtained for the peptides using database matching.

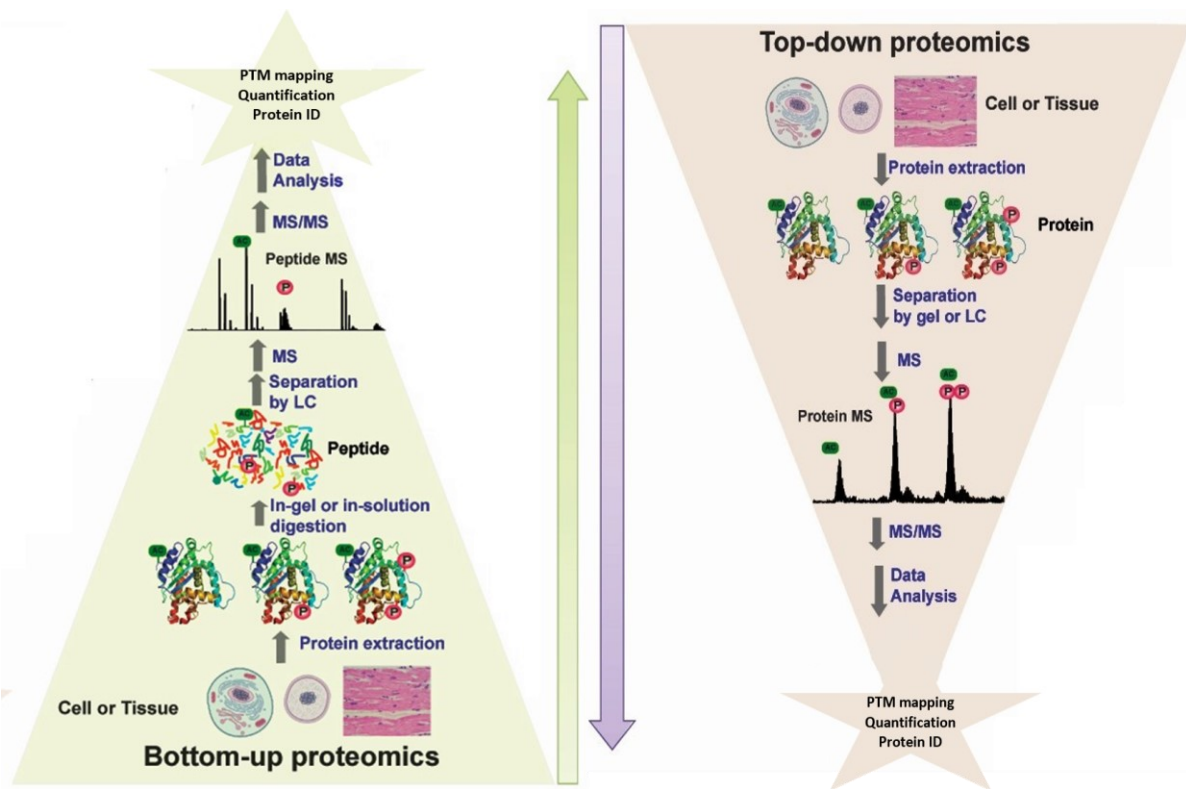
21 A limitation of bottom-up proteomics is a low percentage coverage of the protein sequence is obtained  
22 because only a small and variable fraction of the total peptide population of a protein can be recovered.  
23 Genomic studies have shown that each open reading frame can give rise to several protein isoforms due  
24 to alternative splicing products and differences in the locations and types of post-translational  
25 modification (PTM). In bottom-up proteomics, the limited sequence coverage means much information  
26 about PTMs and alternative splice variants is lost (263–265).

27  
28 **Top-down Proteomics** can characterize intact proteins from complex biological systems. This approach  
29 routinely allows for nearly 100% sequence coverage and full characterization of proteoforms, the



30 specific molecular form of the protein resulting from combinations of genetic variation, alternative  
31 splicing, and post-translational modifications. Fragmentation for tandem mass spectrometry is  
32 accomplished by electron-capture dissociation (ECD) or electron-transfer dissociation (ETD). Proteins  
33 are typically ionized by electrospray ionization and trapped in a Fourier transform ion cyclotron  
34 resonance or quadrupole ion trap mass spectrometer.

35 It involves identifying proteins in complex mixtures without prior digestion into their corresponding  
36 peptide species. The schematic workflow for top-down proteomics includes protein separation, mass  
37 spectrometer detection, and data analysis (**Figure 29**). The main advantages of the top-down strategy  
38 are the potential access to the complete protein sequence and the ability to locate and characterize PTMs.  
39 It also has the ability for protein isoform determination. In addition, the time-consuming protein  
40 digestion required for bottom-up methods is eliminated. It has not been achieved on a large scale due to  
41 a lack of intact protein fractionation methods integrated with tandem mass spectrometry (263, 265, 266).



42  
43  
44

Figure 29 Bottom-up and Top-down proteomics principles (adapted from (267))





## 5.1. Isolation and purification of selenoprotein P

The abundance of SELENOP in human serum exceeds that of plasma glutathione peroxidase (GPx) and selenized albumin (SeAlb) (111). It is typically present in serum at a level of ca. 50 ng/mL. Its concentrations in cultured cells, breast milk, or tissues are an order of magnitude lower. Taking into account the presence of a multitude of proteins in a 1000-fold excess, any characterization of SELENOP by mass spectrometry should be preceded by its isolation and enrichment. The methods are usually based on immunoaffinity precipitation or chromatography (mono- and/or poly-clonal antibodies) (142, 268–272) or chemical affinity (heparin (141, 238, 273) or immobilized transition metals (71, 274).

### 5.1.1. Immunoaffinity precipitation and chromatography

The use of immunoaffinity has been largely explored for the isolation of SELENOP. This strategy is critically dependent on the quality and selectivity of antibodies. The cross-activity of one antibody with an antigen from different species is not granted and must be tested. Moreover, the activity of the antibody is highly variable from the serum of one animal to the other and must also be systematically tested.

The first purification of SELENOP by immunoprecipitation was performed from rat serum, using monoclonal antibodies (269). Subsequently, Akesson *et al.* (143) used the rat monoclonal antibodies for the purification of human SELENOP. Other groups reported the preparation (270, 275) or use (276) of a monoclonal antibody raised against rat SELENOP (270). No cross-reactivity with plasma from five animal species (143) was observed. Commercially available antibodies against murine SELENOP do not cross-react with the human orthologue (274). Recombinant rat SELENOP was efficiently immunoprecipitated by a commercial penta-histidine antibody but not by the tetrahistidine one (71).

Considerable developments in the field of SELENOP antibodies have taken place in recent years driven by the need for the development of ELISA kits (see below). They are based on the use of antibodies prepared by using recombinant mutant SELENOP as immunogen. These expressed SELENOP mutants are characterized by the absence of SeCys which are all replaced by Cys (277) or Ser (278). A recombinant SELENOP commonly used as an immunogen for commercial antibody development encompasses the 60-299 SELENOP sequence without SeCys residues (279). Alternatively, SELENOP purified from human serum was employed as an immunogen (268, 275, 280).

The antibody-based methods for purification and measurement of SELENOP may not allow the distinction among the isoforms (141). Indeed, antibodies are usually directed towards one of its domains (N or C). Consequently, they capture not only full-length SELENOP but also its N- or C-terminal side domain fragments. In vivo, SELENOP is cleaved by plasma kallikrein which generates N-terminal and C-terminal fragments of SELENOP (280). The combined use of antibodies specific for N- or C-terminal SELENOP side domain fragments allows the differentiation between the full-length SELENOP from total SELENOP (truncated and full length) (139, 268, 272).

Technically speaking, immunoprecipitation of SELENOP can be conveniently performed with commercial antibodies conjugated to polystyrene superparamagnetic beads (271). GPx3 is co-immunoprecipitated with SELENOP, resulting in incomplete separations which is likely to be due to the similarity in the structure of the N-terminal part of SELENOP and GPx3 (271). This point has not been addressed by recent studies where combined antibodies specific for the different SELENOP termini were employed.

### 5.1.2. Heparin affinity methods

Selenoprotein P contains two poly-histidine domains and several other histidine and lysine residues and has a predominance of basic compared to acidic amino acids (281). These characteristics are common for proteins that bind proteoglycans (25). The pH- and ionic strength-dependence also support the hypothesis that the binding of selenoprotein P is based on electrostatic interactions. The two apparent binding sites of selenoprotein P on heparin may be explained by a simple charge interaction between the protein and heparin (low-affinity site), and a stronger, histidine-dependent interaction (high-affinity site). While the calculated molar ratio of binding of selenoprotein P is predominated by the low-affinity site, the relative strength of the higher affinity site may make this a more important interaction biologically at neutral pH (231).

These histidine-rich stretches containing up to 10 sequential basic amino acids are present in the 185–198 and 225–234 amino-acid sequences in rats (273). The rat and human SELENOP sequences encode two His-rich regions: the first region consists of 8 (rat) or 9 (human) histidines out of 14 residues, and the second, a stretch of 7 (rat) or 4 (human) consecutive histidines (282). The presence of these stretches confers to SELENOP a feature of binding to heparin (273).

SELENOP binds to heparin as a function of pH. The binding is facilitated by an increase in protonation of histidine residues. Therefore, SELENOP will bind to heparin under acidic conditions but remains unbound at physiological pH (109). The pKa of histidine (7.0) explains the release of SELENOP from heparin at alkaline conditions (273).

Heitland *et al.* were able to isolate SELENOP using heparin column from other serum proteins with a total recovery of selenium (96%) (238). A recovery above 90% was reported (283). Problems linked to nonspecific adsorption of plasma-extracellular glutathione peroxidase (GPx) and albumin on the heparin affinity column were evoked (283). Purified SELENOP can be separated in three peaks using heparin chromatography suggesting its capability to discriminate amongst the isoforms (141).

### 5.1.3. Immobilized metal affinity methods

The mechanism of separation of IMAC Sepharose with metal is using the specificity of SELENOP to have two histidine stretches in positions 185-198 and 225-234 of its amino-acid sequence. This chromatography column is based on the chelating mechanism of immobilized metals. Thanks to the presence of histidine on proteins, a coordination bond is formed between the metals chelated on the stationary phase and the histidine stretch (**Figure 30**). A protein with a lot of histidines will then be retained on the column and will be separated from other proteins with no or few histidine residues. These histidine-rich regions in conjunction with the Cys and SeCys content, are likely responsible for the coordination to heavy metals such as, e.g., mercury (282). The presence of such motifs makes it possible to retain SELENOP on an IMAC-sepharose column loaded with cobalt (274). Co<sup>2+</sup> was found superior to Cu<sup>2+</sup>, Ni<sup>2+</sup>, Zn<sup>2+</sup>, and Cd<sup>2+</sup> for metal affinity LC (274).

The Ni-agarose chromatography was performed using Ni-NTA spin columns and turned out to be efficient for the isolation of SELENOP, prior to SDS PAGE and Western blotting analysis (71).

### 5.1.4. Sequential purifications

In order to increase the purity of the isolated SELENOP, the above discussed steps can be employed in a sequence. Akesson *et al.* reached a 1000-fold purification of SELENOP by combining immunoaffinity LC and heparin (143). The immunoaffinity purified protein was further separated into several forms using heparin-sepharose column (270).

Daegen *et al.* separated plasma into three components (GPx, SELENOP, and Alb) using heparin-sepharose and blue 2-sepharose (to remove SeAlb) (284). A combination of IMAC and heparin offered a 15,000-fold enrichment of SELENOP (274). Isolation of electrophoretically pure SELENOP was reported to be achieved in three steps: heparin agarose, ultrafiltration concentration, anion-exchange, Ni-NTA-agarose (146). The combination of heparin-sepharose CL-GB, Q Sepharose F and Ni-NTA agarose chromatography, followed by desalting by gel filtration, allowed a 13,000-fold purification of SELENOP with an overall yield of 16% (285). The low yield of sequential purification is often due to the multiplication of steps inducing loss of protein. In recent studies, the use of heparin was shown to be the most efficient for SELENOP purification with a yield of 96% (238), however this method does not concentrate the protein.

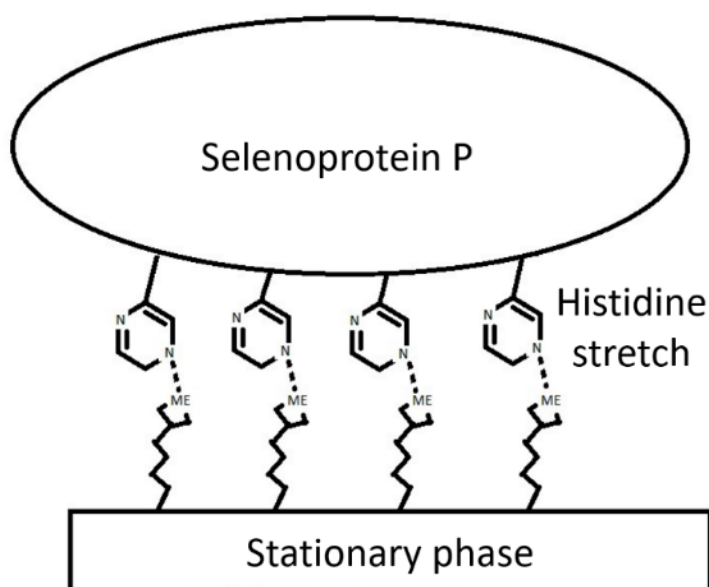


Figure 30 Schematic interaction between SELENOP and IMAC stationary phase

## 5.2. Detection of selenoprotein P

SELENOP can be quantified by measuring the Se response provided that the protein is separated from the other Se-containing species by HPLC. The initial use of hydride generation atomic absorption or fluorescence spectrometry was replaced by ICP-MS because of its higher sensitivity, isotopic specificity and simplicity avoiding the need for post-column chemical conversion of SELENOP to Se or to selenium hydride. Because of the high relative abundance of SELENOP, the challenge of separation is practically limited to SELENOP from selenoalbumin, GPx3, and selenometabolite fraction.

The principle of the methods is based on downscaling and on-line arrangement in different configurations of the three principal techniques discussed above: size-exclusion LC for the separation according to the molecular weight, heparin LC for the selective retention of SELENOP, and Blue-Sepharose column for the selective retention of SeAlb. As a result, the SELENOP signal is obtained in


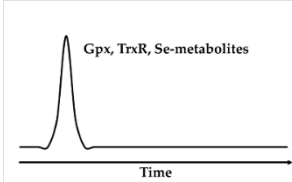
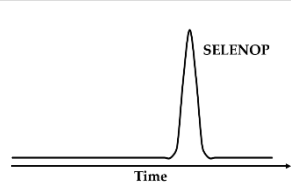

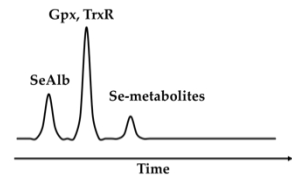
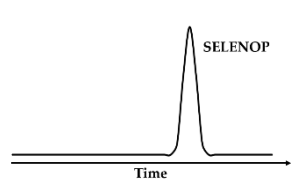

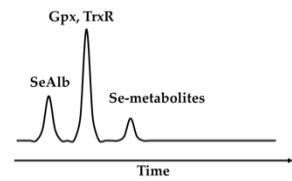
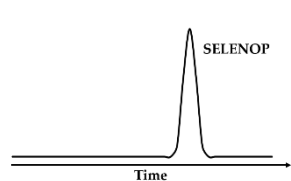

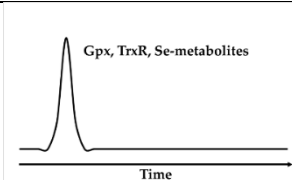
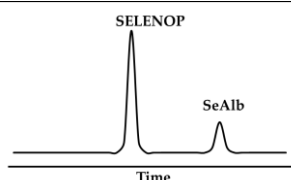
the form of a chromatographic peak, other species may sometimes be separated by SEC. The principle of the proposed arrangements and the type of signal used for quantification is schematically shown in (**Figure 31**).

The most widely used principle for the on-line isolation of SELENOP consists of the retention of SELENOP by affinity using a heparin column while all other selenium species are eluted and detected as a peak in the loading run (238). The subsequent elution run produces a peak corresponding to SelP (**Figure 31a**). The incorporation of a SEC (heparin) column on-line, either preceding (286, 287) (**Figure 31b**) or following (283) (**Figure 31c**), allows the discrimination of the selenium species eluting in the loading run into HMW Se-containing proteins (Se-albumin and GPx) and LMW metabolite fraction.

A more sophisticated version of the system includes a switching valve and a circuit containing a column with an affinity for albumin, allowing for the specific recovery of SelAlb during the loading run for its subsequent quantification (**Figure 31d**) (239, 288–291). It can be refined by the integration of a SEC column into the system (**Figure 31e–f**) (292–295).

Size-exclusion LC alone does not offer a sufficient resolution nor preconcentration to separate SELENOP from SelAlb (296, 297). However, when coupled in-tandem with a SelAlb method, SELENOP appears as a peak partially separated from GPx3 and separated from LMW selenometabolite fraction (**Figure 31g**) (298).

Alternatively, as SELENOP is the only selenium species in serum and cerebrospinal fluid not retained on the anion-exchange column; anion-exchange HPLC (**Figure 31h**) was used to separate it from other species (299–301).

| Schematic configuration  | Schematic chromatogram (Se-specific detection)                                      |  | Refs.                    |
|--|---|--|--------------------------|
|  | Loading run   | Elution run  |                          |
| (a)<br> |  |  | (143, 238, 270)          |
| (b)<br> |  |  | (286, 287)               |
| (c)<br> |  |  | (283)                    |
| (d)<br> |  |  | (239, 283, 284, 288–291) |

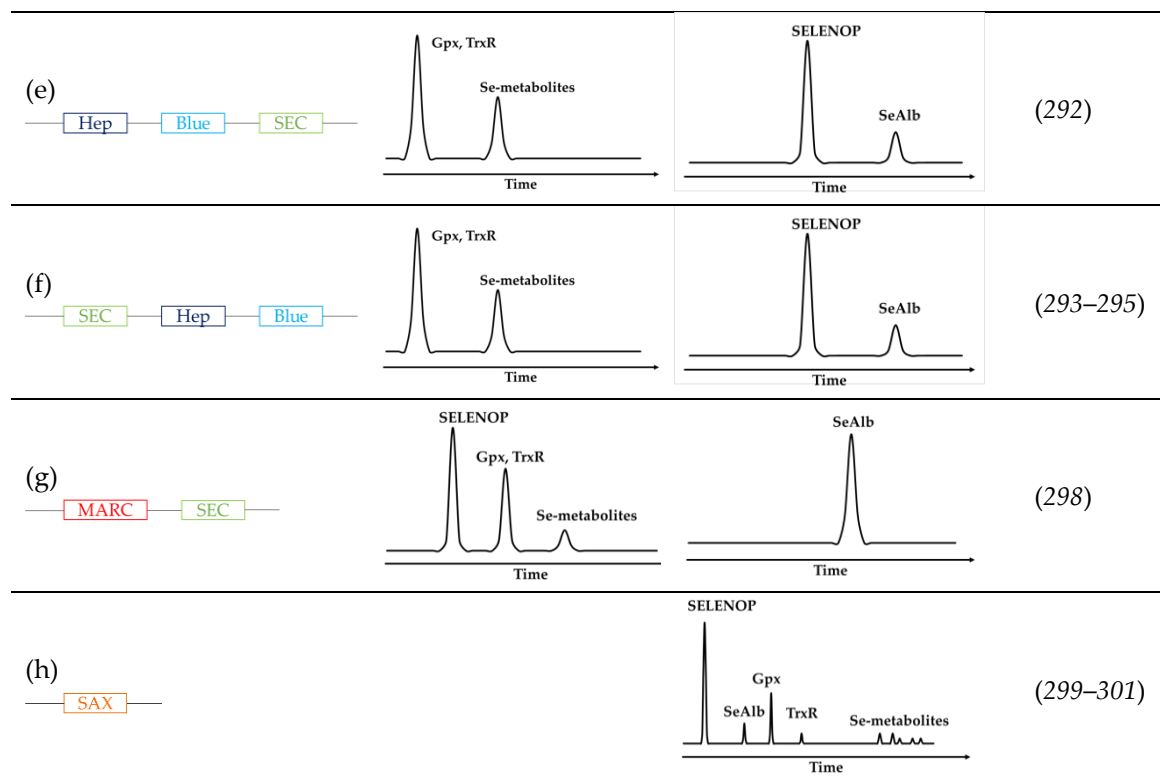


Figure 31 Schematic overview of the principle of HPLC configuration coupled with ICP-MS for SELENOP determination

### 5.3. Characterization of selenoprotein P

The isolated SELENOP can be formally identified without mass spectrometry by the N-terminal amino-acid sequence (or microsequencing) (284). However, the advantage of MS in terms of sensitivity and speed cannot be overestimated. So far, to our knowledge, there have been no mass spectra published for the intact full-length SELENOP and their truncated isoforms. Most of the published MS data concern the analysis of peptides, obtained after tryptic digestion, by MALDI or ESI MS. The latter allows the determination of the peptide sequence upon collision-induced dissociation (MS/MS). The list of the reported peptides allowing the 100% sequence specificity and their correspondence to full-length or truncated isoforms is given in (Table 8).

A number of bioinformatic tools have been developed for the detection of selenoproteins in high throughput MS schemes (302, 303). Several enzymes (such as trypsin or endoproteinase) can be used to lyse the proteins and to obtain different SELENOP characteristic peptides. The inconvenience of bottom-up proteomics approaches is that it is not always possible to identify isoforms from which the peptides are derived. Their advantage is the capability to deal with post-translational modification.

The major challenges in mass spectrometry analysis include the ability to be able to distinguish between isoforms, to complete the characterization of truncated forms and to develop analytical methods for their quantification. The potential of top-down proteomics for this purpose is very promising (304).

#### 5.3.1. Matrix assisted laser desorption/ionisation mass spectrometry

MALDI-MS allowed the discovery in rat plasma of three SELENOP isoforms that have identical N-termini, and differ in the length of the amino-acid chain (141). The full-length SELENOP and the

isoforms were separated by SDS PAGE. They were reduced, alkylated, deglycosylated and digested with trypsin. Additional peptides could be identified by digestion with Glu-C of the SELENOP isolated by heparin, without the need for its subsequent purification by SDS PAGE. Mass spectrometry could identify the C-termini of the isoforms according to the prediction (at the 2nd, 3rd and 7th selenocysteine residue) (141).

MALDI-MS was also used to identify the sites of glycosylation of the full-length SELENOP (145). The procedure was based on a treatment with PNGase F, which cleaves off asparagine-linked carbohydrates and converts the residue asparagine to aspartic acid. Of the five potential glycosylation sites, three located at residues 64, 155 and 169 were occupied, and two at residues 351 and 356 were not occupied. Threonine 346 was variably O-glycosylated. Full-length SELENOP was found to be both N- and O-glycosylated (145).

MALDI-MS was also essential in the identification of Se-S and disulfide linkage sites (145). The strategy of sample preparation for the determination of the oxidation state of the cysteine residues consisted of the alkylation of all free cysteines and selenocysteines in the short form of SELENOP with iodoacetamide, digestion with endoproteinase, and deglycosylation (145). A selenide-sulfide bond was found in the shortened isoform to be analogous to the selenol-thiol pair considered to be redox-active (145). Two selenylsulfide bonds were identified by MALDI-MS in a peptide isolated from a tryptic digest of rat SELENOP (305).

Table 8 List of selenopeptides used for the SELENOP mass spectrometry identification on the basis of a partial sequence

| Matrix            | SELENOP Specific Sequence with SeCys Detected             | Identified Isoform  | Ref.  |
|-------------------|---|---|-------|
| Rat plasma        | <sup>28</sup> GTVTVVALLQASUYLCLLQASRL <sup>51</sup>       | 4 Isoforms:<br>50 kDa (full length)<br>49 kDa (terminated at 351)<br>38 kDa (terminated at 262)<br>36 kDa (terminated at 244) | (141) |
|                   | <sup>239</sup> QGHLESUDMGASEGLQLSLAQR <sup>260</sup>      |   |       |
|                   | <sup>252</sup> GLQLSLAQRKLRRCINQLLCKLSEE <sup>278</sup>   |   |       |
|                   | <sup>298</sup> SGSAITUQCAENLPSLCSUQGLFAEEK <sup>324</sup> |   |       |
| Rat plasma        | <sup>333</sup> SPPAAUHSQHVSPTEASPNUSUNNK <sup>357</sup>   | 1 Isoform terminated at 244   | (145) |
|                   | <sup>348</sup> ASPNUUNNKTKKUKUNLN <sup>366</sup>          |   |       |
| Rat plasma        | <sup>28</sup> GTVTVVALLQASUYLCLLQASR <sup>49</sup>        | <i>n.d.</i>   | (305) |
| Human plasma      | <sup>322</sup> ENLPSLCUQGLR <sup>334</sup>                | <i>n.d.</i>   | (288) |
| Human plasma      | <sup>335</sup> AEENITESCQR <sup>346</sup>                 | 3 Isoforms:<br>45 kDa (terminated at 299)<br>49 kDa ( <i>n.d.</i> )<br>57 kDa ( <i>n.d.</i> )                                 | (271) |
|                   | <sup>312</sup> TGSAITUQCK <sup>321</sup>                  |   |       |
|                   | <sup>322</sup> ENLPSLCUQGLR <sup>334</sup>                |   |       |
| Human breast milk | <sup>312</sup> TGSAITUQCKENLPSLCSUQGLR <sup>334</sup>     | <i>n.d.</i>   | (286) |
|                   | <sup>370</sup> NQAKKUEUPSNC <sup>382</sup>                |   |       |

(Peptides with the same sequence are highlighted in colors)

### 5.3.2. Electrospray mass spectrometry

The basic advantage of electrospray ionization (ESI) MS over MALDI is the possibility to sequence peptides in LC-MS/MS on the basis of the m/z of their b and y fragments. ESI MS was used to verify the sequences of the putative glycosylated peptides in rat SELENOP (145) and the confirmation of the existence of disulfide linkages (145, 305).



High-pressure liquid chromatography (HPLC)-MS/MS was a convenient technique for the identification of selenopeptides in a tryptic digest of purified SELENOP. It allowed the formal confirmation of SELENOP presence in human breast milk (286). A sequence with a coverage of 80% of the theoretical one was reported on the basis of the tryptic digest analysis, and two selenopeptides were formally identified (286).

SELENOP, being a low-abundant protein in serum, was not detected by a regular shotgun proteomics approach (288). The analysis of the fraction purified by heparin allowed the detection of three unique SELENOP peptides identified by only one post-translational modification for each, and a sequence coverage of 41.5% (288). The purification of SELENOP by SDS PAGE and blotting, which was followed by tryptic digestion and HPLC-MS/MS, allowed the identification of 7 SELENOP peptides totalling 115 post-translational modifications (none of which contained selenium) in the 49 kDa SELENOP band in the blot, accounting for a sequence coverage factor of 17.7%. Selenium contained peptides missed by the regular shotgun proteomics procedure. The identification of two selenopeptides increased the sequence coverage to 24.4% (288). Three isoforms of SELENOP were identified by this method (271).

Human SELP still needs a complete MS characterization covering all the selenopeptides. The recent data obtained are summarized in **Table 8**.

The developments in soft ionization mass spectrometry open new perspectives in the detection of SELENOP in broad-scope proteomic studies. The method is based on nano-flow liquid chromatography (LC) with electrospray MS/MS detection and data-independent acquisition MS (306). For instance, label-free proteomics showed selenoprotein P as the most abundant protein in the milk of cows, more precisely, in cows producing milk with A2A2- $\beta$ -casein variants (307). The protocols can be quantitative by using isobaric tagging for relative and absolute Quantification (iTRAQ)(303, 308–310).

## 5.4. Quantification of selenoprotein P

### 5.4.1. Immunoassays

An immunoassay is a biochemical test that measures the presence or concentration of a macromolecule or a small molecule in a solution through an antibody (usually) or an antigen (sometimes). The molecule detected by the immunoassay is often referred to as an "analyte" and is in many cases a protein, although it may be other kinds of molecules of different sizes and types, as long as the proper antibodies the required properties for the assay are developed. Analytes in biological liquids such as serum or urine are frequently measured using immunoassays for medical and research purposes (311). Immunoassays rely on the ability of an antibody to recognize and bind a specific macromolecule in what might be a complex mixture of macromolecules. In immunology, the particular macromolecule bound by an antibody is referred to as an antigen and the area on an antigen to which the antibody binds are called an epitope. This method was extensively used in protein science when antibody is available.

Originally, radioimmunoassay's based on the in-vitro synthesized or partially purified labelled SELENOP preparations were proposed by (107, 269, 312, 313). Nevertheless, due to the cumbersome procedures and restrictive regulations concerning the use of radioactive materials, these assays were only used in very few studies and were not widely adopted by the larger community.

ELISA (enzyme-linked immunosorbent assay) for SELENOP was first developed as early as 2010 (116), but the early ELISA assays were time-consuming and inconvenient for clinical use. However, the



approach is rapidly gaining popularity for the absolute quantification of SELENOP in plasma samples (144, 314). Several kits are commercially available (278, 279, 315–317). The results depend largely on the kit used and caution and criticism are required when comparing data obtained with the different kits (318).

The accuracy of the results depends on the epitope identified by the antibody and its selectivity (activity towards the other proteins). If an antibody recognizes just, for example, the N-terminal, the assays will capture not only full-length SELENOP but also the SELENOP-N-terminal fragment (268). An assay using colloidal gold particles coated with two types of anti-SELENOP monoclonal antibodies, one recognizing the N-terminal side domain and the other recognizing the C-terminal, was developed for measuring full-length selenoprotein P in human serum (268).

The in-plate variation, within-laboratory variation, and between laboratory variation are all typically below 15% with a limit of quantification of 10 ng/mL (144). The accuracy of ELISA (difference with the SRM value) was assessed to be 2.9% (144). Because of the limited presence of mass spectrometry technology in the clinical environment, immunoassays are the most widely used technique for human and animal health status.

#### 5.4.2. Inductively coupled plasma mass spectrometry-based methods

A major problem in the quantification of SELENOP is the non-availability of an authentic SELENOP standard as it is currently practically impossible to obtain recombinant SELENOP in reasonable purity and quantity. Calibration is therefore carried out using a proxy such as selenite, selenomethionine, a peptide characteristic of SELENOP, or recombinant homologue of SELENOP in which the SeCys residues were replaced by Cys.

The standards used for calibration are usually isotopically labelled. However, the term “isotope dilution analysis (IDA)” frequently used in the context of quantification of SELENOP by HPLC-ICP-MS does not bear the original meaning of absolute (traceable to SI units) quantification. As there is not isotopically labeled SELENOP available, the analyte (SELENOP) and the spike used are not in the same chemical form.

The principal quantification strategies of SELENOP using calibration by isotope dilution are based on:

- the measurement, in an HPLC peak, of the intensity ratio between the natural selenium isotope from the SELENOP after HPLC separation of the latter and the enriched Se ( $^{77}\text{Se}$ ,  $^{74}\text{Se}$ ) added post-column as SeMet or selenite (“spike”). The method is referred to as species-unspecific isotope dilution (286, 288, 290, 293, 295).
- the measurement, in an HPLC peak, of the intensity ratio between Se in selenomethionine obtained by the complete proteolysis of the selenoprotein and the isotopically enriched  $^{77}\text{Se}$ Met standard (“spike”). The method can be referred as species-specific isotope dilution on the amino-acid level. The proof of principle was demonstrated by Ruiz Encinar *et al.* (319) and the approach was applied to the SELENOP quantification by Jitaru *et al.* (320).
- the measurement, in an HPLC peak, of the intensity ratio between the Se in a Se-containing peptide obtained from a selenoprotein by tryptic digestion and the isotopically enriched Se ( $^{77}\text{Se}$ ,  $^{74}\text{Se}$ ) in the identical synthetic peptide. The addition of peptide spikes to the plasma samples was followed by tryptic digestion, alkylation, and isotope ration determination using

HPLC-ICP-MS. The principle of the method was demonstrated by Polatajko *et al.* (321). The method was first applied to the quantification of SELENOP by Ballihaut *et al.* (288). Deitrich *et al.* (138) proposed the use of two synthetic peptides (isotopically enriched,  $^{76}\text{Se}$ ) derived from SELENOP for its quantification by IDA-ICP-MS/MS. The disadvantage is the introduction of additional uncertainty due to the necessity of control of the efficiency of the enzymatic digestion by the use of selenopeptides (293).

- the use of a proxy protein as standard. The closest proxy protein has been for the moment a full-length human recombinant SELENOP in which the original 10 SeCys residues (SeCys) were replaced by 10 cysteines (Cys). This replacement was achieved by point mutations of nucleotide triplets coding SeCys to triplets coding Cys in the coding sequence for selenoprotein present in the expression vector used as a template for *E. coli* protein synthesis (289). Selenium was introduced in the polypeptide chain during cell-free protein *E. coli* synthesis in the form of SeMet or  $^{76}\text{Se}$ -Met for the preparation of the SEPP1 standard and an isotopically labelled spike for isotope dilution analysis (322, 323). The standard and spike were purified by SDS PAGE (289). However imperfect the assumption of the similarity of the behaviour of the standard and the spike might be, the use of such an isotopically enriched spike allowed the quantification by standard addition and isotope dilution analysis by ICP-MS after the purification of SELENOP by affinity chromatography.

#### 5.4.3. Gel-electrophoresis-based methods

Isoelectric focusing (IEF) and sodium dodecyl sulphate-polyacrylamide gel-electrophoresis (SDS-PAGE) allows for the separation of full-length and truncated SELENOP forms. The quantification of SELENOP and its isoforms in the produced band(s) can be achieved by the detection of selenium (either radioactive or not) or directly by the detection of the protein (recognized by a specific antibody).

The mature SELENOP has a molecular mass of 41 kDa but migrates as multiple bands, of approximately 50–60 kDa in SDS PAGE, probably due to variations in glycosylation (conserved 2 N-linked—and one O-linked glycosylation) (135). Deglycosylation shifts the migration band from 57 kDa to 43 kDa (313). A small difference can be seen in mobility (69 kDa under nonreducing conditions) and 66 kDa under reducing conditions (285).

#### $^{75}\text{Se}$ Detection

The migration of  $^{75}\text{Se}$  radioactivity in the gel played a fundamental role in the early works, allowing for the discovery and rough characterization of SELENOP (105, 106). The comparison of the radioactivity in the band with that of a standard is a straightforward method of quantification. An additional advantage is a convenient evaluation of SELENOP recovery from the gel. The inconvenience is the need for handling gamma-radioactivity which requires dedicated laboratories. Note that the technique requires that the quantified  $^{75}\text{Se}$  is present in the radioactive form. Whereas it is an elegant quantification technique in animal studies, it is not an option for human SELENOP.

#### Western Blotting Detection

The principle of the method consists of the separation of SELENOP by SDS PAGE and its transfer onto a PVDF membrane. The membranes are subsequently incubated with primary and secondary antibodies and developed with enhanced chemiluminescence. Standard curves were constructed using dilute NIST1950 reference material (71, 316).

The method is particularly attractive in combination with immunoprecipitation (140, 271) allowing the isolation and preconcentration of SELENOP from complex samples.

The selectivity of the method depends less critically on the quality of antibodies than in the case of ELISA as SDS PAGE offers an additional separation step. The method does not account for losses at the different stages of the procedure, but many of these losses are compensated by the calibration with a standard reference material. Western blotting is robust but is not traceable to the SELENOP sequence.

#### *Laser Ablation-ICP MS Detection*

The detection consists of the evaporation of SELENOP present in the band separated by isoelectric focusing (IEF) or SDS PAGE using a laser beam followed by the quantification of selenium in the produced aerosol by ICP-MS. This method was first proposed by Fan *et al.* (324) and later developed for the quantification of selenium proteins by Ballihaut *et al.* (325, 326) and Bianga *et al.* (327).

The identity and purity of the band can be verified by tryptic digestion and ESI MS/MS analysis of the non-ablated part of the gel. Calibration is carried out in a parallel lane using a well-characterized Se-containing protein with a known Se concentration, such as a fully selenized calmodulin (325) or glutathione peroxidase (326).

The LA-ICP-MS detection limits were reported to be 10 times lower for GPx than those of Western blot analyses (328). However, because LA-ICP-MS is sensitive to selenium and the number of Se atoms in SELENOP is ten times bigger than in GPx, similar detection limits to those of Western blot are expected for SELENOP. Indeed, in well-optimized conditions, the reported sensitivity was close to that of radioactivity detection (329). Note that the advent of triple quadrupole ICP-MS offers a considerable margin for improvement of the detection limits as the most abundant <sup>80</sup>Se can be chosen for detection (328). LA-ICP-MS offers a dynamic range of five orders of magnitude which largely surpasses that of Western blotting detection (two orders of magnitude) and of ELISA (one order of magnitude) which is important for the analysis of unknown sample.

#### *5.4.4. Isobaric tagging for relative and absolute quantification*

The use of LC-MS/MS as a way to quantify SELENOP was developed with the advent of new techniques such as label-free quantification (LFQ), and tandem mass tag (330).

The iTRAQ (isobaric tagging for relative and absolute quantification) method is based on the covalent labelling of the N-terminus and side-chain amines of peptides from protein digestions with tags of varying mass. The samples are then pooled and liquid chromatography tandem mass spectrometry (MS/MS). A database search using the fragmentation data allows for the identification of the labelled peptides and hence the corresponding proteins. The fragmentation of the attached tag generates a low-molecular-mass reporter ion that can be used to relatively quantify the peptides and the proteins from which they originated (331).

To enhance the detection and identification of medium- and low-abundance proteins (such as SELENOP), different immuno-depletion methods are usually used. Since lipids interfere with iTRAQ labelling (as well as detection of peptides by mass spectrometry), the serum samples have to be delipidated before the analysis (303).

SELENOP has been reported in iTRAQ-based multiplex quantitative proteomics investigations searching for biomarkers of disease (303, 308–310, 332, 333) or of Se-exposure (334).

ETUDE DES INTERACTIONS DE LA SELENOPROTEINE P ET DE LA VASSOPRESSINE DISELENIEE EN  
PRESENCE D'AURANOFINE ET DE CISPLATINE

Jérémy LAMARCHE – 16 décembre 2021

---



## 6.1. Matrix assisted laser desorption/ionisation mass spectrometry and electrospray ionisation mass spectrometry studies of selenoprotein-metallodrugs adducts

MALDI MS (200, 219, 220) has been used for the analysis of the interactions of gold-based metallodrugs with thioredoxin reductase protein. In this context, auranofin was used as a probe to distinguish between the total and active TrxR in human serum (220). MALDI spectra were recorded on TrxR1 standard solutions before and after incubation with a 10-molar excess of auranofin for 1 h at room temperature. The obtained results where a mass shift of 1058 Da between the two species can be observed (**Figure 32**). Taking into account that the binding of auranofin to the selenol-thiol groups of the enzyme takes place via displacement of the triethyl-phosphine ligand ( $\text{Et}_3\text{P}$ ) to form  $\text{Et}_3\text{PO}$ , a known metabolite of auranofin in vivo (335), a mass increment of 560 Da should be observed for each auranofin label introduced into the enzyme. Consequently, from these MALDI-MS experiments an average stoichiometry could be determined to be 1:2 (TrxR1: auranofin) for each of the two monomers of the protein, which gives a 1:4 stoichiometry (TrxR1: auranofin) for the entire protein (220).

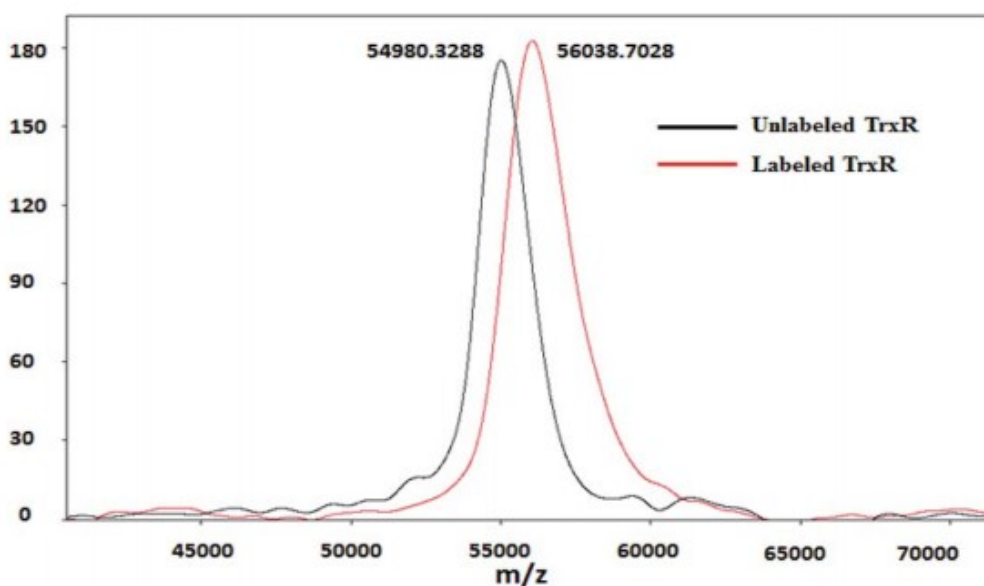


Figure 32 MALDI-MS spectra obtained for a native TrxR1 standard (black trace) and an auranofin labelled TrxR1 standard (red trace) (220).

This interaction was also observed by Bindoli *et al.* where the treatment of rat TrxR1 with gold compounds also resulted in an increase of its mass (**Figure 33**). In the case of auranofin the untreated TrxR1 mass is located at 55,5 kDa while the incubated is at 56.6 kDa which suggests, as in previous case, that 4 fragments of  $\text{AuPEt}_3^+$  are bound to the protein. As gold(III) compounds can undergo reduction processes and loss of the ligands upon protein binding, the results of MALDI MS did not make it possible to accurately assign the number and molecular structures of the gold adducts (219).

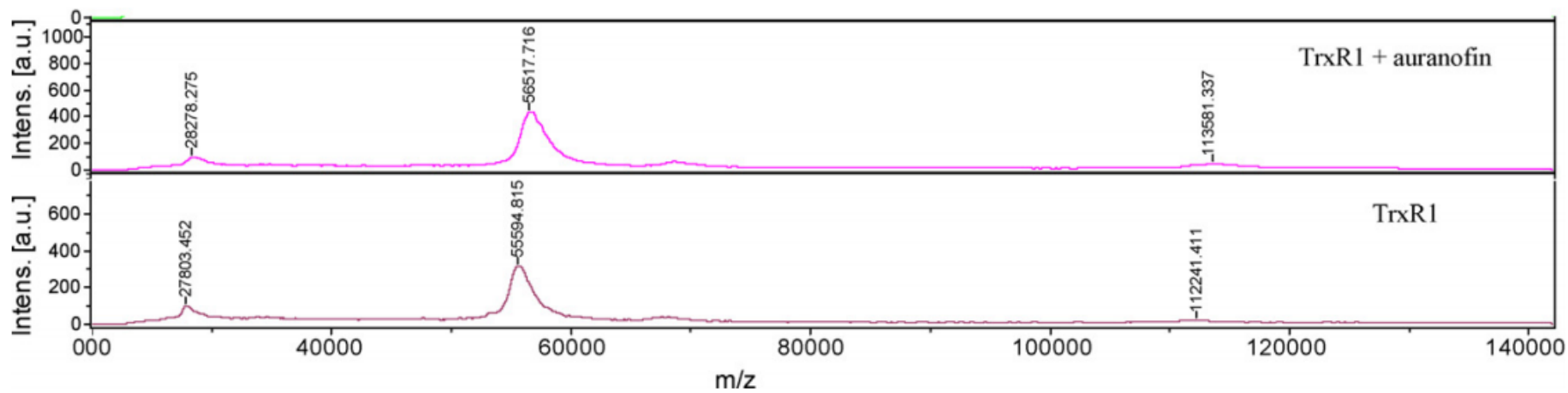
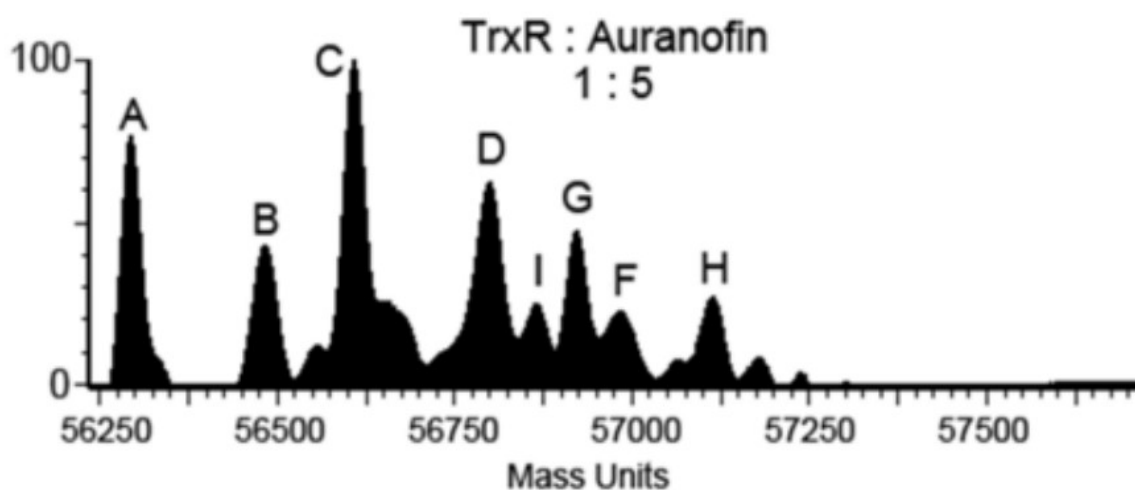


Figure 33 MALDI MS spectra of intact rat TrxR1, pre-reduced with NADPH, alone or after 1 h incubation with auranofin, at 10:1 gold to protein molar ratio, and removal of unbound gold (200)

The only work involving ESI MS concerned a TrxR mutant with a cysteine replacing the selenocysteine (336) reacted with aurothiomalate, aurothiosulfate or auranofin. ESI MS spectra showed complexes containing bare gold atoms bound to the protein, or protein adducts containing gold atoms retaining some of their initial ligand (336). In **Figure 34**, peak A represent the TrxR without gold adduct, the following peak B to H, increase in the mass suggest that Au(I) can bind to several site along with the TrxR mutant without SeCys, this experiment highlight that cysteine moiety can also be involved in the gold binding as well as several other potential sites along TrxR.



*Figure 34 ESI mass spectra, transformed to an absolute mass scale (298) Components A–M correspond to : (A) TrxR; (B) TrxR + Au; (C) TrxR + AuL; (D) TrxR + Au + AuL; (E) TrxR + 2Au; (F) TrxR + 2Au + AuL; (G) TrxR + 2AuL; (H) TrxR + 2Au + 2AuL; (I) TrxR + 3Au; where L represents PEt3. (298)*

## 6.2. Probing the molecular co-occurrence of selenium and gold by high pressure liquid chromatography hyphenated with inductively coupled plasma mass spectrometry

Yan *et al.* (218) showed that the Au(I) N,N-disubstituted cyclic thiourea complex could bind with TrxR. Under near equimolar conditions, they observed inhibition of more than half of TrxR activity, suggesting a strong binding between the complex and the protein, which was verified by ESI-MS. They demonstrated this interaction via SEC-ICP-MS after tryptic digestion of the protein treated with the Au complex. A chromatographic peak corresponding to a peptide fraction shows a co-elution of selenium and gold, reflecting an interaction between these two atoms **Figure 35**. This interaction was then validated by a competitive test between the gold complex and biotinylated iodoacetamide (BIAM), which showed that the alkylation of selenol and thiols by BIAM reduces the reactivity of the gold complex to TrxR, thus confirming that the preferential binding sites for this complex are free cysteines and selenocysteine.

## 6.3. Probing selenoprotein-metallodrugs binding by enzymatic digestion of the adduct

The usual size of the adducts formed between selenoproteins and metals does not allow the direct identification of the binding sites by mass spectrometry. As accessing this information requires



decreasing the size of the species, a possible approach includes the enzymatic digestion of the adducts (e.g., using trypsin) assuming that the binding with metal survives the procedure.

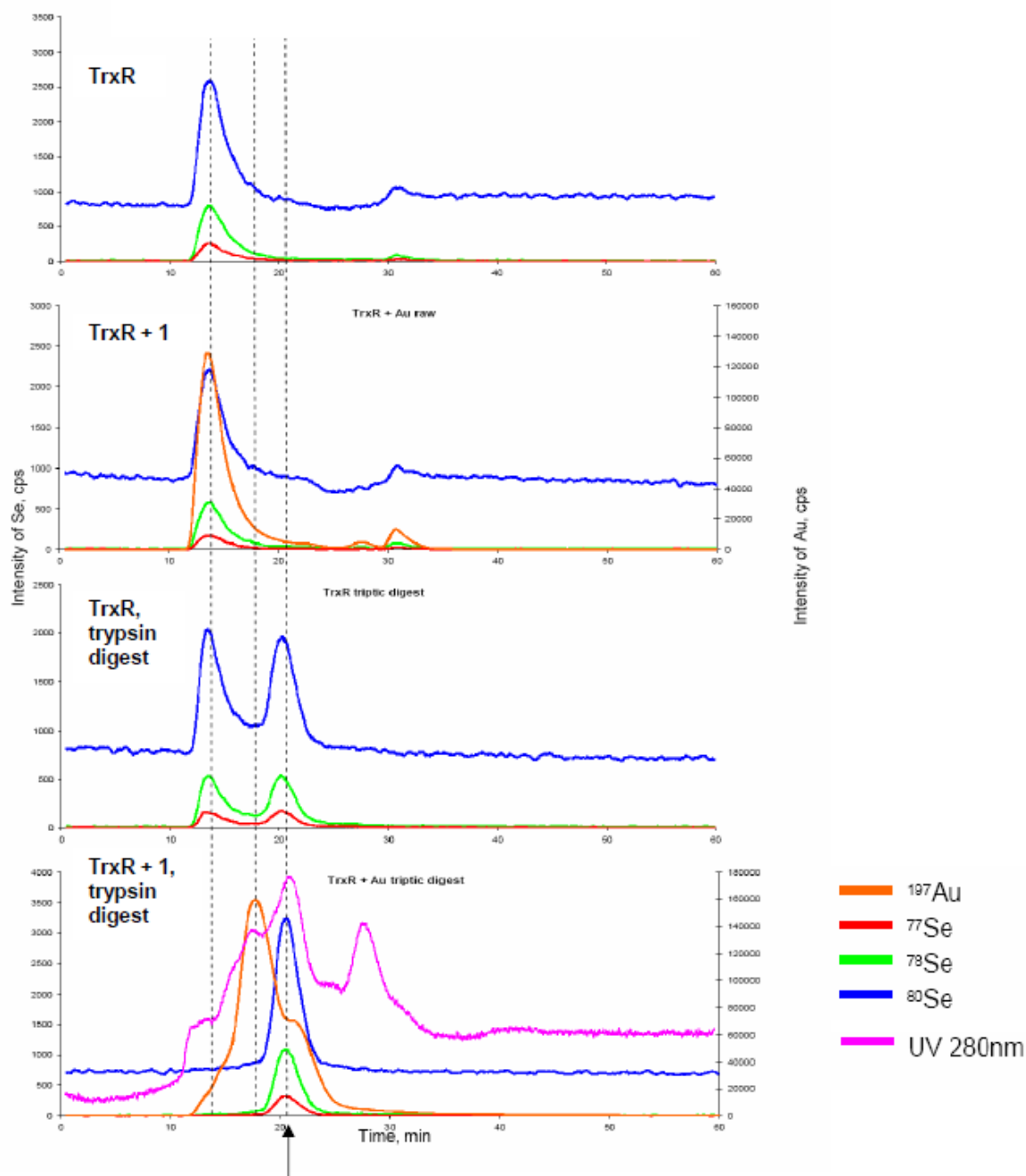


Figure 35 SEC-ICP-MS analysis of TrxR treated with  $[Au(TU)_2]Cl$  (Arrow indicates the peptide fraction co-eluted with Se and Au(218))

An attempt to identify the Au binding site by tryptic digestion of TrxR-Au adduct followed by MALDI resulted in the putative detection of peptide  $^{236}IGEHMEEHGIK^{246}$  and gold adduct. The authors proposed that the binding site for the Au ion occurred on histidine residues (His<sup>239</sup> or His<sup>243</sup>) (220). But, it is important to underline that the analytical procedure might have displaced Au from its initial binding site in the protein and resulted in its secondary binding and the formation of an artifact (220).

Another attempt concerned a TrxR mutant where selenocysteine-498 codon (TGA) was altered to cysteine (TGC) to promote the efficient production of TrxR in *E. coli*, the MALDI MS results suggest that terpyridine-platinum(II) binds directly to the sulfur in the GCCG motif of TrxR (337). In **Figure 36**, Lo *et al.* showed that compared to the TrxR1 mutant, TrxR1 incubated with the terpyridine-platinum display a shift of around 430, which is equivalent to the calculated –SGASILQAGCCG- peptide bound with one terpyridine-platinum moiety. This suggest that for platinum compound the active site of wild type TrxR1 could be located around the –SGASILQAGCUG- motif containing a free selenol moiety that displays higher reactivity than thiol.

Lu *et al.* (212) were able to identify via MALDI the <sup>488</sup>SGGDILQSGCUG<sup>499</sup> peptide of rat TrxR as interacting with arsenic. They speculate that arsenic binds more precisely with the <sup>496</sup>GCUG<sup>499</sup> fragment. As displayed on **Figure 37**, a shift is detected in the SGGDILQSGCUG peptide corresponding to a potential binding of Arsenic with the peptide.

## 6.4. Studies of model selenopeptides and other species

The use of mass spectrometry technique has permitted the study of the interaction between model peptide or LMW selenospecies and gold compounds. *Meier et al.*, (221) showed, via ESI-IT MS and ESI-TOF MS, the molecular interaction of Au (III) complexes with a mixture of amino acids (L-histidine, L-methionine, L-cysteine, L-glutamic acid, methyl seleno-L-cysteine (SeMe-Cys) and seleno-L-cysteine generated in situ). In this study, the different adducts between Au complexes and amino acids were characterized, and binding preferences were described. Molecular reactivity patterns and binding sites have been correlated with inhibition of TrxR. The interaction of complexes with SeCys was proved to cause potent inhibition of TrxR, even going to induce strong antiproliferative activity in some of the cases studied. In addition, the authors point out the importance of evaluating the action of ligands released after coordination with the protein when considering the cytotoxic effects of its complexes (221).

Positive mode electrospray mass spectrometry was used to investigate complexes of cysteine and selenocysteine with auranofin (338). Auranofin has a labile complex, the thioglucose moiety acting as leaving group, which the gold binding primarily to sulfur atoms in bio-molecules. Its mode of action in this respect is similar to Pt-based cancer drugs that employ a leaving group to expose the Pt to bind to the nitrogen in adenine and guanine bases. No experimental evidence was found for a direct complex formation between methylselenocysteine and auranofin. However, in source, dissociation of auranofin and loss of a methyl group from methylselenocysteine, produced a complex involving the gold triethylphosphine moiety and selenocysteine (338).

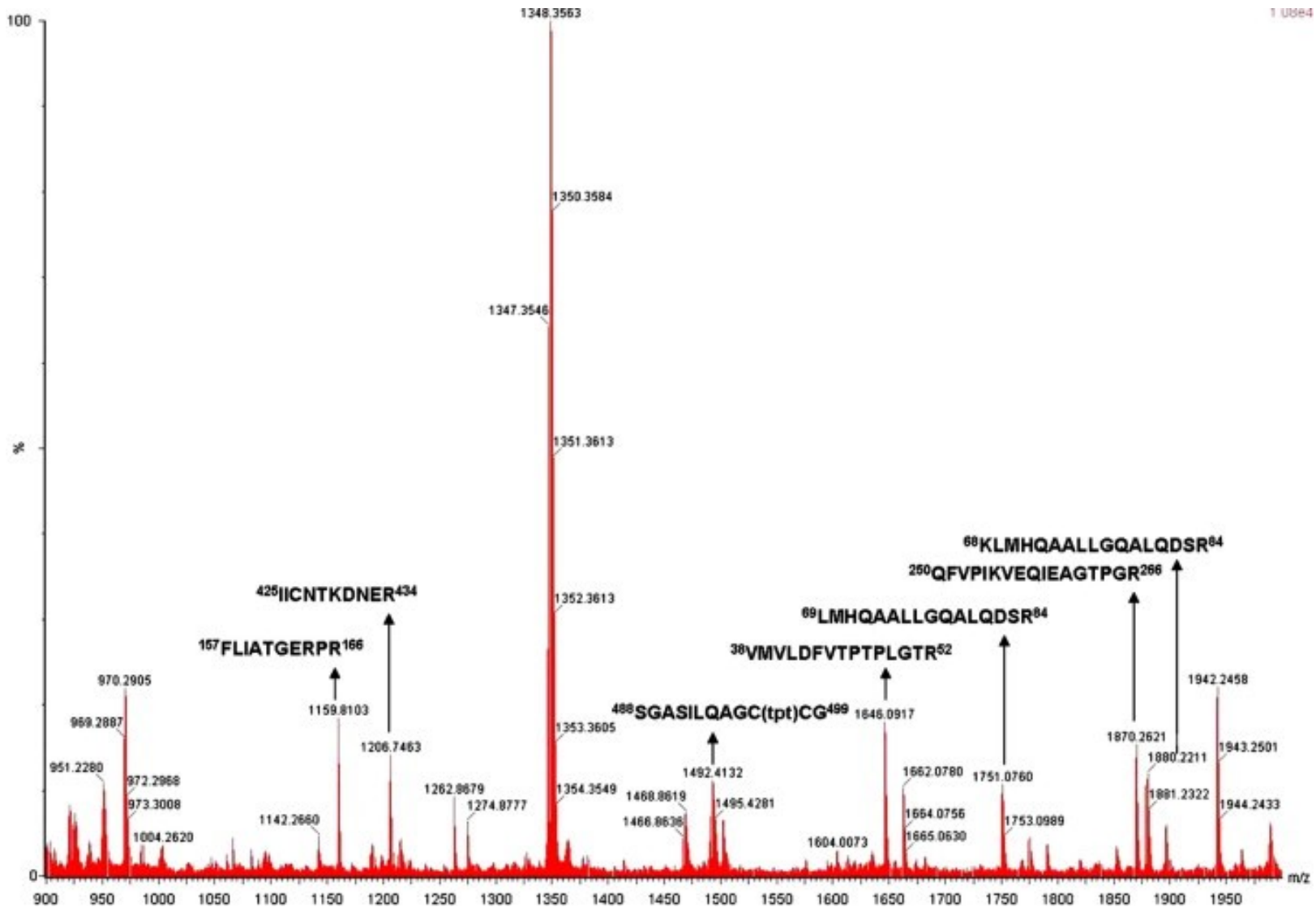


Figure 36 MALDI mass spectrometry of TrxR1 reduced by NADPH and incubated with terpyridine-platinum complex, *tpt* mean TP-Pt(II) (337)

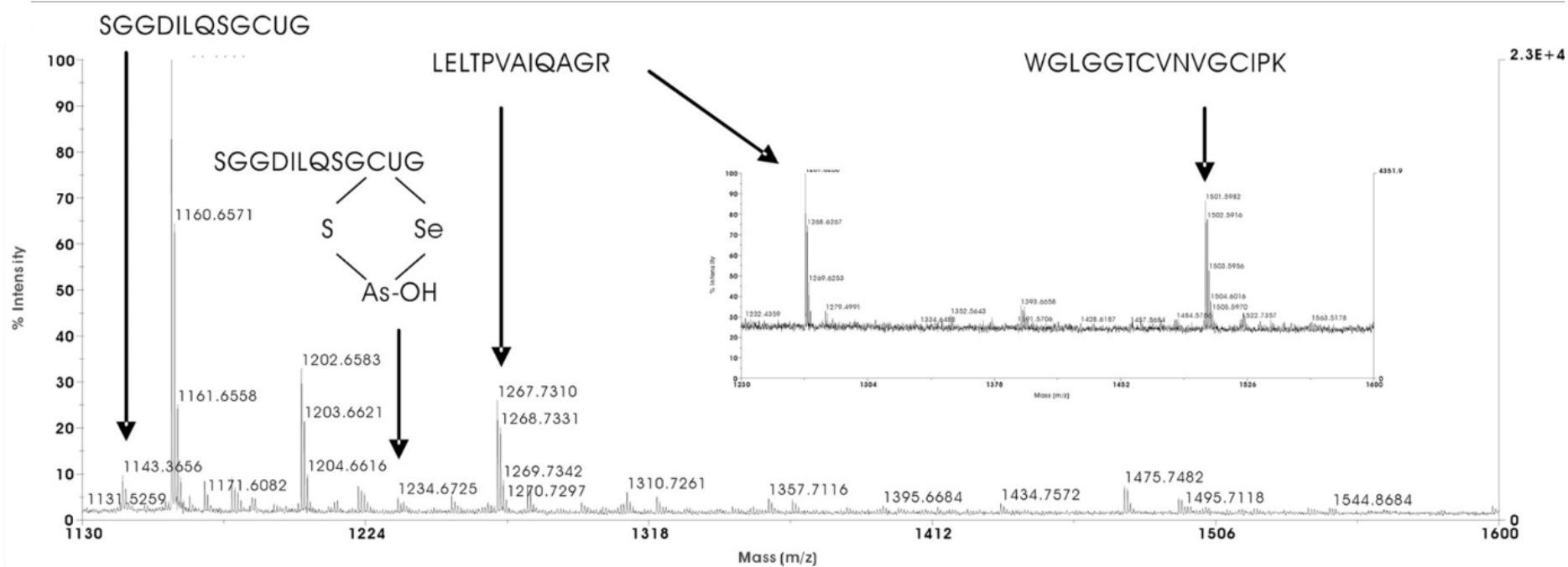


Figure 37 Peptide mass of TrxR-arsenic by MALDI mass spectrometry (294)



The kinetics and thermodynamics of ligand exchange reactions of auranofin with Cys, SeCys, His and Lys were analyzed in aqueous solution by means of DFT (density functional theory calculations). Two distinct reactions paths were followed, leading to the replacement of the thioglucose ligand (path-S) and the triethylphosphane moiety (path-P); selenocysteine was confirmed as the main target for auranofin (199).

Model investigations consisting of a competitive reaction of equimolar amounts of reduced cystamine and selenocystamine with QMs led only to the formation of the selenide adducts thus confirming selective alkylation of selenol at neutral pH as evidenced by ESI-MS analyses (207).

The comprehension of the reactivity on small selenium unity such as amino acids was completed with studies on a bigger model such as the model peptide of TrxR. **Ott *et al.*** (217) showed the coordination between the gold complex  $(PPh_3)AuCl$  and TrxR using a peptide model (Ala-Gly-Cys-Val-Gly-Ala-Gly-Leu-Ile-Lys) containing cysteine. A covalent bond between the Au(I) ion and the protein was detected, cysteine having been identified as the anchoring site of the "naked" Au(I) ion after the loss of its chloride ligand followed by that of phosphine (**Figure 38**). Even if this peptide is not derived from TrxR, the peptide is displaying a certain homology with the N-terminal part of TrxR.

Pratesi *et al.* (222) used a peptide model of the C-terminal motif of human TrxR containing SeCys to study its interactions with auranofin and other di-nuclear cytotoxic complexes of Au (III) using ESI-MS. In this study, the tetra-peptide Gly-[Cys-SeCys]-Gly (with an internal S-Se bridge) did not show any reactivity towards the Au complexes in the absence of reducing agents. In contrast, after pre-reduction with dithiothreitol (DTT), binding between the peptide and auranofin was detected with loss of its ligand tetraacetatethioglucose and retention of  $PEt_3$ . MS/MS analysis revealed that the SeCys residue is the preferential Au coordination site. They also demonstrated the presence of a second coordination site at the Cys residue.

A top-down  $MS^2$  approach confirmed that the preferential coordination site of Au (I) complexes, with its NHC ligand, is indeed the residue of SeCys, and that cysteine plays the role of secondary coordination site (223). The linear di-coordinated gold(I) complexes studied had the same carbene ligand (i.e., 1,3-diethylbenzimidazol-2-ylidene) on one side and a second ligand (chloride, a second NHC ligand (identical to the first one) or triphenylphosphine) on the other. The peptide (most likely through its selenolate group) is able to displace – at least partially – the second ligand from gold(I) coordination; the substitution reaction appears to be progressively more difficult and less efficient upon passing from chloride to carbene to phosphine (223). In **Figure 39**, auranofin is displaying a nice interaction with the peptide, several auranofin adducts are observed from naked gold to  $AuPEt_3^+$  which indicated multiple interaction sites on the peptide with the -CU- peptide region being pointed at the possible anchor for those ligands.

Notably, no reaction takes place in the absence of reducing agents. However, when the peptide was pre-reduced with DTT and treated with the various gold drugs a number of new species of greater molecular mass were formed. Auranofin binding takes place through the replacement of the thiosugar moiety while the phosphine ligand is kept. The preferential binding site, confirmed by MS/MS spectrum, is selenocysteine followed by cysteine; no evidence was obtained for any gold centre bridging the adjacent selenocysteine and cysteine residues nor for peptide binding of bare gold(I) ions (222). On the other hand, with two different gold (III) compounds resulted in the same product identified as a DTT/ $Au(I)_2$ /tetrapeptide species implying that gold (III) reduction has taken place (222).

The comprehension of interaction mechanism on model peptide have also led to the understanding of the reactivity of natural tryptic digestion peptide interaction with gold compounds. MS / MS mass spectrometry technique made it possible to identify several active sites along with the protein. The use of MALDI-TOF-MS showed a significant metallation of TrxR after incubation with an excess of Auranofin (200). In more detail, up to 4 fragments of  $AuPEt_3^+$  (Auranofin ligand) can bind to TrxR1, indicating a large number of binding sites available for the gold atom; as a result, not only selenocysteine (SeCys) but probably also cysteines, methionines and histidines. Another study by **Gabbiani *et al.***, (219) showed a similar reactivity of TrxR with gold-based compounds Au (I) (auranofin and aurothiomalate), but also Au complexes (III)). They were able to demonstrate a quasi-quantitative binding of TrxR1 with these gold complexes, up to 10 equivalents of gold adduct were formed following the incubation of TrxR1 in the presence of these complexes in excess, thus confirming the presence of multiple sites of interactions accessible on the protein other than SeCys.

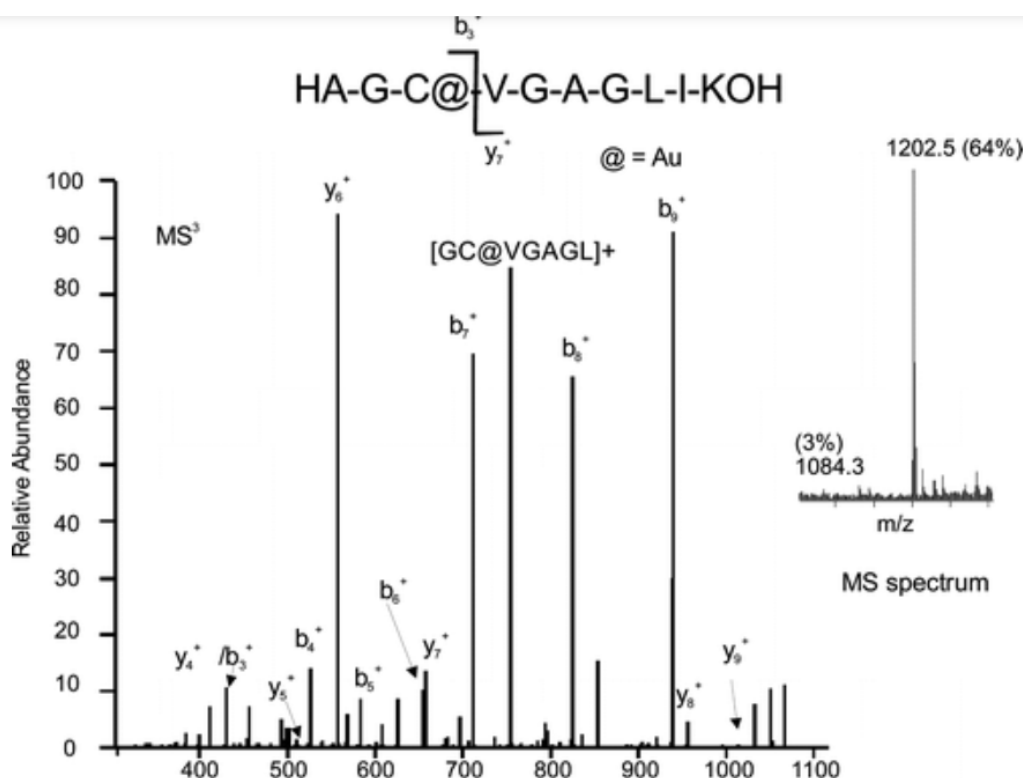


Figure 38 MS/MS spectrum of the molecular ion  $[peptide + Au]^+$  generated by neutral loss of triethylphosphine from the adduct  $[peptide + Au(PEt_3)]^+$  peptide = AGCVGAGLIK (217)

The C-terminal dodecapeptide of thioredoxin reductase containing the characteristic –Gly–Cys–SeCys–Gly metal-binding motif was found able to trigger gold(III)-to-gold(I) reduction of  $Au_2phen$ ,  $AuL12$ , and  $Aubipyc$ ; the main adduct formed corresponded to the binding of a gold(I) ion to the peptide (**Figure 40**)(339). The different coordination sites demonstrated by the further studies are as follows, thiols, selenols, and to a lesser extent, histidines.

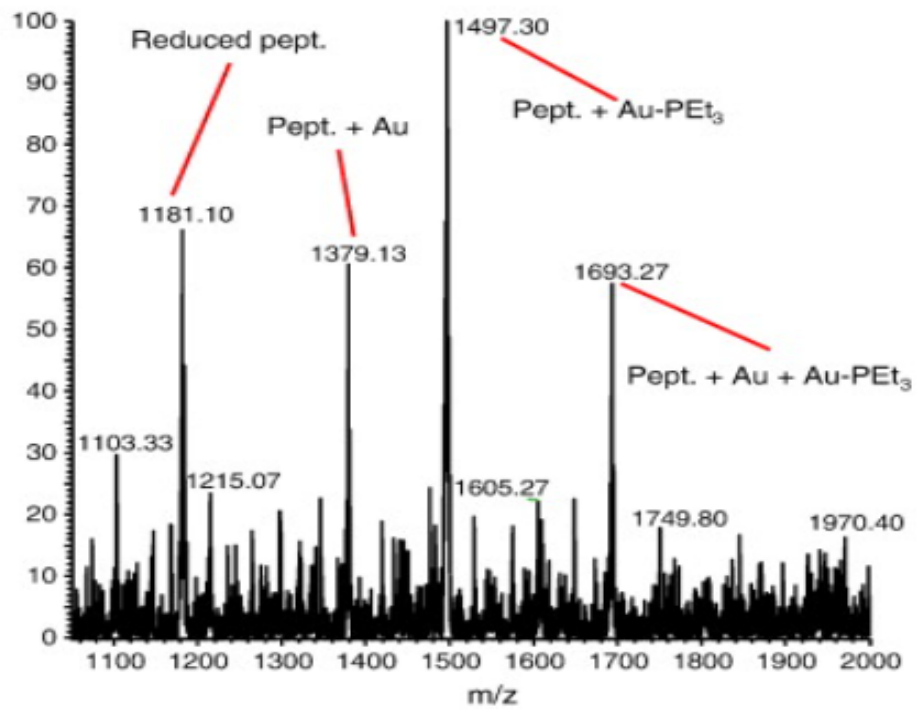


Figure 39 ESI-MS spectrum of the synthetic dodecapeptide Ac-SGGDILQSGCUG-NH<sub>2</sub> incubated with auranofin, acquired in negative ion mode (223)

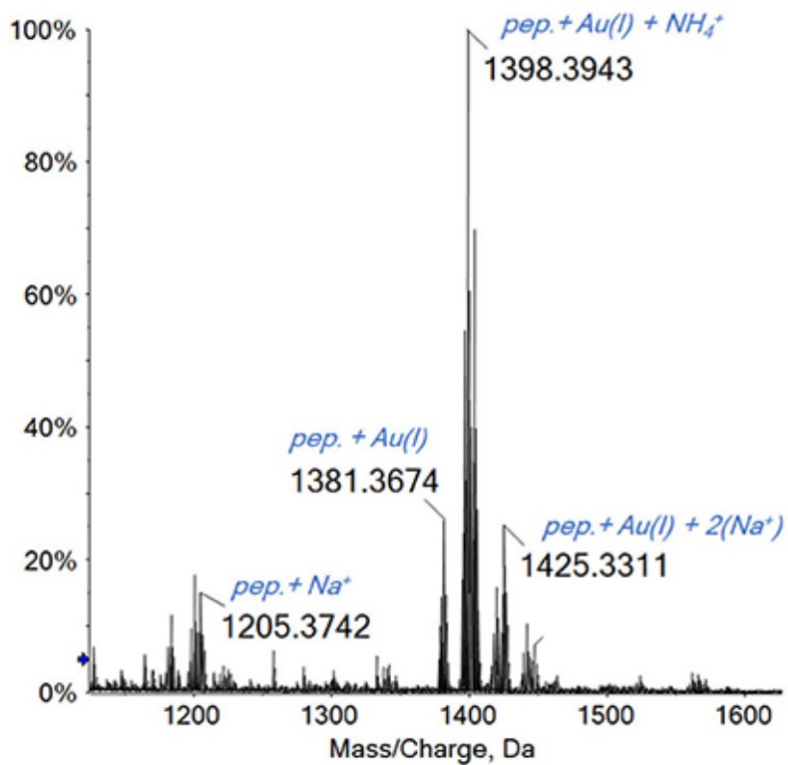


Figure 40 Electrospray ionization spectra of the dodecapeptide with Au<sub>2</sub>ph (339)





Whereas the detoxification effects of selenium by its action on metals, such as e.g. Hg, and inhibitory effects of selenoenzymes have been extensively demonstrated, molecular evidence of the binding environment has been relatively scarce. Studies of probing the selenium binding by molecule-specific techniques, such as mass spectrometry or, by chemical bond-specific techniques, such as extended X-ray absorption fine structure (EXAFS) spectroscopy, have been largely limited to thioredoxin reductase. Consequently, the development of methods allowing an insight into the metal-binding site and the type of liaison induced by such binding is of considerable interest to study further the mechanisms linking selenium to the detoxification of heavy metals or therapeutic action of metallodrugs.

The question is the more important because selenium occurs in biology in several forms, such as selenols (SeH), diselenides (-Se-Se-) and -Se-S- bridges each in potential competition with the sulfur analogues, such as thiols (-SH) and disulfides (-S-S-). The situation is complicated by the role played by the steric availability of Se or S containing sites and the presence of other binding motifs (Lys, His, Met) within the protein structure that can bind the metal and compete with the Se-containing sites.

Selenium in human blood and tissues occurs at the sub nanomolar levels. This fact together with the complexity of the matrix, makes molecular studies in vivo be able to be successfully carried out by only a small number of advanced instrumental techniques, and notably by mass spectrometry. The recent developments in the sensitivity of chromatography with selenium specific detection (ICP MS) and in resolution and sensitivity of electrospray MS offer a number of attractive tools to probe selenium metal interactions. Even so, investigations of model compounds, either isolated from serum, or synthesized for the particularly attractive selenium environment, have their place in molecular studies of Se-metal interactions.

Metallodrugs, such as Pt and Au compounds, have attracted recently a considerable interest as targets for selenium species. As indicated above, they have almost all been limited to an enzyme thioredoxin reductase and its proxies (mimics). An important factor facilitating these studies, in addition to the undeniable interest in the demonstration of TrxR inhibition by metallodrug, has been the possibility of expression of the protein and thus, its availability in pure form. However, TrxR is by far not the most abundant protein in human serum. Several others exist, all containing at least one selenocysteine residue, free or oxidized to form a Se-S or Se-Se bridges. Out of these proteins, the most abundant is SELENOP which has up to 10 selenocysteine residues. While evidence of the formation of stable covalent complexes of SELENOP with heavy metals does exist, there have been virtually no studies probing the specificity of the binding to selenium and the nature of the binding site. One of the reasons for that was the impossibility of the heterogenous expression of SELENOP. Consequently, the protein for the metal interaction studies has to be isolated and purified from natural serum, which can be quite a challenge knowing that the total Se concentration in Se is about 100 ng/ml and SELENOP accounts only for 1/3 to 1/2 of it.

One of the goals of this thesis has therefore been to revisit the SELENOP isolation schemes reported elsewhere in order to develop a method able to produce sufficient quantities of SELENOP to produce measurable Se species-specific signals for mass spectrometric studies of SELENOP interactions with Au and Pt compounds. For this purpose, different types of affinity chromatography, such as IMAC or heparin, standing alone or in sequence, have been revisited. Emphasis has been placed on the optimization of the inter-chromatography concentration steps and the monitoring of SELENOP

recovery. Different chromatographic conditions have been tested to obtain the highest resolution spectrum for each step and to increase the recovery of each step of the purification.

An inherent element of the thesis has been an extensive characterization of the isolate selenoprotein by high resolution high accuracy mass spectrometry. However strange it may sound, very little of mass spectrometry evidence for the amino acid sequence data of SELENOP exists in the literature. Consequently, a method based on the tryptic digestion and HPLC MS/MS spectrometry has had to be developed in order to demonstrate the chemical identity of the isolated and purified protein and acquire support data for the interpretation of data on the SELENOP interactions with Pt and Au compounds.

The ultimate objective relative to SELENOP has been to investigate its binding with auranofin and cisplatin, probing the formation of the SELENOP – metal compounds and acquiring molecular evidence on the binding sites of Au and Pt.

The ease of oxidation of SeCys residues to form Se-Se bonds raises a burning question of their reactivity with metallodrugs. While it is now well documented that auranofin and its analogues bind rapidly and tightly to proteins bearing free cysteines or selenocysteines, the ability of these gold compounds to interact directly with disulfide and diselenide bridges and cleave them is much less understood. This has prompted us to investigate in detail the reactions of auranofin and its analogues with model molecules containing disulfide and diselenide motifs.

For this purpose, we have decided to use, as a model, the selenium analogue ([Se-Se]-AVP, **Figure 41a**) of the hormone vasopressin (AVP, **Figure 41b**, a nonapeptide cyclized by two cysteine residues, best known for its antidiuretic and vasopressor actions (340). [Se-Se]-AVP, in which both AVP Cys residues have been replaced by selenocysteine (SeCys) residues, is characterized by an internal Se-Se bridge and retains full affinity of the AVP towards the vasopressin receptor (341).

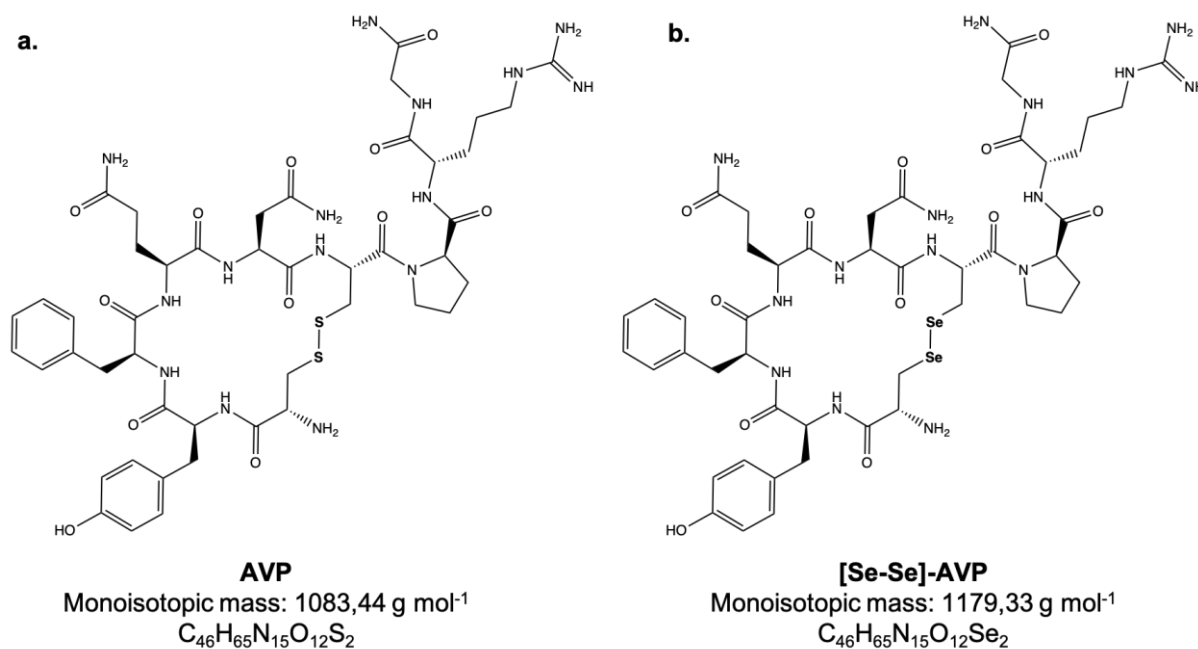


Figure 41 Chemical structure of a) vasopressin and b) selenovasopressin

## ***EXPERIMENTAL SECTION***



## 8.1. Samples

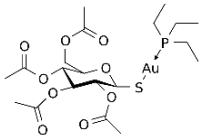
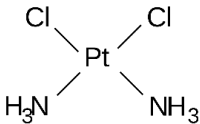
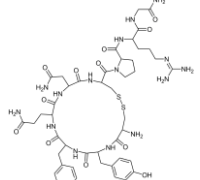
*Human blood serum* was purchased from Pan<sup>TM</sup> Biotech (*Aidenbach, Allemagne*). Serum collection was done aseptically; after being collected, the coagulated blood was centrifuged, then pooled and frozen. Samples are then taken to check the batch's compliance with the defined requirements (determination of the level of endotoxins, control of contamination by viruses, measurement of pH and osmolarity). The serum is then filtered through a succession of filters, the last of which has a porosity of 0.2  $\mu\text{m}$ . The serum is finally packaged in PETG bottles. All these steps are carried out under a laminar flow hood and in class 100 white rooms under aseptic conditions. When received, serum is divided in aliquot of 20mL and stored at  $-80^{\circ}\text{C}$ .

## 8.2. Metallodrugs and model compounds

*Vasopressin and selenovasopressin*. For the vasopressin part of the thesis, auranofin and its analogues were synthesized by the group of Pr. L. Messori (University of Florence, Italy) and Selenovasopressin was synthesized by the group of Pr. G. Subra and Pr. C. Enjalbal (IBB, Montpellier, France). Samples were stored at  $4^{\circ}\text{C}$ .

All commercial reagent used are presented in **Table 9**.

*Table 9 Commercial reagent used*

| Species     | Chemical formula or species   | Provider      | Location                   |
|-------------|---|---------------|----------------------------|
| Auranofin   |  | Sigma-Aldrich | Saint-Louis, Missouri, USA |
| Cisplatine  |  | Sigma-Aldrich | Saint-Louis, Missouri, USA |
| Vasopressin |  | Eurogentec    | Seraing, Belgique          |

## 8.3. Chemicals

All chemicals used during the thesis are presented in **Table 10**.

## 8.4. Buffers

To prepare buffers for the chromatographic separations, chemicals were weighed and dissolved in  $\text{H}_2\text{O}$ . Once the salt was dissolved, pH was adjusted using either ammonia or HCl solution. For organic buffers acetonitrile and  $\text{H}_2\text{O}$  were mixed together in adequate proportions.

*Table 10 : Chemicals used*

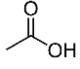
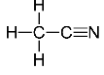
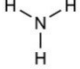
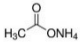
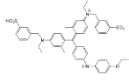
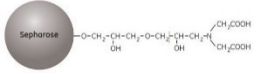
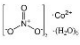
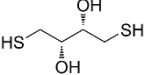
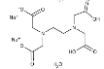
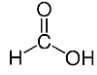
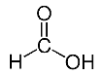
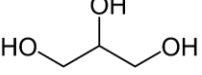
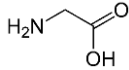
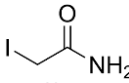
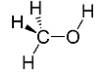
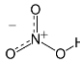
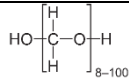
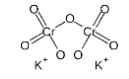
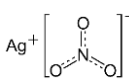

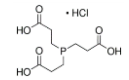
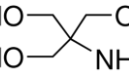
| Species                          | Chemical formula or species   | Provider          | Location                           | Purity  |
|----------------------------------|---|-------------------|------------------------------------|---------|
| Acetic acid                      |    | Sigma-Aldrich     | Saint-Louis, Missouri, USA         | 99%     |
| Acetonitrile                     |    | Honeywell         | Charlotte, North Carolina, USA     | ≥ 99.9% |
| Ammonia solution                 |    | Fisher            | Hampton, New Hampshire, USA        | 35%     |
| Ammonium acetate                 |    | Sigma-Aldrich     | Saint-Louis, Missouri, USA         | ≥ 98%   |
| Bovine serum albumin             | Bovine  | Sigma-Aldrich     | Saint-Louis, Missouri, USA         | ≥ 96%   |
| Brilliant Blue G                 |    | Sigma-Aldrich     | Saint-Louis, Missouri, USA         | 100%    |
| Chelating Sepharose Fast Flow    |    | Cytiva            | Cytiva, Dassel, Germany            | 100%    |
| Cobalt(II) nitrate hexahydrate   |   | Sigma-Aldrich     | Saint-Louis, Missouri, USA         | ≥ 98%   |
| Criterion TGX precast gels 8-16% | Acrylamide gels   | Biorad            | Uppsala, Sweden                    |         |
| Dithiothreitol                   |  | Fisher            | Hampton, New Hampshire, USA        | 100%    |
| EDTA disodium salt 2 hydrate     |  | PanReac AppliChem | Barcelona, Spain                   | 100%    |
| Formic acid                      |  | Merck             | Merck, Kenilworth, New Jersey, USA | ≥ 98%   |
| Formic acid for LC-MS            |  | Merck             | Merck, Kenilworth, New Jersey, USA | ≥ 98%   |
| Glycerol                         |  | Sigma-Aldrich     | Saint-Louis, Missouri, USA         | 100%    |
| Glycine                          |  | Sigma-Aldrich     | Saint-Louis, Missouri, USA         | 100%    |
| Iodoacetamide                    |  | Sigma-Aldrich     | Saint-Louis, Missouri, USA         | 100%    |
| Methanol                         |  | Honeywell         | Saint-Louis, Missouri, USA         | ≥ 99.9% |
| Nitric acid                      |  | Fischer           | Hampton, New Hampshire, USA        | 67%     |

Table 11 : Chemicals used (following)

| Species                                     | Chemical formula or species   | Provider      | Location                    | Purity  |
|---|---|---------------|-----------------------------|---------|
| Paraformaldehyde                            |  | Sigma-Aldrich | Saint-Louis, Missouri, USA  | 95%     |
| Potassium Dichromate                        |  | Sigma-Aldrich | Saint-Louis, Missouri, USA  | 100%    |
| Silver nitrate                              |  | Merck         | Kenilworth, New Jersey, USA | 100%    |
| Sodium Dodecyl sulfate                      |  | Sigma-Aldrich | Saint-Louis, Missouri, USA  | 100%    |
| Tris(2-carboxyethyl)phosphine hydrochloride |  | Sigma-Aldrich | Saint-Louis, Missouri, USA  | 100%    |
| Trizma base                                 |  | Sigma-Aldrich | Saint-Louis, Missouri, USA  | ≥ 99.9% |
| Trypsin from porcine pancreas               | Porcine   | Sigma-Aldrich | Saint-Louis, Missouri, USA  |         |

#### IMAC buffers:

- Buffer A: 0.5 M ammonium acetate pH 7.
- Pre-buffer: 0.5 M ammonium acetate + Formic acid pH 4.1
- Buffer C: 0.5 M ammonium acetate pH 4.1 obtained by mixing 50/50 v/v of Buffer A and PreBuffer
- EDTA washed solution: 200 mM of EDTA pH 7
- Cobalt solution: 0.1 M of  $\text{Co}(\text{NO}_3)_2 \cdot 6\text{H}_2\text{O}$
- EtOH 20% cleaning solution: 20% of ethanol absolute in water

#### Heparin buffers:

- Buffer D: 0.1 M ammonium acetate
- Buffer E: 1.5 M ammonium acetate
- EtOH 20% cleaning solution: 20% of ethanol absolute in MQ water

#### Chromatographic ICP MS buffers:

- Buffer SEC: 25-100 mM ammonium acetate pH 7
- Buffer MonoQ: A: 20 mM Trizma base; B: 20 mM Trizma base, 250 mM  $\text{NH}_4\text{Cl}$  pH 7.5

#### Chromatographic ESI-MS buffers:

- A:  $\text{H}_2\text{O}$  0.1% formic acid
- B: ACN 0.1% formic acid



## 8.5. Instrumentation and materials

### 8.5.1. Sample preparation equipment

All reagents and chemicals were weighed on an analytical balance XT 220A Precisa. The adjustments of pH of chromatographic mobile phases separation were done using a Five-easy pH-meter (Mettler Toledo, Columbus, Ohio, USA). All solutions were prepared using HPLC grade solvent and Milli-Q water (18.2 M $\Omega$  cm) obtained from a water purification system Elix<sup>®</sup> from Millipore, Burlington, Massachusetts, USA). Solutions are loaded on the affinity column using a peristaltic pump from Ismatec<sup>®</sup> (Wertheim, Germany). For samples centrifugation Eppendorf MiniSpin centrifuge by Eppendorf (Hambourg, Allemagne) for small vial and Eppendorf centrifuge 5804 R with a rotor A-4-44 were used. The sample concentration before digestion was carried out using a Freeze-dryer from Cryotec (Saint-Gély-du-Fesc, France). The digestion of samples was carried out using a Digi Prep MS (SCP Science, Villebon-sur-Yvette, France).

The enzymatic digestion of sample was carried out using a heat block Dri-Block<sup>®</sup>, DB200/2 from Techne (Morancé, France) and a mixing devise KS250basic from IKA-Werke (Staufen im Breisgau, Allemagne). All vials' tubes use after the final purification steps are protein Lo-bind grade. All 96 well-microplate, flat bottoms are from Greiner Bio (Madrid, Spain).

### 8.5.2. High pressure liquid chromatography and columns

Several chromatographic systems were used:

#### *For purification steps:*

- An Agilent 1200 Series (Agilent, Tokyo, Japan) pump with a UV-module, automated sampler, and fraction collection module, were used with the IMAC, heparin and SEC column that was previously calibrated for the protein molecular mass and elution volume.
- An Agilent 1200 Series (Agilent, Tokyo, Japan) pump was used to either dilute the sample prior ICP-analysis on purification steps or in analysis mode to purified SELENOP, the HPLC was used with SEC and MONOQ column.
- A Dionex Ultimate 3000 RS (ThermoFischer Scientific, Germering, Germany) was used for reverse-phase chromatography

#### *For MS characterization of selenoprotein P:*

- A UPLC Dionex Ultimate 3000 RS (ThermoFischer Scientific, Germering, Germany) pump was used for reversed-phase HPLC.
- A nanoUPLC Dionex Ultimate 3000 RS (ThermoFischer Scientific, Germering, Germany) was used with C18 Acclaim PepMap<sup>™</sup> that was calibrated using Pierce HeLA Protein Digest Standard from (ThermoFischer Scientific)

#### *For MS characterization of selenoprotein P with auranofin and cisplatin:*

- A nanoUPLC Dionex Ultimate 3000 RS (ThermoFischer Scientific, Germering, Germany) was used with C18 Acclaim PepMap<sup>™</sup> that was calibrated using Pierce HeLA Protein Digest Standard from (ThermoFischer Scientific)

*For MS characterization of vasopressin, selenovasopressin with auranofin:*

- A UPLC Dionex Ultimate 3000 RS (ThermoFischer Scientific) was used with C18 Acclaim™ 120

HPLC operating conditions for all the columns used during the thesis are presented in **Table 12**.

### *8.5.3. Inductively coupled plasma mass spectrometry*

The ICP MS instrument used and illustrated in **Figure 42** was Agilent Model 7700s (Agilent, Tokyo, Japan) equipped with a collision cell with hydrogen as collision gas, to reduce the spectral interferences. The ICP system consisted of a 50 mL/min micro-mist U nebulizer (Glass Expansion, Friedenbachstrasse, Germany), a Scott type spray chamber, a 1 mm i.d. injector torch (Agilent, Tokyo, Japan), and a set of nickel cones (sampler and skimmer cones) for total analysis and platinum cones in the case of coupling with HPLC where organic solvents were used. The experimental parameters, such as plasma power, torch position, the voltage on extraction and focusing lenses were optimized every day by using a tune solution containing 1 µg/L each of Li, Mg, Y, Ce, Tl and Co in 2% HNO<sub>3</sub>. Typical operating conditions are given in **Table 13**.



*Figure 42 ICP-MS Agilent Technologies model 7700s*

### *8.5.4. Electrospray mass spectrometry*

*For selenoprotein P characterization:*

The electrospray ionization mass spectrometer used was Orbitrap LUMOS Fusion (**Figure 43**, *ThermoFisher Scientific*, Germering, Germany) in positive ionisation mode with an ESI ion max NG source.

Table 12 HPLC Column operating conditions

| Column name                              | Company, Location                                    | Interaction  | Mobile phases  | Condition   | Gradient  | Column diameter  | Particle size | Porosity |
|--|--|--|--|---|---|--|---------------|----------|
| IMAC Sepharose                           | Cytiva, Dassel, Germany                              | Chelating metals with reacting histidine exposed protein | A: 0.5M ammonium acetate, pH 7<br>B: 0.5M ammonium acetate, pH 4.1 | Flow: 5mL/min<br>Max Pressure: 20 bar<br>Injection volume: 25mL   | 0-20min 0% B, 20-40min 15% B, 40-55min 15% B, 55-70min 25% B, 70-90min 25% B, 90-100min 35% B, 100-105min 100% B, 105-140min 100% B, 140-141min 0% B, 141-145min 0% B | 2.6cm x 200 mm (loaded with 25mL of Chelating Sepharose Fast flow) | 90 µm         |          |
| Heparin                                  | Cytiva, Dassel, Germany                              | Heparin affinity   | A: 0.1M ammonium acetate<br>B: 1.5M ammonium acetate               | Flow: 5mL/min<br>Max Pressure: 20 bar<br>Injection volume: 1L     | 0-30min 0% B, 30-35min 70% B, 35-40min 100% B, 40-55min 100% B, 55-60min 0% B, 60-70min 0% B  | 1.6cm x 2.5 cm   | 34 µm         |          |
| Superdex™ 75kDa PC3.2/300 GL             | Sigma-Aldrich, Saint-Louis, Missouri, USA            | Pore size  | 0.1M ammonium acetate, pH 7  | Flow: 0.7mL/min<br>Max Pressure: 40 bar<br>Injection volume: 5µL  | Isocratic   | 30cm x 3.2 mm  | 9 µm          |          |
| SEC Acquity UPLC BEH 125 SEC Gold Column | Waters, Etten-Leur, The Netherlands                  | Pore size  | 0.1M ammonium acetate, pH 7  | Flow: 0.3mL/min<br>Max Pressure: 400 bar<br>Injection volume: 5µL | Isocratic   | 4.6 mm x 3.0mm   | 1.7 µm        | 125 Å    |
| C18 Acclaim™ 120                         | ThermoFisher scientific, Waltham, Massachusetts, USA | hydrophobic  | A: H <sub>2</sub> O 0.1% formic acid<br>B: ACN 0.1% formic acid    | Flow: 1mL/min<br>Max Pressure: 310 bar<br>Injection volume: 10µL  | 0-7min 5% B, 7-8min 95% B, 8-9min 95% B, 9-10min 5% B   | 4.6mm x 100mm  | 5 µm          | 120 Å    |
| C18 Acclaim™ RSLC                        | ThermoFisher scientific, Waltham, Massachusetts, USA | hydrophobic  | A: H <sub>2</sub> O 0.1% formic acid<br>B: ACN 0.1% formic acid    | Flow: 0.3mL/min<br>Max Pressure: 600 bar<br>Injection volume: 5µL | 0-5min 5% B, 5-35min 55% B, 35-36min 90% B, 36-40min 90% B, 40-41min 5% B, 41-50min 5% B  | 2.1x250mm  | 2.2 µm        | 120 Å    |
| C18 Acclaim PepMap™                      | ThermoFisher scientific, Waltham, Massachusetts, USA | hydrophobic  | A: H <sub>2</sub> O 0.1% formic acid<br>B: ACN 0.1% formic acid    | Flow: 0.3µL/min<br>Max Pressure: 700 bar<br>Injection volume: 3µL | 0-5min 0% B, 5-10min 10% B, 10-110min 25% B, 110-120min 40% B, 120-121min 90% B, 121-130min 90% B, 130-131min 5% B, 131-140min 0% B                                   | 75 µm x 50cm   | 2 µm          | 100 Å    |
| Isolute C4 SPE columns                   | Biotage, Uppsala, Sweden                             | hydrophobic  | MeOH   | Flow: 2mL/min   | Cleaning process: 50% MeOH, 5% MeOH 0.1% FA<br>3x Sample loading<br>Cleaning of non-retained species: 5% MeOH Removing of the SELENOP: 80% MeOH                       |  | 59 µm         | 54 Å     |

If used with nanoUPLC Dionex Ultimate 3000 RS, the ESI source was replaced by a TriVersa Nanomate (Advion, Ithaca, New York, USA) using an injection chip with a coupler. The following parameters were adjusted: capillary temperature, carrier gas temperature, shielding gas pressure and spray voltage. Data processing was carried out in the Thermo XCalibur program and with Proteome discoverer for the experimental masses, Expasy software were used for the generation of theoretical masses. Optimized ESI conditions used during analysis have been grouped in **Table 14**.

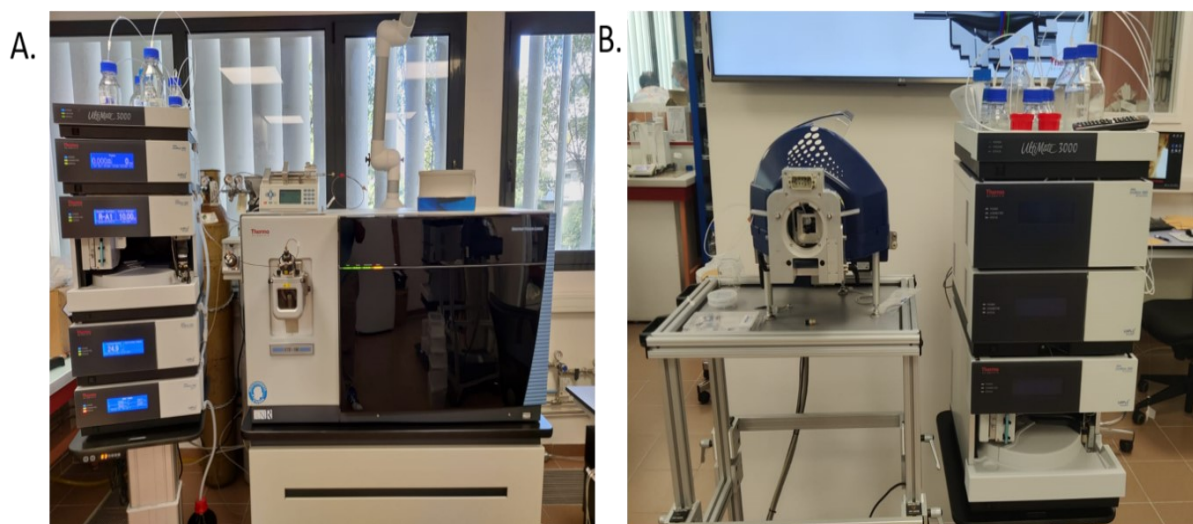
*For Selenovassopressin/auranofin interaction:*

The electrospray ionization mass spectrometer used was a Q Exactive plus quadrupole-orbitrap hybrid mass spectrometer (**Figure 44**, Thermofisher Scientific, Germering, Germany) in positive ionisation mode. The following parameters were adjusted: capillary temperature, carrier gas temperature, shielding gas pressure and spray voltage. Data processing was carried out in the Thermo XCalibur program used for the generation of theoretical masses and their comparison with experimental ones. Optimized ESI conditions used during analysis have been summarized in **Table 15**.

*Table 13 ICP-MS operating conditions*

| <b>Cones</b>                             | <i>Nickel</i> | <i>Platinum</i> |
|--|---------------|-----------------|
| <b>Plasma generator power</b>            | 1550 W        | 1550 W          |
| <b>Plasma gas flow rate</b>              | 1 L/min       | 0.64 L/min      |
| <b>Reaction gas (H<sub>2</sub>) rate</b> | 4.5 mL/min    | 4.5 mL/min      |
| <b>Optional gas (O<sub>2</sub>)</b>      | 0%            | 7.5%            |
| <b>Extraction lenses voltage</b>         | 4V            | 4 V             |
| <b>Focusing lenses voltage</b>           | -180 V        | -180 V          |
| <b>Quadrupole focus</b>                  | -10 V         | -10 V           |
| <b>Octopole bias</b>                     | -18 V         | -18 V           |
| <b>Quadrupole bias</b>                   | -15 V         | -15 V           |

*Figure 43 ESI-MS Orbitrap LUMOS Fusion A) with UPLC and B) TriVersa Nanomate and nanoUPLC*



*Table 14 ESI-MS LUMOS operating parameters*

|                              |                 |
|------------------------------|-----------------|
| <b>Polarization mode (V)</b> | Positive (1800) |
|------------------------------|-----------------|

|   |   |
|---|---|
| <b>Resolution</b>                         | 120000 for Ms (for Ms <sup>n</sup> 15000/30000) |
| <b>AGC</b>                                | 4.0e <sup>5</sup>                               |
| <b>Scan range</b>                         | 250-2000  |
| <b>Detector type</b>                      | Orbitrap  |
| <b>Activation type</b>                    | CID   |
| <b>Isolation mode</b>                     | Quadrupole                                      |
| <b>Ion transfer tube temperature (°C)</b> | 275   |
| <b>Max injection time (ms)</b>            | 50  |
| <b>RF Lens (%)</b>                        | 30  |
| <b>Chip SOFT Spraying voltage (kV)</b>    | 1.8   |



Figure 44 ESI-MS Orbitrap LUMOS Fusion with UPLC

Table 15 ESI-MS Q Exactive operating parameters

|                                |                   |
|--------------------------------|-------------------|
| <b>Polarization mode</b>       | Positive          |
| <b>Resolution</b>              | 140000            |
| <b>AGC</b>                     | 3.0e <sup>6</sup> |
| <b>Scan range</b>              | 300-2000          |
| <b>Detector type</b>           | Orbitrap          |
| <b>Activation type</b>         | CID               |
| <b>Isolation mode</b>          | Quadrupole        |
| <b>Max injection time (ms)</b> | 500               |
| <b>RF Lens (%)</b>             | 30                |
| <b>Spraying voltage (kV)</b>   | 3.8               |

Both ESI-MS instruments were calibrated weekly using a Pierce LTQ Velos ESI Positive Ion Calibration solution.

## 8.6. Methods

The following part describes the optimized methods used to isolate SeIP from human blood serum and for the studies of interaction of SeIP and SeAVP with auranofin.

### 8.6.1. Purification of selenoprotein P

Human blood serum was removed from a -80 °C freezer, and an aliquot of 20 mL was thawed at room temperature for 1 h. Once liquid, the aliquot is centrifuged and then, 7.5 mL of serum was recovered and diluted in 7.5 mL of water. This new aliquot is used for the purification, the rest of the 20 mL aliquot is kept at -20°C in a freezer for other analysis.

#### *Immobilized metal affinity chromatography separation*

The IMAC column was loaded with 25 mL of IMAC Chelating Sepharose (*on the right*) and kept at 4°C in 20% of ethanol when it was not used. A peristaltic pump was used for the loading of solutions.

The IMAC column was washed before every experiment using a 0.2 M EDTA solution at pH7, followed by 5 column volumes of water at 4mL/min. A freshly prepared solution of 0.1 M of  $\text{Co}(\text{NO}_3)_2$  was then loaded. The non-retained  $\text{Co}^{2+}$  was washed from the column with water. The column was then conditioned with 0.5M ammonium acetate pH 7 as a running buffer.

Serum samples were thawed each morning prior to the experiment, and centrifuged. Then, a 7.5mL aliquot was diluted twice with water. After the column was conditioned, the sample was loaded on the column at 2mL/min.



The column was then integrated into the dual-HPLC system coupled online with ICP-MS as shown in **Figure 45**. The separation of SELENOP from other proteins was followed using UV and ICP-MS. For this purpose, an online setup was developed and presented in detail in **Figure 46**.

The elution was realised with the first HPLC column at 5mL/min with the gradient presented in **Table 12**. The eluate was split into a 0.5 mL/min flow directed to UV-ICP MS and 4.5 mL/min to the fraction collector. Fractions were collected between 100 and 115 min. The rest of the flow that was directed through the UV module was split again with a second HPLC with water at 0.5mL/min to dilute by the solution prior ICP-MS analysis. This step was used to reduce the salt content of the solution to avoid clogging of the nebuliser, and to avoid sending a huge salt concentration into the ICP where  $^{59}\text{Co}$ ,  $^{60}\text{Ni}$  and  $^{78}\text{Se}$   $^{80}\text{Se}$  isotope were measured. After fraction collection, the solution was kept at 4°C to be used for heparin affinity separation.

The optimization of this method will be discussed in detail in **Chapter 9.1.1** (Results and discussion Section)

#### *Heparin affinity separation*

The heparin column was washed prior to each experiment using water (5 column volumes) and 0.1 M ammonium acetate buffer (5 volume) using a peristaltic pump at 1mL/min.

The solution collected after IMAC separation was diluted 10 times with and pH was adjusted to 5.8. The solution was then loaded overnight on a Heparin Hitrap<sup>TM</sup> 5mL column.

The column was then integrated into the dual HPLC system coupled online with an ICP-MS instrument as shown in **Figure 45**. The system was the same one as for IMAC, the only difference was the column used.



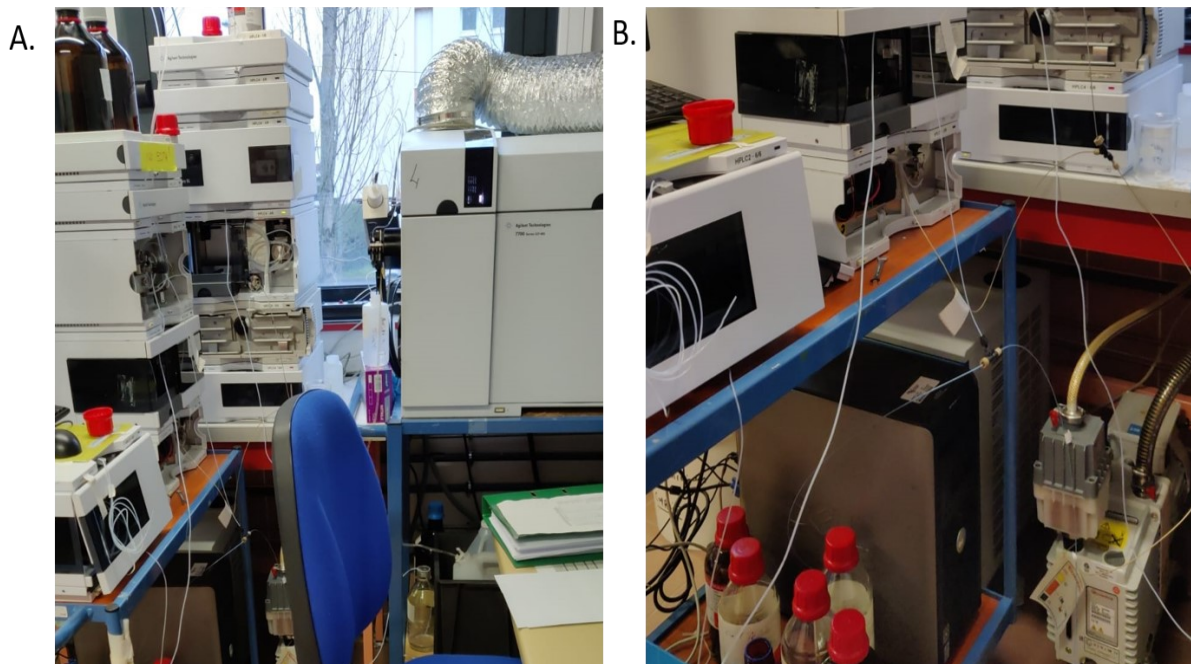


Figure 45 Dual-HPLC system coupled with ICP-MS A. DI-HPLC-ICP-MS, B. Split and capillary system used to connect the column with UV, ICP and dilution HPLC and fraction collector

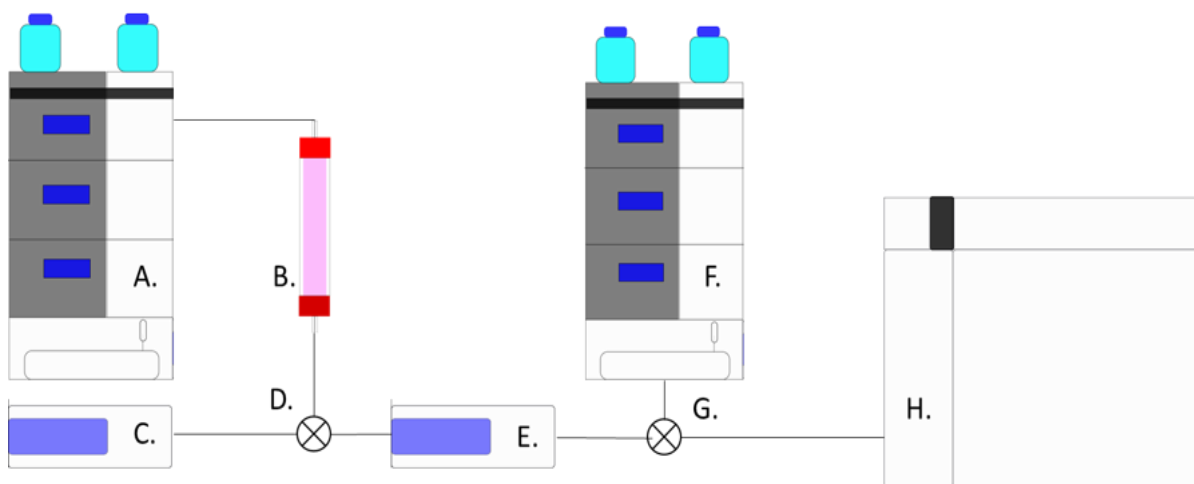


Figure 46 Schematic representation of the Dual-HPLC coupled with ICP-MS A. Separation HPLC with phase A and B, B. IMAC column loaded with serum, C. Fraction collection module, D. Split between column end, fraction collection and UV module, E. UV module, F. Dilution HPLC, G. Second split between UV end, Dilution HPLC and ICP-MS, H. ICP-MS

The elution was realised with the first HPLC column at 5mL/min with the following gradient with the gradient presented in **Table 12**.

The eluate flow was split into 0.5mL/min directed to UV-ICP MS and 4.5mL/min to the fraction collector. Fractions were collected between 34 and 38 min. Similar to the IMAC, the solution is also diluted with the second HPLC at 0.5 mL of water prior injection on ICP-MS.  $^{59}\text{Co}$ ,  $^{60}\text{Ni}$  and  $^{78}\text{Se}$   $^{80}\text{Se}$  isotopes were monitored. After fraction collection, the solution was kept at 4°C to be used for concentration, characterization and quantification methods.

### *Concentration method*

To realise further analysis on the sample, the  $\approx 20$  mL of Heparin fraction was concentrated. An SPE column Isolute C4 on visiprep 24™ DL from *Supelco* was used (Sigma-Aldrich, Saint-Louis, Missouri, USA) (*Figure 47*).



*Figure 47 SPE system used for SELENOP*

The column was washed using 20 mL of 50% MeOH, and 20 mL of 0.1% FA a solution in 5% MeOH. The sample was loaded 3 times on the SPE column. After the loading, the column was washed with 5 mL of 5% MeOH. Finally, the SELENOP was removed using 1 mL of 80% MeOH.

The solution was concentrated using SpeedVac concentrator plus (*Eppendorf, Hambourg, Allemagne*) at 30°C for 1 h. The final volume of the sample was 150  $\mu$ L.

Several other methods were used to concentrate the sample, they will be discussed in *Chapter 9.1.4* (Results and Discussion Section).

## *8.6.2. Quantification of selenoprotein P*

### *Total selenium quantification*

During the purification steps, aliquots of 1 mL were collected to quantify the recovery and concentration of selenium in serum. In the specific case of concentration methods, the whole sample was used.

Samples were frozen using liquid nitrogen and then dried using a freeze-dryer for 12h. After the drying process, a volume of 100  $\mu$ L of conc. HNO<sub>3</sub> was added to each sample. The samples were incubated overnight at 60 °C using a DigiPrep. Samples were then diluted with 2% HNO<sub>3</sub> and analysed by ICP-MS. Isotopes <sup>74</sup>Se, <sup>76</sup>Se, <sup>77</sup>Se, <sup>78</sup>Se, <sup>80</sup>Se, <sup>82</sup>Se were monitored, each sample was analysed in duplicate or triplicate as a function of the initial volume.



### *Protein quantification method*

Protein concentration was measured using a DC Protein Assay Kit from (Bio-Rad, Hercules, California, USA). The kit contains 3 solutions Reagent A, an alkaline copper tartrate solution, Reagent B, a dilute folin reagent and reagent S, a surfactant solution.

The DC (detergent compatible) protein assay is a colorimetric assay for protein concentration following detergent solubilization. The reaction is similar to the Lowry assay, but has been modified to save time. The DC protein assay requires a single 15-min incubation, and absorbance remains stable for at least 2 h.

A volume of 20  $\mu\text{L}$  of reagent S is diluted in 1 mL of reagent A. This new solution will be called A' and remained stable for 1 week. In the case of precipitation, the solution was heated and vortexed. Calibration solutions were prepared using BSA diluted in water at concentrations from 0 to 5  $\mu\text{g}/\mu\text{L}$ . The solutions were kept for 1 y at  $-24^{\circ}\text{C}$ . A 5 $\mu\text{L}$  sample aliquot and calibration solution were pipetted into the 96 well-microplates. Each sample or calibration solution was analysed in triplicate. A volume of 25 $\mu\text{L}$  of solution A' was added to each well, followed by addition of 200  $\mu\text{L}$  of reagent B. The solution was homogenized and incubated for 15 min.

Using a SPECTROstar<sup>nano</sup> (**Figure 48**), the absorbance was measured at 750nm.



Figure 48 Spectrophotometer SPECTROstarnano

### *8.6.3. Characterisation of selenoprotein P*

#### *Polyacrylamide gel electrophoresis*

The samples were dissolved (v/v) in a loading buffer containing 50mM of Trizma base (pH 7.5), 100 mM DTT, 2% (w/v) of SDS, 10% (v/v) of glycerol, 0.1% (w/v) of blue of bromophenol. A 5- $\mu\text{L}$  aliquot of each sample was loaded on the precast gel Criterion<sup>TM</sup>TGX<sup>TM</sup> 8-16% in each side of the gel a protein

ladder from Precision Plus Protein™ Dual Color Standards from Bio-rad (Hercule, California, USA) was added with a ladder from 10-250 kDa to determine the protein mass.

The electrophoresis was carried out at 100V for 1 h 30 min in a running buffer composed of 25 mM Trizma base, 3.5 mM of SDS and 192 mM of glycine. The gel was then removed and gently shaken for 1h in a coloration solution composed of 0.1% (w/v) of blue of bromophenol, 25% of methanol and 10% acetic acid. After 1h, the gel was transferred into another bath containing a destaining solution with 30% ethanol and 5% glycerol.

The gel was placed on a *slimlite reading plate* (Kaisercraft, Sydney, Australia) and a picture was taken using a cellphone.

#### *Bottom-up proteomics approach*

The samples were buffered to pH 7.5 to fall within the reactivity range of trypsin digestion activity. The samples were incubated at 37 ° up to 70 °C in the presence of DTT 1:10 eqs for 30 min and then let react with 1:10 eqs IAM (eqs were calculated thanks to protein dosage). Then 1:50eq of Trypsin was added and incubated overnight at 37°C. The reaction was stopped by addition of 1µL of formic acid. Samples were kept at -80 °C prior to analysis.

Two methods were used to identify SELENOP peptides in the samples:

- The first method used was nanoUPLC-TriVersa Nanomate-MS (Lumos). A nanoC18 column was placed at 40°C. The mobile phases were: A - 0.1% formic acid and B, 0.1% formic acid in 90% acetonitrile. The flow rate was 10 µL/min. Elution was performed with the gradient presented in **Table 11**. The sample injection volume was 3µL.
- The second method is using the UPLC-ESI-MS (Lumos). A C18 column was placed at 40°C. The mobile phases were: A - 0.1% formic, and B- 0.1% formic acid in 90% acetonitrile. The flow rate was 300 µL/min. Sample elution was performed with the gradient presented in **Table 12**. The sample injection volume was 10 µL.

#### *8.6.4. Studies of interaction between selenoprotein P and metallodrugs (auranofin and cisplatin)*

Stock solutions at 0.6 mM of Auranofin, and 0.1mM Cisplatin were prepared by dissolving the sample in DMSO.

For auranofin, aliquots of SELENOP (10µL) solution were diluted with 2 mM ammonium acetate buffer (pH 7.0). 10eq of DTT or TCEP were added to the peptide solution. Then, 3 to 10 equivalents of auranofin were added to protein solution. The mixtures were left under stirring overnight at 37 °C up to 70 °C in a water bath.

For cisplatin, aliquots of SELENOP (10µL) solution were diluted with 2 mM ammonium acetate buffer (pH 7.0). 10 eqs of DTT or TCEP were added to SELENOP solution. Then, 3 to 10 eqs of cisplatin were added to the protein solution. The mixture was left under stirring overnight at 37 °C up to 70 °C in a water bath.

The samples were then incubated overnight at 37 °C in the presence of 1:50eq of trypsin under stirring. After being neutralized with 1µL of formic acid, the sample was frozen and kept at -80°C until analysis.

Liquid chromatography separations were performed by nanoUHPLC. Data obtained from on-line detection by MS were used for the identification of the reaction products.

#### *8.6.5. Studies of interactions between vasopressin, diselenovasopressin and auranofin*

Stock solutions of AVP 0.92 mM, [Se-Se]-AVP 0.85mM, DTT 0.4 M and TCEP 0.1 M were prepared by dissolving the samples in ultrapure water.

Stock solutions (10 mM) of auranofin, Au(PEt<sub>3</sub>)Cl, Au(PEt<sub>3</sub>)Br, Au(PEt<sub>3</sub>)I, and Au(PEt<sub>3</sub>)<sub>2</sub> were prepared by dissolving the sample in DMSO.

##### *Reduction studies*

For the reduction of [Se-Se]-AVP, aliquots of its stock solution were diluted with ammonium acetate solution 2 mM (pH 7.0) to 0.1 mM final peptide concentration. Then, aliquots of DTT or TCEP stock solution were added in peptide to reducing agent ratios 1:10, 1:100, 1:200 and 1:400 (1 mM, 10 mM, 20 mM, and 40 mM, reducing agent concentration respectively). Those mixtures were explored over different T (from 37 °C up to 70 °C) and at incubation time (from 30 min up to 5 h).

[Se-Se]-AVP aliquots were also incubated, without reducing agents, at 70 °C overnight in a water bath under stirring.

##### *Incubation with gold(I) compounds*

Aliquots of peptide stock solution were diluted with 2 mM ammonium acetate solution pH 7.0 to 0.1 mM final peptide concentration. Then, 3 equivalent of gold (I) compounds (AF, Et<sub>3</sub>PAuCl, Et<sub>3</sub>PauBr, Et<sub>3</sub>PauI or [Au(PEt<sub>3</sub>)<sub>2</sub>]Cl were added to the peptide solution (0.3 mM of final gold (I) compound concentration). The mixtures were left under stirring overnight at 37 °C or 70 °C in a water bath.

After the incubation, all solutions were sampled and diluted to a final peptide concentration of 6 μM using 2 mM ammonium acetate pH 7, 2% (v/v) of ACN and used for LC-MS analysis.

##### *LC-MS analysis*

After the incubation, all solutions were sampled and diluted to a final peptide concentration of 6 μM using 2 mM ammonium acetate pH 7.0, 20% (v/v) of ACN and 0.1% (v/v) of formic acid and used for LC-MS analysis.

Separation and identification of samples were performed by LC-MS/MS (Q-Exactive).

## ***RESULTS AND DISCUSSION SECTION***



This section describes the development of a methodology to isolate and quantify SELENOP from serum. For this purpose, a multiaffinity chromatography separation has been developed. ICP-MS was used to monitor the selenium signal. The combination of IMAC affinity chromatography first described by Sidenius *et al.* (274) and the well-known heparin affinity chromatography extensively described over the last decade (143, 238, 270) has been revisited. The aim was to separate SELENOP from the other proteins present in human serum and to preconcentrate it for the purpose of characterization and studies of interactions with metalldrugs.

## 9.1. Purification of selenoprotein P from serum

### 9.1.1. Optimisation of immobilized metal affinity chromatography

SELENOP possesses two histidine stretches (cf. **Figure 11**.) which are responsible for its retention by IMAC chromatography and offer the possibility to separate it from other seral proteins. Cobalt (II) has been chosen as the chelated ion in the stationary phase according to Sidenius *et al.* (274).

#### *Initial experiments*

Initially, serum aliquots of 20 mL were filtered using 0.45 µm filter to remove potential protein precipitate before injection on IMAC column. However, the recovery of selenium turned out to be poor. About 50% of the serum selenium content was retained on the filter, reducing considerably the amount of selenium to be injected on the IMAC column and thus potentially diminishing the recovery of SELENOP. Therefore, filtration was abandoned and the sample was prepared as described in **Chapter 8.6.1 (Experimental section)**. The centrifugation was implemented to remove the potential clot. Less than 1% of serum selenium content was detected in the clot.

The initial IMAC Sepharose column used was prepared with 50 mL of Chelating Sepharose resin. A solution of 25 mL at 0.1 M of Co<sup>2+</sup> was loaded on the column. The preparation of the column described in Chapter 8.6.1, took 3h with ca. 750 mL of solvent used. The initial gradient lasted 6.5 h and used 2.5 L of buffer A and 1L of buffer C (cf. **section 8.4**). A volume of 15 mL of sample was taken for each experiment. Originally, the experiment was not performed online, but 40 fractions were collected from the elution time range between 200 and 300 min. 10 µL of each fraction was diluted in 100 µL of HNO<sub>3</sub> 2% and injected on ICP-MS. **Figure 49** shows that the signal of selenium was low meaning that sample selenium concentration seems low. Little information was obtained on the loss of selenium during sample loading, corresponding to Fraction 0 (F0).

Following this initial experiment, it was attempted to improve the efficiency of the IMAC purification steps using a different stationary phase (Sepharose 6 fast flow from Cytiva (Dassel, Germany)). However, almost no Se signal was observed. After this result, a new chelating sepharose phase (Chelating Sepharose fast flow from Cytiva (Dassel, Germany)) was purchased and investigated. This second phase was giving results that was matching the initial work performed by Ouerdane *et al.* in our lab.

To determine where the loss of selenium was occurring, the initial experiment was modified. A split was installed to divide the flow 1/5, to the ICP MS and to the fraction collector, respectively. As it is presented in **Figure 50**, a considerable improvement was observed in terms of the Se signal intensity. The origin of the low signal that was observed in the initial experiment was coming from the dilution factor. The fractions were diluted 10 times, which reduced the signal from 2500 cps to 250 cps. To improve the signal on the ICP and reduce the salt content, a new HPLC was introduced in the system to

dilute the sample prior to injection on ICP, adding a second split connected to the flow going to ICP and adding 0.5 mL of MQ water to the 1/5 flow resulted in a dilution. A two-fold dilution was decided as a compromise between signal and salt concentration.

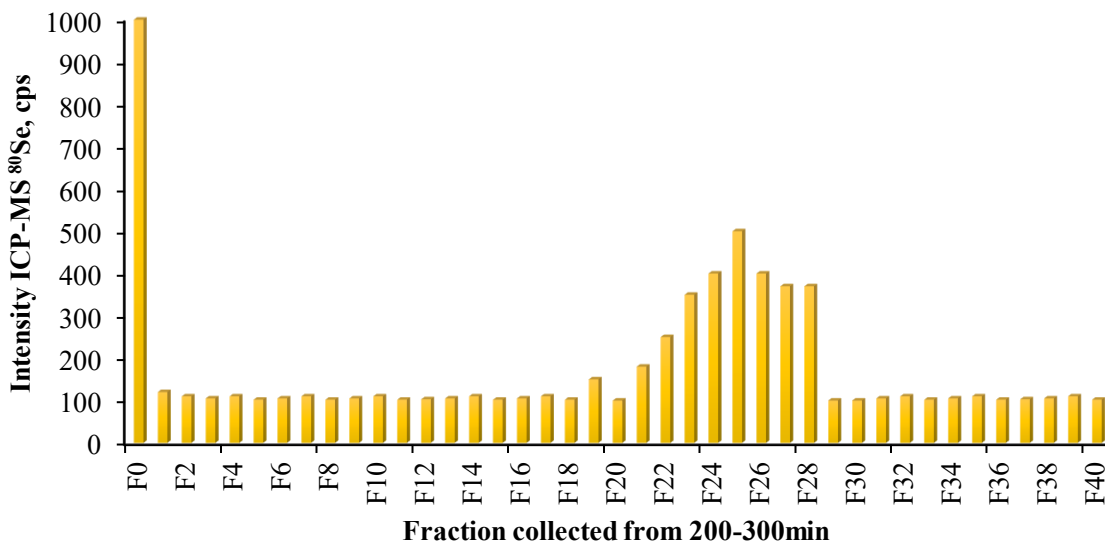


Figure 49 Chromatogram of the initial SELENOP purification method using fraction collection

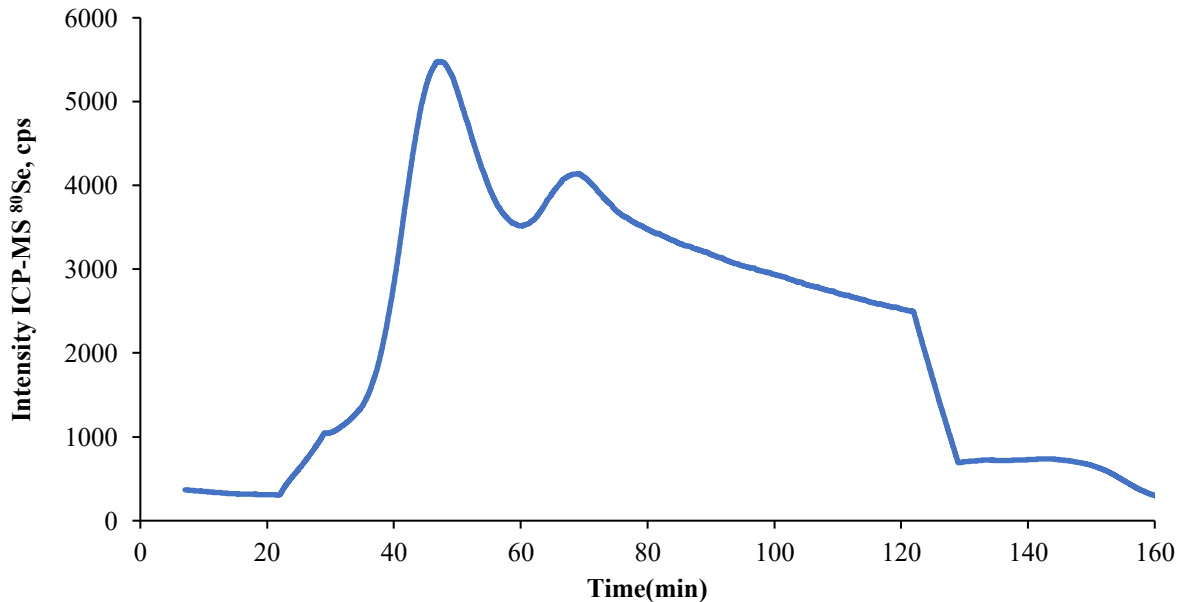


Figure 50 Online analysis of IMAC purification of SELENOP with initial gradient from 200-360min

### The miniaturisation of the experiment

A major problem about the purification of SELENOP was linked to solvent and sample consumption and the duration of the experiment. A complete purification via IMAC of SELENOP took originally 12h. Therefore, to reduce the time of the experiment, it was attempted to downscale the experiment.

The column volume was first reduced to 5 mL as the initial volume of the column was 50 mL, every parameter was reduced by 10. The amount of serum used was tested from 0.5 to 1.5 mL to see if the

column capacity was still enough to handle 1.5 mL. As your result showed, 750  $\mu$ L was the best compromise to obtain the maximum signal for SELENOP. The duration of the experiment was reduced to 1h, but the amount of Se recovered was very low, less than 1ng of selenium and judged to be too low to perform other purifications steps efficiently.

A compromise between time and sample quantity was found. First, the column volume was reduced from 50 mL to 25 mL, thus reducing the time of the experiment twice. Then, the optimization of the gradient allowed the reduction of the overall time by 2.5 to reach the final time of the experiment of 145 min.

#### *Influence of temperature on loading and binding of selenoprotein P*

In proteomics, the degradation of proteins is the main concern during long purification methods. In our case, the purification was performed at room temperature, due to the ICP localisation. However, the loading was technically possible at 4°C. Experiments were performed to answer the question of whether the loading temperature influenced the final result.

Two comparative experiments were performed in similar conditions with only the loading temperature as a different parameter. One experiment was performed with loading at room temperature (20°C) and the other one was performed in the cold room at 4°C. As illustrated in **Figure 51**, about 2/3 of the signal was lost with the loading at 4 °C. This phenomenon can be explained because SELENOP is potentially less active at cold temperatures and does not appropriately interact with  $\text{Co}^{2+}$  present in the stationary phase. Consequently, the SELENOP binding was less efficient and the amount of non-retained selenospecies increased.

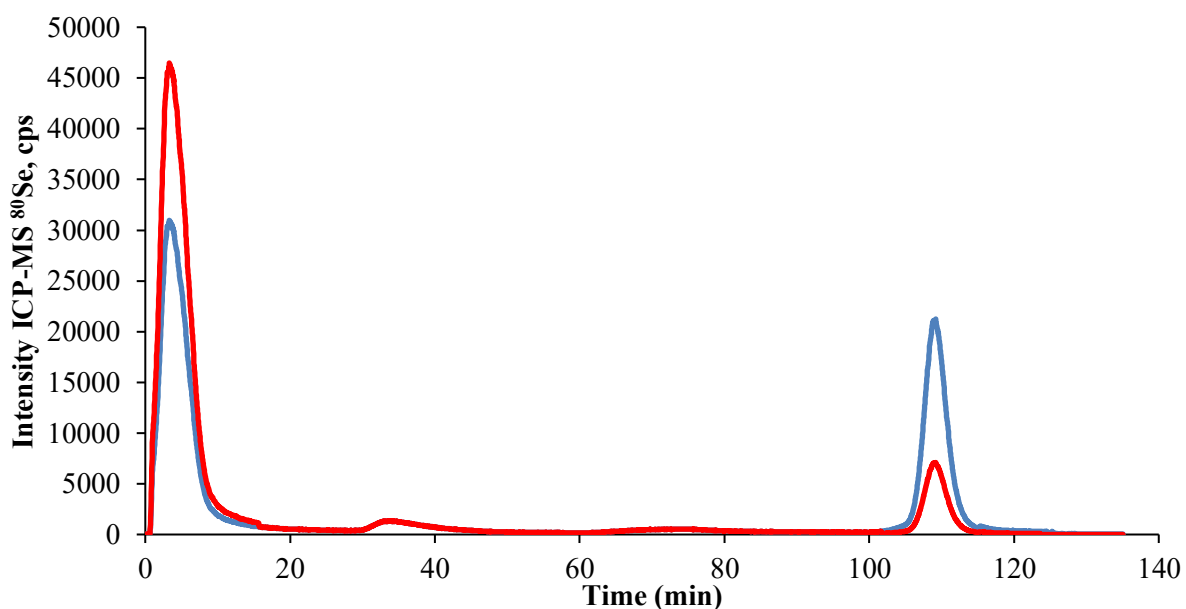


Figure 51 Comparative experiment of the effect of temperature in the binding of SELENOP with IMAC stationary phase (red curve 4°C, blue curve 20°C)

#### *Influence of $\text{Co}^{2+}$ concentration and non-chelating $\text{Co}^{2+}$ on loading and binding of selenoprotein P*



Experiments were performed to test the influence of  $\text{Co}^{2+}$  excess on the binding capacity of IMAC. The  $\text{Co}^{2+}$  concentration was set to 1 M of  $\text{Co}^{2+}$ . However, no significant difference was observed between 0.1 M and 1 M concentrations. A solution (pH 7.4) of 20 mM imidazole, 20 mM sodium phosphate and 0.5 M NaCl, was also tested to increase the binding, the solution is used to clean the column after the chelation of the metal to remove all non-chelating  $\text{Co}^{2+}$  that are free and could impair the correct binding of the protein with the stationary phase. This solution was supposed to remove unbound  $\text{Co}^{2+}$  from the column but no significant difference between experiments with or without these cleaning steps was observed.

### 9.1.2. Optimized selenoprotein P purification using immobilized metal affinity chromatography

The optimization resulted in the purification of SELENOP illustrated in **Figure 52**. Two Se peaks with a similar area can be observed. The first peak corresponds to the non-retained fraction of selenium-containing among others, Gpx and proteins with low or no histidine that could be observed by the UV signal. ICP-MS obtained this chromatogram after a dilution by 2 using MQ water introduced by the second HPLC. Proteins with histidine stretches are retained on the column. In order to remove them, a pH gradient from 7 to 4.1 was applied. SELENOP was eluted from the column at 100 min with 100% of Buffer C (0.5 M Ammonium acetate, pH 4.1). The UV signal shows that the amount of protein decreased during the gradient; there was no absorbance when SELENOP was collected. Therefore, it can be concluded that the majority of proteins are not retained on the column and that SELENOP could have been considerably enriched. Note that the results are similar to those reported by Reyes *et al.* (290). Even if the affinity column used was not the same, the morphology of the chromatogram was the same with a first peak corresponding to the non-retained species is observed from 0 to 15min and the second peak corresponding to SELENOP is observed from 105 to 118 min. Depending on the Se isotope followed, the height difference between both peaks can vary,  $^{80}\text{Se}$  was selected for the high signal in cps obtained but the spectrum with  $^{78}\text{Se}$  display and a smaller difference between the first and the second peak, that difference in height can be explained by the fact that  $^{78}\text{Se}$  has less interferences than  $^{80}\text{Se}$  which can overestimate the signal of  $^{80}\text{Se}$ .

**Table 16** shows the synthesis of all the parameters used in the optimized IMAC procedure. The optimization allowed us to obtain narrow peaks with good reproducibility. Indeed, for 7 experiments, a standard deviation of the SeLP peak was less than a minute.

### 9.1.3. Repurification of selenoprotein P using heparin affinity

In order to increase the purity of the SELENOP isolated by IMAC, a second purification step using its affinity to heparin was developed like the one from Heitland *et al.* (174). SELENOP was loaded overnight at pH 5.8 on the column at 4°C after being diluted 10 times. Using a salt gradient of 1.5 M of ammonium acetate, SELENOP was removed from the column. As it was shown in **Figure 53**, SELENOP eluted at 38 min with a gradient of 75% of Buffer E. No other selenoproteins were observed, indicating that the separation made with IMAC was sufficient to remove other seleno-species. The UV trace showed however, that SELENOP was not the only protein remaining on the column which means that IMAC was not sufficient to separate SELENOP from other proteins, confirming the need for a second purification step.

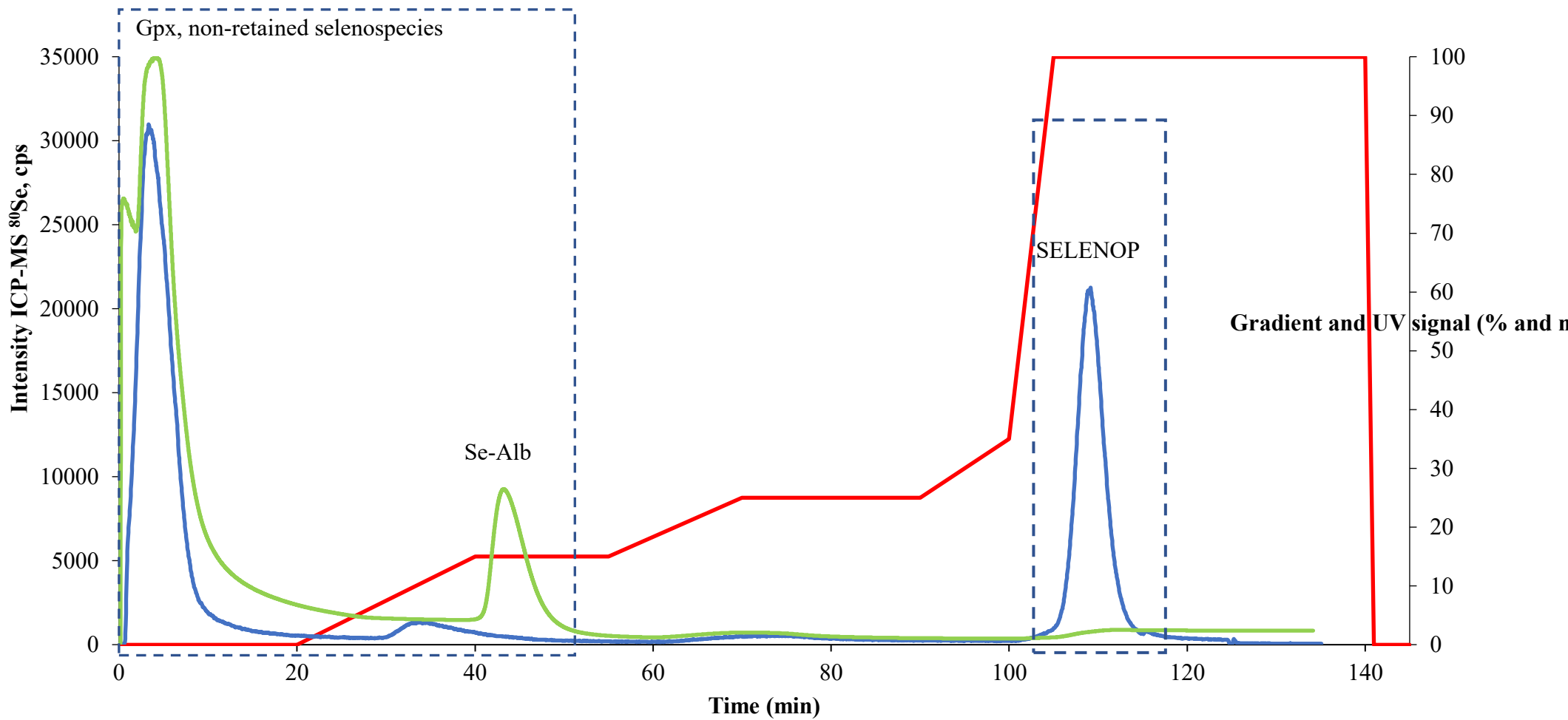


Figure 52 Chromatogram of IMAC purification (Phase IMAC Sepharose, Mobile phase (A :0.5M ammonium acetate, C: 0.5M ammonium acetate) Gradient described in red correspond to the percentage of C with UV 254nm

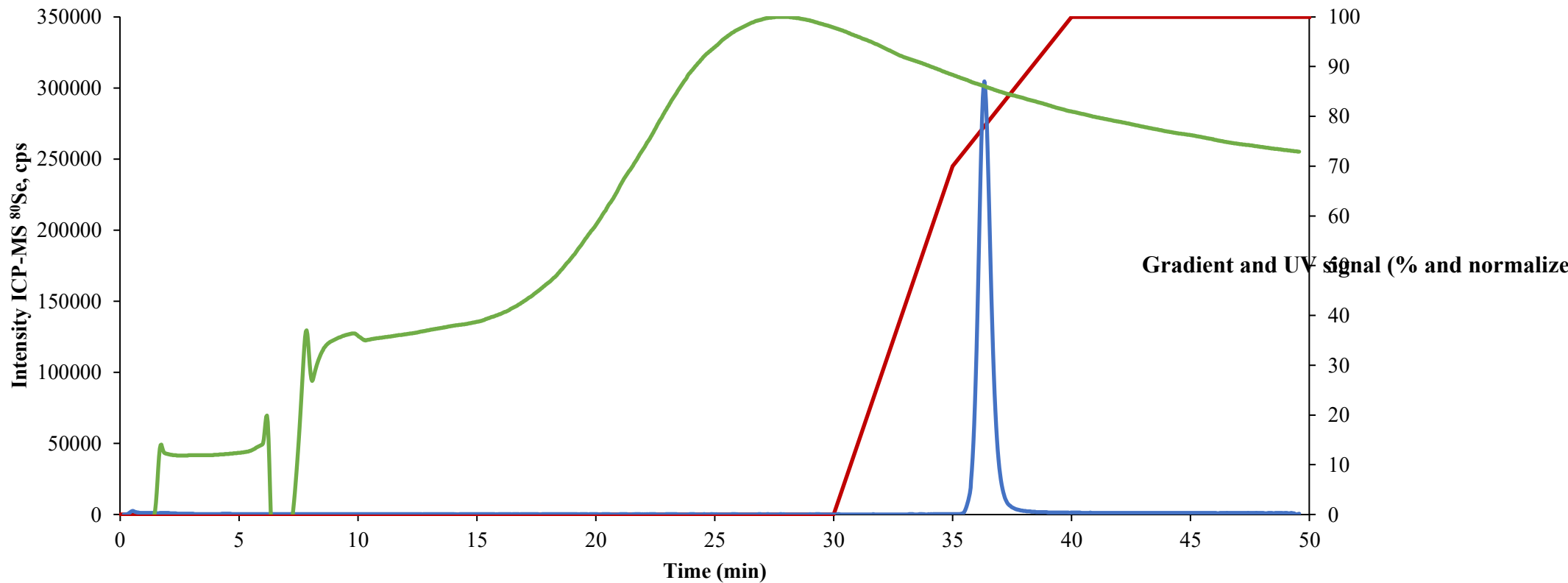


Figure 53 Chromatogram of repurification of SELENOP (Phase Heparin, Mobile phase (D :0.1M ammonium acetate, E: 1.5M ammonium acetate) Gradient described in red correspond to the percentage of E with UV 254nm

During the conception of the Heparin purification, we have tested some parameters to obtain the graph presented above. The first crucial parameter is the size of the column. Heparin Hitrap is commercially available in 2 forms 1mL and 5mL column. When working with a 1mL column, a 10% recovery was obtained after Heparin by quantification even if the amount of serum introduced in the IMAC was changed. To overcome that problem, increasing the size of the column was decided, and using a 5mL column gave much better recovery (71%).

Another parameter that was checked is temperature. Heparin is used mainly at low temperatures (4°C), but we decided to check if working at 20°C could improve the binding of the protein to the column. Unfortunately, no real difference was observed between the two temperatures, so the loading of the SELENOP solution was maintained on heparin at 4°C to avoid possible degradation overnight.

*Table 16 Parameters used to increase the efficiency and recovery of IMAC chromatography*

| Parameters                            | Threshold                           | Results (fixed parameter)                      |
|---------------------------------------|-------------------------------------|--|
| Sample Amount                         | 0.5-15mL                            | 7.5mL of serum for each experiment.            |
| Stationary phase amount (column size) | 5-50mL                              | 25mL of stationary phase.                      |
| Temperature                           | 4-20°C                              | 20°C.  |
| Metal concentration                   | 0.1-1 M Co <sup>2+</sup>            | 0.1 M of Co <sup>2+</sup>                      |
| Pre-column cleaning                   | With/Without Imidazole solution     | without cleaning the non-bind Co <sup>2+</sup> |
| Type of stationary phase              | IMAC Fast Flow/ Sepharose Fast flow | Sepharose Fast flow                            |
| Pre-filtration of Serum               | With/Without                        | no filtration was made.                        |
| Dilution of sample prior analysis     | From x2 to x10                      | x2 dilution.                                   |

The final parameter that was changed is pH, the heparin column was used at a pH of 7, but unfortunately, the SELENOP was not well retained on the column and working with a pH of 5.8 was displaying the best result (**Figure 54**), so the pH was fixed at 5.8. Using pH 5.8 was helped us to improve by 5 the signal of selenium compared to the one with pH 7 and to reduce the peak width.

#### *9.1.4. Concentration of selenoprotein P after heparin separation*

The purification of protein results in most of the cases in a heavy dilution of the sample. To reduce this effect, it is widespread to concentrate the protein afterwards using the cut-off filters.

For the purpose of concentration SELENOP eluted from the heparin column, we investigated a number of cut-off filters summarized in **Table 17** and centrifugation.

However, more than 99% of the selenium was lost on either of the filters, so other concentration methods needed to be considered and tested.

One of them was freeze-drying. However, due to a relatively large volume (20mL) collected after heparin purification, it was time-consuming. More important, no SELENOP protein could be recovered after freeze-drying. One hypothesis to explain this phenomenon is that the protein had precipitated during freeze-drying. In such a case, urea is recommended to facilitate the solubilization of the protein. However, even with an 8 M concentration of urea, the protein was not resolubilized and could not be observed in gel or in ESI-MS analysis after tryptic digestion.

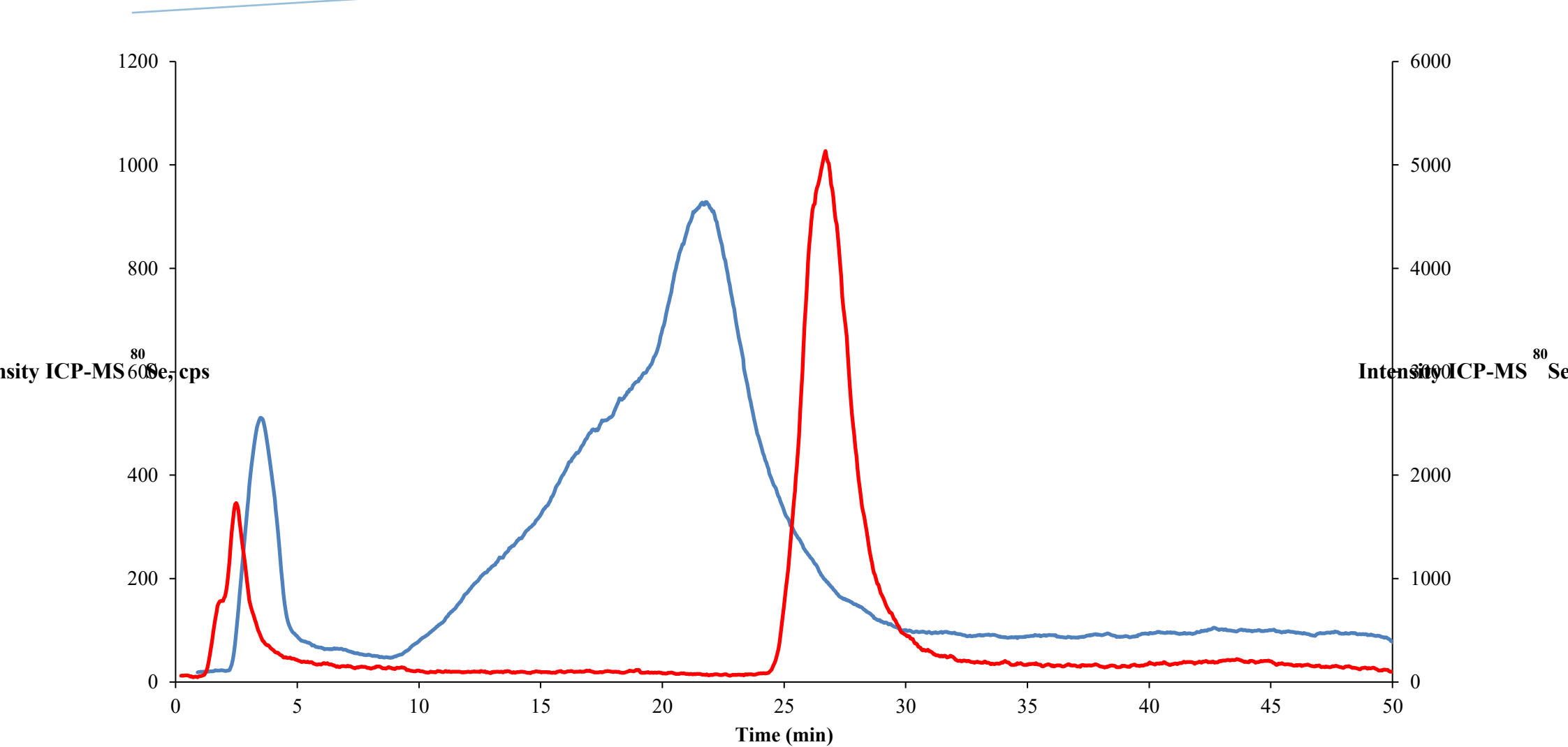


Figure 54 Effect of pH on the SELENOP retention by heparin (Blue curve pH 7, Red curve pH 5.8)

However, more than 99% of the selenium was lost on either of the filters, so other concentration methods needed to be considered and tested.

One of them was freeze-drying. However, due to a relatively large volume (20mL) collected after heparin purification, it was time-consuming. More important, no SELENOP protein could be recovered after freeze-drying. One hypothesis to explain this phenomenon is that the protein had precipitated during the freeze-drying. In such a case, urea is recommended to facilitate the solubilization of the protein. However, even with an 8 M concentration of urea, the protein was not resolubilized and could not be observed in gel or in ESI-MS analysis after tryptic digestion.

*Table 17 Ultracentrifugation filter use for cut-off procedure*

| Type of cut-off filter | Size (MWCO) | Filter materials      | Company, location                               |
|------------------------|-------------|-----------------------|---|
| Amicon® Ultra          | 10K         | Regenerated cellulose | Sigma-Aldrich,<br>Saint-Louis, Missouri,<br>USA |
| Amicon® Ultra 15       | 30K         | Regenerated cellulose | Sigma-Aldrich,<br>Saint-Louis, Missouri,<br>USA |
| Amicon® Ultra 0.5      | 100K        | Regenerated cellulose | Sigma-Aldrich,<br>Saint-Louis, Missouri,<br>USA |
| Vivaspin 20            | 10K         | HY                    | Sartorius, Aubagne,<br>France                   |
| Vivaspin 20            | 10K         | PES                   | Sartorius, Aubagne,<br>France                   |
| Vivacon 500            | 30K         | HY                    | Sartorius, Aubagne,<br>France                   |
| Vivaspin 500           | 100K        | HY                    | Sartorius, Aubagne,<br>France                   |

To overcome this problem, the use of solid-phase extraction (SPE) was investigated to concentrate the protein. SPE allows extraction, purification and enrichment in analytes before their quantification. It is fast (less than 30 min) and easy to perform. In addition, small amounts of solvents are handled, and it is entirely suitable for the pre-treatment of complex samples such as urine, blood, food, water (342–345). This technique was evoked by Jitaru *et al.* (239) in the context of SELENOP speciation in order to remove Cl and Br interferents in ICP MS detection.

A C4 stationary phase was selected being one available in our lab. It offered the capacity to retain SELENOP and remove potential interferents from the fraction collected after heparin purification. SELENOP could be eluted after several rinses with 80% MeOH. The solution obtained was then concentrated by evaporation under a vacuum. By optimizing this technique, it was possible to reach the recovery of SeIP of 3% (in terms of total selenium concentration of serum) and 14% (in terms of the selenium concentration after Heparin purification).

The massive loss of selenium after heparin purification is a significant issue that still needs to be investigated. Other techniques, such as immunoprecipitation, using magnetic beads to pull the protein out of the solution, are here of potential interest and should be tested in the future.



## 10.1. Size exclusion chromatography

The following columns were used to SEC column (**Table 18**).

*Table 18 Column used to obtain an analytical peak of SELENOP*

| Column named                             | Interaction | Column diameter | Stationary phase                              | Particule size | Porosity |
|--|-------------|-----------------|---|----------------|----------|
| Superdex™ 75kDa PC3.2/300 GL             | Pore size   | 30cm x 3.2 mm   | Composite of cross-linked agarose and dextran | 9 µm           |          |
| SEC Acquity UPLC BEH 125 SEC Gold Column | Pore size   | 4.6 mm x 3.0mm  | BEH   | 1.7 µm         | 125 Å    |

The sample after SPE contained about 80 ppb of selenium. With this concentration, a signal of at least 10,000 cps was supposed to be produced by SEC – ICP MS. However, regardless of the SEC column used, no signal above 3000 cps was observed. As no sufficient selenium signal was obtained, a Gpx sample was tried at 55 ppb of Gpx to see if the problem was coming from the column or from the SELENOP sample. In **Figure 55**, the theoretical concentration of selenium in Gpx is supposed to be less than 1ppb, the signal difference being massive, with a factor x10. The signal observed for SELENOP does not match the selenium concentration that we obtained. The problem was similar with the fast SEC Acquity UPLC BEH 125 SEC Gold Column, where the SELENOP peak was not sufficiently intense after the elution (**Figure 56**). The selenium signal presented in the figure is extremely low and does not fit the selenium concentration.

Knowing that SELENOP theoretical size is below 75 kDa, what was observed on SEC, was not expected. Therefore, the SELENOP should not have been stuck before or in the column. One hypothesis that could explain why a low signal is detected for SELENOP is the following. The signal of SELENOP is not detected because only a small amount of the protein passes through the column. The rest of the protein could interact with another non-Se protein. As a result, the complex form will have a mass above 100 kDa, making it difficult for SELENOP to pass inside the column pore.

## 10.2. Sodium dodecylsulfate-polyacrylamide gel electrophoresis

SDS-PAGE electrophoresis was used to evaluate the degree of purification and to check for the presence of potential isoforms of SELENOP. Using a pre-cast gel from Biorad at 8-16%, the sample of concentrated.

SELENOP was loaded on the gel and eluted. The result obtained using protein detection with Brilliant blue dye (Blue Coomassie staining) is presented in **Figure 57**.

Protein bands could be identified in the region between 75kDa and 50 kDa. This region corresponds to the region where SELENOP and its isoforms are expected to be observed (143). It is therefore very likely that the two bands observed correspond to 55kDa and 61kDa SELENOP isoforms. Note that a band of 200 kDa close to the starting zone of the gel can also be observed.



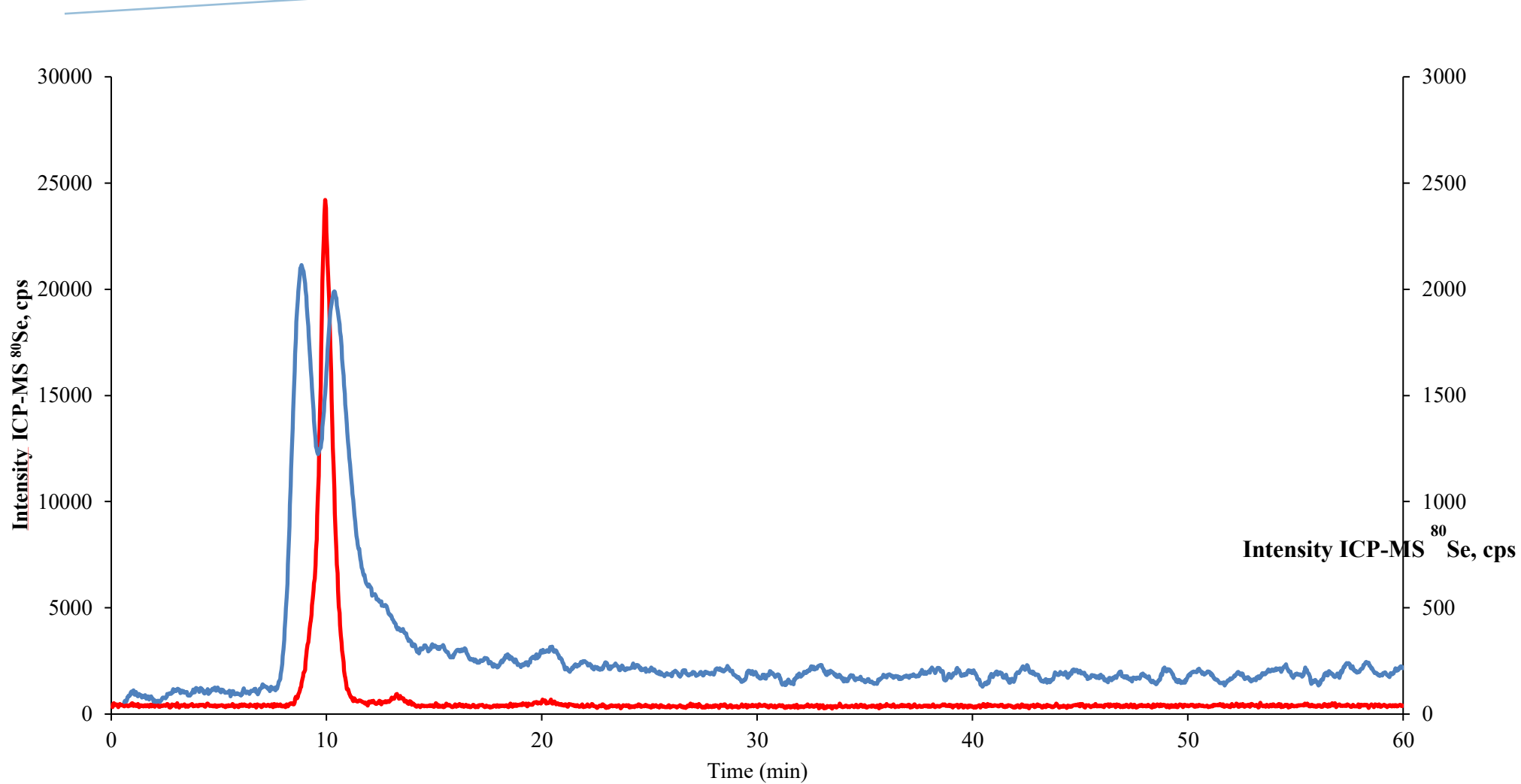


Figure 55 Chromatogram obtain using Superdex<sup>TM</sup> 75kDa PC3.2/300 GL with 0.1 M ammonium acetate pH 7 of SELENOP (blue) and Gpx (red) at respectively 77 ppb and 0.17 ppb of selenium

The dye use is not optimal for such a low concentration, making it challenging to interpret a result correctly.

Other staining techniques can be used to improve the gel. The fluorescent staining method and silver staining are two methods that could be considered when working with low protein concentration. Another method that could also help to interpret the gel is Western blotting or immunoblotting.

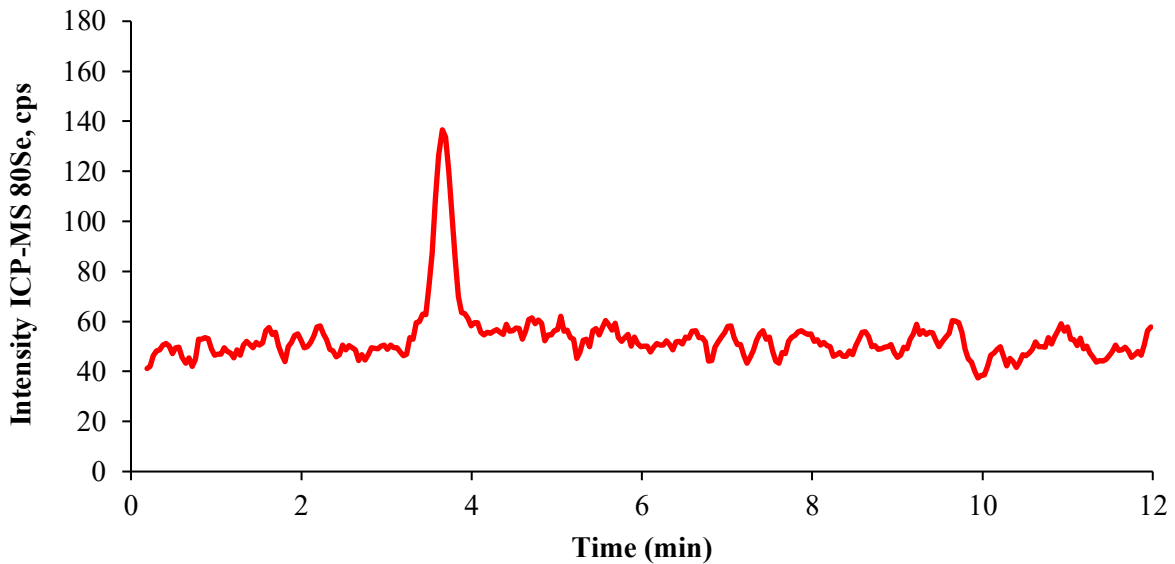


Figure 56 Chromatogram obtained using SEC Acquity UPLC BEH 125 Gold with 0.1 M ammonium acetate pH 7

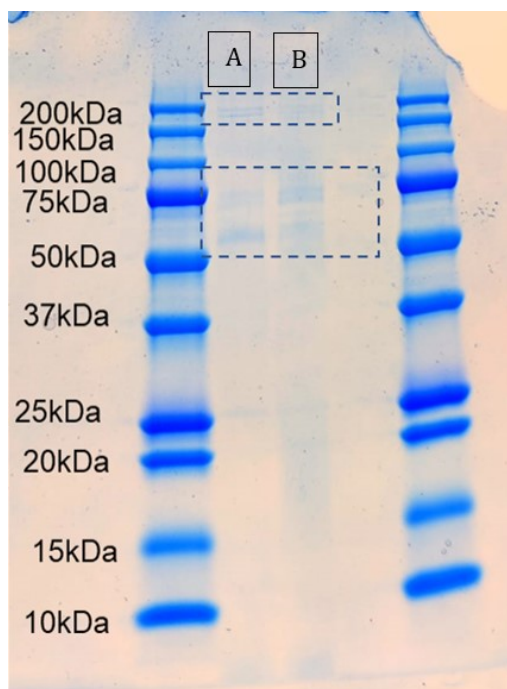


Figure 57 SDS-PAGE gel electrophoresis of two purification experiments using Blue Coomassie staining

### 10.3. Electrospray ionisation mass spectrometry analysis

SELENOP is too big to be observed intact in ESI MS. In order to be characterized, it has to be cut enzymatically into peptides that can be identified and sequenced by electrospray MS/MS. Trypsin, used in bottom-up proteomics, is the most common enzyme used. By comparing the masses of the proteolytic peptides and/or their tandem mass spectra with those predicted from a sequence database or annotated peptide spectra in a peptide spectral library, peptides can be identified and multiple peptide identifications assembled to identify the protein.

To perform the characterization, a sample of SELENOP was first derivatized using 10eq of DTT and IAM. The protein was then digested overnight in the presence of 1/50 eq of trypsin at pH 8. The sample was diluted by 2 and then injected on Acclaim™ RSLC C18 column connected to an ESI mass spectrometer operated in positive mode. All the detected peptides are summarized in **Table 19**. In **Figure 59**, the presence of 5 peptides was observed. The extracted ion chromatograms (XICs) show that the peptide concentrations were low. Most of the peptides presented in **table 19 row 2-5** diverge from the theoretical mass with a difference of around 114.043 corresponding to carbamidomethylation (CAM) of SeCys and Cys. For entry **table 19 row 1**, the mass difference was 772.0092. This mass corresponds to the carbamidomethylation of SeCys but also the O-glycosylation of Thr with a mass of 656.132. This mass corresponded to the O-glycosylation N-acetylneuraminic acid, N-Acetylneuraminic acid galactose, N-acetylgalactosamine presented in **Figure 58**. This structure of glycosylation was elucidated by successive loss of 291.095 (N-Acetylneuraminic acid galactose (NeuNAcGal)), 162.053 (N-acetylneuraminic acid (NeuNAc)) and 203.079 (N-acetylgalactosamine (GalNAc)) corresponding to the fragmentation of 772.009 mass difference (**Figure 60**).

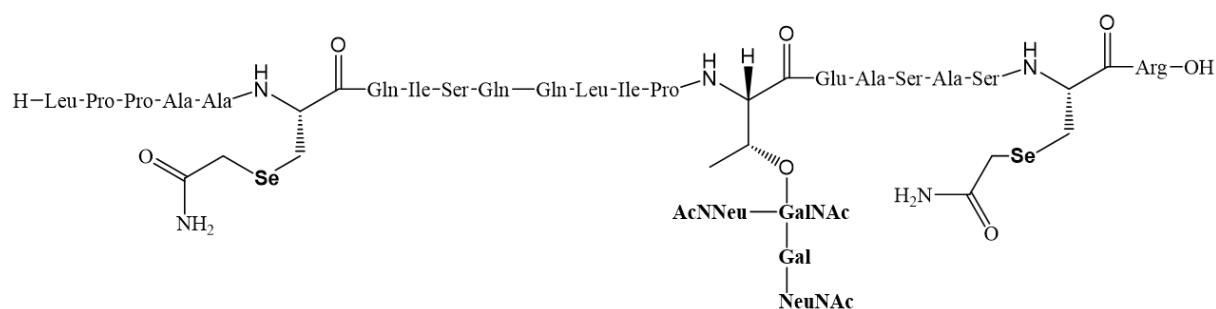


Figure 58 Peptide LPPAAUQISQQIIPTEASASUR with the site of post-translational modification

Another characterization was performed using C18 Acclaim PepMap™ column by nanoHPLC - ESI-MS (positive mode). The sample of SELENOP was first derivatized using 10eq of DTT and IAM. The protein was then digested overnight in the presence of 1/50 eq of Trypsin at pH 8. The sample was diluted by 2 prior to injection. **Figure 61** shows the presence of 3 peptides, the XICs show that peptides concentration was higher than above due to the pre-concentration and desalting on a pre-column. The result obtained are similar to the previous one with the exception that fewer peptides were observed but their concentrations were greatly improved can be observed in the XICs.

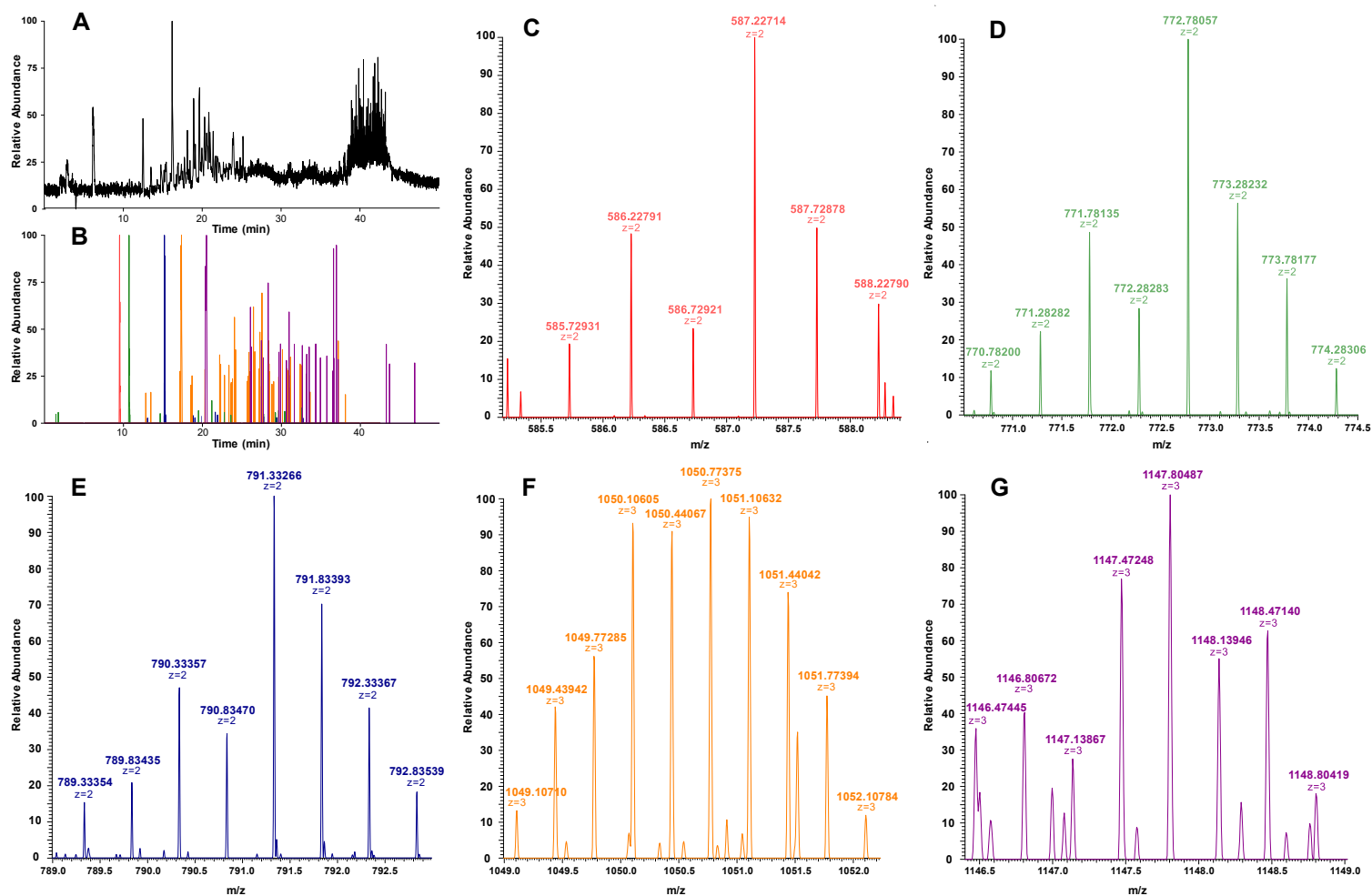


Figure 59 A. LC-MS chromatogram of SELENOP digested with trypsin 1/50 with C18 column, B. XIC of SELENOP peptide, C. MS spectrum of peak at tR = 11.18 min, D. MS spectrum of peak at tR = 12.59 min, E. MS spectrum of peak at tR = 17.85 min, F. MS spectrum of peak at tR = 20.40 min, G. MS spectrum of peak at tR = 20.51 min

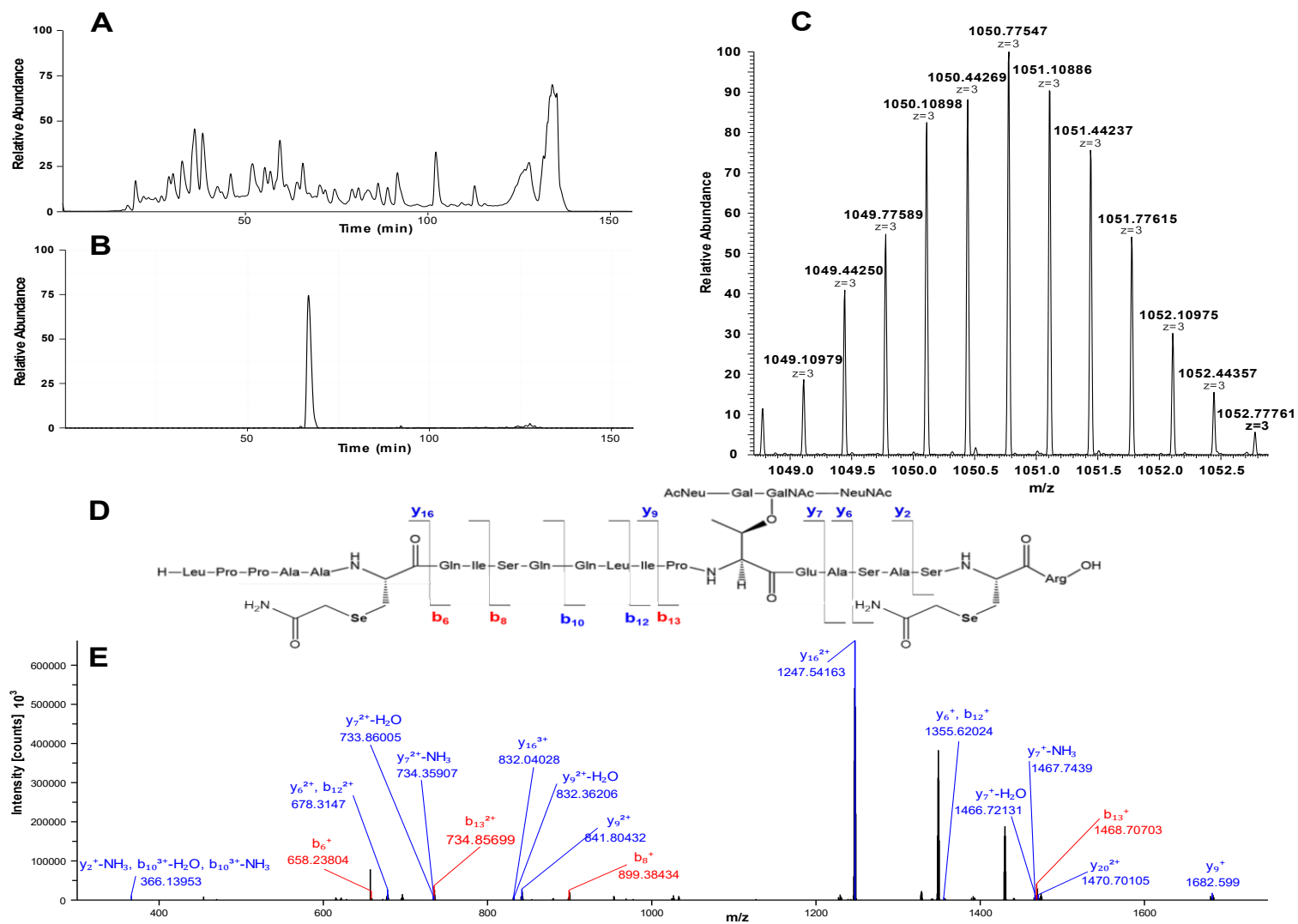


Figure 60 A. TIC, B. XIC, C. MS, D; peptide sequence and E. MS/MS spectrum of LPPAUQISQQLIPTEASASUR at m/z 1050.7748 (z=3)

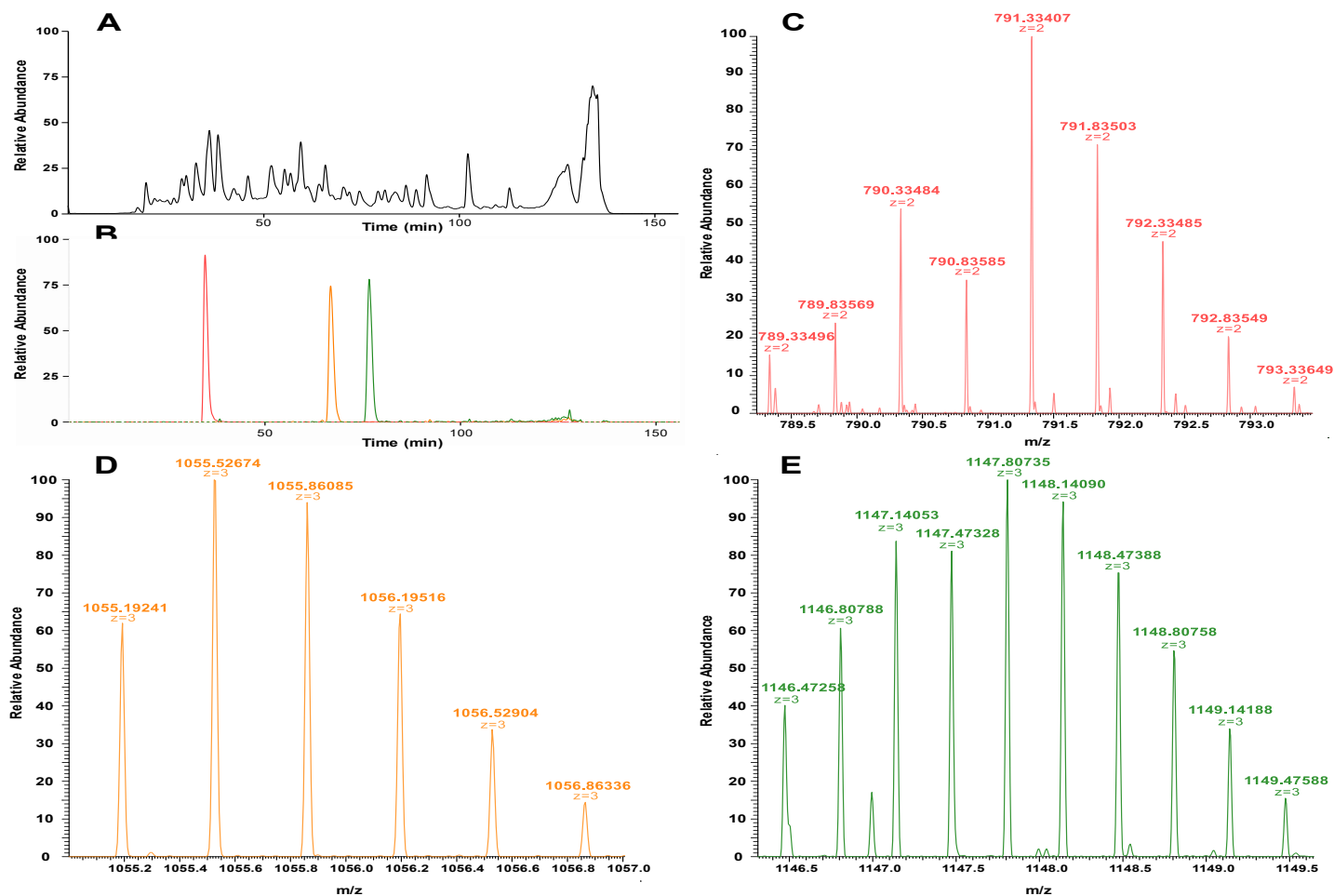


Figure 61 A. LC-MS chromatogram of SELENOP digested with trypsin 1/50 with nano C18 column, B. XIC of SELENOP peptide, C. MS spectrum of peak at tR = 35.08 min (red), D. MS spectrum of peak at tR = 67.04 min (orange), E. MS spectrum of peak at tR = 76.73 min (green)

Table 19 Observed MS products obtain by LC-ESI-MS analysis in positive mode of SELENOP

| Entry, n° | Peptide                                  | Theoretical peptide mass with PTMs | Experimental mass | Observed ions, m/z   |
|-----------|--|------------------------------------|-------------------|--|
| 1         | LPPAA <u>U</u> QISQQLIPTEASAS <u>U</u> R | 3150.1932                          | 3152.3212         | 1050.7737<br>(z=3)<br>1050.7753<br>(z=3)<br>1147.8073<br>(z=3) |
| 2         | DQDPMLNSNGSVTVVALLQAS <u>U</u> YLCILQASK | 3443.5958                          | 3443.4220         | 1147.8048<br>(z=3)<br>791.3326<br>(z=2)                        |
| 3         | ENLPSLCS <u>U</u> QGLR                   | 1581.6463                          | 1582.6652         | 791.3333<br>(z=2)  |
| 4         | AEENITESCQ <u>U</u> R                    | 1544.5419                          | 1545.5609         | 772.7804<br>(z=2)  |
| 5         | TGSAIT <u>U</u> QCK                      | 1173.0704                          | 1174.4542         | 587.2271<br>(z=2)  |

All the peptides observed by mass spectrometry were unique to SELENOP which mean that these peptides are confirming that the SELENOP is present in our sample. Moreover, they all display the specific pattern of selenium.

As mentioned above, another band of protein was observed in gels. This protein could be identified as  $\alpha$ -2-macroglobulin (or rather its fragment as the size of the original protein is 725 kDa). **Figure 62-63** shows the MS spectrum of the peptide corresponding to  $\alpha$ -2-macroglobulin. The peptides presented in **table 20 row 2-3** are diverge from theoretical mass with a difference around 57.0215 corresponding to carbamidomethylation (CAM) of Cys. The peptides listed in **table 20** are unique to human  $\alpha$ -2-macroglobulin.

Table 20 Observed MS products obtain by LC-ESI-MS analysis in positive mode of  $\alpha$ -2-macroglobulin

| Entry, n° | Peptide                         | Theoretical peptide mass | Experimental mass | Observed ions, m/z                         |
|-----------|---------------------------------|--------------------------|-------------------|--|
| 1         | HNVYINGITYTPVSSTNEKDMYSFLEDMGLK | 3566.68180               | 3567.7116         | 1090.23272<br>(z=3)<br>1090.23455<br>(z=3) |
| 2         | VYDYIYETDEFAIAEYNAPCSK          | 2544.06456               | 2545.0952         | 1275.04760<br>(z=2)<br>1275.04896<br>(z=2) |
| 3         | YNILPEKEEFPFALGVQTLPTQCDEPK     | 3169.54213               | 3170.58288        | 1056.86096<br>(z=3)<br>1055.52917<br>(z=3) |

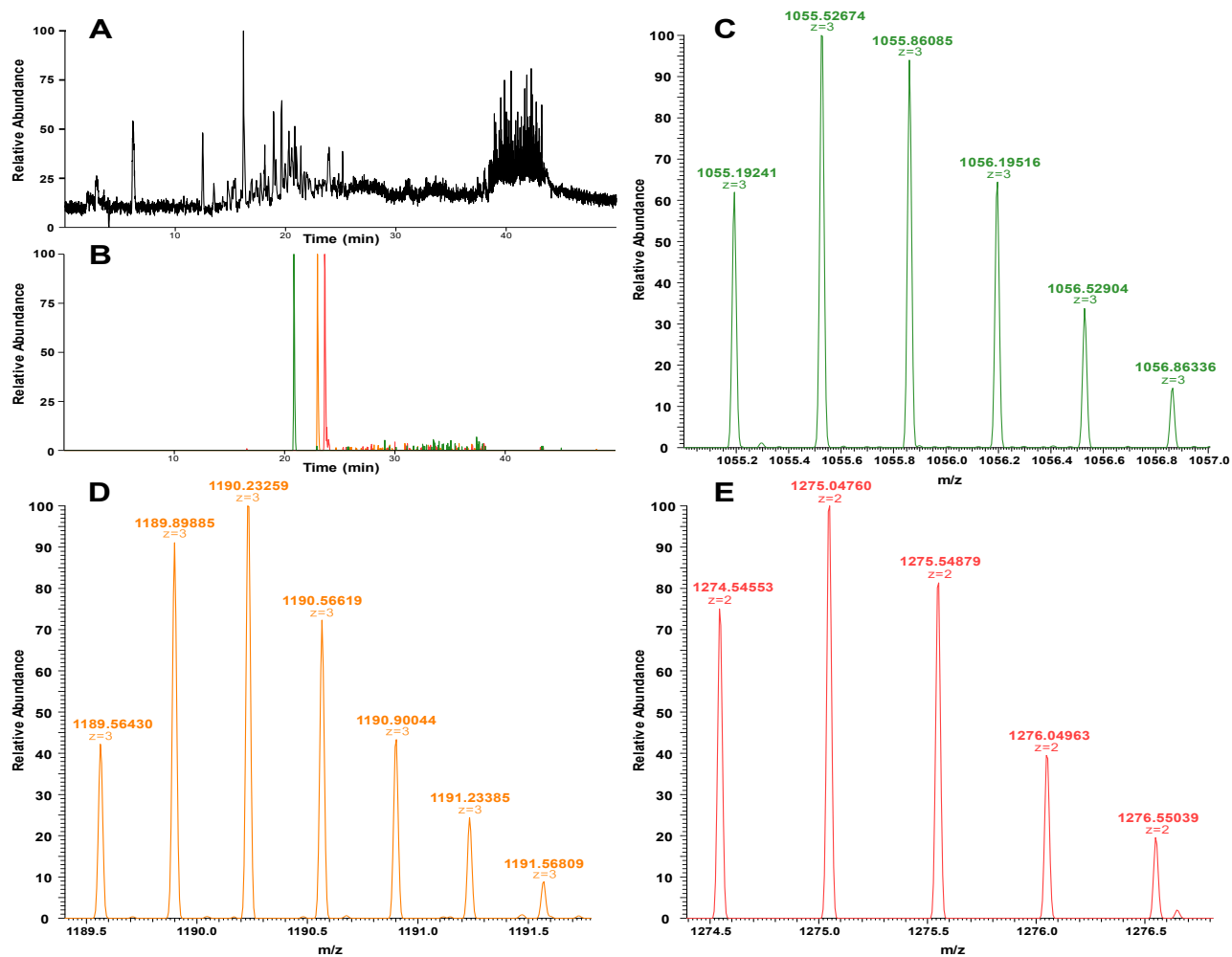


Figure 62 A. LC-MS chromatogram of  $\alpha$ -2-macroglobulin digested with trypsin 1/50 with C18 column, B. XIC of  $\alpha$ -2-macroglobulin peptide, C. MS spectrum of peak at  $t_R = 20.84$  min, D. MS spectrum of peak at  $t_R = 22.98$  min, E. MS spectrum of peak at  $t_R = 23.63$  min



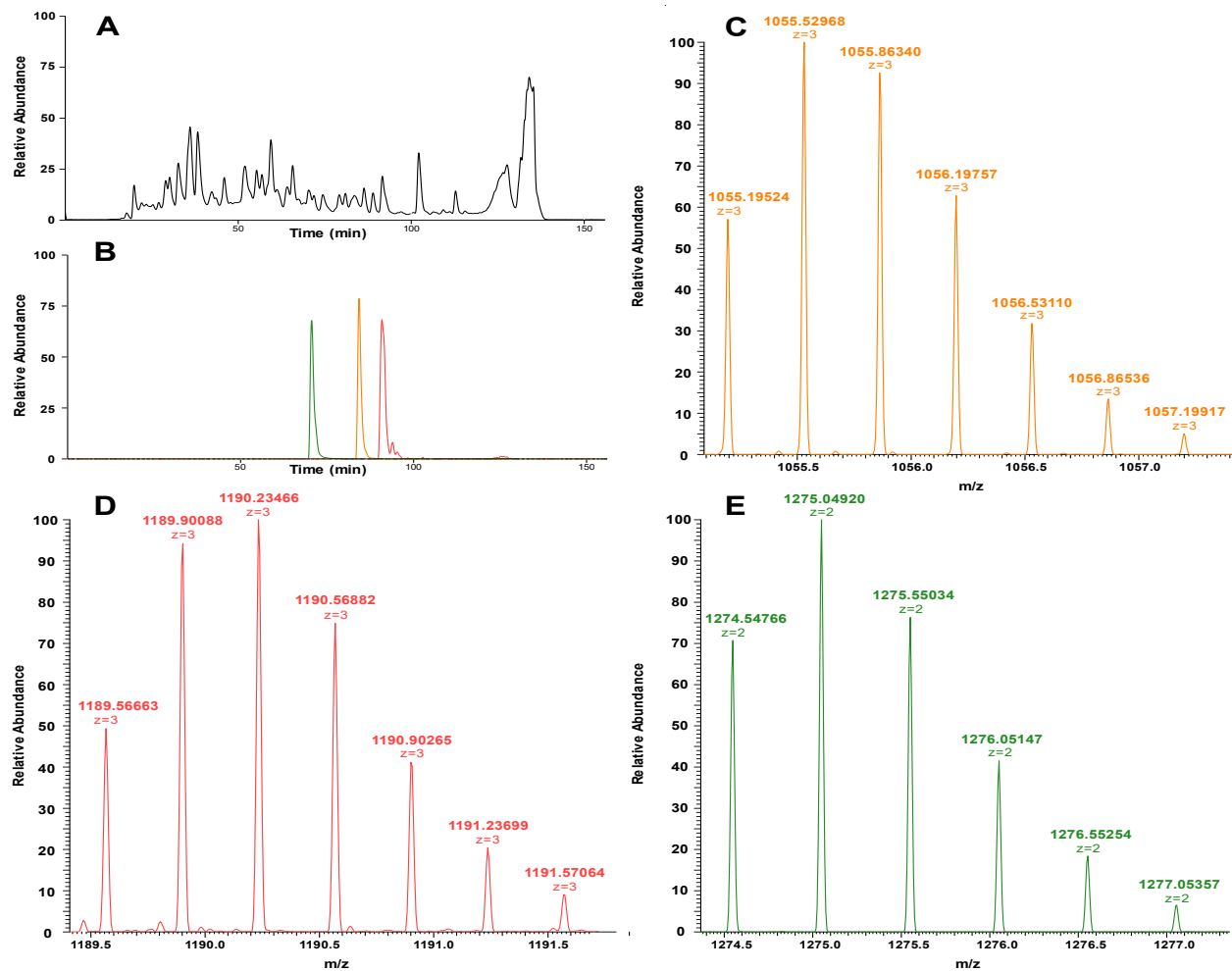


Figure 63 A. LC-MS chromatogram of  $\alpha$ -2-macroglobulin digested with trypsin 1/50 with nanoC18 column, B. XIC of  $\alpha$ -2-macroglobulin peptide, C. MS spectrum of peak at  $t_R = 70.47$  min, D. MS spectrum of peak at  $t_R = 84.20$  min, E. MS spectrum of peak at  $t_R = 91.31$  min

## 10.4. Quantification

To determine the overall recovery of the purification, two techniques of quantifications were used, one based on UV absorption and the other one on total selenium quantification.

### *Protein quantification*

In order to carry out SDS-PAGE and to determine the amount of trypsin needed for enzymatic digestion, the determination of protein content in the sample was of paramount importance. For that we used a commercial kit from Biorad using UV absorbance to detect the protein presence in the sample. Undiluted samples were used. Three replicates were carried out.

**Table 21** presents the results obtained. The limit of detection for this technique was 0.44 g/L and the limit of quantification was 2.7g/L. The values obtained were between both the LQ and the LD meaning that SELENOP could not be quantified precisely but it could be detected. These results cannot be used to quantify SELENOP without selenium quantification, especially knowing that another protein was detected in the gel.

*Table 21 Protein content obtained using commercial kit DTCm Protein assay kit (\* concentration of selenium was calculated considering that MW of SELENOP = 43174 and that SELENOP is containing 10 SeCys)*

| Sample<br>(n= number of<br>replicate) | Concentration<br>in g/L | RSD<br>(%) | Concentration of<br>selenium in ng<br>(Se)/mL* | LD<br>(g/L) | LQ<br>(g/L) | R <sup>2</sup> |
|---------------------------------------|-------------------------|------------|--|-------------|-------------|----------------|
| A (n=3)                               | 0.69 (±0.004)           | 0.5        | 13x10 <sup>3</sup> (±73)                       |             |             |                |
| B (n=3)                               | 0.69 (±0.006)           | 1          | 13x10 <sup>3</sup> (±109)                      |             |             |                |
| C (n=3)                               | 0.60 (±0.021)           | 3          | 11x10 <sup>3</sup> (±384)                      | 0.44        | 2.7         | 0.1554         |
| Total (n=9)                           | 0.66 (±0.047)           | 7          | 12x10 <sup>2</sup> (±859)                      |             |             |                |

### *Total selenium quantification*

To quantify the selenium amount, samples were collected along with all the purification/concentration steps. The samples were lyophilized, and diluted with 2% HNO<sub>3</sub>. Selenium isotopes <sup>76</sup>Se, <sup>77</sup>Se, <sup>78</sup>Se, <sup>80</sup>Se, <sup>82</sup>Se were monitored. A standard was established in the range from 0.5 to 50 ppb (selenite in 2%HNO<sub>3</sub>). **Table 21** shows that 67 ppb of total selenium was detected in serum fitting the range of values reported earlier by Heitland *et al.* (238) and in other studies using isotope dilution - ICP MS (138, 289).

The results in **Table 21** confirm that a significant amount of selenium was lost at the final step of the purification and the concentration step was hardly successful.

*Table 22 Selenium content obtained using ICP-MS and by following <sup>76</sup>Se, <sup>77</sup>Se, <sup>78</sup>Se, <sup>80</sup>Se, <sup>82</sup>Se isotope*

| Sample (n= number of<br>replicate)         | Concentration of selenium in<br>ng (Se)/mL | RSD<br>(%) | LD<br>(ng<br>(Se)/mL) | LQ<br>(ng<br>(Se)/mL) |
|--|--|------------|-----------------------|-----------------------|
| Serum (n=6)                                | 67.32 (±3.68)                              | 5          |                       |                       |
| Elution peak 1 of IMAC (n=3)               | 4 (±1.1)                                   | 26         |                       |                       |
| Elution peak 2 of IMAC<br>(SELENOP) (n=7)  | 3 (± 0.4)                                  | 13         | 0.04                  | 0.25                  |
| Elution peak of Heparin<br>(SELENOP) (n=6) | 4 (± 0.8)                                  | 20         |                       |                       |
| SELENOP post SPE C4 (n=2)                  | 77 (± 6.2)                                 | 7          |                       |                       |

**Table 22** confirms that the recoveries at each step of purification are far from quantitative. The difference between the first IMAC peak and the one containing SELENOP could be linked to a problem of column

capacity. The overall recovery of IMAC is 87% which is correct knowing that two small peaks of selenium could be seen in **Figure 53**. A selenium loss is observed during Heparin separation with a loss of 29% of IMAC selenium. The *Heparin* column capacity could have been reached when we compare the recovery presented in **Table 22** to the 96% of recovery using Heparin reported by Heitland *et al.* (238). The remaining drawback of the developed methodology's is the loss of 86% of the selenium content during the final concentration step.

A considerable difference was observed when comparing the result of selenium content obtained to the one calculated with the protein quantification. There is a difference of x120, meaning that the quantified protein does not entirely correspond to the SELENOP concentration. Moreover, the concentration of SELENOP in the sample calculated should be 0.004 g/L. In the literature, the concentration of  $\alpha$ -2-macroglobulin is considered to be around 2-4g/L (346, 347). However, the SELENOP concentration is comprised between 0.002 to 0.003 g/L in serum if we used the interval presented by Heitland *et al.* (241).

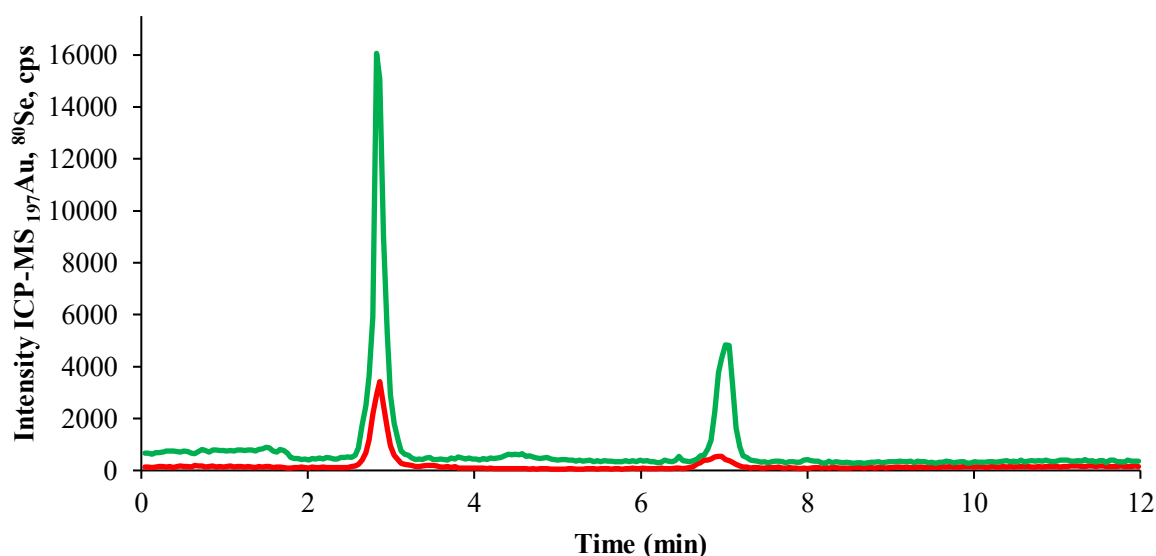
*Table 23 Selenium recovery obtained using ICP-MS and by following <sup>76</sup>Se, <sup>77</sup>Se, <sup>78</sup>Se, <sup>80</sup>Se, <sup>82</sup>Se isotope*

| <b>Sample (n= number of replicate)</b>         | <b>Mass of selenium (ng)</b> | <b>Recovery from serum (%)</b> | <b>Recovery from IMAC (%)</b> | <b>Recovery from Heparin (%)</b> |
|--|------------------------------|--------------------------------|-------------------------------|----------------------------------|
| <i>Serum (n=6)</i>                             | 448                          |                                |                               |                                  |
| <i>Elution peak 1 of IMAC (n=3)</i>            | 239                          | 53                             |                               |                                  |
| <i>Elution peak 2 of IMAC (SELENOP) (n=7)</i>  | 155                          | 35                             |                               |                                  |
| <i>Elution peak of Heparin (SELENOP) (n=6)</i> | 99                           | 24                             | 71                            |                                  |
| <i>SELENOP post SPE (n=2)</i>                  | 10                           | 3                              | 10                            | 14                               |

The objective of this part was to study the interaction between the SELENOP and metallodrugs such as auranofin and cisplatin. For this purpose, a methodology needed to be developed to study the protein-metallodrug interaction and to characterize the binding sites.

## 11.1. Interaction of auranofin and cisplatin with full-length selenoprotein P

The explored principle of the method was based on size-exclusion chromatography with the simultaneous ICP MS detection of selenium and the metal. This should allow to identifying intact SELENOP, a SELENOP-metal adduct and free metallodrug. However, auranofin was shown not to elute completely from the column. Moreover, as it was shown in **Figure 64**, selenoproteins can react with the gold left on the column producing a peak at the elution volume of SELENOP.



*Figure 64 Chromatogram of the SELENOP and auranofin co-elution after the injection of SELENOP on a column contaminated with traces of auranofin (green  $^{197}\text{Au}$ , red  $^{80}\text{Se}$ )*

To see if the phenomenon was reproducible, another experiment was performed by manually reproducing the potential interaction, SELENOP sample after purification was incubated with DTT and auranofin and cisplatin for 1h. The sample was then injected into the same SEC column, and the isotope of gold, platinum and selenium were followed. As presented in **Figure 64**, a co-elution is observed between Au and Se. That observation confirmed what was observed in **Figure 65**: possible interaction between Au and peptide from SELENOP. The co-elution was also observed with platinum compound, but it seems that this interaction was not necessarily linked to the selenopeptide of SELENOP (**Figure 66**). In order to obtain a deeper insight in these interactions, the protein is digested by trypsin and the binding of the two analysed metallodrugs with the individual peptides was probed.

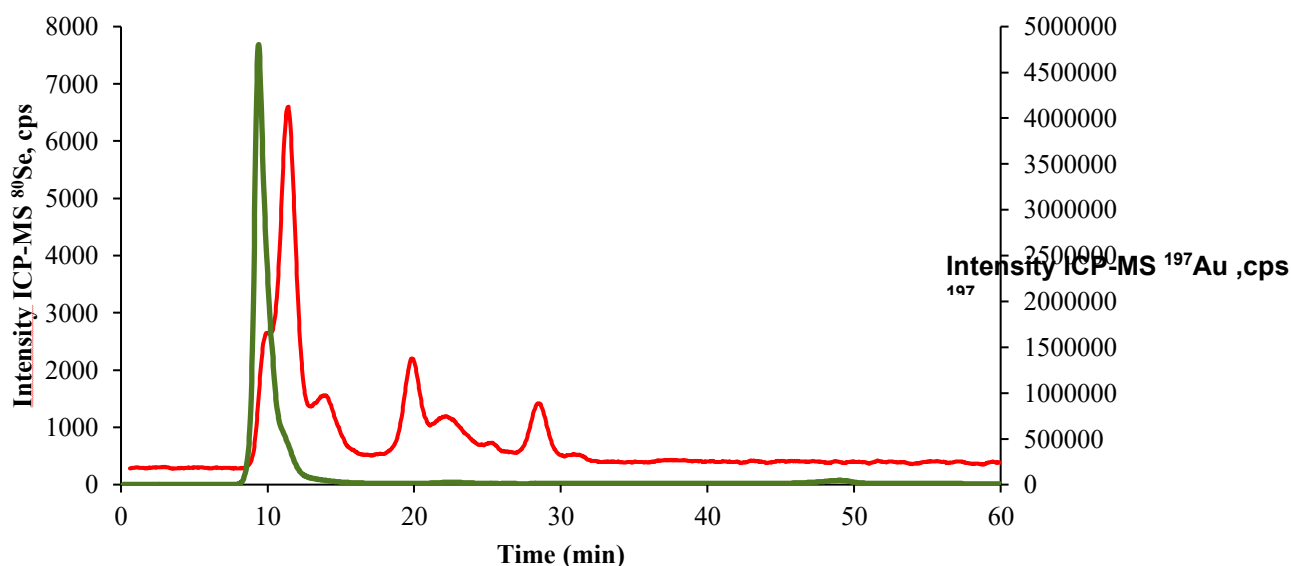


Figure 65 Chromatogram of the interaction between SELENOP and auranofin after DTT and incubation during 1h at 37°C observed by SEC (red  $^{80}\text{Se}$ , green  $^{197}\text{Au}$ )

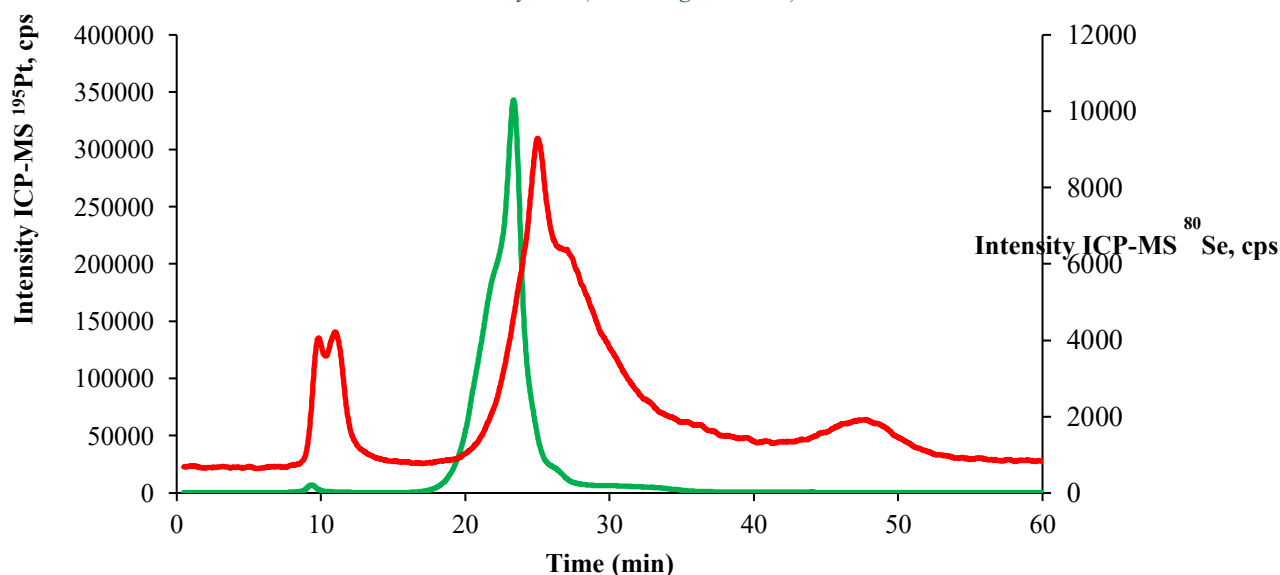


Figure 66 Chromatogram of the interaction between SELENOP and cisplatin after DTT treatment and incubation during 1h at 37°C observed by SEC (red  $^{80}\text{Se}$ , green  $^{195}\text{Pt}$ )

## 11.2. Identification of the interaction between selenoprotein P and metallodrugs on the peptide level

### 11.2.1. Auranofin

The reactions of SELENOP with the gold compounds were investigated using reversed-phase nanoHPLC with electrospray MS/MS detection (LC-MS).

To detect the peptide sequence interacting with gold, the isotopic profile of selenopeptide was studied for SeCys containing peptide (**Figure 67**). MS/MS data were used to confirm the presence of PTMs (such as glycosylation) and metalation on the peptide sequence.

### *S-Au peptide*

**Table 24** summarizes all the peptides with Cys-moiety that were observed by mass spectrometry and were displaying gold adducts. In this table, all peptides were manually verified, to fit mass shift induced by the interaction of gold moiety with Cys, however due to the low concentration, most of the MS/MS spectrum obtained for all the peptides are not exploitable. All the data presented in red are therefore considered as potential interactions that need to be validated.

*Table 24 Observed MS of SELENOP peptides interacting with gold (Red data are not supported by MS/MS characterisation)*

| Peptide sequence               | Theoretical peptide mass | Experimental mass | Modification observed  | Observed ion, m/z  |
|--------------------------------|--------------------------|-------------------|--|--------------------|
| MWRSLGLALALCLLPSSGGTESQDQSSLCK | 3379.6664                | 3379.65772        | +315.14<br>AuPEt <sub>3</sub> (C1)                                 | 676.7367<br>(z= 5) |
| RCINQLLC                       | 1592.771                 | 1591.76556        | +315.14<br>AuPEt <sub>3</sub> (C1,<br>C2)                          | 531.5852<br>(z=3)  |
| PYVEEAIKIAYCEKK                | 2099.0683                | 2099.08248        | +315.14<br>AuPEt <sub>3</sub> (C1)                                 | 700.69416<br>(z=3) |
| NQLLCKLPTDSELAPR               | 2113.0927                | 2113.10865        | +315.14<br>AuPEt <sub>3</sub> (C1)                                 | 705.36955<br>(z=3) |
| MWRSLGLALALCLLPSSGGT           | 2290.1954                | 2290.22128        | +15.99<br>Oxidation on<br>M1<br>+315.14<br>AuPEt <sub>3</sub> (C1) | 573.55532<br>(z=4) |
| TTLKDEDFCK                     | 1514.7012                | 1515.7063         | +315.14<br>AuPEt <sub>3</sub> (C1)                                 | 757.85315<br>(z=2) |
| TTLKDEDFCKR                    | 1670.8023                | 1671.80664        | +315.14<br>AuPEt <sub>3</sub> (C1)                                 | 835.90332<br>(z=2) |

The MS/MS data shown in **Figure 68**, corresponding to the first peptide presented in **Table 24**, allowed the finding that the +315.14 addition was located in the first half of the peptide, and more precisely on the cysteine. With this data we could confirm that one AuPEt<sub>3</sub><sup>+</sup> ligand directly binds the Cys. When compared with the supposed sulfur isotopic profile the less intense peaks are missing. This could be explained by the fact that the sample was too diluted. The concentration of the sample is yet again primordial to obtain better data and more information on the peptide interaction with gold compounds.

**Table 24 (rows 2,3,4,5,6 and 7)** demonstrates the formation of AuPEt<sub>3</sub><sup>+</sup> adduct (+315.14 uma) potentially corresponding to the binding of Au(I) to Cys. Unfortunately, without more accurate MS/MS data, the mass shift alone is not sufficient to confirm the metal-peptide binding site (MS spectrum are presented in **Annexe 1 Figures 1 to 6**).

C24H52O13N11SeS: C24 H52 O13 N11 Se1 S1 pa Chrg 3

C24H52O13N11SeS: C24 H52 O13 N11 Se1 S1 pa Chrg 5

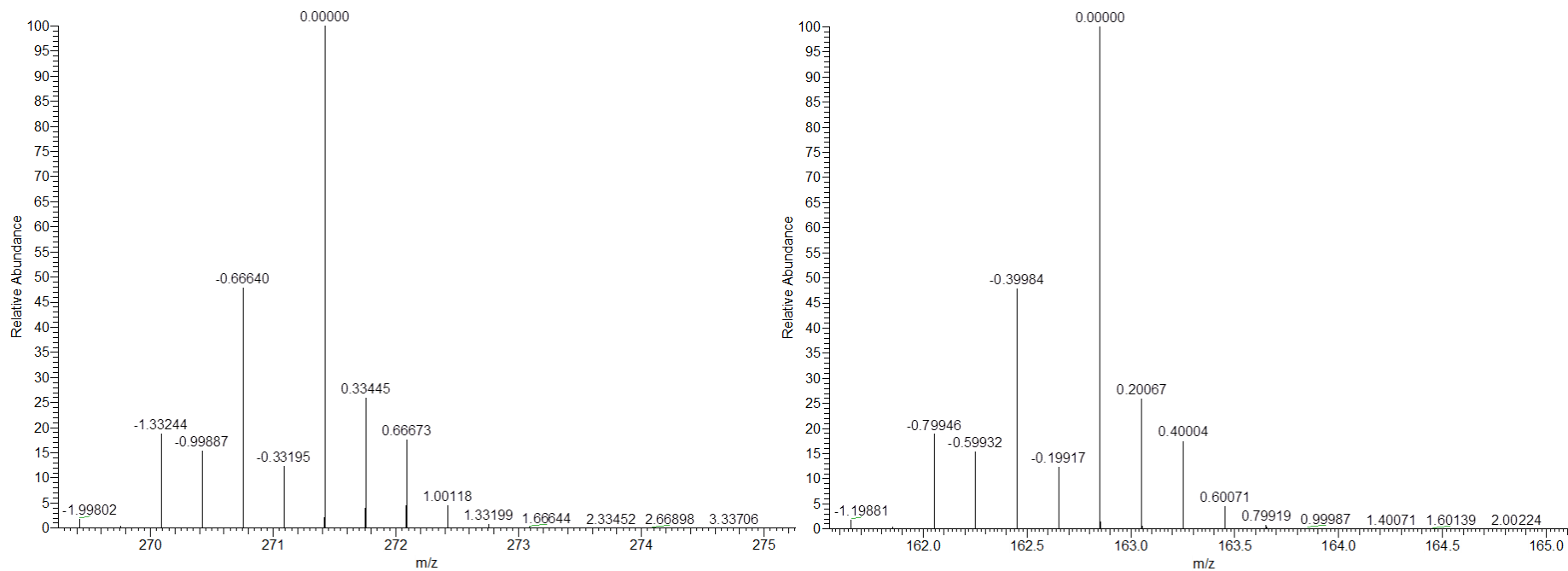


Figure 67 Theoretical isotopic profile of peptide containing S-Se moiety

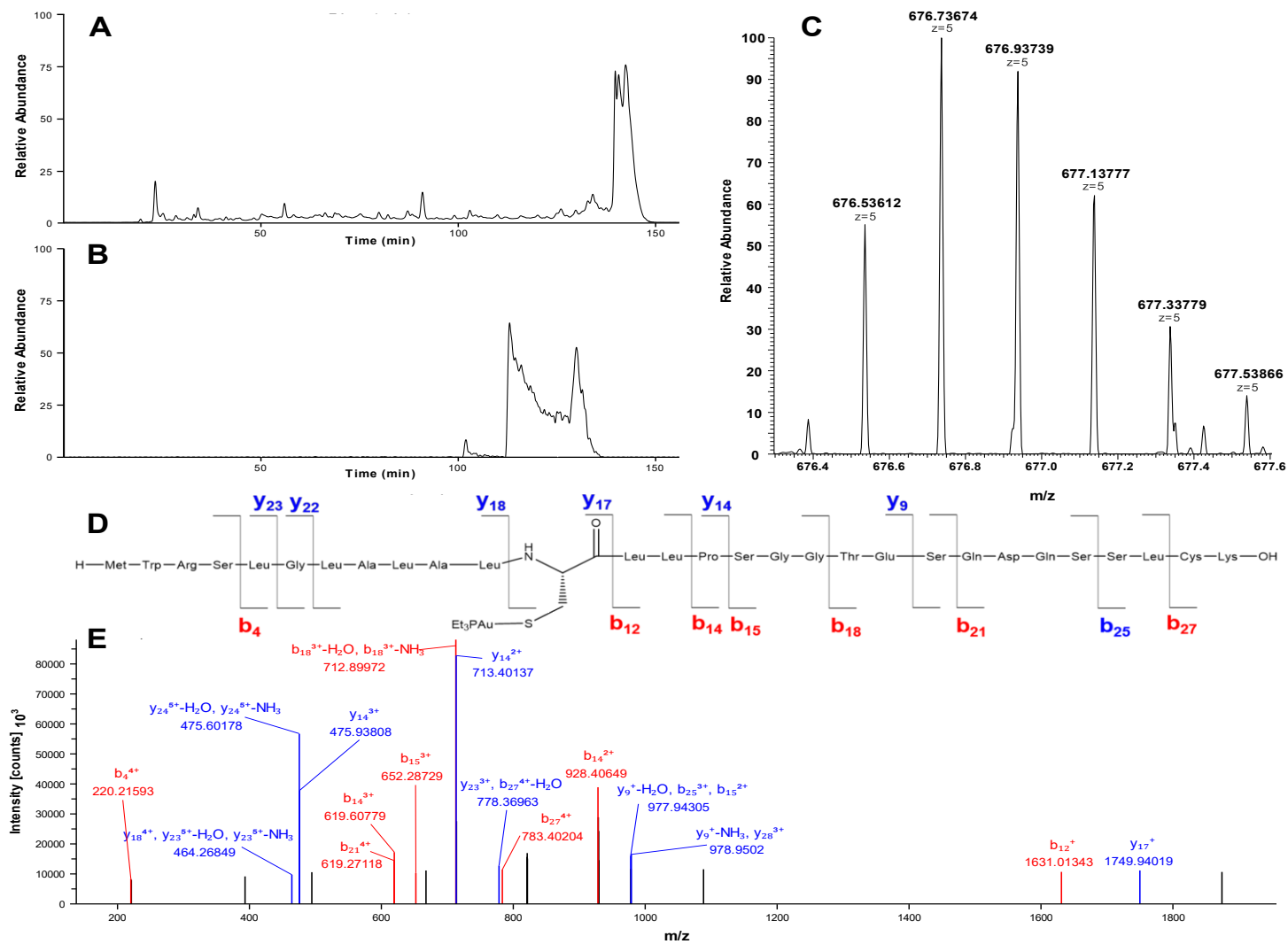


Figure 68 A. TIC, B. XIC, C. MS, D. peptide sequence and E. MS/MS spectrum of MWRSLGLALALLPSGGTESQDQSSLCK at m/z 676.7367 (z=5)



### Se-Au peptide

**Table 25** summarizes all the peptides showing the Se isotopic pattern and potentially forming gold adducts. All the peptides highlighted in red were manually verified, to fit the selenopeptide isotopic pattern, however due to low concentration, most of the MS/MS spectra obtained could not be exploited. The data presented are therefore considered as indications of potential and not effective interactions between Au-SeCys.

The peptide in **Table 25 row 1** is the only gold adduct peptide for which a sufficient amount of quality MS/MS could be obtained. The MS data confirm the presence of 3 AuPEt<sub>3</sub><sup>+</sup> adducts on the SeCys of this sequence (three times the mass shift of 315.14) (**Figure 69**).

*Table 25 Observed MS peptide obtain by LC-ESI-MS analysis in positive mode (Red data are data without correct MS/MS validation)*

| Peptide sequence             | Theoretical peptide mass | Experimental mass | Modification observed  | Observed ion m/z |
|------------------------------|--------------------------|-------------------|--|------------------|
| LPPAAUQISQQLIPTEASASURUKNQAK | 4103.5734                | 4103.61838        | +315.14x 3 AuPEt <sub>3</sub> (U1/U2/U3)<br>+58 ACN/OH <sup>-</sup> adduct   | 1368.8786 (z=3)  |
| PMLNSNGSVTVVALLQASUYLCILQASK | 3952.8734                | 3953.7744         | +315.14x2 AuPEt <sub>3</sub> (U1 and C1)<br>+315.14 AuPEt <sub>3</sub> (M1)  | 988.44360 (z=4)  |
| LQASUYLCILQASKLEDLRVK        | 3492.594615              | 3492.5284         | +315.14 AuPEt <sub>3</sub> (U1 or C1)<br>+ 83 ACN adducts<br>+656.227615 O-glycosylation N-acetylneuraminic acid, N-Acetylneuraminic acid galactose, N-acetylgalactosamine (S1 or S2)  | 698.50568 (z=5)  |
| TGSAITUQCKENLPSLCSUQGLRA     | 4061.57696               | 4061.77516        | +315.14x2 AuPEt <sub>3</sub> (U1 or C1, C2 or U2)<br>+ 198.03 Au <sup>+</sup> (U1 or C1, C2 or U2)<br>+656.227615 O-glycosylation N-acetylneuraminic acid, N-Acetylneuraminic acid galactose, N-acetylgalactosamine (T1 or T2, S1 or S2 or S3) | 1016.44379 (z=4) |

**Table 25 (rows 2,3,4)** demonstrate the formation of AuPEt<sub>3</sub><sup>+</sup> adducts (+315.14 uma) potentially correspond to the binding of Au(I) to SeCys. Unfortunately, without more accurate MS/MS data, the mass shift alone is not sufficient to confirm the metal-peptide binding site (MS/MS spectrum are presented in **Annexe 1 Figures 7 to 9**).

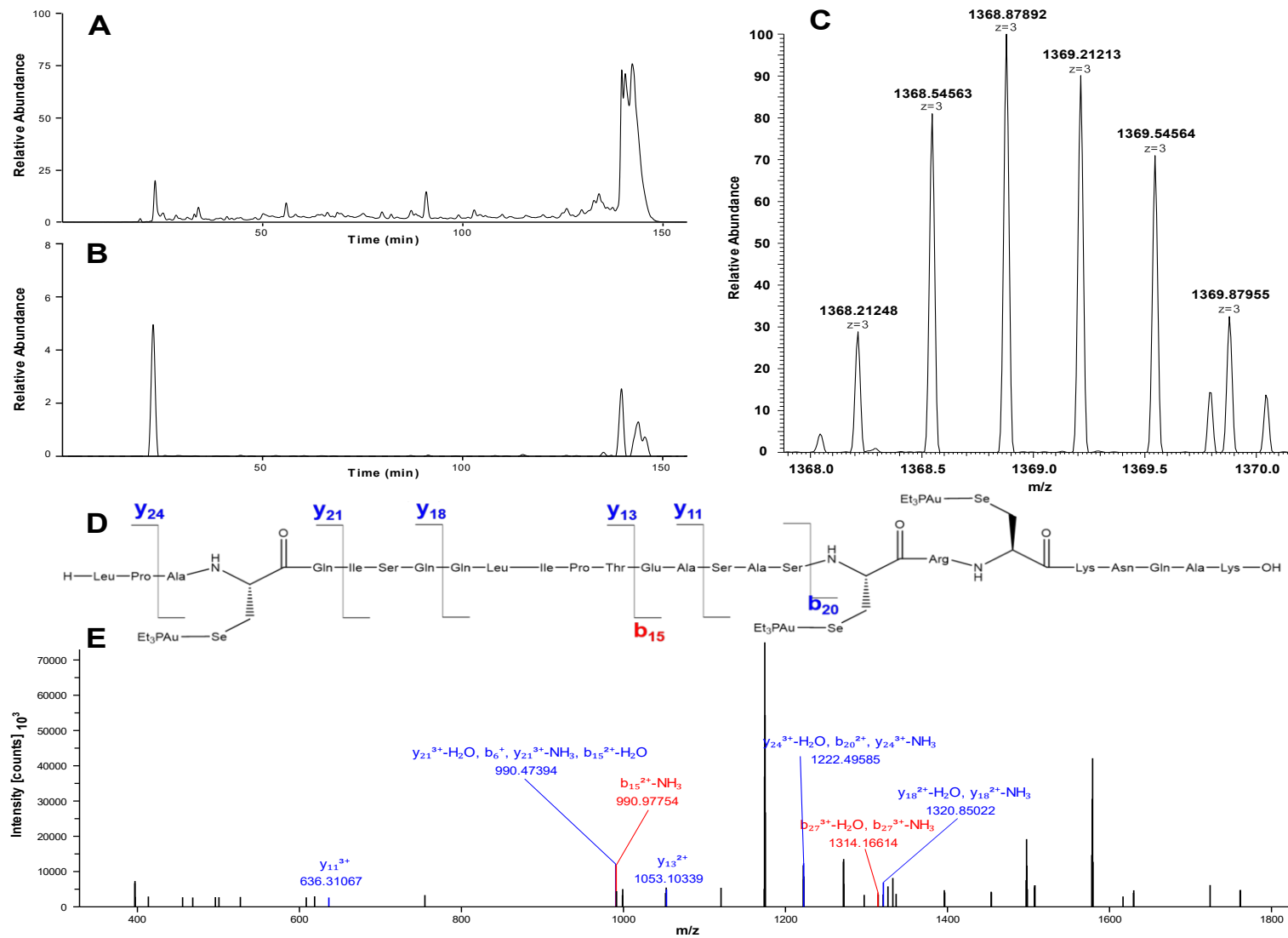


Figure 69 A. TIC, B. XIC, C. MS, D. peptide sequence and E. MS/MS spectrum of LPPAAUQISQQLIPTSEASASURUKNQAK at m/z 1368.8786 (z=3)

As presented in the precedent part, the presence of an interaction between SELENOP and auranofin is verified. However, the low concentration of the sample and some parameters are not optimal to obtain more consequent information on this interaction. The phenomenon that was observed by ICP on the purified SELENOP (**Figure 65 and 66**) seems to be explained by mass shift observed on digested peptides after protein metalation and the MS/MS fragmentation pattern of two of them showing the involvement of Cys and SeCys in the binding with Au.

### 11.2.2. Cisplatin

The reactions of SELENOP with the platin compounds were investigated using reversed-phase nanoHPLC with electrospray MS/MS detection (LC- MS).

To detect the peptide where the interaction between Pt and Cys or SeCys, isotopic profiles of sulfur/selenium/platin were used to confirm the presence of the peptide having interacted with the drug (**Figure 70**). MS/MS data were used to confirm the presence of the PTMs (glycosylation) and metalation (metallodrug fragment) on the peptide sequence.

In **Table 26**, we present the peptides that we were able to detect and characterize by MS/MS. The first peptide displays multiples cisplatin rbinding on all the Cys and also an O-glycosylation on the Ser. The MS/MS data allowed us to locate each modification as presented in **Figure 71**.

Table 26 Observed MS peptide obtain by LC-ESI-MS analysis in positive mode

| Peptide sequence              | Theoretical peptide mass | Experimental mass | Modification observed  | Observed ion m/z |
|-------------------------------|--------------------------|-------------------|--|------------------|
| AYCEKCKGNCSTTLK               | 3575.8332                | 3575.99073        | +83 ACN adducts<br>+261.97 Cisplatin x<br>3<br>(C1, C2, C3)<br>+947.32029 O-glycosylation N-acetylneuraminic acid, N-Acetylneuraminic acid galactose, 2 N-acetylgalactosamine (S1)   | 716.20437 (z=5)  |
| TUQCKENLPSLUSCQGLRAEENITESCQR | 4734.442015              | 4736.37464        | +261.97x2 Cisplatin (U1, U2)<br>+656.227615 O-glycosylation N-acetylneuraminic acid, N-Acetylneuraminic acid galactose, N-acetylgalactosamine (T2)<br>+64 ACN/Na <sup>+</sup> adduct | 948.68207 (z=5)  |

The second observed peptide is particularly interesting because it corresponds to a three miss-cleaved in SELENOP that contains 3 SeCys residues, two of them interacting with a Pt as presented in **Figure 72**.

NOCHSeSPt: N1 O1 C1 H1 Se1 S1 Pt1 pa Chrg 5

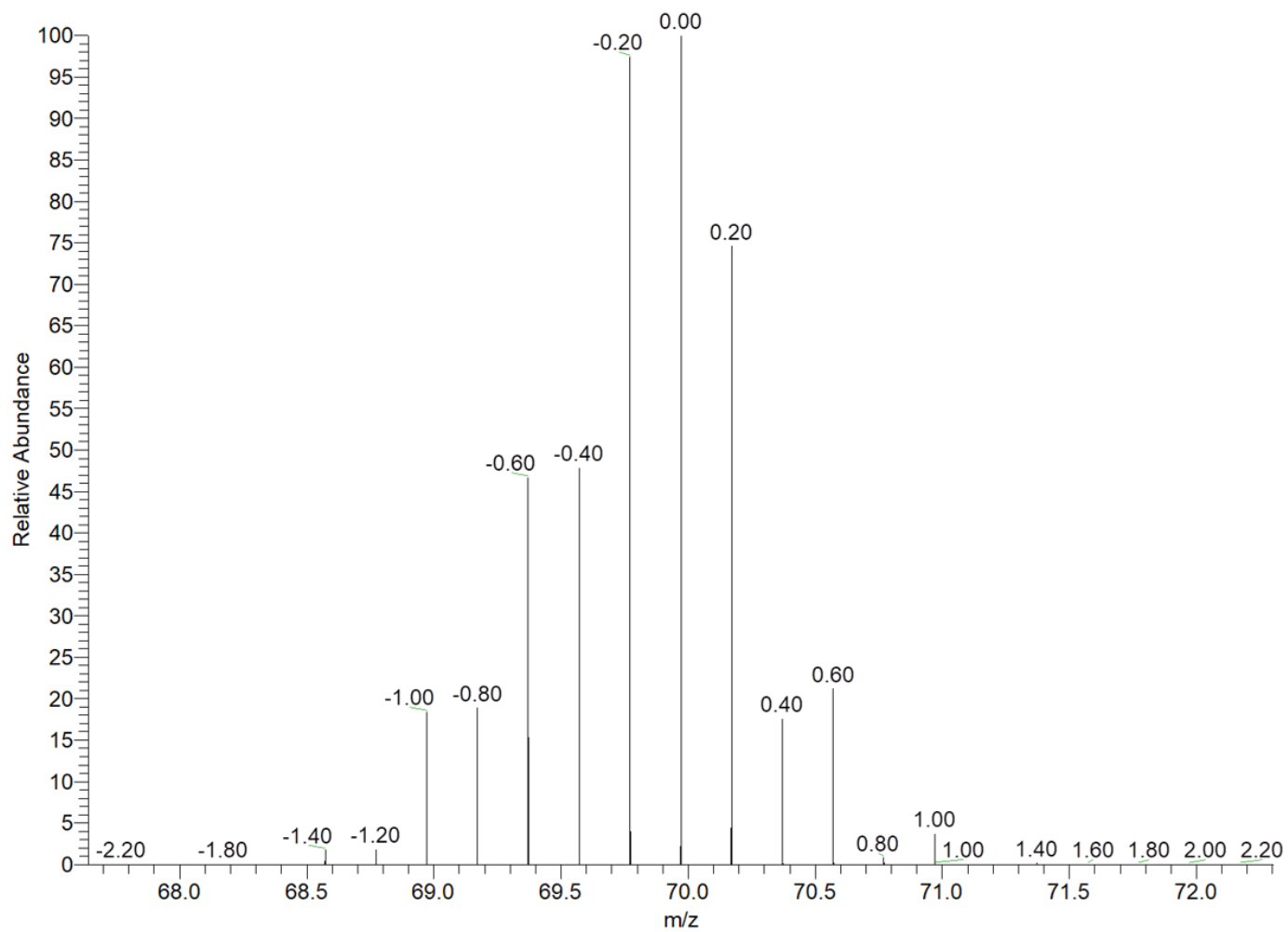


Figure 70 Theoretical isotopic profile of peptide containing S-Se-Pt moiety

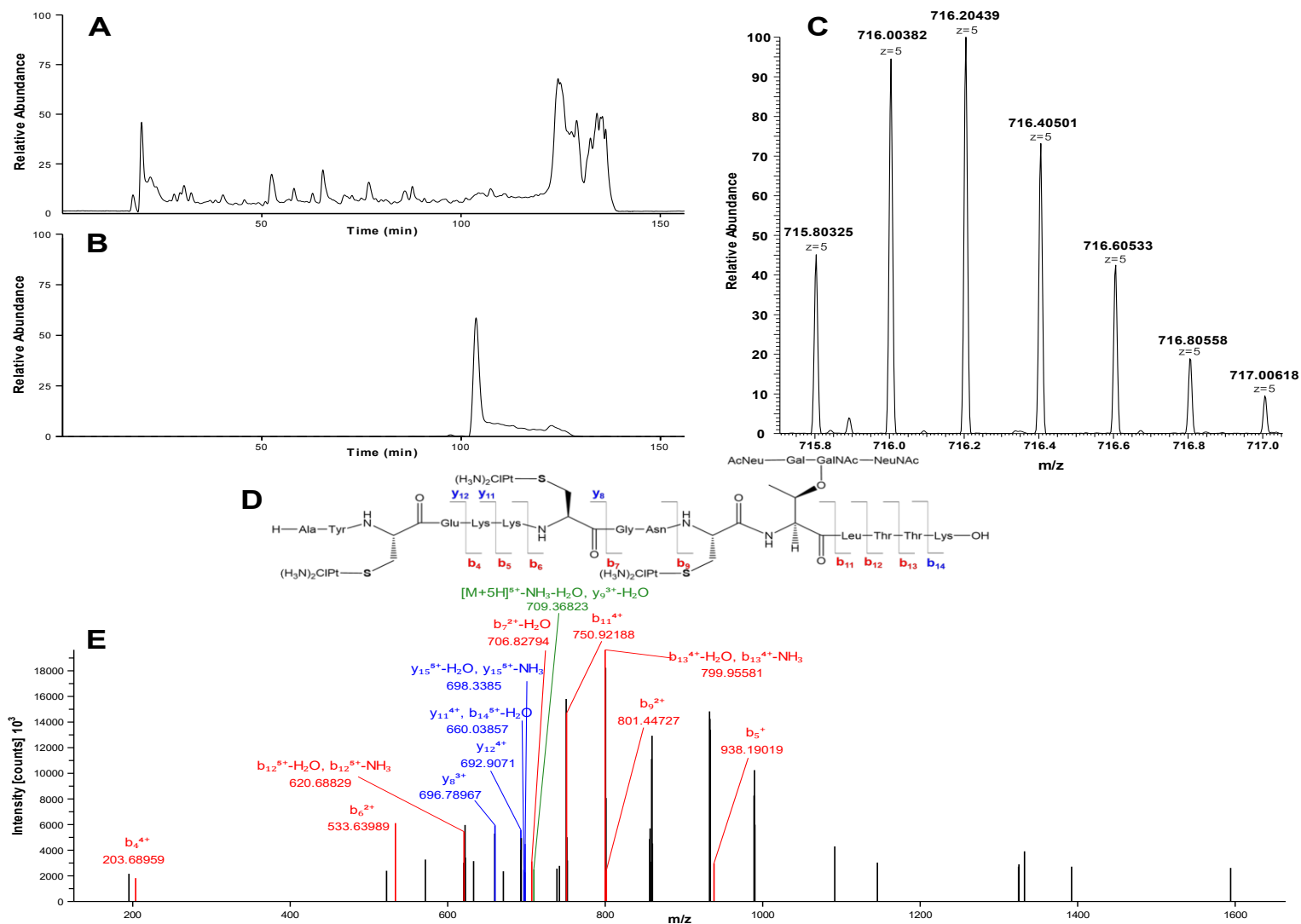


Figure 71 A. TIC, B. XIC, C. MS, D. peptide sequence and E. MS/MS spectrum of AYCEKKCGNCSLTLK at m/z 716.20437 (z=5)

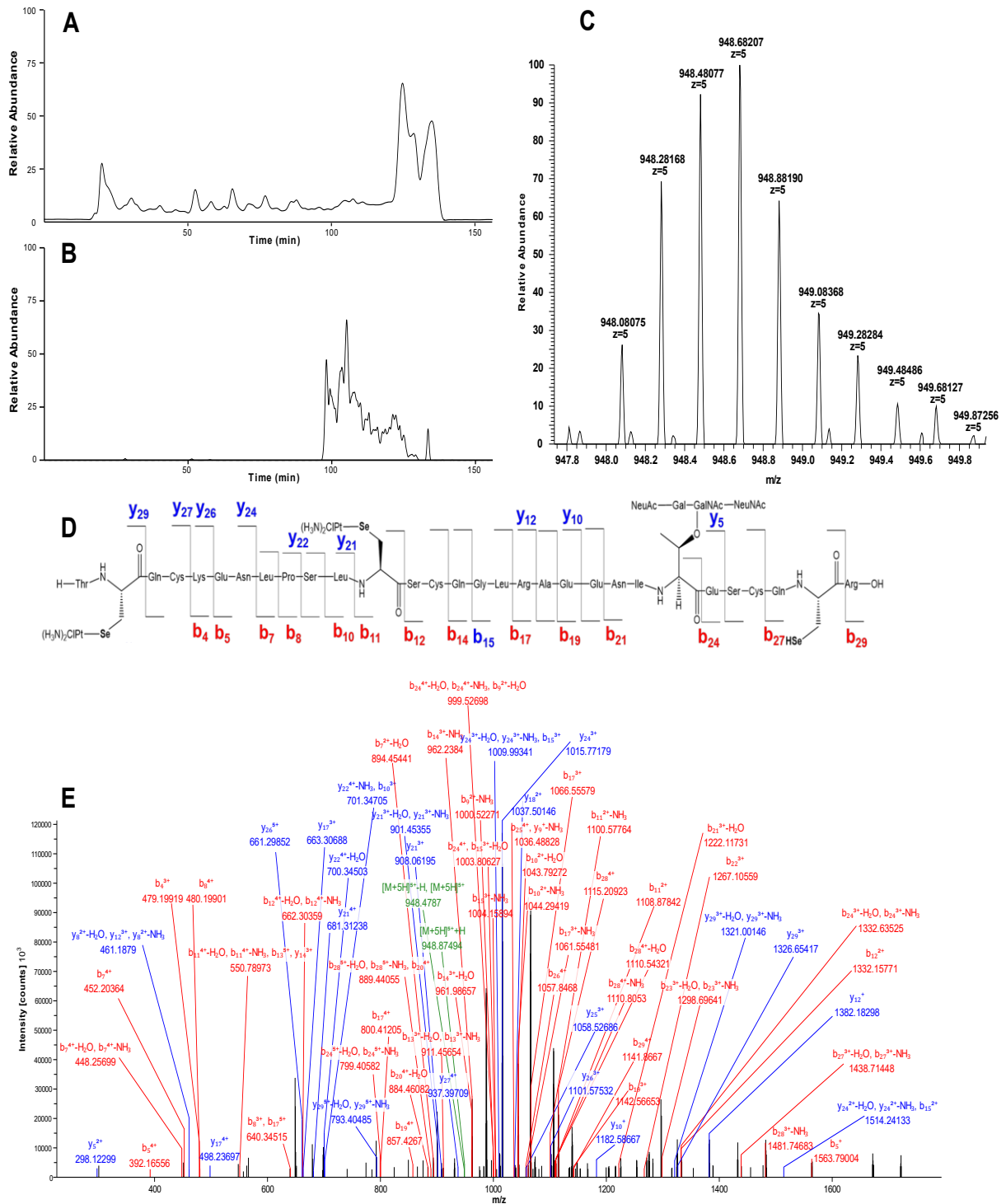


Figure 72 A. TIC, B. XIC, C. MS, D. peptide sequence and E. MS/MS spectrum of  
 TUQCKENLPLSLUSCQGLRAEENITESCQR at  $m/z$  948.68207 ( $z=5$ )

This peptide shows that SeCys platination is possible under our experimental conditions, and seems to prevail over Cys platination.

However, some experiment needs to be conducted on the model peptide to determine if the difference in term of platination could be linked to a stronger interaction or to the effect of some reagents used for the peptide digestion such as trypsin, that could impair the binding.

**Figure 73** is regrouping the four metaled peptides that were observed and characterized by MS/MS displaying either  $\text{AuPEt}_3^+$  or  $\text{Pt}(\text{NH}_3)_2\text{Cl}^+$ . These metalations obtained were mainly located on Cys and SeCys. These are preliminary results which need to be improved. However, they allow to better explain our first ICP-MS data showing the interaction of the purified SELENOP with the analyzed metallodrugs.

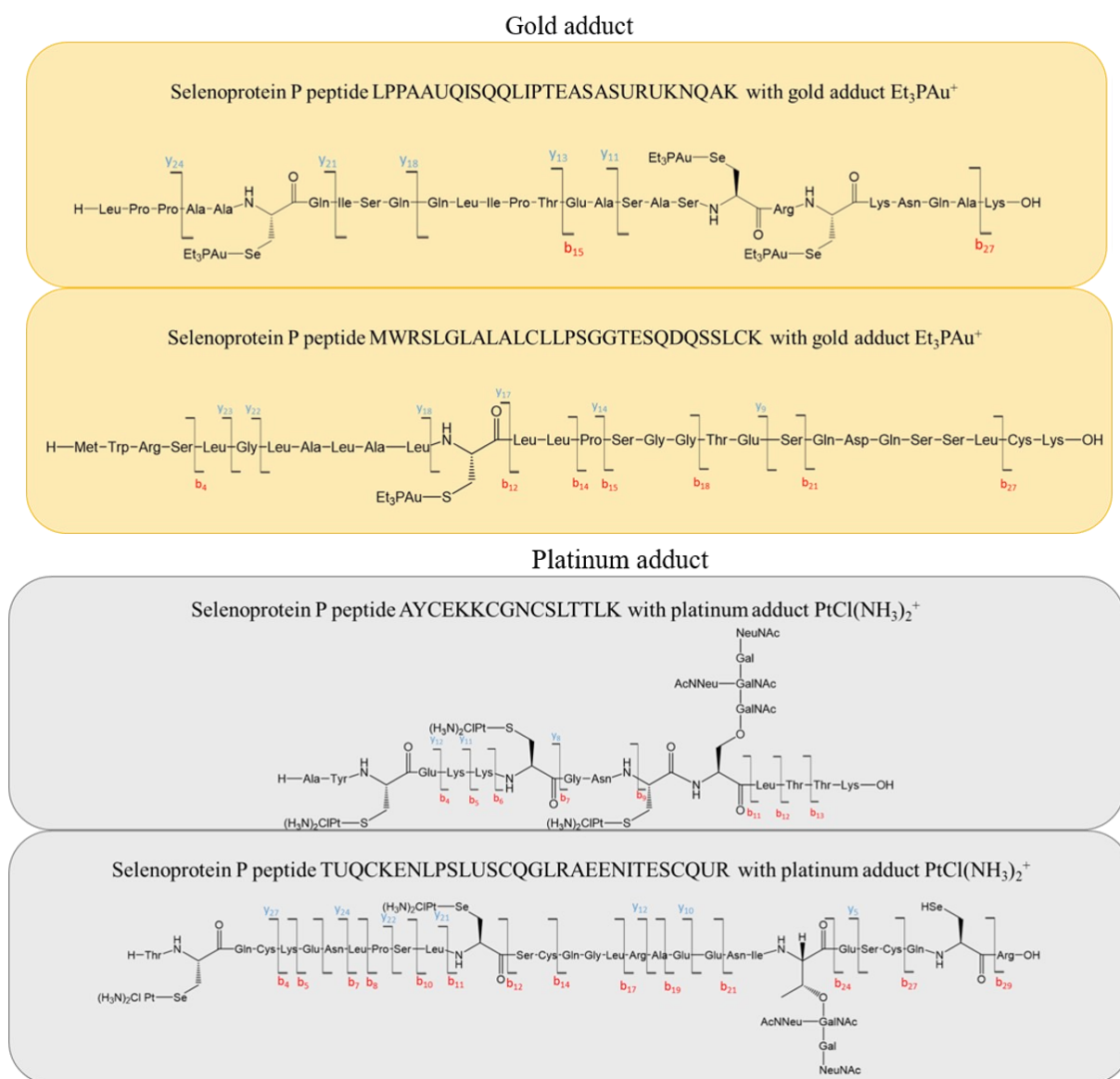


Figure 73 Selenoprotein P peptide displaying a metallodrug (auranofin or cisplatin) adduct and the MS/MS fragmentation of the peptide used to determine the binding site

In order to investigate the effect of the replacement of S by Se on the conditions of the reduction of the S-S and Se-Se bonds by medicinal gold(I) compounds, this section presents the reactions of auranofin and its strict analogues (**Figure 41**) with vasopressin and its diselenide counterpart (**Figure 41**) using reversed-phase HPLC coupled with electrospray MS/MS detection.

## 12.1. Unreacted peptides characterization

Our first objective was to characterize our starting peptides AVP (**Annexe 1 Table 1 entry 1**) and [Se-Se]-AVP (**Annexe 1 Table 1 entry 2**) by LC-MS, **Figure 74 and 75**, respectively.

The presence of two selenium atoms in [Se-Se]-AVP confers the characteristic isotopic pattern of the its mono- and di-charged ions (**Figure 76**).

## 12.2. Disulfide and diselenide reduction

First, we tried to reduce both compounds through classical methods by using DTT or TCEP as reductants. The reduction took place quite easily in the case of the disulfide bond when employing classical incubation protocols with DTT or TCEP (10 eq. with respect to the peptide), for 30 min at 37 °C (**Annexe 1 Figure 10, Annexe 1 Table 1 entry 3**). In contrast, the same experimental protocol did not result in any [Se-Se]-AVP reduction. Reduction of the latter was possible only after prolonged incubation of the peptide (at least 3h) with an elevated concentration of DTT (20 mM) at high temperature (70 °C), thus indicating the by far higher stability of diselenide bond in comparison with the disulfide bond. Notably, the latter reduction procedure generated two different products (**Figure 77**). By comparing the relative intensity of their isotopic peaks (**Figure 78**), it appeared that only one Se atom was conserved in the peptide structure. The reduction probably favours the degradation of one of the SeCys residues. MS/MS experiments on these two products revealed that Se is preserved either at the N-terminus (**Figure 79**) or in the middle of the sequence (**Figure 80 and 81, Annexe 1 Table 1 entry 5**). In the latter case, we observed at the N-terminus the likely formation of a pyruvoyl group, a hydrolysis product of the unsaturated amino acid dehydroalanine, formed by  $\beta$ -elimination of SeCys (348).

## 12.3. Effect of temperature on the reduction of the diselenide peptide

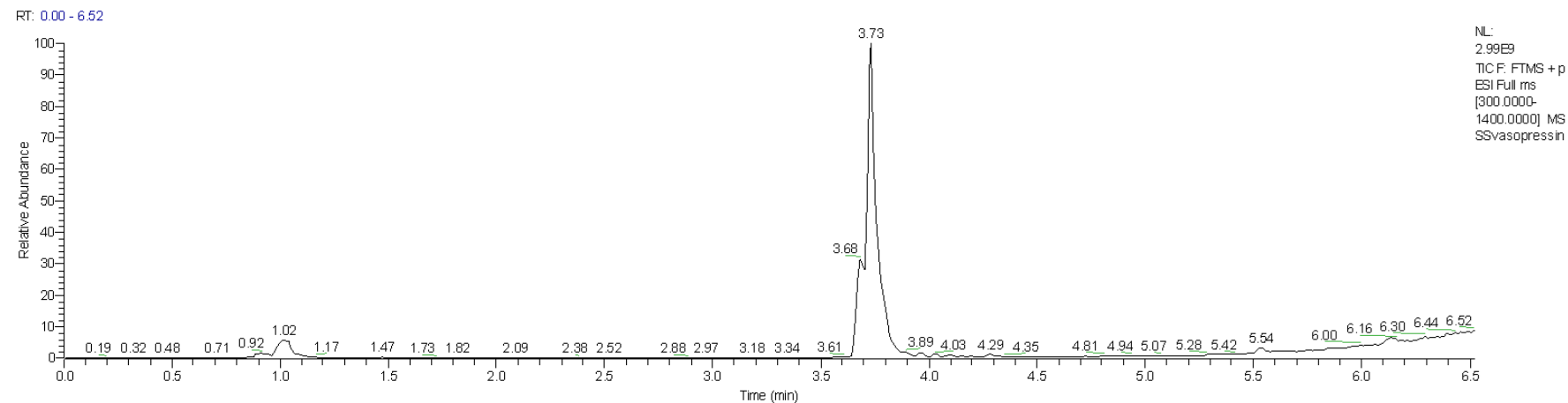
To discriminate between the effects induced on [Se-Se]-AVP by DTT or by temperature, we incubated the peptide at 70 °C in the absence of a reducing agent. We observed a partial conversion of the peptide into dimers (**Figure 82 and Annexe 1 Table 1 entry 5**). This result suggests that high temperature favors the formation of dimers, most likely through the disruption of intramolecular diselenide bridges and the establishment of intermolecular ones. Even after heating, only one Se atom is conserved in the peptide structure and is probably involved in the dimer formation.



AVP

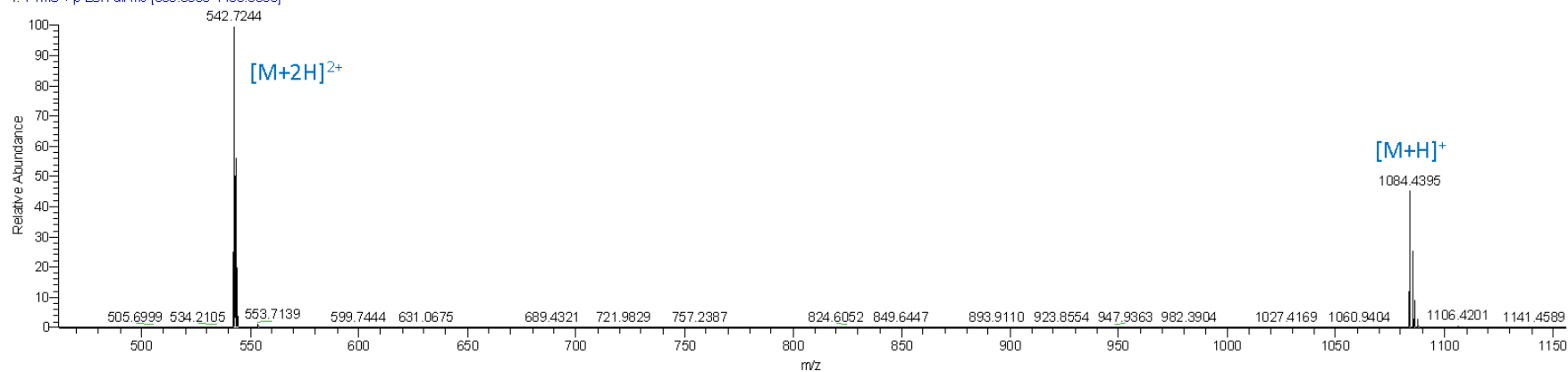
D:\Master...\26032021\LC\SSvasopressin

03/26/21 13:58:08



A

SSvasopressin #462-470 RT: 3.72-3.76 AV: 4 NL: 7.81E8  
T: FTMS + p ESI Full ms (300.0000-1400.0000)



B

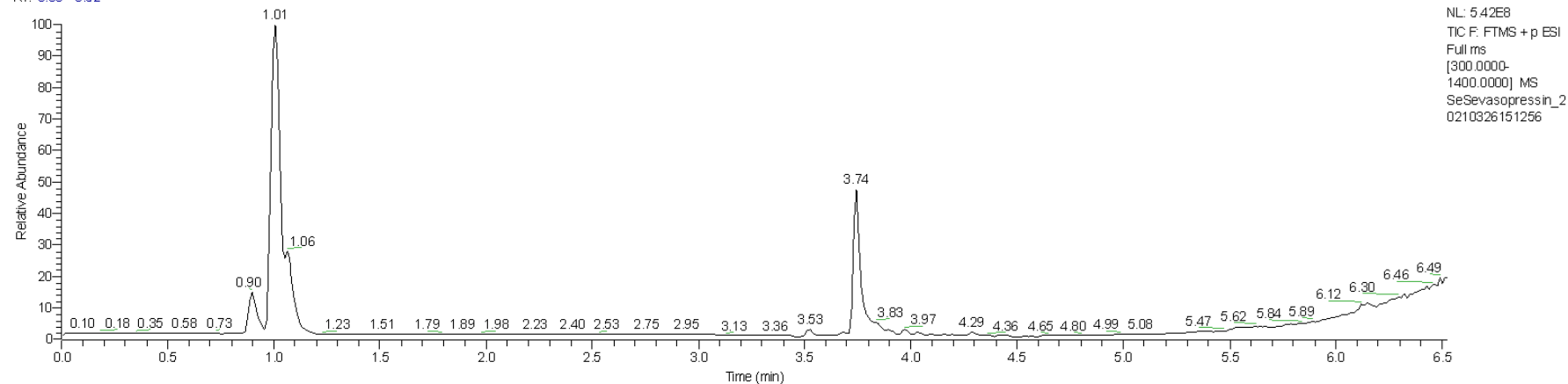
Figure 74 LC-MS of unreacted AVP. (A) TIC, (B) MS spectrum of peak at tR= 3.73 min

[Se-Se]-AVP

SeSevasopressin\_20210326151256

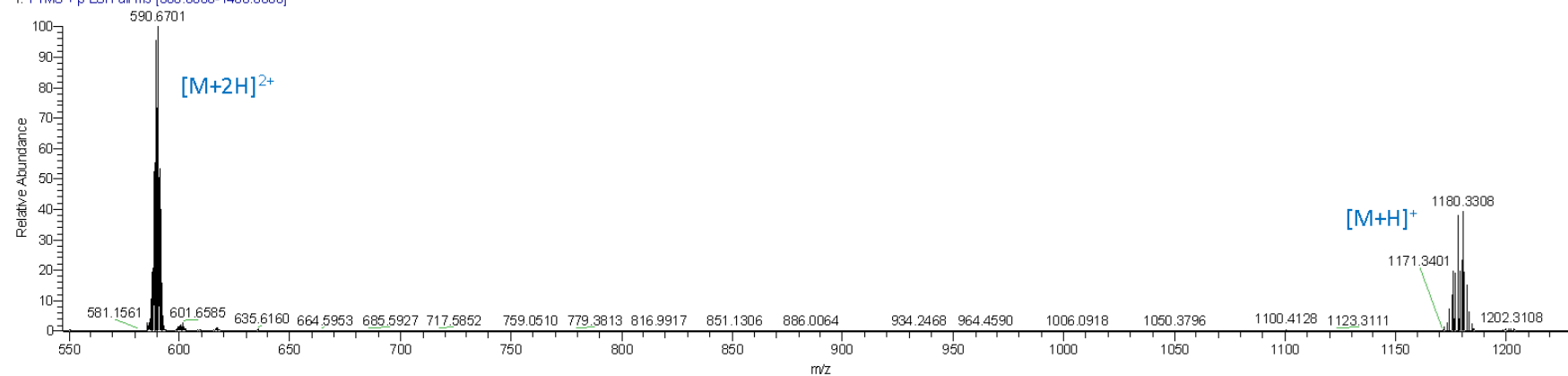
03/26/21 15:14:12

RT: 0.00 - 6.52



A

SeSevasopressin\_20210326151256 #536-544 RT: 3.72-3.75 AV: 4 NL: 1.90E7  
T: FTMS + p ESI Full ms [300.0000-1400.0000]



B

Figure 75 LC-MS of unreacted [Se-Se]-AVP. (A) TIC, (B) MS spectrum of peak at  $t_R = 3.74$  min

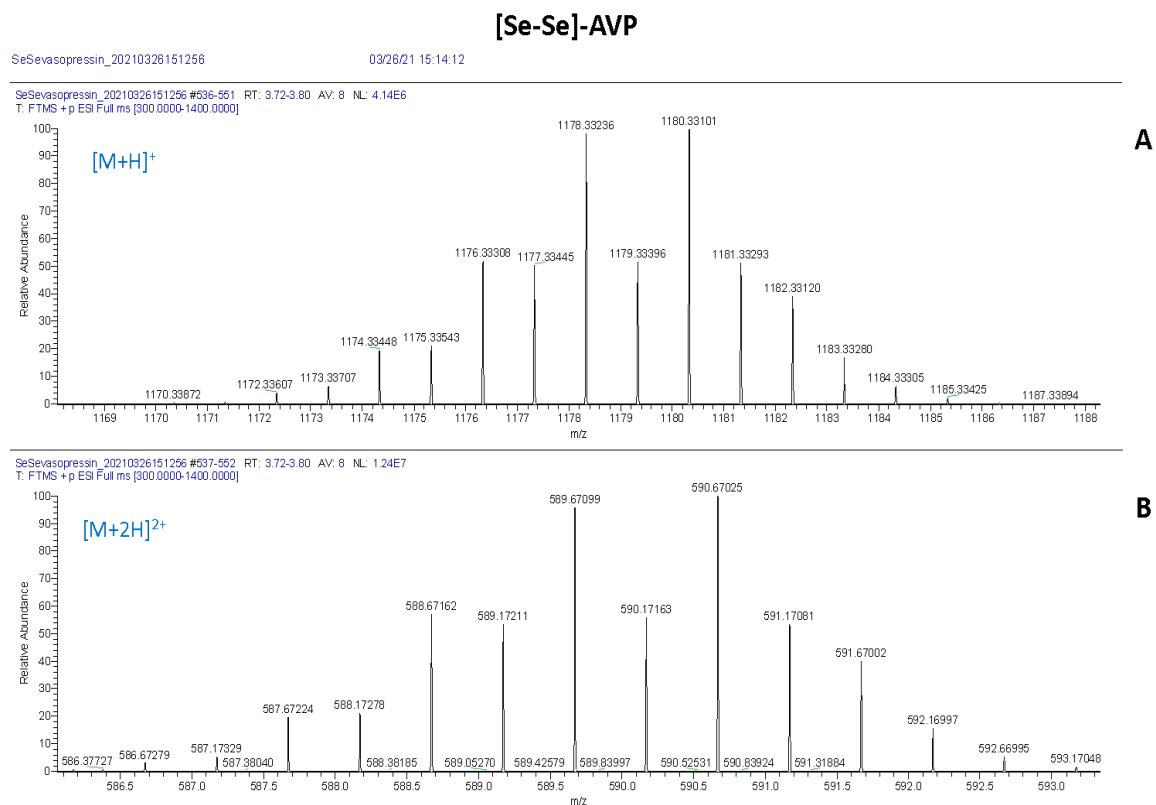


Figure 76 MS isotopic pattern of the unreacted [Se-Se]-AVP for mono- ( $m/z = 1180.3310$ ) and di- ( $m/z = 590.6702$ ) charged ion

## 12.4. Reaction of auranofin with reduced peptides (thiol or selenol)

The reaction of AVP, in its reduced form, with auranofin and its analogues proceeded as expected showing a partial metalation of AVP by auranofin and its chloro-analogue  $\text{AuPEt}_3\text{Cl}$  either by Au(I) or by  $\text{AuPEt}_3^+$  ion (**Figure 83 and 84**). This result is in line with previous observations (222). However, it implies that while the reaction of auranofin with the disulfide group can occur at physiological temperature in a reducing environment, it cannot with the diselenide bridge. Indeed, the latter can undergo reductive cleavage only at a very high temperature and in the presence of a large quantity of DTT.

## 12.5. Reaction of gold(I) compounds with the oxidized peptide (S-S and Se-Se)

Subsequently, we explored the reactivity of the S-S and Se-Se bridges when vasopressin and its Se-Se analogue were challenged with auranofin and its analogues in the absence of reducing agents. We had assumed that given the large affinity of the soft gold(I) ion to either the S or Se atoms, these compounds might induce direct S-S and Se-Se bridge cleavage. However, the precise experimental conditions under which such bridge cleavage occurs had to be defined.

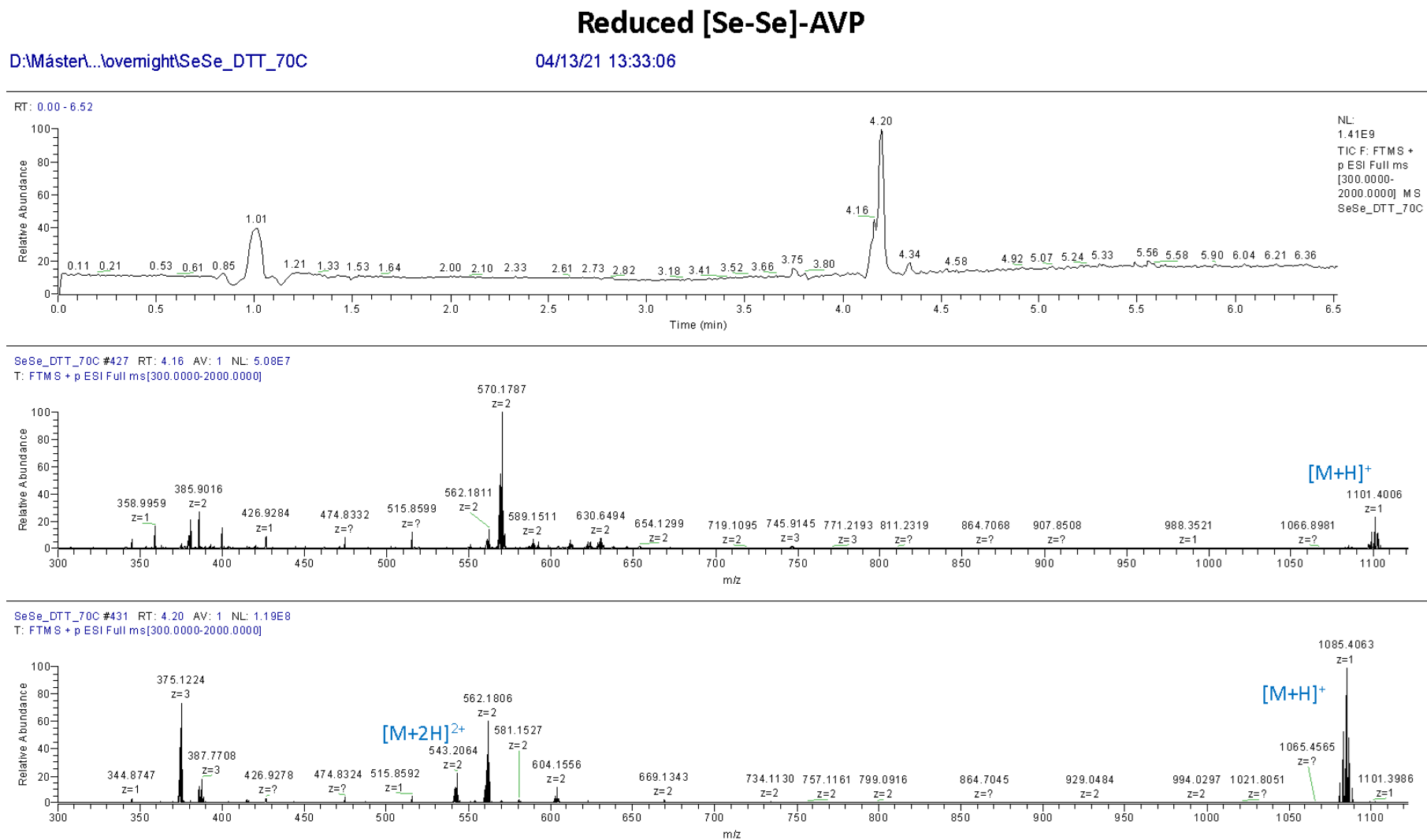


Figure 77 LC-MS of reduced [Se-Se]-AVP. (A) TIC. (B) MS spectrum of peak at  $t_R = 4.16$  min. (C) MS spectrum of peak at  $t_R = 4.20$  min.

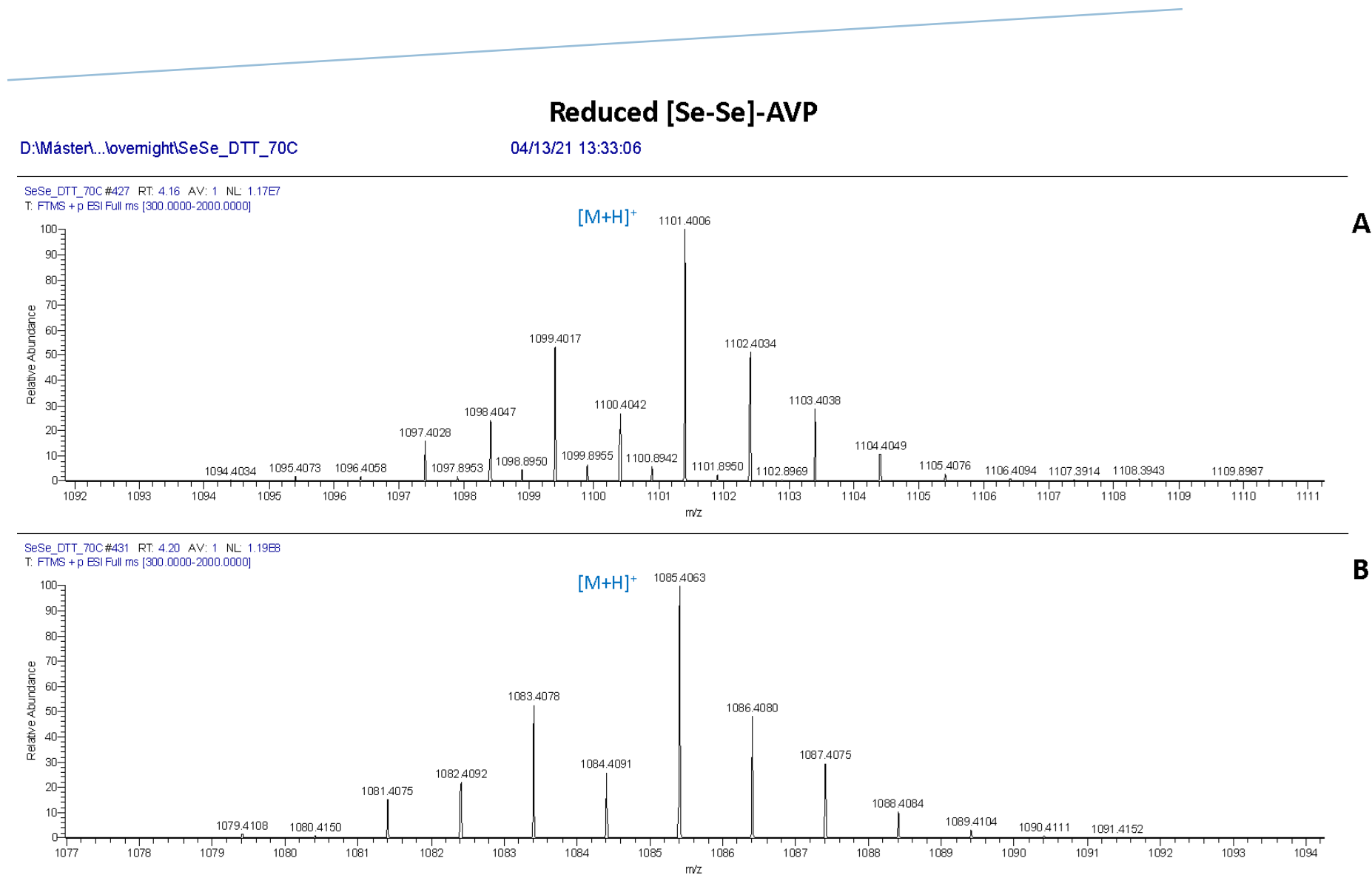


Figure 78 LC-MS of reduced [Se-Se]-AVP. (A) MS spectrum of peak at tR = 4.16 min. (B) MS spectrum of peak at tR = 4.20 min.

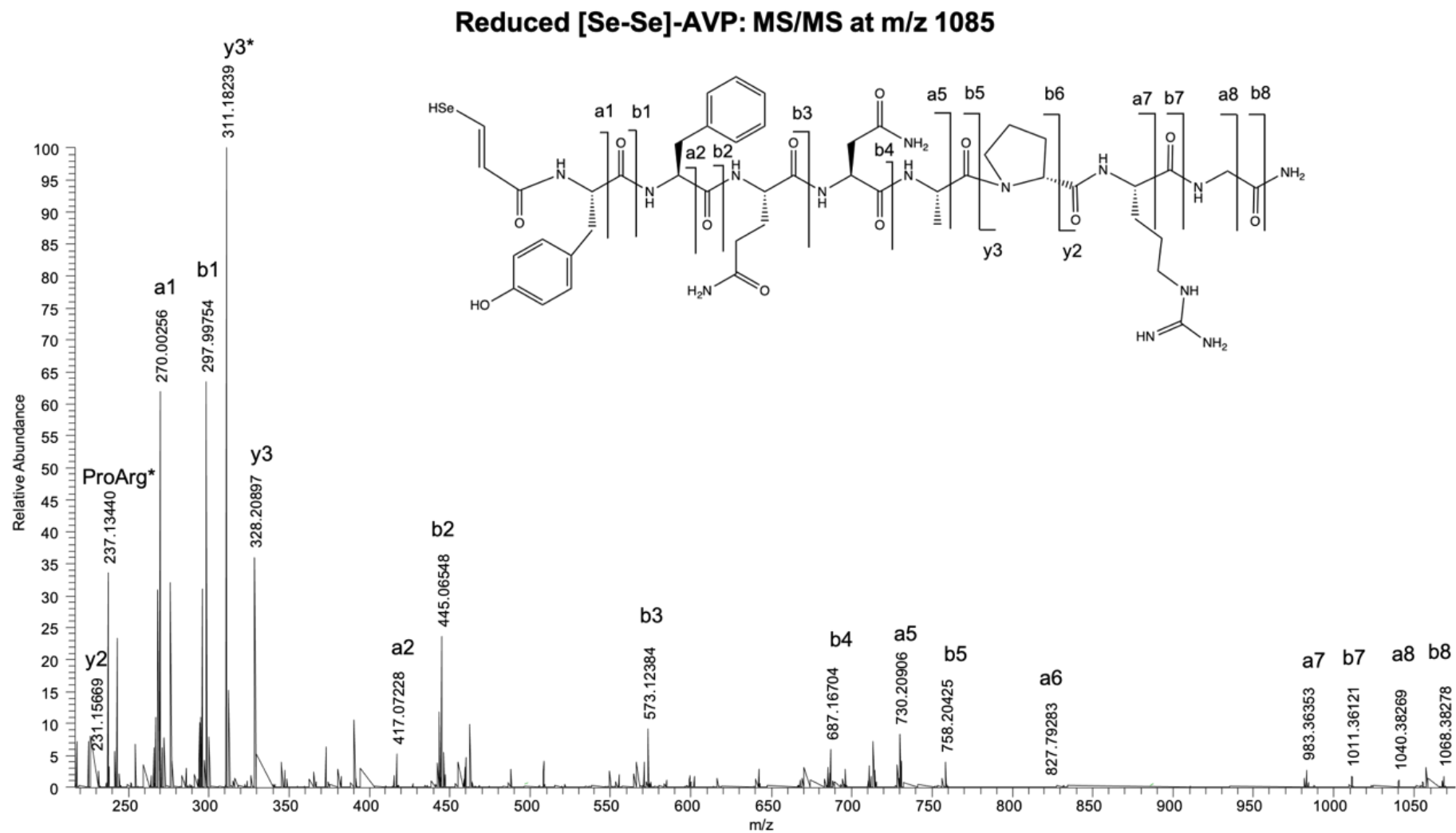


Figure 79 MS/MS of reduced [Se-Se]-AVP at m/z= 1085 (z=1). Principal fragments at HCD = 30.

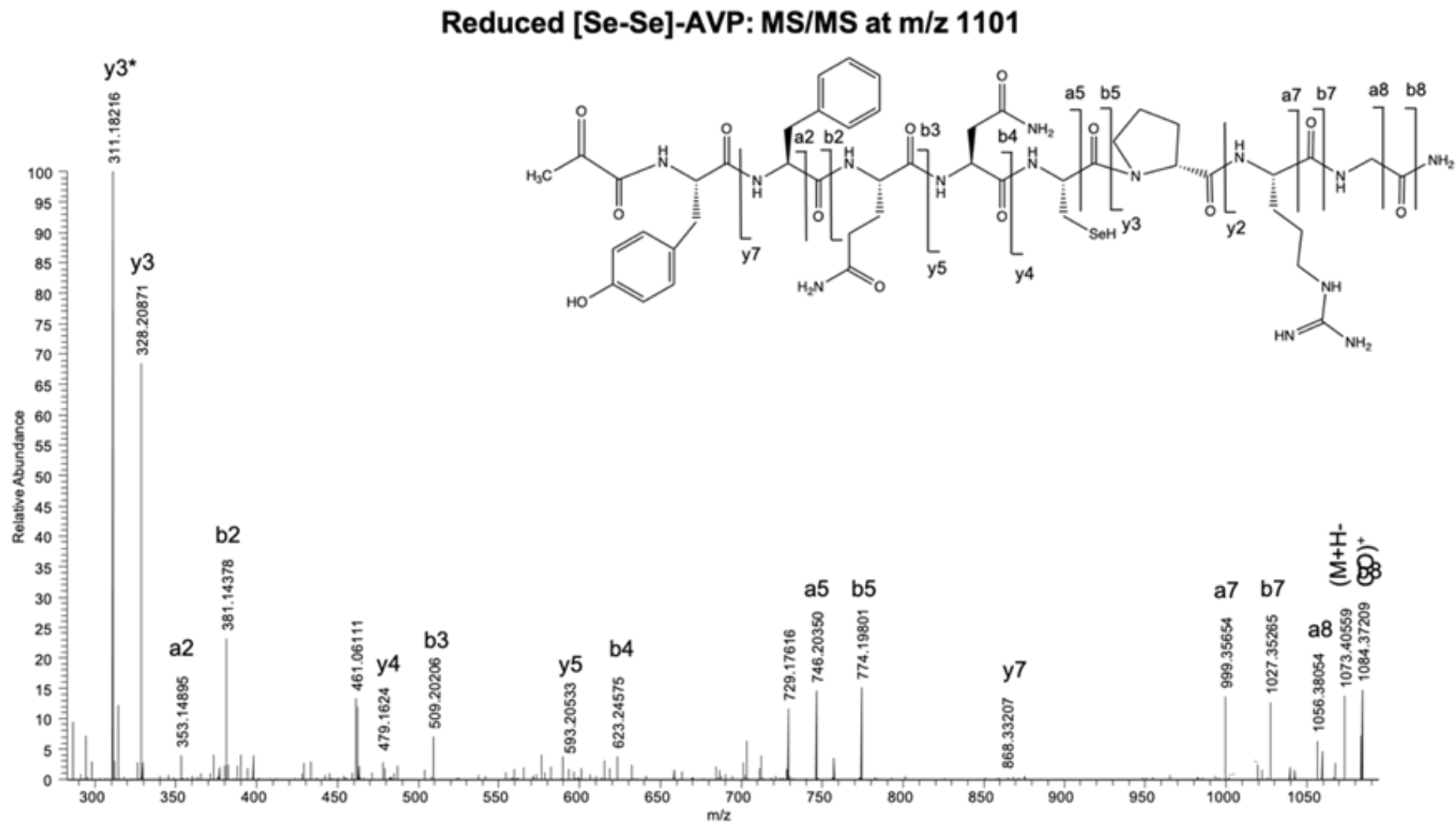


Figure 80 MS/MS of reduced [Se-Se]-AVP at m/z=1101.3960 (z=1). Principal fragments at HCD = 30

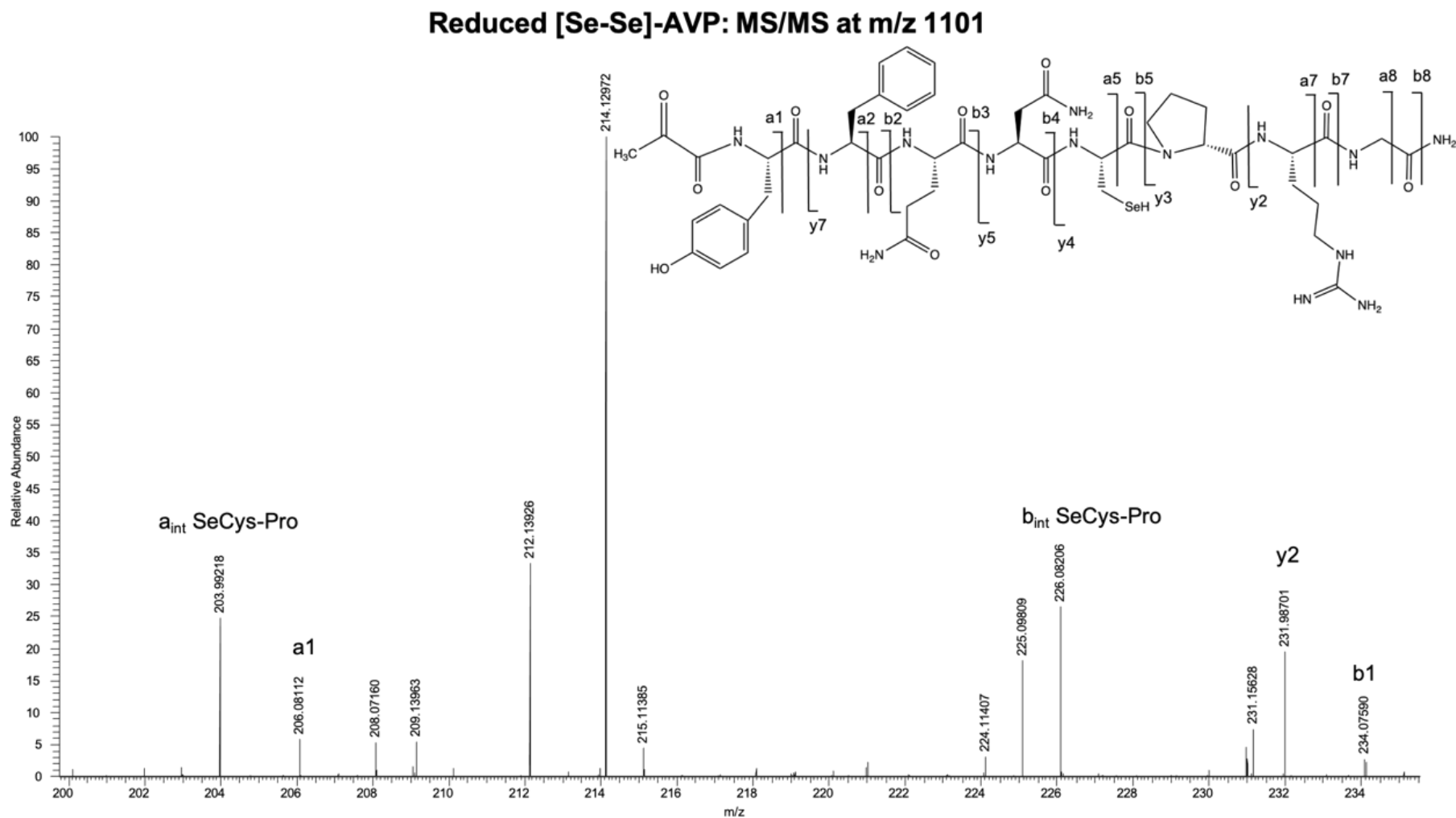


Figure 81 MS/MS of reduced [Se-Se]-AVP at m/z=1101.3960 (z=1). Principal fragments at HCD = 35



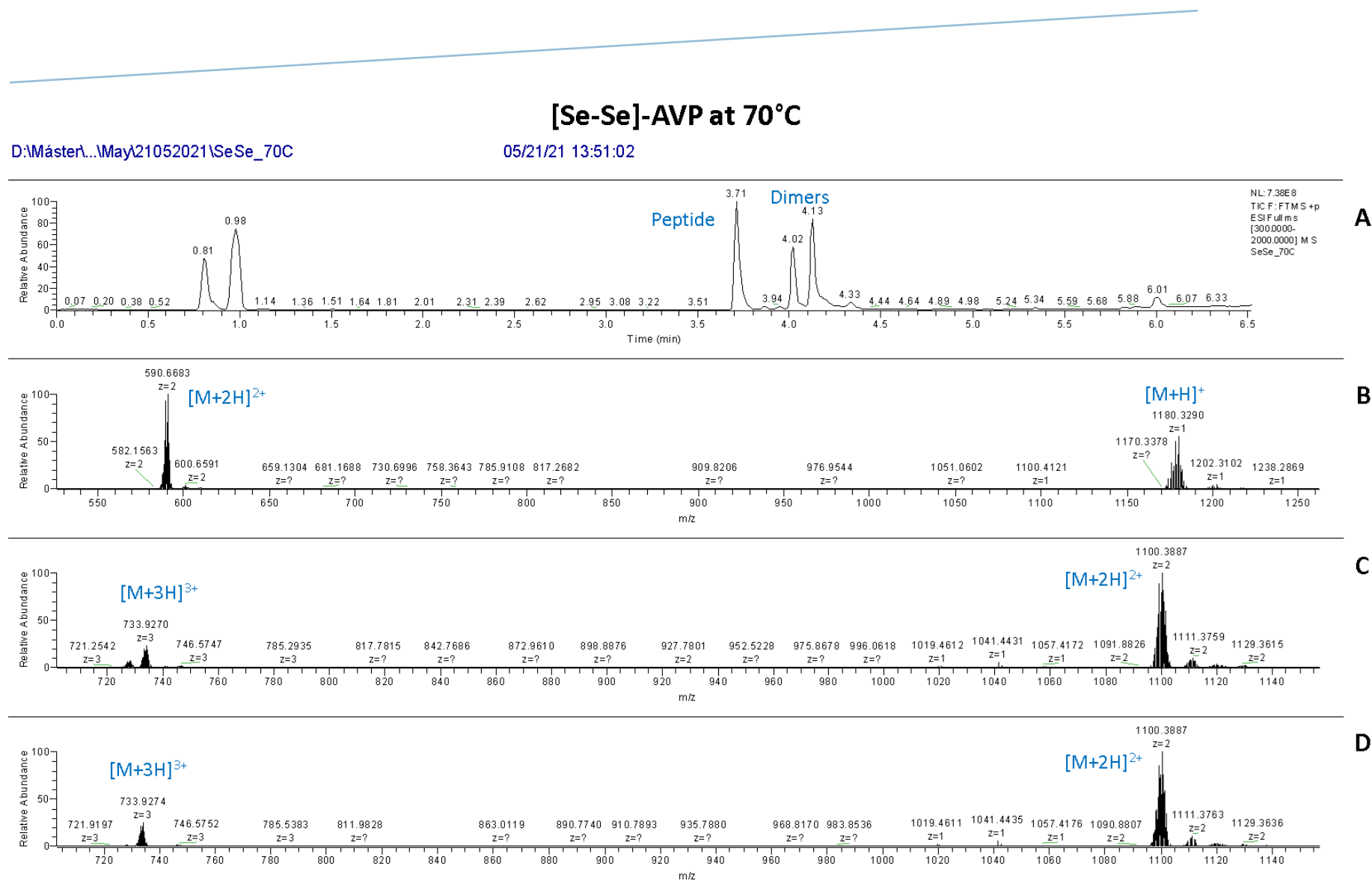
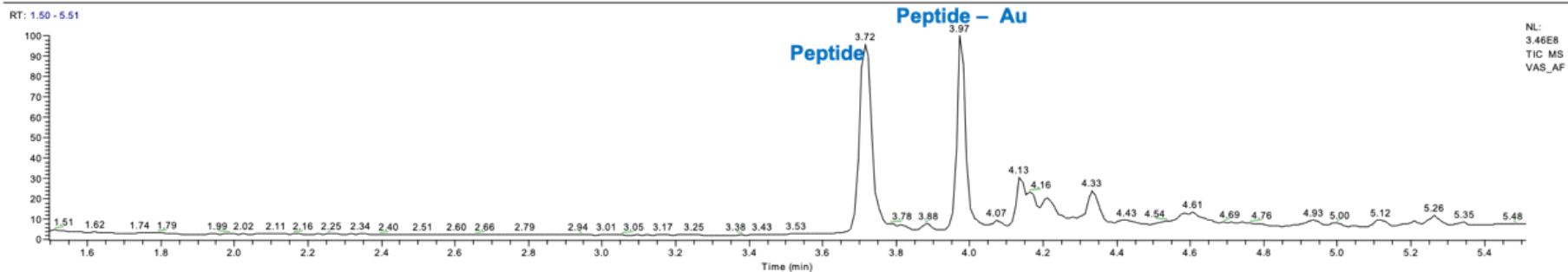


Figure 82 LC-MS of [Se-Se]-AVP incubated overnight at 70 °C. (A) TIC. (B) MS spectrum of peak at tR = 3.71 minutes. (C) MS spectrum of peak at tR = 4.02 minutes. (D) MS spectrum of peak at tR = 4.13 minutes

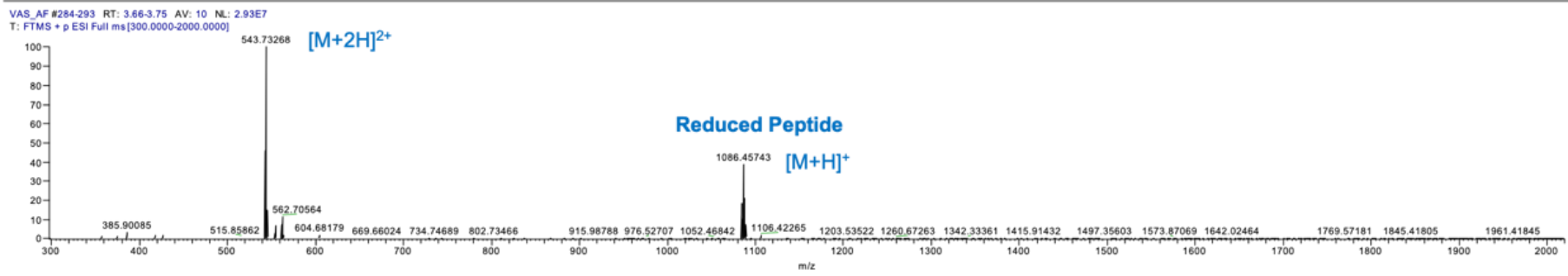
### Reduced AVP after incubation with AF at 37°C

D:\Luisa\gold\April\29042021\VAS\_AF

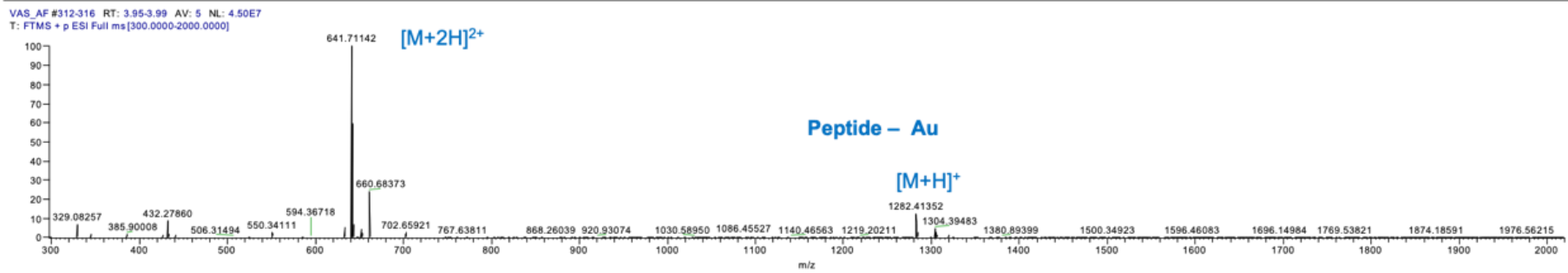
04/29/21 11:22:45



A



B



C

Figure 83 LC-MS of reduced AVP incubated with AF overnight at 37 °C. (A) TIC. (B) MS spectrum of peak at tR = 3.72 minutes. (C) MS spectrum of peak at tR = 3.97 minutes.

Reduced AVP after incubation with Et<sub>3</sub>PAuCl at 37°C

D:\Luisa\gold\April29042021\VAS\_AFCI

04/29/21 11:00:17

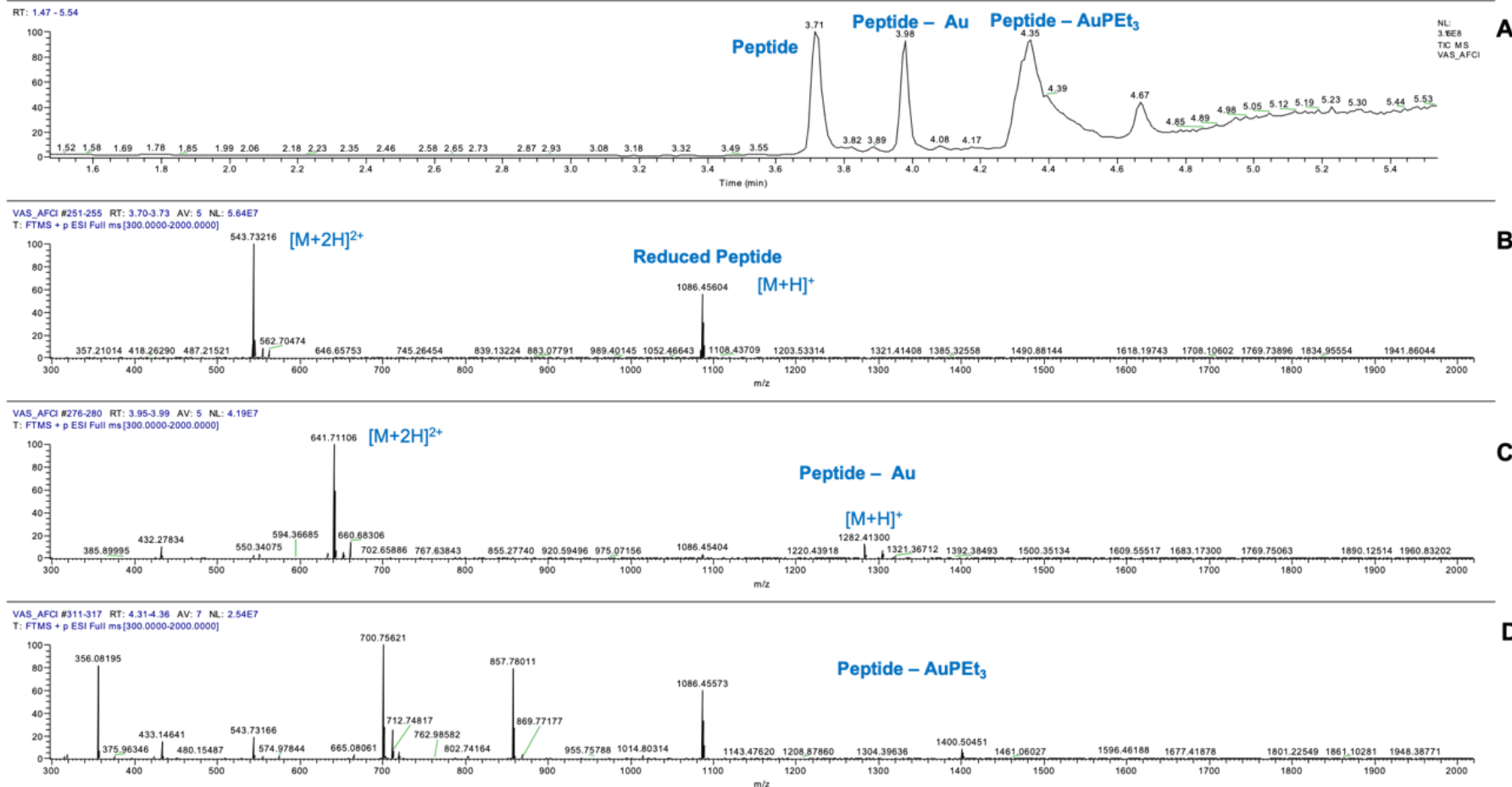


Figure 84 LC-MS of reduced AVP incubated with Et<sub>3</sub>PAuCl overnight at 37 °C. (A) TIC. (B) MS spectrum of peak at t<sub>R</sub> = 3.72 minutes. (C) MS spectrum of peak at t<sub>R</sub> = 3.97 minutes. (D) MS spectrum of peak at t<sub>R</sub> = 4.35 minutes

### 12.5.1. *Comparison of reactivity at 37°C and at 70°C*

Quite surprisingly, upon working at 37°C, we realized that an important quantity of unreacted peptides was still present and only small amounts of peptide-AuPEt<sub>3</sub> adduct were formed. Yet, by performing the same experiment at 70°C, a much higher degree of peptide metalation was observed (**Figure 85 and 86**). Interestingly, also in the case of S-S vasopressin, the high temperature favours the formation of a pyruvoyl group at the N-terminus of the sequence (41) (**Annexe 1 Table 1 entry 7**).

### 12.5.2. *Comparison of reactivity between auranofin analogues*

We noticed that auranofin and all its tested analogues were able, at 70°C, to form gold adducts with both S-S and Se-Se vasopressin (**Annexe 1 Figure 11 to 18**). The adducts were characterized by MS/MS experiments revealing on both peptides the presence of two AuPEt<sub>3</sub> moieties, one forming an ion via a cationization mechanism and the other one directly bound to S or Se, in AVP and [Se-Se]-AVP, respectively (**Figure 87 and 88, Annexe 1 Table 1**). Interestingly, among the tested gold compounds, auranofin yielded the least extended metalation. Its lower reactivity can be explained by the better leaving group ability of the -Cl, -Br, -I ligands substituting the auranofin thiosugar moiety in its analogues.

### 12.5.3. *Comparison of reactivity of the S-S and Se-Se bridges*

Upon comparing the LC profiles of S-S or Se-Se vasopressin reacting with gold compounds at high temperature, it appears that the reactivity of all Au(I) compounds with [Se-Se]-AVP is much higher than that with AVP. This can be seen in **Figures 85a and 86a** showing the LC-MS of the two peptides incubated with Et<sub>3</sub>PAuCl. Indeed, while [Se-Se]-AVP is almost completely converted into its gold adduct, AVP reacts only partially and a large amount of unreacted peptide is still present in the reaction medium after the same incubation time. This observation further demonstrates that the affinity of these gold(I) compounds for Se are much bigger than that for S.

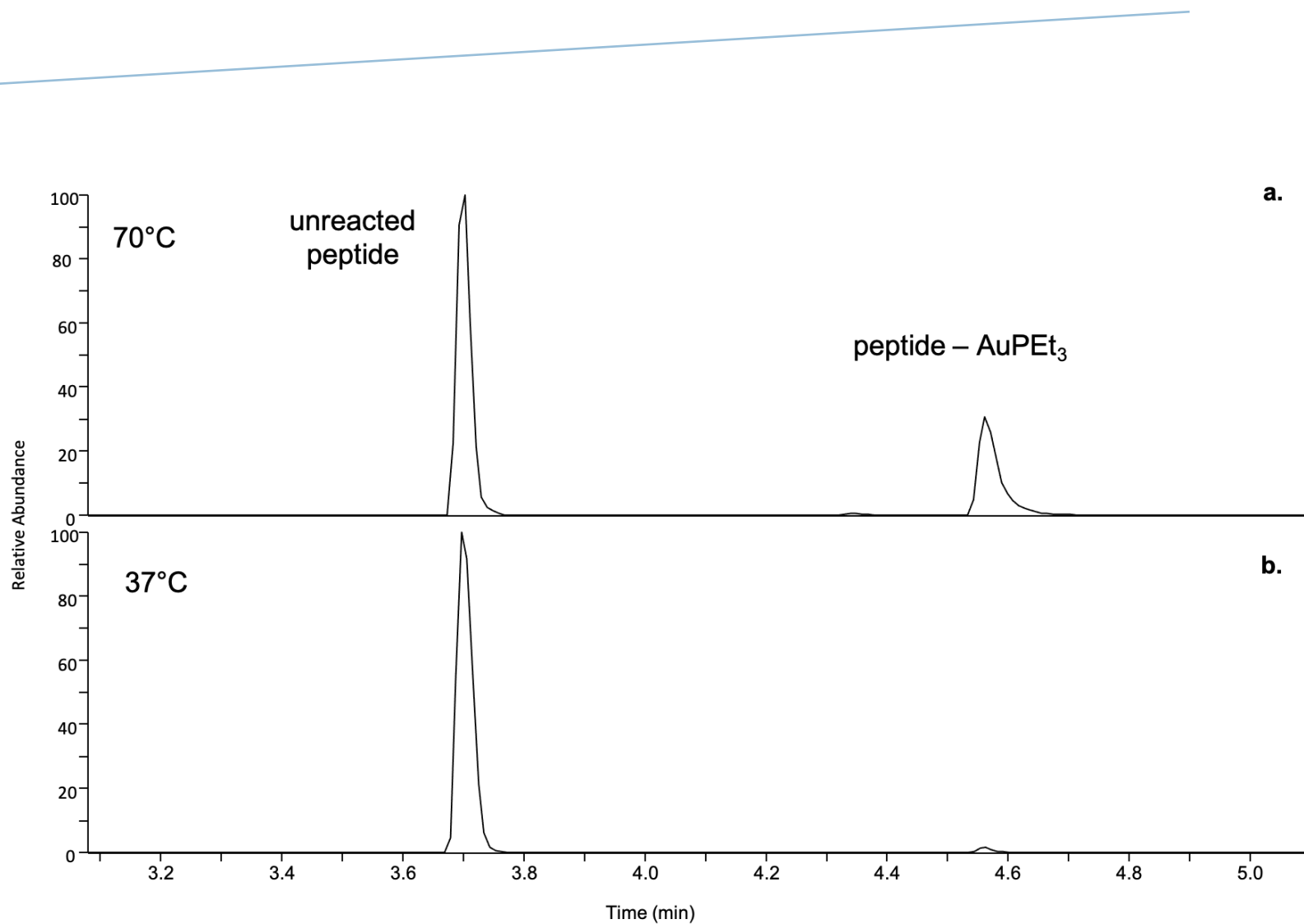


Figure 85 LC-MS of AVP incubated with Et<sub>3</sub>PAuCl at 70 °C (a) and 37 °C (b). XIC of ions m/z 1084.44 (AVP, t<sub>R</sub>=3.70) and 1367.49 (peptide-AuPEt<sub>3</sub>, t<sub>R</sub>=4.56)

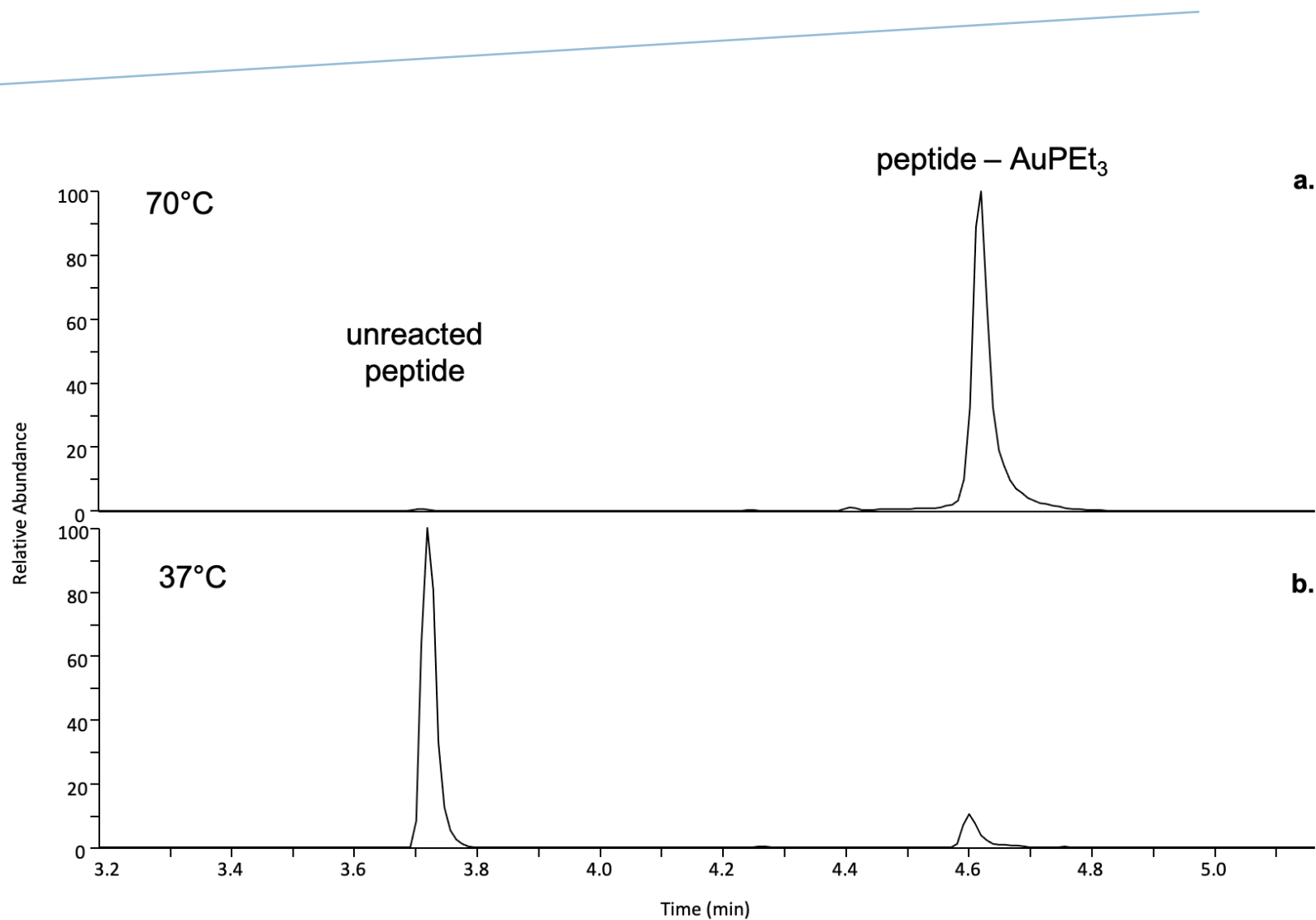


Figure 86 LC-MS of [Se-Se]-AVP incubated with Et<sub>3</sub>PAuCl at 70 °C (a) and 37 °C (b). XIC of ions m/z 1180.33 (unreacted peptide, t<sub>R</sub>=3.70) and 1415.44 (peptide–AuPEt<sub>3</sub>, t<sub>R</sub>=4.62)

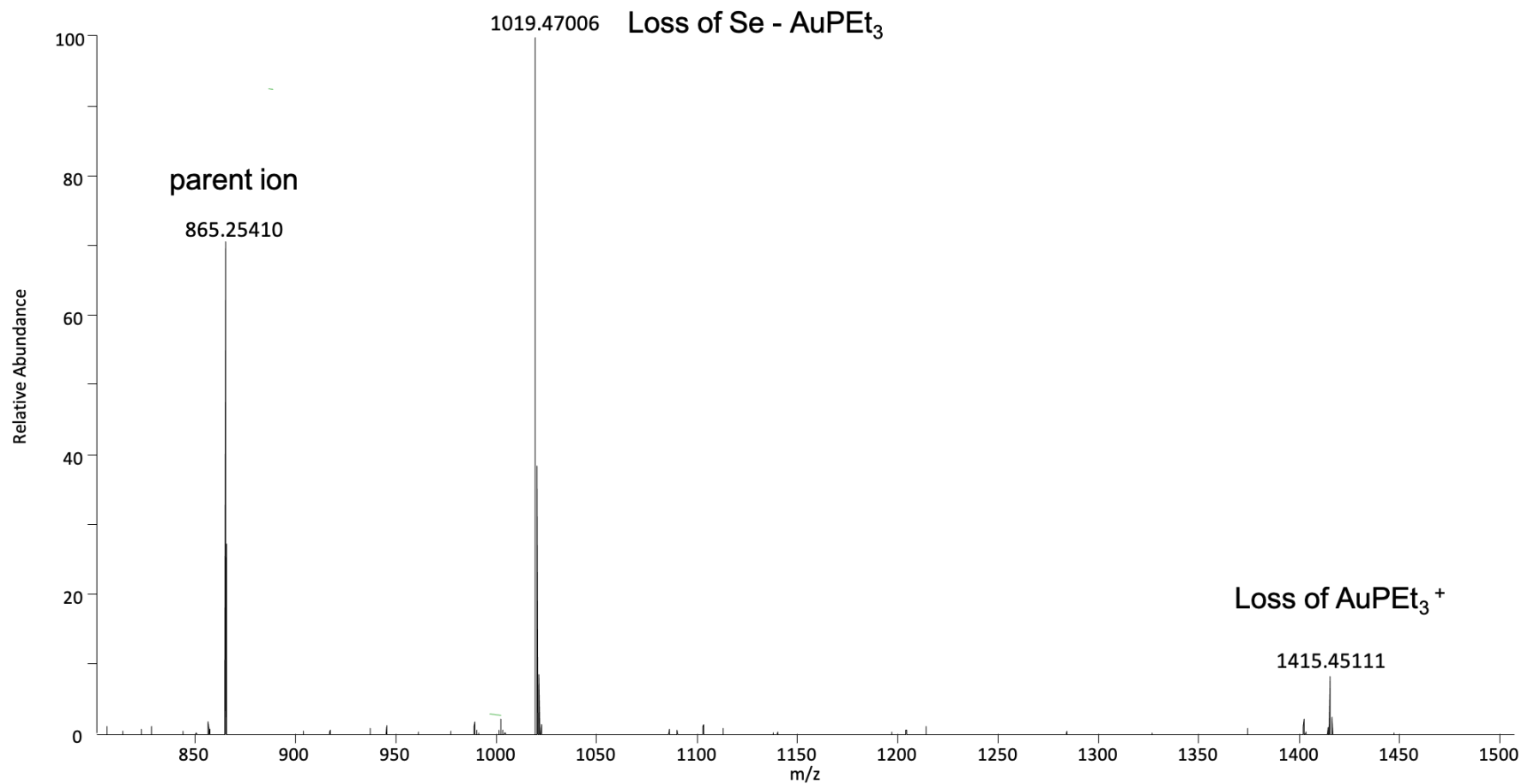


Figure 87 MS/MS of AVP incubated with Et<sub>3</sub>PAuI at m/z 841.2799 (z=2). Principal fragments at HCD = 20.

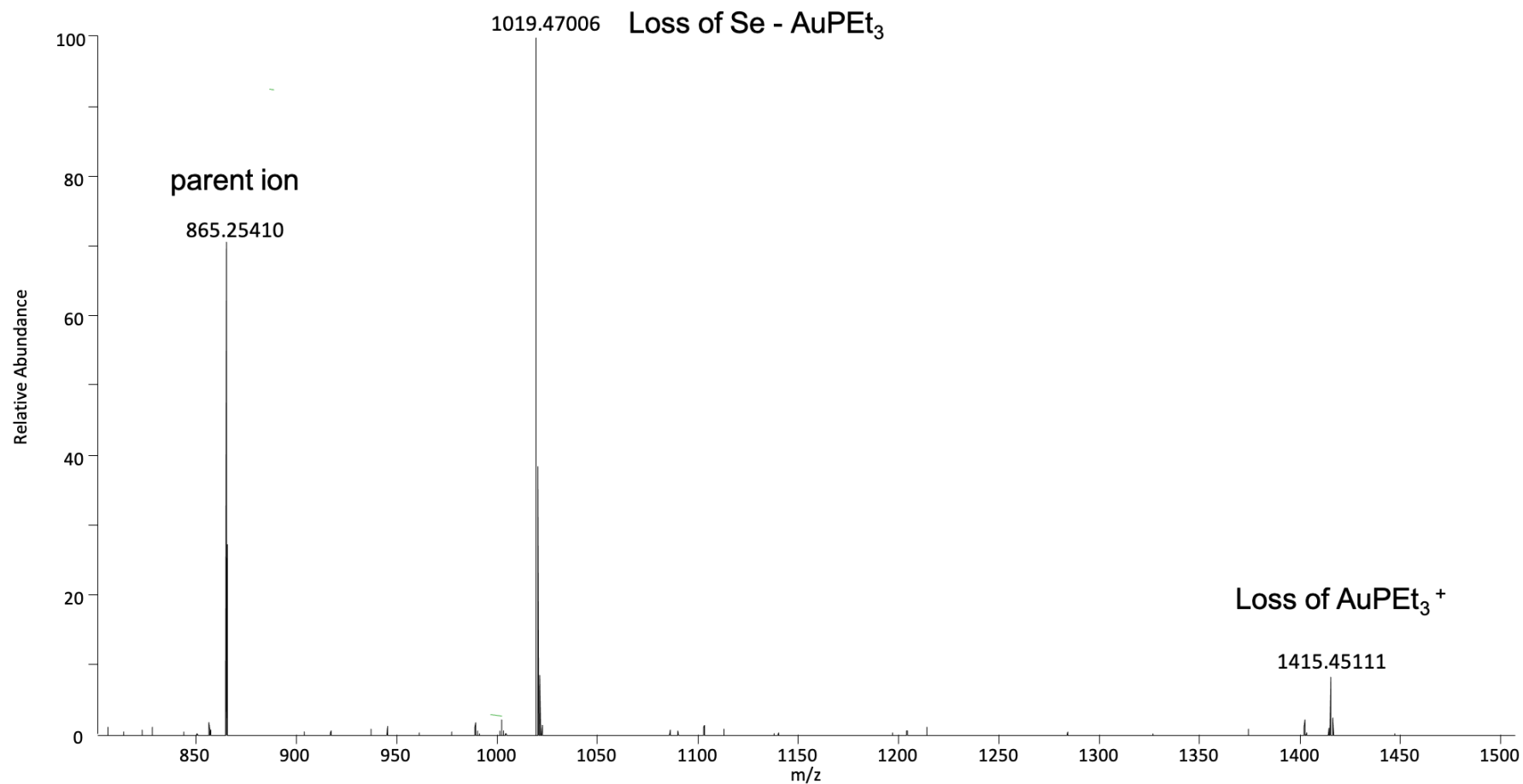


Figure 88 MS/MS of [Se-Se]-AVP incubated with Et3PAuI at m/z 865.2541 (z=2). Principal fragments at HCD = 20



The developed SELENOP purification method allowed relatively pure SELENOP to be obtained for studies of its interactions with metallodrugs. The separation of SELENOP from other selenoproteins was achieved using the double affinity IMAC-Heparin column. The SELENOP could be easily separated from the other proteins present in serum as observed by SDS-PAGE. The achieved methodological improvements offer a viable method to purify SELENOP from serum in quantities sufficient of studies of its interactions with metals.

The recoveries of 14% measured may seem low but there are impossible to be compared with literature studies as this is to our knowledge the first time where such recoveries were systematically measured at each step of the procedure. The major source of losses is the concentration step after heparin-affinity purification generating a large volume of dilute solution. The non-specific affinity to the SPE filtration used maybe one reason but the presence of  $\alpha$ -2-macroglobulin in the eluate opens the possibility of the formation of SELENOP-  $\alpha$ -2-macroglobulin adducts. This may also be the reason for the missing of some SELENOP at the elution volume in size-exclusion chromatography. Another open question is why the amount of SELENOP measured with the protein kit is slightly different than that obtained by other techniques such as total selenium quantification.

In terms of quantification of SELENOP in serum, our results are similar to those reported in the literature, meaning that the matrix effect of serum is not that important and does not necessarily require the use of more sophisticated quantification techniques such as isotope dilution ICP MS.

The characterisation of the purified SELENOP allowed us to detect new selenopeptides that were not detected so far in the literature. On the four-peptide presented in the literature, we identified three of them by MS characterization and 2 new peptide that were not published were also detected. One of these peptides was displaying a O-glycosylation that was elucidated thank to MS/MS data. The total number of SeCys that were identified (six of them) thank to the 5 peptides, is to our knowledge the highest reported SeCys detected so far for SELENOP, meaning that only the 4 last peptides located at the *N-terminus* of SELENOP need to be identified.

In terms of SELENOP purification, using magnetic bead coated with streptavidin and VICAT reagent containing biotin residue, a fishing-like methodology was imagined to selectively target selenium-containing species and more specifically SeCys containing protein from complex medium (349). The interest of VICAT reagents is the possibility to remove them using light-cleavable moiety or by elution to obtain either the selenoproteins with or without a mass tag that could be used to perform quantification of the protein using ESI-MS methodology. The method could eventually help us to overcome the dilution problem that was observed during the purification of SELENOP.

The availability of the purified SELENOP, allowed the observation, for the first time, of the formation of adducts with auranofin and cisplatin. The metalation site was preserved after tryptic digestion. Several peptides that were displaying interactions between Cys, SeCys and the metallodrugs studies could be observed. These results corroborate the hypothesis that SELENOP can interact with metallodrugs via SeCys and Cys residues. Two peptides were obtained with an  $\text{AuPEt}_3^+$  adducts on either Cy and SeCys amino acids, and two peptides were obtained with a  $\text{PtCl}(\text{NH}_3)_2^+$  adducts also on Cys and SeCys, the binding site were determined using the fragmentation data obtained by MS/MS. The four peptides obtained are specific to SELENOP, and displayed different sequences. These observations were possible owing to the excellent sensitivity of the state-of-the-art mass spectrometer. Cisplatin and auranofin both preferentially interact with Cys, SeCys. However, their binding mechanism should be different due to their own chemistry.

For the moment, studies of the interactions of selenols and diselenides with metals and metallocompounds are still largely dependent on the availability of model compounds. The studies on selenovasopressin offer clear insight into the comparative reactivity of medicinal gold compounds with biomolecules containing disulfide or diselenide bonds. Gold(I) compounds are able to react with S-S or Se-Se at high temperature (70°C) by forming adducts where the AuPEt<sub>3</sub><sup>+</sup> ligand is directly bonded to S or Se. On the other hand, no reaction occurs between the investigated gold compounds and oxidized S-S or Se-Se vasopressins under physiological conditions (37°C) in the absence of reducing agents.

The disulfide bridge, at 37 °C, is more prone to reduction than the diselenide bridge. Consequently, upon adding a reducing agent the S-S bond can be cleaved and can form adducts with Au(I) compounds. In contrast, reduction of the Se-Se bond is more difficult to obtain and takes place only at high temperatures. At 70°C, the gold compounds are able to cleave both the disulfide and diselenide bridge and form the corresponding adducts. The reaction occurs preferentially for the Se-Se over the S-S bond probably because of the softer character of the selenolate group.

In view of the apparent strength of the Se-Au bond, our results further support the view that SeCys containing proteins (25 in humans) are preferential and likely targets of soft Lewis's electrophiles, such as heavy metals, e.g. Hg, Pb, As, Cd involved in environmental and human toxicology, and metallic compounds (containing Au, Ag, Pt, etc.) employed as therapeutic agents. However, the quick and facile reactions of metal compounds with the selenocysteine group take place only when the SeCys is present in its selenol or selenolate (reduced) form. In contrast, when SeCys has formed a Se-Se bridge, these reactions take place only at temperatures much higher than physiological ones. These results offer an interesting perspective to the research focus on the interaction of metallodrug and plasma proteins.

## Reference

1. J. Trofast, Undersökning af en ny Mineral-kropp, funnen i de orenare sorterna af det vid Fahlun tillverkade svaflet. *Chem. Int.* **33**, 16–19 (2011).
2. I. Rosenfeld, *Selenium: geobotany, biochemistry, toxicity, and nutrition* / (Academic Press, 1964).
3. M. J. Yaeger, R. D. Neiger, L. Holler, T. L. Fraser, D. J. Hurley, I. S. Palmer, The effect of subclinical selenium toxicosis on pregnant beef cattle. *J. Vet. Diagn. Investig. Off. Publ. Am. Assoc. Vet. Lab. Diagn. Inc.* **10**, 268–273 (1998).
4. L. N. Vernie, Selenium in carcinogenesis. *Biochim. Biophys. Acta BBA - Rev. Cancer.* **738**, 203–217 (1984).
5. J. Pinsent, The need for selenite and molybdate in the formation of formic dehydrogenase by members of the Coli-aerogenes group of bacteria. *Biochem. J.* **57**, 10–16 (1954).
6. K. Schwarz, C. M. Foltz, Selenium as an integral part of factor 3 against dietary necrotic liver degeneration. *J. Am. Chem. Soc.* **79**, 3292–3293 (1957).
7. M. Walter, U. E. J, Trace elements in human and animal nutrition. 5th ed. (1986).
8. World Health Organization, Food and Agriculture Organization of the United Nations, International Atomic Energy Agency, Eds., *Trace elements in human nutrition and health* (World Health Organization, Geneva, 1996).
9. H. J. Reich, R. J. Hondal, Why Nature Chose Selenium. *ACS Chem. Biol.* **11**, 821–841 (2016).
10. J. Risher, *Toxicological Profile for Selenium (Update)* (DIANE Publishing, 2011).
11. L. A. Wessjohann, A. Schneider, M. Abbas, W. Brandt, Selenium in chemistry and biochemistry in comparison to sulfur. *Biol. Chem.* **388**, 997–1006 (2007).
12. O. A. Levander, Metabolic interrelationships between arsenic and selenium. *Environ. Health Perspect.*, 6 (1977).
13. R. E. Huber, R. S. Criddle, Comparison of the chemical properties of selenocysteine and selenocystine with their sulfur analogs. *Arch. Biochem. Biophys.* **122**, 164–173 (1967).
14. J. Cioslowski, P. Piskorz, M. Schimeczek, G. Boche, Diversity of Bonding in Methyl Ate Anions of the First- and Second-Row Elements. *J. Am. Chem. Soc.* **120**, 2612–2615 (1998).
15. E. J. Corey, C. U. Kim, New and highly effective method for the oxidation of primary and secondary alcohols to carbonyl compounds. *J. Am. Chem. Soc.* **94**, 7586–7587 (1972).
16. S. M. Bachrach, D. W. Demoin, M. Luk, J. V. Miller, Nucleophilic Attack at Selenium in Diselenides and Selenosulfides. A Computational Study. *J. Phys. Chem. A.* **108**, 4040–4046 (2004).
17. Alexandros. Makriyannis, W. H. H. Guenther, H. G. Mautner, Selenol esters as specific reagents of the acylation of thiol groups. *J. Am. Chem. Soc.* **95**, 8403–8406 (1973).

18. N. J. Mitchell, L. R. Malins, X. Liu, R. E. Thompson, B. Chan, L. Radom, R. J. Payne, Rapid Additive-Free Selenocystine–Selenoester Peptide Ligation. *J. Am. Chem. Soc.* **137**, 14011–14014 (2015).
19. A. L. Adams, D. Macmillan, Investigation of peptide thioester formation via N→Se acyl transfer. *J. Pept. Sci. Off. Publ. Eur. Pept. Soc.* **19**, 65–73 (2013).
20. N. A. McGrath, R. T. Raines, Chemoselectivity in Chemical Biology: Acyl Transfer Reactions with Sulfur and Selenium. *Acc. Chem. Res.* **44**, 752–761 (2011).
21. G. J. Fredericks, P. R. Hoffmann, Selenoprotein K and protein palmitoylation. *Antioxid. Redox Signal.* **23**, 854–862 (2015).
22. D. A. Martens, D. L. Suarez, Selenium Speciation of Marine Shales, Alluvial Soils, and Evaporation Basin Soils of California. *J. Environ. Qual.* **26**, 424–432 (1997).
23. E. Dumont, F. Vanhaecke, R. Cornelis, Selenium speciation from food source to metabolites: a critical review. *Anal. Bioanal. Chem.* **385**, 1304–1323 (2006).
24. N. Terry, A. Zayed, M. P. Souza, A. Tarun, Selenium in Higher Plants. *Annu. Rev. Plant Physiol. Plant Mol. Biol.* **51**, 401–432 (2000).
25. L. Schomburg, U. Schweizer, J. Köhrle, Selenium and selenoproteins in mammals: extraordinary, essential, enigmatic. *Cell. Mol. Life Sci. CMLS.* **61**, 1988–1995 (2004).
26. P. D. Whanger, Selenocompounds in plants and animals and their biological significance. *J. Am. Coll. Nutr.* **21**, 223–232 (2002).
27. G. Roy, B. K. Sarma, P. P. Phadnis, G. Muges, Selenium-containing enzymes in mammals: Chemical perspectives. *J. Chem. Sci.* **117**, 287–303 (2005).
28. A. Läuchli, Selenium in Plants: Uptake, Functions, and Environmental Toxicity. *Bot. Acta.* **106**, 455–468 (1993).
29. I. Schröder, S. Rech, T. Krafft, J. M. Macy, Purification and characterization of the selenate reductase from *Thauera selenatis*. *J. Biol. Chem.* **272**, 23765–23768 (1997).
30. M. Björnstedt, S. Kumar, A. Holmgren, Selenodiglutathione is a highly efficient oxidant of reduced thioredoxin and a substrate for mammalian thioredoxin reductase. *J. Biol. Chem.* **267**, 8030–8034 (1992).
31. S. Kumar, M. Björnstedt, A. Holmgren, Selenite is a substrate for calf thymus thioredoxin reductase and thioredoxin and elicits a large non-stoichiometric oxidation of NADPH in the presence of oxygen. *Eur. J. Biochem.* **207**, 435–439 (1992).
32. C. Garbisu, S. Gonzalez, W. H. Yang, B. C. Yee, D. L. Carlson, A. Yee, N. R. Smith, R. Otero, B. B. Buchanan, T. Leighton, Physiological mechanisms regulating the conversion of selenite to elemental selenium by *Bacillus subtilis*. *BioFactors Oxf. Engl.* **5**, 29–37 (1995).
33. K. Bierla, J. Szpunar, A. Yiannikouris, R. Lobinski, Comprehensive speciation of selenium in selenium-rich yeast. *TrAC Trends Anal. Chem.* **41**, 122–132 (2012).
34. A. Böck, K. Forchhammer, J. Heider, W. Leinfelder, G. Sawers, B. Veprek, F. Zinoni, Selenocysteine: the 21st amino acid. *Mol. Microbiol.* **5**, 515–520 (1991).

35. S. Pinitglang, A. B. Watts, M. Patel, J. D. Reid, M. A. Noble, S. Gul, A. Bokth, A. Naeem, H. Patel, E. W. Thomas, S. K. Sreedharan, C. Verma, K. Brocklehurst, A classical enzyme active center motif lacks catalytic competence until modulated electrostatically. *Biochemistry*. **36**, 9968–9982 (1997).
36. D. Steinmann, T. Nauser, W. H. Koppenol, Selenium and sulfur in exchange reactions: a comparative study. *J. Org. Chem.* **75**, 6696–6699 (2010).
37. R. G. Pearson, Hard and Soft Acids and Bases. *J. Am. Chem. Soc.* **85**, 7 (1963).
38. R. Mousa, R. Notis Dardashti, N. Metanis, Selenium and Selenocysteine in Protein Chemistry. *Angew. Chem. Int. Ed.* **56**, 15818–15827 (2017).
39. S. Dery, P. Sai Reddy, L. Dery, R. Mousa, R. Notis Dardashti, N. Metanis, Insights into the deselenization of selenocysteine into alanine and serine. *Chem. Sci.* **6**, 6207–6212 (2015).
40. N. Metanis, E. Keinan, P. E. Dawson, Traceless Ligation of Cysteine Peptides using Selective Deselenization. *Angew. Chem. Int. Ed Engl.* **49**, 7049–7053 (2010).
41. K. Wiśniewski, J. Finnman, M. Flipo, R. Galyean, C. D. Schteingart, On the mechanism of degradation of oxytocin and its analogues in aqueous solution. *Pept. Sci.* **100**, 408–421 (2013).
42. M. J. Axley, A. Böck, T. C. Stadtman, Catalytic properties of an Escherichia coli formate dehydrogenase mutant in which sulfur replaces selenium. *Proc. Natl. Acad. Sci. U. S. A.* **88**, 8450–8454 (1991).
43. M. J. Berry, A. L. Maia, J. D. Kieffer, J. W. Harney, P. R. Larsen, Substitution of cysteine for selenocysteine in type I iodothyronine deiodinase reduces the catalytic efficiency of the protein but enhances its translation. *Endocrinology*. **131**, 1848–1852 (1992).
44. C. Rocher, J. L. Lalanne, J. Chaudière, Purification and properties of a recombinant sulfur analog of murine selenium-glutathione peroxidase. *Eur. J. Biochem.* **205**, 955–960 (1992).
45. M. Maiorino, K. D. Aumann, R. Brigelius-Flohé, D. Doria, J. van den Heuvel, J. McCarthy, A. Roveri, F. Ursini, L. Flohé, Probing the presumed catalytic triad of selenium-containing peroxidases by mutational analysis of phospholipid hydroperoxide glutathione peroxidase (PHGPx). *Biol. Chem. Hoppe. Seyler.* **376**, 651–660 (1995).
46. N. Metanis, E. Keinan, P. E. Dawson, Synthetic Seleno-Glutaredoxin 3 Analogues Are Highly Reducing Oxidoreductases with Enhanced Catalytic Efficiency. *J. Am. Chem. Soc.* **128**, 16684–16691 (2006).
47. S. Hazebrouck, L. Camoin, Z. Faltin, A. D. Strosberg, Y. Eshdat, Substituting selenocysteine for catalytic cysteine 41 enhances enzymatic activity of plant phospholipid hydroperoxide glutathione peroxidase expressed in Escherichia coli. *J. Biol. Chem.* **275**, 28715–28721 (2000).
48. H.-Y. Kim, D. E. Fomenko, Y.-E. Yoon, V. N. Gladyshev, Catalytic Advantages Provided by Selenocysteine in Methionine-S-Sulfoxide Reductases. *Biochemistry*. **45**, 13697–13704 (2006).
49. H.-Y. Kim, V. N. Gladyshev, Different catalytic mechanisms in mammalian selenocysteine- and cysteine-containing methionine-R-sulfoxide reductases. *PLoS Biol.* **3**, e375 (2005).
50. G. M. Lacourciere, T. C. Stadtman, Catalytic properties of selenophosphate synthetases: comparison of the selenocysteine-containing enzyme from Haemophilus influenzae with the

- corresponding cysteine-containing enzyme from *Escherichia coli*. *Proc. Natl. Acad. Sci. U. S. A.* **96**, 44–48 (1999).
51. S. M. Kanzok, A. Fechner, H. Bauer, J. K. Ulschmid, H.-M. Müller, J. Botella-Munoz, S. Schneuwly, R. H. Schirmer, K. Becker, Substitution of the Thioredoxin System for Glutathione Reductase in *Drosophila melanogaster*. *Science*. **291**, 643–646 (2001).
  52. Z. P. Wu, D. Hilvert, Selenosubtilisin as a glutathione peroxidase mimic. *J. Am. Chem. Soc.* **112**, 5647–5648 (1990).
  53. G. Casi, G. Roelfes, D. Hilvert, Selenoglutaredoxin as a Glutathione Peroxidase Mimic. *ChemBioChem*. **9**, 1623–1631 (2008).
  54. S. Boschi-Muller, S. Muller, A. Van Dorsselaer, A. Böck, G. Branlant, Substituting selenocysteine for active site cysteine 149 of phosphorylating glyceraldehyde 3-phosphate dehydrogenase reveals a peroxidase activity. *FEBS Lett.* **439**, 241–245 (1998).
  55. L. Ding, Z. Liu, Z. Zhu, G. Luo, D. Zhao, J. Ni, Biochemical characterization of selenium-containing catalytic antibody as a cytosolic glutathione peroxidase mimic. *Biochem. J.* **332 ( Pt 1)**, 251–255 (1998).
  56. J.-Q. Liu, M.-S. Jiang, G.-M. Luo, G.-L. Yan, J.-C. Shen, Conversion of trypsin into a selenium-containing enzyme by using chemical mutation. *Biotechnol. Lett.* **20**, 693–696 (1998).
  57. Y. Sun, T. Li, H. Chen, K. Zhang, K. Zheng, Y. Mu, G. Yan, W. Li, J. Shen, G. Luo, Selenium-containing 15-mer peptides with high glutathione peroxidase-like activity. *J. Biol. Chem.* **279**, 37235–37240 (2004).
  58. X. Ren, P. Jemth, P. G. Board, G. Luo, B. Mannervik, J. Liu, K. Zhang, J. Shen, A semisynthetic glutathione peroxidase with high catalytic efficiency. Selenogluthione transferase. *Chem. Biol.* **9**, 789–794 (2002).
  59. D. Dimastrogiovanni, M. Anselmi, A. E. Miele, G. Boumis, L. Petersson, F. Angelucci, A. D. Nola, M. Brunori, A. Bellelli, Combining crystallography and molecular dynamics: The case of *Schistosoma mansoni* phospholipid glutathione peroxidase. *Proteins Struct. Funct. Bioinforma.* **78**, 259–270 (2010).
  60. F. Zinoni, A. Birkmann, T. C. Stadtman, A. Böck, Nucleotide sequence and expression of the selenocysteine-containing polypeptide of formate dehydrogenase (formate-hydrogen-lyase-linked) from *Escherichia coli*. *Proc. Natl. Acad. Sci. U. S. A.* **83**, 4650–4654 (1986).
  61. I. Chambers, J. Frampton, P. Goldfarb, N. Affara, W. McBain, P. R. Harrison, The structure of the mouse glutathione peroxidase gene: the selenocysteine in the active site is encoded by the “termination” codon, TGA. *EMBO J.* **5**, 1221–1227 (1986).
  62. X. Q. Wu, H. J. Gross, The length and the secondary structure of the D-stem of human selenocysteine tRNA are the major identity determinants for serine phosphorylation. *EMBO J.* **13**, 241–248 (1994).
  63. N. Hubert, C. Sturchler, E. Westhof, P. Carbon, A. Krol, The 9/4 secondary structure of eukaryotic selenocysteine tRNA: more pieces of evidence. *RNA*. **4**, 1029–1033 (1998).



64. C. Baron, A. Böck, The length of the aminoacyl-acceptor stem of the selenocysteine-specific tRNA(Sec) of *Escherichia coli* is the determinant for binding to elongation factors SELB or Tu. *J. Biol. Chem.* **266**, 20375–20379 (1991).
65. S. Commans, A. Böck, Selenocysteine inserting tRNAs: an overview. *FEMS Microbiol. Rev.* **23**, 335–351 (1999).
66. J. Rudinger, R. Hillenbrandt, M. Sprinzl, R. Giegé, Antideterminants present in minihelix(Sec) hinder its recognition by prokaryotic elongation factor Tu. *EMBO J.* **15**, 650–657 (1996).
67. B. A. Carlson, B. J. Lee, P. A. Tsuji, R. Tobe, J. M. Park, U. Schweizer, V. N. Gladyshev, D. L. Hatfield, in *Selenium: Its Molecular Biology and Role in Human Health*, D. L. Hatfield, U. Schweizer, P. A. Tsuji, V. N. Gladyshev, Eds. (Springer International Publishing, Cham, 2016), pp. 3–12.
68. A. A. Turanov, X.-M. Xu, B. A. Carlson, M.-H. Yoo, V. N. Gladyshev, D. L. Hatfield, Biosynthesis of Selenocysteine, the 21st Amino Acid in the Genetic Code, and a Novel Pathway for Cysteine Biosynthesis. *Adv. Nutr.* **2**, 122–128 (2011).
69. N. Esaki, T. Nakamura, H. Tanaka, K. Soda, Selenocysteine lyase, a novel enzyme that specifically acts on selenocysteine. Mammalian distribution and purification and properties of pig liver enzyme. *J. Biol. Chem.* **257**, 4386–4391 (1982).
70. A. Small-Howard, N. Morozova, Z. Stoytcheva, E. P. Forry, J. B. Mansell, J. W. Harney, B. A. Carlson, X. Xu, D. L. Hatfield, M. J. Berry, Supramolecular Complexes Mediate Selenocysteine Incorporation In Vivo. *Mol. Cell. Biol.* **26**, 2337–2346 (2006).
71. R. M. Tujebajeva, P. R. Copeland, X.-M. Xu, B. A. Carlson, J. W. Harney, D. M. Driscoll, D. L. Hatfield, M. J. Berry, Decoding apparatus for eukaryotic selenocysteine insertion. *EMBO Rep.* **1**, 158–163 (2000).
72. J. Donovan, P. R. Copeland, Threading the Needle: Getting Selenocysteine Into Proteins. *Antioxid. Redox Signal.* **12**, 881–892 (2010).
73. L. Flohé, The labour pains of biochemical selenology: the history of selenoprotein biosynthesis. *Biochim. Biophys. Acta.* **1790**, 1389–1403 (2009).
74. M. W. Pitts, C. N. Byrns, A. N. Ogawa-Wong, P. Kremer, M. J. Berry, Selenoproteins in Nervous System Development and Function. *Biol. Trace Elem. Res.* **161**, 231–245 (2014).
75. M. Rederstorff, A. Krol, A. Lescure, Understanding the importance of selenium and selenoproteins in muscle function. *Cell. Mol. Life Sci.* **63**, 52–59 (2006).
76. D. M. Driscoll, L. Chavatte, Finding needles in a haystack. *EMBO Rep.* **5**, 140–141 (2004).
77. A. Holmgren, Thioredoxin. *Annu. Rev. Biochem.* **54**, 237–271 (1985).
78. E. S. J. Arnér, Focus on mammalian thioredoxin reductases — Important selenoproteins with versatile functions. *Biochim. Biophys. Acta BBA - Gen. Subj.* **1790**, 495–526 (2009).
79. J. Bernal, in *Reference Module in Neuroscience and Biobehavioral Psychology* (Elsevier, 2017).
80. M. Conrad, J. P. Friedmann Angeli, in *Comprehensive Toxicology (Third Edition)*, C. A. McQueen, Ed. (Elsevier, Oxford, 2018), pp. 260–276.

81. J. Lamarche, L. Ronga, J. Szpunar, R. Lobinski, Characterization and Quantification of Selenoprotein P: Challenges to Mass Spectrometry. *Int. J. Mol. Sci.* **22** (2021), doi:10.3390/ijms22126283.
82. A. V. Lobanov, D. L. Hatfield, V. N. Gladyshev, Eukaryotic selenoproteins and selenoproteomes. *Biochim. Biophys. Acta.* **1790**, 1424–1428 (2009).
83. X. Ren, L. Zou, X. Zhang, V. Branco, J. Wang, C. Carvalho, A. Holmgren, J. Lu, Redox Signaling Mediated by Thioredoxin and Glutathione Systems in the Central Nervous System. *Antioxid. Redox Signal.* **27**, 989–1010 (2017).
84. J. Ceccarelli, L. Delfino, E. Zappia, P. Castellani, M. Borghi, S. Ferrini, F. Tosetti, A. Rubartelli, The redox state of the lung cancer microenvironment depends on the levels of thioredoxin expressed by tumor cells and affects tumor progression and response to prooxidants. *Int. J. Cancer.* **123**, 1770–1778 (2008).
85. D. L. Kirkpatrick, G. Ehrmantraut, S. Stettner, M. Kunkel, G. Powis, Redox Active Disulfides: The Thioredoxin System as a Drug Target. *Oncol. Res. Featur. Preclin. Clin. Cancer Ther.* **9**, 351–356 (1997).
86. G. Bjørklund, L. Zou, J. Wang, C. T. Chasapis, M. Peana, Thioredoxin Reductase as a Pharmacological Target. *Pharmacol. Res.*, 105854 (2021).
87. S. Fulvio, A. Francesco, B. Giovanna, C. Daniela, D. Gianni, E. M. Adriana, B. Andrea, Thioredoxin Reductase and its Inhibitors. *Curr. Protein Pept. Sci.* **15**, 621–646 (2014).
88. E. Chupakhin, M. Krasavin, Thioredoxin reductase inhibitors: updated patent review (2017-present). *Expert Opin. Ther. Pat.* **31**, 745–758 (2021).
89. K. F. Tonissen, G. Di Trapani, Thioredoxin system inhibitors as mediators of apoptosis for cancer therapy. *Mol. Nutr. Food Res.* **53**, 87–103 (2009).
90. M. Selenius, A.-K. Rundlöf, E. Olm, A. P. Fernandes, M. Björnstedt, Selenium and the Selenoprotein Thioredoxin Reductase in the Prevention, Treatment and Diagnostics of Cancer. *Antioxid. Redox Signal.* **12**, 867–880 (2010).
91. S. Prast-Nielsen, H.-H. Huang, D. L. Williams, Thioredoxin glutathione reductase: Its role in redox biology and potential as a target for drugs against neglected diseases. *Biochim. Biophys. Acta BBA - Gen. Subj.* **1810**, 1262–1271 (2011).
92. G. Boumis, G. Giardina, F. Angelucci, A. Bellelli, M. Brunori, D. Dimastrogiovanni, F. Saccoccia, A. E. Miele, Crystal structure of Plasmodium falciparum thioredoxin reductase, a validated drug target. *Biochem. Biophys. Res. Commun.* **425**, 806–811 (2012).
93. A. Cimini, R. Gentile, F. Angelucci, E. Benedetti, G. Pitari, A. Giordano, R. Ippoliti, Neuroprotective effects of PrxI over-expression in an in vitro human Alzheimer's disease model. *J. Cell. Biochem.* **114**, 708–715 (2013).
94. M. Peana, C. T. Chasapis, G. Simula, S. Medici, M. A. Zoroddu, A Model for Manganese interaction with Deinococcus radiodurans proteome network involved in ROS response and defense. *J. Trace Elem. Med. Biol.* **50**, 465–473 (2018).



95. F. Saccoccia, F. Angelucci, G. Boumis, M. Brunori, A. E. Miele, D. L. Williams, A. Bellelli, On the mechanism and rate of gold incorporation into thiol-dependent flavoreductases. *J. Inorg. Biochem.* **108**, 105–111 (2012).
96. R. Xiaoyuan, Z. Lili, H. Arne, Targeting Bacterial Antioxidant Systems for Antibiotics Development. *Curr. Med. Chem.* **27**, 1922–1939 (2020).
97. J. Zhang, X. Li, X. Han, R. Liu, J. Fang, Targeting the Thioredoxin System for Cancer Therapy. *Trends Pharmacol. Sci.* **38**, 794–808 (2017).
98. Y. Liu, Y. Li, S. Yu, G. Zhao, Recent advances in the development of thioredoxin reductase inhibitors as anticancer agents. *Curr. Drug Targets.* **13**, 1432–1444 (2012).
99. S. E. Jackson-Rosario, W. T. Self, Targeting selenium metabolism and selenoproteins: Novel avenues for drug discovery. *Metallomics.* **2**, 112–116 (2010).
100. Q. Cheng, T. Sandalova, Y. Lindqvist, E. S. J. Arnér, Crystal Structure and Catalysis of the Selenoprotein Thioredoxin Reductase 1. *J. Biol. Chem.* **284**, 3998–4008 (2009).
101. J. Baclaocos, D. Santesmasses, M. Mariotti, K. Bierła, M. B. Vetick, S. Lynch, R. McAllen, J. J. Mackrill, G. Loughran, R. Guigó, J. Szpunar, P. R. Copeland, V. N. Gladyshev, J. F. Atkins, Processive Recoding and Metazoan Evolution of Selenoprotein P: Up to 132 UGAs in Molluscs. *J. Mol. Biol.* **431**, 4381–4407 (2019).
102. L. Jiang, Q. Liu, in *Selenoproteins: Methods and Protocols*, L. Chavatte, Ed. (Springer, New York, NY, 2018), *Methods in Molecular Biology*, pp. 29–39.
103. R. F. Burk, Effect of Dietary Selenium Level on <sup>75</sup>Se Binding to Rat Plasma Proteins. *Proc. Soc. Exp. Biol. Med.* **143**, 719–722 (1973).
104. J. T. Rotruck, A. L. Pope, H. E. Ganther, A. B. Swanson, D. G. Hafeman, W. G. Hoekstra, Selenium: Biochemical Role as a Component of Glutathione Peroxidase. *Science.* **179**, 588–590 (1973).
105. K. P. McConnell, R. M. Burton, T. Kute, P. J. Higgins, Selenoproteins from rat testis cytosol. *Biochim. Biophys. Acta BBA - Gen. Subj.* **588**, 113–119 (1979).
106. M. Motsenbocker, A. L. Tappel, A selenocysteine-containing selenium-transport protein in rat plasma. *Biochim. Biophys. Acta BBA - Gen. Subj.* **719**, 147–153 (1982).
107. M. Persson-Moschos, W. Huang, T. S. Srikumar, B. Akesson, S. Lindeberg, Selenoprotein P in serum as a biochemical marker of selenium status. *The Analyst.* **120**, 833–836 (1995).
108. V. N. Gladyshev, E. S. Arnér, M. J. Berry, R. Brigelius-Flohé, E. A. Bruford, R. F. Burk, B. A. Carlson, S. Castellano, L. Chavatte, M. Conrad, P. R. Copeland, A. M. Diamond, D. M. Driscoll, A. Ferreira, L. Flohé, F. R. Green, R. Guigó, D. E. Handy, D. L. Hatfield, J. Hesketh, P. R. Hoffmann, A. Holmgren, R. J. Hondal, M. T. Howard, K. Huang, H.-Y. Kim, I. Y. Kim, J. Köhrle, A. Krol, G. V. Kryukov, B. J. Lee, B. C. Lee, X. G. Lei, Q. Liu, A. Lescure, A. V. Lobanov, J. Loscalzo, M. Maiorino, M. Mariotti, K. Sandeep Prabhu, M. P. Rayman, S. Rozovsky, G. Salinas, E. E. Schmidt, L. Schomburg, U. Schweizer, M. Simonović, R. A. Sunde, P. A. Tsuji, S. Tweedie, F. Ursini, P. D. Whanger, Y. Zhang, Selenoprotein Gene Nomenclature. *J. Biol. Chem.* **291**, 24036–24040 (2016).

109. R. F. Burk, K. E. Hill, Selenoprotein P—Expression, functions, and roles in mammals. *Biochim. Biophys. Acta BBA - Gen. Subj.* **1790**, 1441–1447 (2009).
110. M. Michaelis, O. Gralla, T. Behrends, M. Scharpf, T. Endermann, E. Rijntjes, N. Pietschmann, B. Hollenbach, L. Schomburg, Selenoprotein P in seminal fluid is a novel biomarker of sperm quality. *Biochem. Biophys. Res. Commun.* **443**, 905–910 (2014).
111. M. A. Reeves, P. R. Hoffmann, The human selenoproteome: recent insights into functions and regulation. *Cell. Mol. Life Sci.* **66**, 2457–2478 (2009).
112. R. F. Burk, K. E. Hill, R. Read, T. Bellew, Response of rat selenoprotein P to selenium administration and fate of its selenium. *Am. J. Physiol.* **261**, E26-30 (1991).
113. S. Yoneda, K. T. Suzuki, Equimolar Hg-Se complex binds to selenoprotein P. *Biochem. Biophys. Res. Commun.* **231**, 7–11 (1997).
114. M. Fujii, K. Saijoh, K. Sumino, Regulation of selenoprotein P mRNA expression in comparison with metallothionein and osteonectin mRNAs following cadmium and dexamethasone administration. *Kobe J. Med. Sci.* **43**, 13–23 (1997).
115. G. F. Combs, Biomarkers of selenium status. *Nutrients.* **7**, 2209–2236 (2015).
116. Y. Xia, K. E. Hill, P. Li, J. Xu, D. Zhou, A. K. Motley, L. Wang, D. W. Byrne, R. F. Burk, Optimization of selenoprotein P and other plasma selenium biomarkers for the assessment of the selenium nutritional requirement: a placebo-controlled, double-blind study of selenomethionine supplementation in selenium-deficient Chinese subjects. *Am. J. Clin. Nutr.* **92**, 525–531 (2010).
117. J. Hoeflich, B. Hollenbach, T. Behrends, A. Hoeg, H. Stosnach, L. Schomburg, The choice of biomarkers determines the selenium status in young German vegans and vegetarians. *Br. J. Nutr.* **104**, 1601–1604 (2010).
118. R. Hurst, C. N. Armah, J. R. Dainty, D. J. Hart, B. Teucher, A. J. Goldson, M. R. Broadley, A. K. Motley, S. J. Fairweather-Tait, Establishing optimal selenium status: results of a randomized, double-blind, placebo-controlled trial. *Am. J. Clin. Nutr.* **91**, 923–931 (2010).
119. N. Kikuchi, K. Satoh, T. Satoh, N. Yaoita, M. A. H. Siddique, J. Omura, R. Kurosawa, M. Nogi, S. Sunamura, S. Miyata, H. Misu, Y. Saito, H. Shimokawa, Diagnostic and Prognostic Significance of Serum Levels of SeP (Selenoprotein P) in Patients With Pulmonary Hypertension. *Arterioscler. Thromb. Vasc. Biol.* **39**, 2553–2562 (2019).
120. D. L. Vu, K. Saurav, M. Mylenko, K. Ranglová, J. Kuta, D. Ewe, J. Masojídek, P. Hrouzek, In vitro bioaccessibility of selenoamino acids from selenium (Se)-enriched *Chlorella vulgaris* biomass in comparison to selenized yeast; a Se-enriched food supplement; and Se-rich foods. *Food Chem.* **279**, 12–19 (2019).
121. R. A. Heller, Q. Sun, J. Hackler, J. Seelig, L. Seibert, A. Cherkezov, W. B. Minich, P. Seemann, J. Diegmann, M. Pilz, M. Bachmann, A. Ranjbar, A. Moghaddam, L. Schomburg, Prediction of survival odds in COVID-19 by zinc, age and selenoprotein P as composite biomarker. *Redox Biol.* **38**, 101764 (2021).
122. A. Moghaddam, R. A. Heller, Q. Sun, J. Seelig, A. Cherkezov, L. Seibert, J. Hackler, P. Seemann, J. Diegmann, M. Pilz, M. Bachmann, W. B. Minich, L. Schomburg, Selenium Deficiency Is Associated with Mortality Risk from COVID-19. *Nutrients.* **12**, 2098 (2020).

123. J. C. Eckers, A. L. Kalen, W. Xiao, E. H. Sarsour, P. C. Goswami, Selenoprotein P Inhibits Radiation-Induced Late Reactive Oxygen Species Accumulation and Normal Cell Injury. *Int. J. Radiat. Oncol.* **87**, 619–625 (2013).
124. M. Temur, F. N. Taşgöz, N. Kender Ertürk, Elevated circulating Selenoprotein P levels in patients with polycystic ovary syndrome. *J. Obstet. Gynaecol.* **0**, 1–5 (2021).
125. Y. Takata, Y.-B. Xiang, R. F. Burk, H. Li, K. E. Hill, H. Cai, J. Gao, W. Zheng, X.-O. Shu, Q. Cai, Plasma selenoprotein P concentration and lung cancer risk: results from a case–control study nested within the Shanghai Men’s Health Study. *Carcinogenesis.* **39**, 1352–1358 (2018).
126. J. Köhrle, Selenium in Endocrinology—Selenoprotein-Related Diseases, Population Studies, and Epidemiological Evidence. *Endocrinology.* **162** (2021), doi:10.1210/endo/bqaa228.
127. D. J. Hughes, V. Fedirko, M. Jenab, L. Schomburg, C. Méplan, H. Freisling, H. B. Bueno-de-Mesquita, S. Hybsier, N.-P. Becker, M. Czuban, A. Tjønneland, M. Outzen, M.-C. Boutron-Ruault, A. Racine, N. Bastide, T. Kühn, R. Kaaks, D. Trichopoulos, A. Trichopoulou, P. Lagiou, S. Panico, P. H. Peeters, E. Weiderpass, G. Skeie, E. Dagrùn, M.-D. Chirlaque, M.-J. Sánchez, E. Ardanaz, I. Ljuslinder, M. Wennberg, K. E. Bradbury, P. Vineis, A. Naccarati, D. Palli, H. Boeing, K. Overvad, M. Dorronsoro, P. Jakszyn, A. J. Cross, J. R. Quirós, M. Stepien, S. Y. Kong, T. Duarte-Salles, E. Riboli, J. E. Hesketh, Selenium status is associated with colorectal cancer risk in the European prospective investigation of cancer and nutrition cohort. *Int. J. Cancer.* **136**, 1149–1161 (2015).
128. C. W. Barrett, V. K. Reddy, S. P. Short, A. K. Motley, M. K. Lintel, A. M. Bradley, T. Freeman, J. Vallance, W. Ning, B. Parang, S. V. Poindexter, B. Fingleton, X. Chen, M. K. Washington, K. T. Wilson, N. F. Shroyer, K. E. Hill, R. F. Burk, C. S. Williams, Selenoprotein P influences colitis-induced tumorigenesis by mediating stemness and oxidative damage. *J. Clin. Invest.* **125**, 2646–2660 (2015).
129. M. P. Rayman, Selenium and human health. *The Lancet.* **379**, 1256–1268 (2012).
130. J. Xi, Q. Zhang, J. Wang, R. Guo, L. Wang, Factors Influencing Selenium Concentration in Community-Dwelling Patients with Type 2 Diabetes Mellitus. *Biol. Trace Elem. Res.* **199**, 1657–1663 (2021).
131. Z.-H. Zhang, G.-L. Song, Roles of Selenoproteins in Brain Function and the Potential Mechanism of Selenium in Alzheimer’s Disease. *Front. Neurosci.* **15**, 215 (2021).
132. H. Misu, T. Takamura, H. Takayama, H. Hayashi, N. Matsuzawa-Nagata, S. Kurita, K. Ishikura, H. Ando, Y. Takeshita, T. Ota, M. Sakurai, T. Yamashita, E. Mizukoshi, T. Yamashita, M. Honda, K. Miyamoto, T. Kubota, N. Kubota, T. Kadowaki, H.-J. Kim, I. Lee, Y. Minokoshi, Y. Saito, K. Takahashi, Y. Yamada, N. Takakura, S. Kaneko, A Liver-Derived Secretory Protein, Selenoprotein P, Causes Insulin Resistance. *Cell Metab.* **12**, 483–495 (2010).
133. Y. Saito, Selenoprotein P as a significant regulator of pancreatic  $\beta$  cell function. *J. Biochem. (Tokyo).* **167**, 119–124 (2020).
134. Y.-C. Huang, T.-L. Wu, H. Zeng, W.-H. Cheng, Dietary Selenium Requirement for the Prevention of Glucose Intolerance and Insulin Resistance in Middle-Aged Mice. *J. Nutr.* **151**, 1894–1900 (2021).

135. R. Tsutsumi, Y. Saito, Selenoprotein P; P for Plasma, Prognosis, Prophylaxis, and More. *Biol. Pharm. Bull.* **43**, 366–374 (2020).
136. K. E. Hill, R. S. Lloyd, J. G. Yang, R. Read, R. F. Burk, The cDNA for rat selenoprotein P contains 10 TGA codons in the open reading frame. *J. Biol. Chem.* **266**, 10050–10053 (1991).
137. R. F. Burk, K. E. Hill, Some properties of selenoprotein P. *Biol. Trace Elem. Res.* **33**, 151–153 (1992).
138. C. L. Deitrich, S. Cuello-Núñez, D. Kmiotek, F. A. Torma, M. E. del Castillo Busto, P. Fisicaro, H. Goenaga-Infante, Accurate Quantification of Selenoprotein P in Plasma Using Isotopically Enriched Seleno-peptides and Species-Specific Isotope Dilution with HPLC Coupled to ICP-MS/MS. *Anal. Chem.* **88**, 6357–6365 (2016).
139. Y. Saito, N. Sato, M. Hirashima, G. Takebe, S. Nagasawa, K. Takahashi, Domain structure of bi-functional selenoprotein P. *Biochem. J.* **381**, 841–846 (2004).
140. A. A. Turanov, R. A. Everley, S. Hybsier, K. Renko, L. Schomburg, S. P. Gygi, D. L. Hatfield, V. N. Gladyshev, Regulation of Selenocysteine Content of Human Selenoprotein P by Dietary Selenium and Insertion of Cysteine in Place of Selenocysteine. *PLOS ONE*. **10**, e0140353 (2015).
141. S. Ma, K. E. Hill, R. M. Caprioli, R. F. Burk, Mass Spectrometric Characterization of Full-length Rat Selenoprotein P and Three Isoforms Shortened at the C Terminus: Evidence that three UGA codons in the mRNA open reading frame have alternative functions of specifying selenocysteine insertion or translation termination. *J. Biol. Chem.* **277**, 12749–12754 (2002).
142. C. Méplan, F. Nicol, B. T. Burtle, L. K. Crosley, J. R. Arthur, J. C. Mathers, J. E. Hesketh, Relative Abundance of Selenoprotein P Isoforms in Human Plasma Depends on Genotype, Se Intake, and Cancer Status. *Antioxid. Redox Signal.* **11**, 2631–2640 (2009).
143. B. Akesson, T. Bellew, R. F. Burk, Purification of selenoprotein P from human plasma. *Biochim. Biophys. Acta.* **1204**, 243–249 (1994).
144. S. Hybsier, T. Schulz, Z. Wu, I. Demuth, W. B. Minich, K. Renko, E. Rijntjes, J. Köhrle, C. J. Strasburger, E. Steinhagen-Thiessen, L. Schomburg, Sex-specific and inter-individual differences in biomarkers of selenium status identified by a calibrated ELISA for selenoprotein P. *Redox Biol.* **11**, 403–414 (2017).
145. S. Ma, K. E. Hill, R. F. Burk, R. M. Caprioli, Mass spectrometric identification of N- and O-glycosylation sites of full-length rat selenoprotein P and determination of selenide-sulfide and disulfide linkages in the shortest isoform. *Biochemistry.* **42**, 9703–9711 (2003).
146. V. Mostert, I. Lombeck, J. Abel, A Novel Method for the Purification of Selenoprotein P from Human Plasma. *Arch. Biochem. Biophys.* **357**, 326–330 (1998).
147. H. Steinbrenner, L. Alili, D. Stuhlmann, H. Sies, P. Brenneisen, Post-translational processing of selenoprotein P: implications of glycosylation for its utilisation by target cells. *Biol. Chem.* **388**, 1043–1051 (2007).
148. V. M. Labunskyy, D. L. Hatfield, V. N. Gladyshev, Selenoproteins: Molecular Pathways and Physiological Roles. *Physiol. Rev.* **94**, 739–777 (2014).
149. T. Makovec, Cisplatin and beyond: molecular mechanisms of action and drug resistance development in cancer chemotherapy. *Radiol. Oncol.* **53**, 148–158 (2019).

150. B. Rosenberg, L. Van Camp, E. B. Grimley, A. J. Thomson, The inhibition of growth or cell division in *Escherichia coli* by different ionic species of platinum(IV) complexes. *J. Biol. Chem.* **242**, 1347–1352 (1967).
151. D. J. Evans, D. J. Searles, E. Mittag, Fluctuation theorem for Hamiltonian Systems: Le Chatelier's principle. *Phys. Rev. E.* **63**, 051105 (2001).
152. S. Dasari, P. B. Tchounwou, Cisplatin in cancer therapy: molecular mechanisms of action. *Eur. J. Pharmacol.* **740**, 364–378 (2014).
153. S. A. Aldossary, Review on Pharmacology of Cisplatin: Clinical Use, Toxicity and Mechanism of Resistance of Cisplatin. *Biomed. Pharmacol. J.* **12**, 7–15 (2019).
154. V. Hellberg, I. Wallin, S. Eriksson, E. Hernlund, E. Jerremalm, M. Berndtsson, S. Eksborg, E. S. J. Arnér, M. Shoshan, H. Ehrsson, G. Laurell, Cisplatin and oxaliplatin toxicity: importance of cochlear kinetics as a determinant for ototoxicity. *J. Natl. Cancer Inst.* **101**, 37–47 (2009).
155. M. A. C. Morelli, A. Ostuni, P. L. Cristinziano, D. Tesauro, A. Bavoso, Interaction of cisplatin with a CCHC zinc finger motif. *J. Pept. Sci.* **19**, 227–232 (2013).
156. E. Serinan, Z. Altun, S. Aktaş, E. Çeçen, N. Olgun, Comparison of Cisplatin with Lipoplatin in Terms of Ototoxicity. *J. Int. Adv. Otol.* **14**, 211–215 (2018).
157. I. Momose, T. Onodera, M. Kawada, Potential Anticancer Activity of Auranofin. *Yakugaku Zasshi.* **141**, 315–321 (2021).
158. C. A. Bulman, C. M. Bidlow, S. Lustigman, F. Cho-Ngwa, D. Williams, J. Alberto A. Rascón, N. Tricoche, M. Samje, A. Bell, B. Suzuki, K. C. Lim, N. Supakordej, P. Supakordej, A. R. Wolfe, G. M. Knudsen, S. Chen, C. Wilson, K.-H. Ang, M. Arkin, J. Gut, C. Franklin, C. Marcellino, J. H. McKerrow, A. Debnath, J. A. Sakanari, Repurposing Auranofin as a Lead Candidate for Treatment of Lymphatic Filariasis and Onchocerciasis. *PLoS Negl. Trop. Dis.* **9**, e0003534 (2015).
159. T. Onodera, I. Momose, M. Kawada, Potential Anticancer Activity of Auranofin. *Chem. Pharm. Bull. (Tokyo).* **67**, 186–191 (2019).
160. X. Zhang, K. Selvaraju, A. A. Saei, P. D'Arcy, R. A. Zubarev, E. S. J. Arnér, S. Linder, Repurposing of auranofin: Thioredoxin reductase remains a primary target of the drug. *Biochimie.* **162**, 46–54 (2019).
161. J. Hu, H. Zhang, M. Cao, L. Wang, S. Wu, B. Fang, Auranofin Enhances Ibrutinib's Anticancer Activity in EGFR-Mutant Lung Adenocarcinoma. *Mol. Cancer Ther.* **17**, 2156–2163 (2018).
162. S. J. Ralph, S. Nozuhur, R. A. ALHulais, S. Rodríguez-Enriquez, R. Moreno-Sánchez, Repurposing drugs as pro-oxidant redox modifiers to eliminate cancer stem cells and improve the treatment of advanced stage cancers. *Med. Res. Rev.* **39**, 2397–2426 (2019).
163. C. Nardon, N. Pettenuzzo, D. Fregona, Gold Complexes for Therapeutic Purposes: an Updated Patent Review (2010-2015). *Curr. Med. Chem.* **23**, 3374–3403 (2016).
164. A. Casini, L. Messori, Molecular mechanisms and proposed targets for selected anticancer gold compounds. *Curr. Top. Med. Chem.* **11**, 2647–2660 (2011).



165. C. Marzano, V. Gandin, A. Folda, G. Scutari, A. Bindoli, M. P. Rigobello, Inhibition of thioredoxin reductase by auranofin induces apoptosis in cisplatin-resistant human ovarian cancer cells. *Free Radic. Biol. Med.* **42**, 872–881 (2007).
166. M. Coronello, E. Mini, B. Caciagli, M. A. Cinellu, A. Bindoli, C. Gabbiani, L. Messori, Mechanisms of cytotoxicity of selected organogold(III) compounds. *J. Med. Chem.* **48**, 6761–6765 (2005).
167. A. Markowska, B. Kasprzak, K. Jaszczyńska-Nowinka, J. Lubin, J. Markowska, Noble metals in oncology. *Contemp. Oncol. Poznan Pol.* **19**, 271–275 (2015).
168. E. S. J. Arnér, A. Holmgren, The thioredoxin system in cancer. *Semin. Cancer Biol.* **16**, 420–426 (2006).
169. E. Schuh, C. Pflüger, A. Citta, A. Folda, M. P. Rigobello, A. Bindoli, A. Casini, F. Mohr, Gold(I) Carbene Complexes Causing Thioredoxin 1 and Thioredoxin 2 Oxidation as Potential Anticancer Agents. *J. Med. Chem.* **55**, 5518–5528 (2012).
170. T. C. Karlenius, K. F. Tonissen, Thioredoxin and Cancer: A Role for Thioredoxin in all States of Tumor Oxygenation. *Cancers.* **2**, 209–232 (2010).
171. L. Ronconi, D. Fregona, The Midas touch in cancer chemotherapy: from platinum- to gold-dithiocarbamate complexes. *Dalton Trans. Camb. Engl.* **2003**, 10670–10680 (2009).
172. A. Bergamo, G. Sava, Ruthenium complexes can target determinants of tumour malignancy. *Dalton Trans.*, 1267–1272 (2007).
173. F. Lentz, A. Drescher, A. Lindauer, M. Henke, R. A. Hilger, C. G. Hartinger, M. E. Scheulen, C. Dittrich, B. K. Keppler, U. Jaehde, in collaboration with C. E. S. for A. D. Research-EWIV, Pharmacokinetics of a novel anticancer ruthenium complex (KP1019, FFC14A) in a phase I dose-escalation study. *Anticancer. Drugs.* **20**, 97–103 (2009).
174. C. G. Hartinger, M. A. Jakupec, S. Zorbas-Seifried, M. Groessler, A. Egger, W. Berger, H. Zorbas, P. J. Dyson, B. K. Keppler, KP1019, A New Redox-Active Anticancer Agent – Preclinical Development and Results of a Clinical Phase I Study in Tumor Patients. *Chem. Biodivers.* **5**, 2140–2155 (2008).
175. T. Schilling, K. B. Keppler, M. E. Heim, G. Niebch, H. Dietzfelbinger, J. Rastetter, A.-R. Hanauske, Clinical phase I and pharmacokinetic trial of the new titanium complex budotitane. *Invest. New Drugs.* **13**, 327–332 (1995).
176. K. Strohsfeldt, M. Tacke, Bioorganometallic fulvene-derived titanocene anti-cancer drugs. *Chem. Soc. Rev.* **37**, 1174–1187 (2008).
177. I. Ott, R. Gust, Non Platinum Metal Complexes as Anti-cancer Drugs. *Arch. Pharm. (Weinheim).* **340**, 117–126 (2007).
178. M. A. Jakupec, B. K. Keppler, Gallium in Cancer Treatment. *Curr. Top. Med. Chem.* **4**, 1575–1583 (2004).
179. G. Jaouen, A. Vessières, S. Top, Ferrocifen type anti cancer drugs. *Chem. Soc. Rev.* **44**, 8802–8817 (2015).
180. N. Muhammad, Z. Guo, Metal-based anticancer chemotherapeutic agents. *Curr. Opin. Chem. Biol.* **19**, 144–153 (2014).

181. C. G. Hartinger, P. J. Dyson, Bioorganometallic chemistry—from teaching paradigms to medicinal applications. *Chem. Soc. Rev.* **38**, 391–401 (2009).
182. A. Bergamo, G. Sava, Linking the future of anticancer metal-complexes to the therapy of tumour metastases. *Chem. Soc. Rev.* **44**, 8818–8835 (2015).
183. K. D. Mjos, C. Orvig, Metallodrugs in Medicinal Inorganic Chemistry. *Chem. Rev.* **114**, 4540–4563 (2014).
184. G. Gasser, I. Ott, N. Metzler-Nolte, Organometallic Anticancer Compounds. *J. Med. Chem.* **54**, 3–25 (2011).
185. C.-P. Tan, Y.-Y. Lu, L.-N. Ji, Z.-W. Mao, Metallomics insights into the programmed cell death induced by metal-based anticancer compounds. *Metallomics.* **6**, 978–995 (2014).
186. N. P. E. Barry, P. J. Sadler, Exploration of the medical periodic table: towards new targets. *Chem. Commun.* **49**, 5106–5131 (2013).
187. G. Jaouen, N. Metzler-Nolte, *Medicinal Organometallic Chemistry* (Springer, 2010).
188. G. Gasser, *Inorganic Chemical Biology: Principles, Techniques and Applications* (John Wiley & Sons, 2014).
189. S. Spreckelmeyer, C. Orvig, A. Casini, Cellular Transport Mechanisms of Cytotoxic Metallodrugs: An Overview beyond Cisplatin. *Molecules.* **19**, 15584–15610 (2014).
190. E. W. Price, C. Orvig, Matching chelators to radiometals for radiopharmaceuticals. *Chem. Soc. Rev.* **43**, 260–290 (2014).
191. S. H. van Rijt, P. J. Sadler, Current applications and future potential for bioinorganic chemistry in the development of anticancer drugs. *Drug Discov. Today.* **14**, 1089–1097 (2009).
192. A. Naganuma, T. Tanaka, K. Maeda, R. Matsuda, J. Tabata-Hanyu, N. Imura, The interaction of selenium with various metals in vitro and in vivo. *Toxicology.* **29**, 77–86 (1983).
193. F. Di Sarra, B. Fresch, R. Bini, G. Saielli, A. Bagno, Reactivity of Auranofin with Selenols and Thiols – Implications for the Anticancer Activity of Gold(I) Compounds. *Eur. J. Inorg. Chem.* **2013**, 2718–2727 (2013).
194. A. Casini, A. Guerri, C. Gabbiani, L. Messori, Biophysical characterisation of adducts formed between anticancer metallodrugs and selected proteins: New insights from X-ray diffraction and mass spectrometry studies. *J. Inorg. Biochem.* **102**, 995–1006 (2008).
195. A. Casini, J. Reedijk, Interactions of anticancer Pt compounds with proteins: an overlooked topic in medicinal inorganic chemistry? *Chem. Sci.* **3**, 3135–3144 (2012).
196. A. de Almeida, B. L. Oliveira, J. D. G. Correia, G. Soveral, A. Casini, Emerging protein targets for metal-based pharmaceutical agents: An update. *Coord. Chem. Rev.* **257**, 2689–2704 (2013).
197. S. Abhishek, S. Sivadas, M. Satish, W. Deeksha, E. Rajakumara, Dynamic Basis for Auranofin Drug Recognition by Thiol-Reductases of Human Pathogens and Intermediate Coordinated Adduct Formation with Catalytic Cysteine Residues. *ACS Omega.* **4**, 9593–9602 (2019).
198. S. Talbot, R. Nelson, W. T. Self, Arsenic trioxide and auranofin inhibit selenoprotein synthesis: implications for chemotherapy for acute promyelocytic leukaemia. *Br. J. Pharmacol.* **154**, 940–948 (2008).

199. H. F. Dos Santos, Reactivity of auranofin with S-, Se- and N-containing amino acids. *Comput. Theor. Chem.* **1048**, 95–101 (2014).
200. A. Bindoli, M. P. Rigobello, G. Scutari, C. Gabbiani, A. Casini, L. Messori, Thioredoxin reductase: A target for gold compounds acting as potential anticancer drugs. *Coord. Chem. Rev.* **253**, 1692–1707 (2009).
201. L. Kou, S. Wei, P. Kou, Current Progress and Perspectives on Using Gold Compounds for the Modulation of Tumor Cell Metabolism. *Front. Chem.* **9**, 638 (2021).
202. F. Chiara, A. Gambalunga, M. Sciacovelli, A. Nicolli, L. Ronconi, D. Fregona, P. Bernardi, A. Rasola, A. Trevisan, Chemotherapeutic induction of mitochondrial oxidative stress activates GSK-3 $\alpha/\beta$  and Bax, leading to permeability transition pore opening and tumor cell death. *Cell Death Dis.* **3**, e444 (2012).
203. M. Pia Rigobello, L. Messori, G. Marcon, M. Agostina Cinellu, M. Bragadin, A. Folda, G. Scutari, A. Bindoli, Gold complexes inhibit mitochondrial thioredoxin reductase: consequences on mitochondrial functions. *J. Inorg. Biochem.* **98**, 1634–1641 (2004).
204. S. Urig, K. Fritz-Wolf, R. Réau, C. Herold-Mende, K. Tóth, E. Davioud-Charvet, K. Becker, Undressing of Phosphine Gold(I) Complexes as Irreversible Inhibitors of Human Disulfide Reductases. *Angew. Chem. Int. Ed.* **45**, 1881–1886 (2006).
205. E. Viry, E. Battaglia, V. Deborde, T. Müller, R. Réau, E. Davioud-Charvet, D. Bagrel, A sugar-modified phosphole gold complex with antiproliferative properties acting as a thioredoxin reductase inhibitor in MCF-7 cells. *ChemMedChem.* **3**, 1667–1670 (2008).
206. C. Schmidt, B. Karge, R. Misgeld, A. Prokop, R. Franke, M. Brönstrup, I. Ott, Gold(I) NHC Complexes: Antiproliferative Activity, Cellular Uptake, Inhibition of Mammalian and Bacterial Thioredoxin Reductases, and Gram-Positive Directed Antibacterial Effects. *Chem. - Eur. J.* **23**, 1869–1880 (2017).
207. A. Citta, A. Folda, A. Bindoli, P. Pigeon, S. Top, A. Vessières, M. Salmain, G. Jaouen, M. P. Rigobello, Evidence for Targeting Thioredoxin Reductases with Ferrocenyl Quinone Methides. A Possible Molecular Basis for the Antiproliferative Effect of Hydroxyferrocifens on Cancer Cells. *J. Med. Chem.* **57**, 8849–8859 (2014).
208. V. Scalcon, A. Citta, A. Folda, A. Bindoli, M. Salmain, I. Ciofini, S. Blanchard, J. de Jesús Cázares-Marinero, Y. Wang, P. Pigeon, G. Jaouen, A. Vessières, M. P. Rigobello, Enzymatic oxidation of ansa-ferrocifen leads to strong and selective thioredoxin reductase inhibition in vitro. *J. Inorg. Biochem.* **165**, 146–151 (2016).
209. V. Scalcon, S. Top, H. Z. S. Lee, A. Citta, A. Folda, A. Bindoli, W. K. Leong, M. Salmain, A. Vessières, G. Jaouen, M. P. Rigobello, Osmocenyl-tamoxifen derivatives target the thioredoxin system leading to a redox imbalance in Jurkat cells. *J. Inorg. Biochem.* **160**, 296–304 (2016).
210. V. Scalcon, M. Salmain, A. Folda, S. Top, P. Pigeon, H. Z. Shirley Lee, G. Jaouen, A. Bindoli, A. Vessières, M. P. Rigobello, Tamoxifen-like metallocifens target the thioredoxin system determining mitochondrial impairment leading to apoptosis in Jurkat cells†. *Metallomics.* **9**, 949–959 (2017).
211. P. Mura, M. Camalli, A. Bindoli, F. Sorrentino, A. Casini, C. Gabbiani, M. Corsini, P. Zanello, M. Pia Rigobello, L. Messori, Activity of Rat Cytosolic Thioredoxin Reductase Is Strongly



- Decreased by *trans* -[Bis(2-amino-5- methylthiazole)tetrachlororuthenate(III)]: First Report of Relevant Thioredoxin Reductase Inhibition for a Ruthenium Compound. *J. Med. Chem.* **50**, 5871–5874 (2007).
212. J. Lu, E.-H. Chew, A. Holmgren, Targeting thioredoxin reductase is a basis for cancer therapy by arsenic trioxide. *Proc. Natl. Acad. Sci.* **104**, 12288–12293 (2007).
213. E. S. J. Arnér, H. Nakamura, T. Sasada, J. Yodoi, A. Holmgren, G. Spyrou, Analysis of the inhibition of mammalian thioredoxin, thioredoxin reductase, and glutaredoxin by cis-diamminedichloroplatinum (II) and its major metabolite, the glutathione-platinum complex. *Free Radic. Biol. Med.* **31**, 1170–1178 (2001).
214. S. Prast-Nielsen, M. Cebula, I. Pader, E. S. J. Arnér, Noble metal targeting of thioredoxin reductase — covalent complexes with thioredoxin and thioredoxin-related protein of 14kDa triggered by cisplatin. *Free Radic. Biol. Med.* **49**, 1765–1778 (2010).
215. R. Millet, S. Urig, J. Jacob, E. Amtmann, J.-P. Moulinoux, S. Gromer, K. Becker, E. Davioud-Charvet, Synthesis of 5-Nitro-2-furancarbohydrazides and Their cis-Diamminedichloroplatinum Complexes as Bitopic and Irreversible Human Thioredoxin Reductase Inhibitors. *J. Med. Chem.* **48**, 7024–7039 (2005).
216. S. I. Hashemy, J. S. Ungerstedt, F. Z. Avval, A. Holmgren, Motexafin Gadolinium, a Tumor-selective Drug Targeting Thioredoxin Reductase and Ribonucleotide Reductase. *J. Biol. Chem.* **281**, 10691–10697 (2006).
217. I. Ott, X. Qian, Y. Xu, D. H. W. Vlecken, I. J. Marques, D. Kubutat, J. Will, W. S. Sheldrick, P. Jesse, A. Prokop, C. P. Bagowski, A Gold(I) Phosphine Complex Containing a Naphthalimide Ligand Functions as a TrxR Inhibiting Antiproliferative Agent and Angiogenesis Inhibitor. *J. Med. Chem.* **52**, 763–770 (2009).
218. K. Yan, C.-N. Lok, K. Bierla, C.-M. Che, Gold(I) complex of N,N'-disubstituted cyclic thiourea with in vitro and in vivo anticancer properties—potent tight-binding inhibition of thioredoxin reductase. *Chem. Commun.* **46**, 7691–7693 (2010).
219. C. Gabbiani, G. Mastrobuoni, F. Sorrentino, B. Dani, M. P. Rigobello, A. Bindoli, M. A. Cinellu, G. Pieraccini, L. Messori, A. Casini, Thioredoxin reductase, an emerging target for anticancer metallodrugs. Enzyme inhibition by cytotoxic gold(III) compounds studied with combined mass spectrometry and biochemical assays. *Med Chem Commun.* **2**, 50–54 (2011).
220. J. Gómez-Espina, E. Blanco-González, M. Montes-Bayón, A. Sanz-Medel, HPLC-ICP-MS for simultaneous quantification of the total and active form of the thioredoxin reductase enzyme in human serum using auranofin as an activity-based probe. *J. Anal. At. Spectrom.* **31**, 1895–1903 (2016).
221. S. M. Meier, C. Gerner, B. K. Keppler, M. A. Cinellu, A. Casini, Mass Spectrometry Uncovers Molecular Reactivities of Coordination and Organometallic Gold(III) Drug Candidates in Competitive Experiments That Correlate with Their Biological Effects. *Inorg. Chem.* **55**, 4248–4259 (2016).
222. A. Pratesi, C. Gabbiani, M. Ginanneschi, L. Messori, Reactions of medicinally relevant gold compounds with the C-terminal motif of thioredoxin reductase elucidated by MS analysis. *Chem. Commun.* **46**, 7001–7003 (2010).

223. A. Pratesi, C. Gabbiani, E. Michelucci, M. Ginanneschi, A. M. Papini, R. Rubbiani, I. Ott, L. Messori, Insights on the mechanism of thioredoxin reductase inhibition by Gold N-heterocyclic carbene compounds using the synthetic linear Selenocysteine containing C-terminal peptide hTrxR(488-499): An ESI-MS investigation. *J. Inorg. Biochem.* **136**, 161–169 (2014).
224. M. A. Baker, A. L. Tappel, Effects of ligands on gold inhibition of selenium glutathione peroxidase. *Biochem. Pharmacol.* **35**, 2417–2422 (1986).
225. J. Chaudiere, A. L. Tappel, Interaction of gold(I) with the active site of selenium-glutathione peroxidase. *J. Inorg. Biochem.* **20**, 313–325 (1984).
226. J. R. Roberts, C. F. Shaw, Inhibition of Erythrocyte Selenium-Glutathione Peroxidase by Auranofin Analogues and Metabolites. *Biochem. Pharmacol.* **55**, 1291–1299 (1998).
227. W. Ashraf, A. A. Isab, <sup>31</sup>P NMR studies of Redox reactions of Bis (Trialkylphosphine) Gold(I) Bromide (Alkyl = Methyl, Ethyl) with Disulphide and Diselenide ligands. *J. Coord. Chem.* **57**, 337–346 (2004).
228. J. Szpunar, Bio-inorganic speciation analysis by hyphenated techniques. *Analyst.* **125**, 963–988 (2000).
229. M. Zachariou, *Affinity Chromatography: Methods and Protocols* (Springer Science & Business Media, 2008).
230. P. L. R. Bonner, *Protein Purification* (Taylor & Francis, 2007).
231. G. E. Arteel, S. Franken, J. Kappler, H. Sies, Binding of Selenoprotein P to Heparin: Characterization with Surface Plasmon Resonance. *Biol. Chem.* **381**, 265–268 (2000).
232. D. E. Brooks, C. A. Haynes, D. Hritcu, B. M. Steels, W. Müller, Size exclusion chromatography does not require pores. *Proc. Natl. Acad. Sci. U. S. A.* **97**, 7064–7067 (2000).
233. I. Molnár, C. Horváth, Reverse-phase chromatography of polar biological substances: separation of catechol compounds by high-performance liquid chromatography. *Clin. Chem.* **22**, 1497–1502 (1976).
234. R. S. Abidin, Murine polyomavirus VLPs as a platform for cytotoxic T cell epitope-based influenza vaccine candidates (2016), doi:10.14264/uql.2017.36.
235. S. C. Wilschefski, M. R. Baxter, Inductively Coupled Plasma Mass Spectrometry: Introduction to Analytical Aspects. *Clin. Biochem. Rev.* **40**, 115–133 (2019).
236. T. Hyotylainen, S. Wiedmer, *Chromatographic Methods in Metabolomics* (Royal Society of Chemistry, 2013).
237. R. Thomas, *Practical Guide to ICP-MS: A Tutorial for Beginners, Third Edition* (CRC Press, 2013).
238. P. Heitland, H. D. Köster, Biomonitoring of selenoprotein P in human serum by fast affinity chromatography coupled to ICP-MS. *Int. J. Hyg. Environ. Health.* **221**, 564–568 (2018).
239. P. Jitaru, M. Prete, G. Cozzi, C. Turetta, W. Cairns, R. Seraglia, P. Traldi, P. Cescon, C. Barbante, Speciation analysis of selenoproteins in human serum by solid-phase extraction and affinity HPLC hyphenated to ICP-quadrupole MS. *J. Anal. At. Spectrom.* **23**, 402–406 (2008).

240. M. Iglesias, N. Gilon, E. Poussel, J.-M. Mermet, Evaluation of an ICP-collision/reaction cell-MS system for the sensitive determination of spectrally interfered and non-interfered elements using the same gas conditions. *J. Anal. At. Spectrom.* **17**, 1240–1247 (2002).
241. J. Darrouzès, M. Bueno, G. Lespes, M. Potin-Gautier, Operational optimisation of ICP - Octopole collision/reaction cell - MS for applications to ultratrace selenium total and speciation determination. *J. Anal. At. Spectrom.* **20**, 88–94 (2005).
242. L. Balcaen, E. Bolea-Fernandez, M. Resano, F. Vanhaecke, Inductively coupled plasma – Tandem mass spectrometry (ICP-MS/MS): A powerful and universal tool for the interference-free determination of (ultra)trace elements – A tutorial review. *Anal. Chim. Acta.* **894**, 7–19 (2015).
243. E. Bulska, B. Wagner, Quantitative aspects of inductively coupled plasma mass spectrometry. *Philos. Trans. R. Soc. Math. Phys. Eng. Sci.* **374**, 20150369 (2016).
244. M. Wang, W.-Y. Feng, Y.-L. Zhao, Z.-F. Chai, ICP-MS-based strategies for protein quantification. *Mass Spectrom. Rev.* **29**, 326–348 (2010).
245. J. Szpunar, Advances in analytical methodology for bioinorganic speciation analysis: metallomics, metalloproteomics and heteroatom-tagged proteomics and metabolomics. *Analyst.* **130**, 442–465 (2005).
246. R. Lobiński, D. Schaumlöffel, J. Szpunar, Mass spectrometry in bioinorganic analytical chemistry. *Mass Spectrom. Rev.* **25**, 255–289 (2006).
247. H. Andrén, I. Rodushkin, A. Stenberg, D. Malinovsky, D. C. Baxter, Sources of mass bias and isotope ratio variation in multi-collector ICP-MS: optimization of instrumental parameters based on experimental observations. *J. Anal. At. Spectrom.* **19**, 1217–1224 (2004).
248. Q. Xie, R. Kerrich, Isotope ratio measurement by hexapole ICP-MS : mass bias effect, precision and accuracy. *J. Anal. At. Spectrom.* **17**, 69–74 (2002).
249. M. Haldimann, B. Zimmerli, C. Als, H. Gerber, Direct determination of urinary iodine by inductively coupled plasma mass spectrometry using isotope dilution with iodine-129. *Clin. Chem.* **44**, 817–824 (1998).
250. D. Schaumlöffel, R. Lobinski, Isotope dilution technique for quantitative analysis of endogenous trace element species in biological systems. *Int. J. Mass Spectrom.* **242**, 217–223 (2005).
251. S. Forcisi, F. Moritz, B. Kanawati, D. Tziotis, R. Lehmann, P. Schmitt-Kopplin, Liquid chromatography-mass spectrometry in metabolomics research: mass analyzers in ultra high pressure liquid chromatography coupling. *J. Chromatogr. A.* **1292**, 51–65 (2013).
252. R. A. Zubarev, A. Makarov, Orbitrap Mass Spectrometry. *Anal. Chem.* **85**, 5288–5296 (2013).
253. A. G. Marshall, C. L. Hendrickson, High-resolution mass spectrometers. *Annu. Rev. Anal. Chem. Palo Alto Calif.* **1**, 579–599 (2008).
254. F. Hillenkamp, M. Karas, R. C. Beavis, B. T. Chait, Matrix-Assisted Laser Desorption/Ionization Mass Spectrometry of Biopolymers. *Anal. Chem.* **63**, 1193A-1203A (1991).
255. M. Karas, R. Krüger, Ion Formation in MALDI: The Cluster Ionization Mechanism. *Chem. Rev.* **103**, 427–440 (2003).

256. H. Steen, M. Mann, The ABC's (and XYZ's) of peptide sequencing. *Nat. Rev. Mol. Cell Biol.* **5**, 699–711 (2004).
257. C. L. Ward-Deitrich, E. Whyte, C. Hopley, M. P. Rayman, Y. Ogra, H. Goenaga-Infante, Systematic study of the selenium fractionation in human plasma from a cancer prevention trial using HPLC hyphenated to ICP-MS and ESI-MS/MS. *Anal. Bioanal. Chem.* **413**, 331–344 (2021).
258. K. Coufalíková, I. Benešová, T. Vaculovič, V. Kanický, J. Preisler, LC coupled to ESI, MALDI and ICP MS – A multiple hyphenation for metalloproteomic studies. *Anal. Chim. Acta.* **968**, 58–65 (2017).
259. M. E. Swartz, UPLC<sup>TM</sup>: An Introduction and Review. *J. Liq. Chromatogr. Relat. Technol.* **28**, 1253–1263 (2005).
260. J. M. Saz, M. L. Marina, Application of micro- and nano-HPLC to the determination and characterization of bioactive and biomarker peptides. *J. Sep. Sci.* **31**, 446–458 (2008).
261. J. Sproß, S. Brauch, F. Mandel, M. Wagner, S. Buckenmaier, B. Westermann, A. Sinz, Multidimensional nano-HPLC coupled with tandem mass spectrometry for analyzing biotinylated proteins. *Anal. Bioanal. Chem.* **405**, 2163–2173 (2013).
262. Y. Wagner, A. Sickmann, H. E. Meyer, G. Daum, Multidimensional nano-HPLC for analysis of protein complexes. *J. Am. Soc. Mass Spectrom.* **14**, 1003–1011 (2003).
263. B. T. Chait, CHEMISTRY: Mass Spectrometry: Bottom-Up or Top-Down? *Science.* **314**, 65–66 (2006).
264. L. C. Gillet, A. Leitner, R. Aebersold, Mass Spectrometry Applied to Bottom-Up Proteomics: Entering the High-Throughput Era for Hypothesis Testing. *Annu. Rev. Anal. Chem.* **9**, 449–472 (2016).
265. N. L. Kelleher, H. Y. Lin, G. A. Valaskovic, D. J. Aaserud, E. K. Fridriksson, F. W. McLafferty, Top Down versus Bottom Up Protein Characterization by Tandem High-Resolution Mass Spectrometry. *J. Am. Chem. Soc.* **121**, 806–812 (1999).
266. A. M. Belov, thesis.
267. Z. R. Gregorich, Y.-H. Chang, Y. Ge, Proteomics in Heart Failure: Top-down or Bottom-up? *Pflugers Arch.* **466**, 1199–1209 (2014).
268. M. Tanaka, Y. Saito, H. Misu, S. Kato, Y. Kitta, Y. Takeshita, T. Kanamori, T. Nagano, M. Nakagen, T. Urabe, T. Takamura, S. Kaneko, K. Takahashi, N. Matsuyama, Development of a Sol Particle Homogeneous Immunoassay for Measuring Full-Length Selenoprotein P in Human Serum. *J. Clin. Lab. Anal.* **30**, 114–122 (2014).
269. J.-G. Yang, J. Morrison-Plummer, R. F. Burk, Purification and Quantitation of a Rat Plasma Selenoprotein Distinct from Glutathione Peroxidase Using Monoclonal Antibodies. *J. Biol. Chem.* **262**, 13372–13375 (1987).
270. S. Himeno, H. S. Chittum, R. F. Burk, Isoforms of Selenoprotein P in Rat Plasma: evidence for a full-length form and another form that terminates at the second UGA in the open reading frame. *J. Biol. Chem.* **271**, 15769–15775 (1996).

271. G. Ballihaut, L. E. Kilpatrick, E. L. Kilpatrick, W. C. Davis, Multiple forms of selenoprotein P in a candidate human plasma standard reference material. *Metallomics*. **4**, 533 (2012).
272. S. M. Oo, H. Misu, Y. Saito, M. Tanaka, S. Kato, Y. Kita, H. Takayama, Y. Takeshita, T. Kanamori, T. Nagano, M. Nakagen, T. Urabe, N. Matsuyama, S. Kaneko, T. Takamura, Serum selenoprotein P, but not selenium, predicts future hyperglycemia in a general Japanese population. *Sci. Rep.* **8**, 16727 (2018).
273. R. J. Hondal, S. Ma, R. M. Caprioli, K. E. Hill, R. F. Burk, Heparin-binding histidine and lysine residues of rat selenoprotein P. *J. Biol. Chem.* **276**, 15823–15831 (2001).
274. U. Sidenius, O. Farver, O. Jøns, B. Gammelgaard, Comparison of different transition metal ions for immobilized metal affinity chromatography of selenoprotein P from human plasma. *J. Chromatogr. B. Biomed. Sci. App.* **735**, 85–91 (1999).
275. Y. Saito, Y. Watanabe, E. Saito, T. Honjoh, K. Takahashi, Production and Application of Monoclonal Antibodies to Human Selenoprotein P. *J. Health Sci.* **47**, 346–352 (2001).
276. G. E. Olson, V. P. Winfrey, S. K. Nagdas, K. E. Hill, R. F. Burk, Apolipoprotein E receptor-2 (ApoER2) mediates selenium uptake from selenoprotein P by the mouse testis. *J. Biol. Chem.* **282**, 12290–12297 (2007).
277. S. Hybsier, Z. Wu, T. Schulz, C. J. Strasburger, J. Köhrle, W. B. Minich, L. Schomburg, Establishment and characterization of a new ELISA for selenoprotein P. *Perspect. Sci.* **3**, 23–24 (2015).
278. A. E. Altinova, O. T. Iyidir, C. Ozkan, D. Ors, M. Ozturk, O. Gulbahar, N. Bozkurt, F. B. Toruner, M. Akturk, N. Cakir, M. Arslan, Selenoprotein P is not elevated in gestational diabetes mellitus. *Gynecol. Endocrinol.* **31**, 874–876 (2015).
279. A. Baran, J. Nowowiejska, J. A. Krahel, T. W. Kaminski, M. Maciaszek, I. Flisiak, Higher Serum Selenoprotein P Level as a Novel Inductor of Metabolic Complications in Psoriasis. *Int. J. Mol. Sci.* **21**, E4594 (2020).
280. Y. Wang, Y. Zou, T. Wang, S. Han, X. Liu, Y. Zhang, S. Su, H. Zhou, X. Zhang, H. Liang, A spatial study on serum selenoprotein P and Keshan disease in Heilongjiang Province, China. *J. Trace Elem. Med. Biol. Organ Soc. Miner. Trace Elem. GMS.* **65**, 126728 (2021).
281. R. F. Burk, K. E. Hill, Selenoprotein P. A Selenium-Rich Extracellular Glycoprotein. *J. Nutr.* **124**, 1891–1897 (1994).
282. K. T. Suzuki, C. Sasakura, S. Yoneda, Binding sites for the (Hg-Se) complex on selenoprotein P. *Biochim. Biophys. Acta BBA - Protein Struct. Mol. Enzymol.* **1429**, 102–112 (1998).
283. Y. Suzuki, T. Sakai, N. Furuta, Isolation of Selenoprotein-P and Determination of Se Concentration Incorporated in Proteins in Human and Mouse Plasma by Tandem Heparin Affinity and Size-exclusion Column HPLC-ICPMS. *Anal. Sci.* **28**, 221–221 (2012).
284. J. T. Deagen, J. A. Butler, B. A. Zachara, P. D. Whanger, Determination of the Distribution of Selenium between Glutathione Peroxidase, Selenoprotein P, and Albumin in Plasma. *Anal. Biochem.* **208**, 176–181 (1993).
285. Y. Saito, T. Hayashi, A. Tanaka, Y. Watanabe, M. Suzuki, E. Saito, K. Takahashi, Selenoprotein P in Human Plasma as an Extracellular Phospholipid Hydroperoxide Glutathione Peroxidase :

- isolation and enzymatic characterization of human selenoprotein P. *J. Biol. Chem.* **274**, 2866–2871 (1999).
286. A. Arias-Borrego, B. Callejón-Leblic, G. Rodríguez-Moro, I. Velasco, J. L. Gómez-Ariza, T. García-Barrera, A novel HPLC column switching method coupled to ICP-MS/QTOF for the first determination of selenoprotein P (SELENOP) in human breast milk. *Food Chem.* **321**, 126692 (2020).
287. K. Shigeta, K. Sato, N. Furuta, Determination of selenoprotein P in submicrolitre samples of human plasma using micro-affinity chromatography coupled with low flow ICP-MS. *J. Anal. At. Spectrom.* **22**, 911 (2007).
288. G. Ballihaut, L. E. Kilpatrick, W. C. Davis, Detection, Identification, and Quantification of Selenoproteins in a Candidate Human Plasma Standard Reference Material. *Anal. Chem.* **83**, 8667–8674 (2011).
289. M. E. del C. Busto, C. Oster, S. Cuello-Nuñez, C. L. Deitrich, A. Raab, A. Konopka, W. D. Lehmann, H. Goenaga-Infante, P. Fisicaro, Accurate quantification of selenoproteins in human plasma/serum by isotope dilution ICP-MS: focus on selenoprotein P. *J. Anal. At. Spectrom.* **31**, 1904–1912 (2016).
290. L. H. Reyes, J. M. Marchante-Gayón, J. I. G. Alonso, A. Sanz-Medel, Quantitative speciation of selenium in human serum by affinity chromatography coupled to post-column isotope dilution analysis ICP-MS. *J. Anal. At. Spectrom.* **18**, 1210–1216 (2003).
291. M. Roman, A. Lapolla, P. Jitaru, A. Sechi, C. Cosma, G. Cozzi, P. Cescon, C. Barbante, Plasma selenoproteins concentrations in type 2 diabetes mellitus—a pilot study. *Transl. Res.* **156**, 242–250 (2010).
292. S. Letsiou, Y. Lu, T. Nomikos, S. Antonopoulou, D. Panagiotakos, C. Pitsavos, C. Stefanadis, S. A. Pergantis, High-throughput quantification of selenium in individual serum proteins from a healthy human population using HPLC on-line with isotope dilution inductively coupled plasma-MS. *PROTEOMICS*. **10**, 3447–3457 (2010).
293. B. Callejón-Leblic, G. Rodríguez-Moro, A. Arias-Borrego, A. Pereira-Vega, J. L. Gómez-Ariza, T. García-Barrera, Absolute quantification of selenoproteins and selenometabolites in lung cancer human serum by column switching coupled to triple quadrupole inductively coupled plasma mass spectrometry. *J. Chromatogr. A*. **1619**, 460919 (2020).
294. M. A. García-Sevillano, T. García-Barrera, J. L. Gómez-Ariza, Simultaneous speciation of selenoproteins and selenometabolites in plasma and serum by dual size exclusion-affinity chromatography with online isotope dilution inductively coupled plasma mass spectrometry. *Anal. Bioanal. Chem.* **406**, 2719–2725 (2014).
295. C. Santos, E. García-Fuentes, B. Callejón-Leblic, T. García-Barrera, J. L. Gómez-Ariza, M. P. Rayman, I. Velasco, Selenium, selenoproteins and selenometabolites in mothers and babies at the time of birth. *Br. J. Nutr.* **117**, 1304–1311 (2017).
296. Y. Anan, Y. Hatakeyama, M. Tokumoto, Y. Ogra, Chromatographic Behavior of Selenoproteins in Rat Serum Detected by Inductively Coupled Plasma Mass Spectrometry. *Anal. Sci.* **29**, 787–792 (2013).



297. Y. Suzuki, Y. Hashiura, T. Sakai, T. Yamamoto, T. Matsukawa, A. Shinohara, N. Furuta, Selenium metabolism and excretion in mice after injection of <sup>82</sup>Se-enriched selenomethionine. *Metallomics*. **5**, 445–452 (2013).
298. O. Palacios, J. Ruiz Encinar, D. Schaumlöffel, R. Lobinski, Fractionation of selenium-containing proteins in serum by multiaffinity liquid chromatography before size-exclusion chromatography-ICPMS. *Anal. Bioanal. Chem.* **384**, 1276–1283 (2006).
299. N. Solovyev, A. Berthele, B. Michalke, Selenium speciation in paired serum and cerebrospinal fluid samples. *Anal. Bioanal. Chem.* **405**, 1875–1884 (2013).
300. M. Xu, L. Yang, Q. Wang, Quantification of selenium-tagged proteins in human plasma using species-unspecific isotope dilution ICP-DRC-qMS coupled on-line with anion exchange chromatography. *J. Anal. At. Spectrom.* **23**, 1545–1549 (2008).
301. F. Maass, B. Michalke, D. Willkommen, C. Schulte, L. Tönges, M. Boerger, I. Zerr, M. Bähr, P. Lingor, Selenium speciation analysis in the cerebrospinal fluid of patients with Parkinson's disease. *J. Trace Elem. Med. Biol.* **57**, 126412 (2020).
302. Y. Zhang, J. Zheng, Bioinformatics of Metalloproteins and Metalloproteomes. *Mol. Basel Switz.* **25**, E3366 (2020).
303. L. Jing, C. E. Parker, D. Seo, M. W. Hines, N. Dicheva, Y. Yu, D. Schwinn, G. S. Ginsburg, X. Chen, Discovery of biomarker candidates for coronary artery disease from an APOE-knock out mouse model using iTRAQ-based multiplex quantitative proteomics. *Proteomics*. **11**, 2763–2776 (2011).
304. L. M. Smith, N. L. Kelleher, Proteoforms as the next proteomics currency. *Science*. **359**, 1106–1107 (2018).
305. S. Ma, K. E. Hill, R. F. Burk, R. M. Caprioli, Mass spectrometric determination of selenenylsulfide linkages in rat selenoprotein P. *J. Mass Spectrom. JMS*. **40**, 400–404 (2005).
306. R. Bruderer, J. Muntel, S. Müller, O. M. Bernhardt, T. Gandhi, O. Cominetti, C. Macron, J. Carayol, O. Rinner, A. Astrup, W. H. M. Saris, J. Hager, A. Valsesia, L. Dayon, L. Reiter, Analysis of 1508 Plasma Samples by Capillary-Flow Data-Independent Acquisition Profiles Proteomics of Weight Loss and Maintenance [S]. *Mol. Cell. Proteomics*. **18**, 1242–1254 (2019).
307. X. Wang, Z. Yu, X. Zhao, R. Han, D. Huang, Y. Yang, G. Cheng, Comparative proteomic characterization of bovine milk containing  $\beta$ -casein variants A1A1 and A2A2, and their heterozygote A1A2. *J. Sci. Food Agric.* **101**, 718–725 (2021).
308. R. N. Cole, I. Ruczinski, K. Schulze, P. Christian, S. Herbrich, L. Wu, L. R. Devine, R. N. O'Meally, S. Shrestha, T. N. Boronina, J. D. Yager, J. Groopman, K. P. West, The plasma proteome identifies expected and novel proteins correlated with micronutrient status in undernourished Nepalese children. *J. Nutr.* **143**, 1540–1548 (2013).
309. X. Shen, B. Huo, T. Wu, C. Song, Y. Chi, iTRAQ-based proteomic analysis to identify molecular mechanisms of the selenium deficiency response in the Przewalski's gazelle. *J. Proteomics*. **203**, 103389 (2019).

310. B. Yan, B. Chen, S. Min, Y. Gao, Y. Zhang, P. Xu, C. Li, J. Chen, G. Luo, C. Liu, iTRAQ-based Comparative Serum Proteomic Analysis of Prostate Cancer Patients with or without Bone Metastasis. *J. Cancer*. **10**, 4165–4177 (2019).
311. R. M. Lequin, Enzyme Immunoassay (EIA)/Enzyme-Linked Immunosorbent Assay (ELISA). *Clin. Chem*. **51**, 2415–2418 (2005).
312. K. E. Hill, Y. Xia, B. Åkesson, M. E. Boeglin, R. F. Burk, Selenoprotein P Concentration in Plasma is an Index of Selenium Status in Selenium-Deficient and Selenium-Supplemented Chinese Subjects. *J. Nutr*. **126**, 138–145 (1996).
313. R. Read, T. Bellew, J. G. Yang, K. E. Hill, I. S. Palmer, R. F. Burk, Selenium and amino acid composition of selenoprotein P, the major selenoprotein in rat serum. *J. Biol. Chem*. **265**, 17899–17905 (1990).
314. B. Hollenbach, N. G. Morgenthaler, J. Struck, C. Alonso, A. Bergmann, J. Köhrle, L. Schomburg, New assay for the measurement of selenoprotein P as a sepsis biomarker from serum. *J. Trace Elem. Med. Biol*. **22**, 24–32 (2008).
315. M. Chen, B. Liu, D. Wilkinson, A. T. Hutchison, C. H. Thompson, G. A. Wittert, L. K. Heilbronn, Selenoprotein P is elevated in individuals with obesity, but is not independently associated with insulin resistance. *Obes. Res. Clin. Pract*. **11**, 227–232 (2017).
316. O. Brodin, J. Hackler, S. Misra, S. Wendt, Q. Sun, E. Laaf, C. Stoppe, M. Björnstedt, L. Schomburg, Selenoprotein P as Biomarker of Selenium Status in Clinical Trials with Therapeutic Dosages of Selenite. *Nutrients*. **12**, 1067 (2020).
317. S. J. Yang, S. Y. Hwang, H. Y. Choi, H. J. Yoo, J. A. Seo, S. G. Kim, N. H. Kim, S. H. Baik, D. S. Choi, K. M. Choi, Serum Selenoprotein P Levels in Patients with Type 2 Diabetes and Prediabetes: Implications for Insulin Resistance, Inflammation, and Atherosclerosis. *J. Clin. Endocrinol. Metab*. **96**, E1325–E1329 (2011).
318. Y. Saito, H. Misu, H. Takayama, S. Takashima, S. Usui, M. Takamura, S. Kaneko, T. Takamura, N. Noguchi, Comparison of Human Selenoprotein P Determinants in Serum between Our Original Methods and Commercially Available Kits. *Biol. Pharm. Bull*. **41**, 828–832 (2018).
319. J. R. Encinar, D. Schaumlöffel, Y. Ogra, R. Lobinski, Determination of Selenomethionine and Selenocysteine in Human Serum Using Speciated Isotope Dilution-Capillary HPLC–Inductively Coupled Plasma Collision Cell Mass Spectrometry. *Anal. Chem*. **76**, 6635–6642 (2004).
320. P. Jitaru, H. Goenaga-Infante, S. Vaslin-Reimann, P. Fiscaro, A systematic approach to the accurate quantification of selenium in serum selenoalbumin by HPLC–ICP-MS. *Anal. Chim. Acta*. **657**, 100–107 (2010).
321. A. Polatajko, J. R. Encinar, D. Schaumlöffel, J. Szpunar, Quantification of a selenium-containing protein in yeast extract via an accurate determination of a tryptic peptide by species-specific isotope dilution capillary HPLC-ICP MS. *Chem. Anal.*, 265–278 (2005).
322. A. Konopka, D. Winter, W. Konopka, M. Estela del Castillo Busto, S. Nunez, H. Goenaga-Infante, P. Fiscaro, W. D. Lehmann, [Sec-to-Cys]selenoprotein – a novel type of recombinant, full-length selenoprotein standard for quantitative proteomics. *J. Anal. At. Spectrom*. **31**, 1929–1938 (2016).



323. A. Konopka, N. Zinn, C. Wild, W. D. Lehmann, in *Shotgun Proteomics: Methods and Protocols*, D. Martins-de-Souza, Ed. (Springer, New York, NY, 2014; [https://doi.org/10.1007/978-1-4939-0685-7\\_23](https://doi.org/10.1007/978-1-4939-0685-7_23)), *Methods in Molecular Biology*, pp. 337–363.
324. T. W.-M. Fan, E. Pruszkowski, S. Shuttleworth, Speciation of selenoproteins in Se-contaminated wildlife by gel electrophoresis and laser ablation-ICP-MS. *J. Anal. At. Spectrom.* **17**, 1621–1623 (2002).
325. G. Ballihaut, L. Tastet, C. Pécheyran, B. Bouyssiere, O. Donard, R. Grimaud, R. Lobinski, Biosynthesis, purification and analysis of selenomethionyl calmodulin by gel electrophoresis-laser ablation-ICP-MS and capillary HPLC-ICP-MS peptide mapping following in-gel tryptic digestion. *J. Anal. At. Spectrom.* **20**, 493–499 (2005).
326. G. Ballihaut, C. Pécheyran, S. Mounicou, H. Preud'homme, R. Grimaud, R. Lobinski, G. Ballihaut, R. Grimaud, R. Lobinski, Multimode detection (LA-ICP-MS, MALDI-MS and nanoHPLC-ESI-MS2) in 1D and 2D gel electrophoresis for selenium-containing proteins. *TrAC Trends Anal. Chem.* **26**, 183–190 (2007).
327. J. Bianga, Z. Touat-Hamici, K. Bierla, S. Mounicou, J. Szpunar, L. Chavatte, R. Lobinski, Speciation analysis for trace levels of selenoproteins in cultured human cells. *J. Proteomics.* **108**, 316–324 (2014).
328. J. Sonet, S. Mounicou, L. Chavatte, Nonradioactive Isotopic Labeling and Tracing of Selenoproteins in Cultured Cell Lines. *Methods Mol. Biol. Clifton NJ.* **1661**, 193–203 (2018).
329. G. Ballihaut, F. Claverie, C. Pécheyran, S. Mounicou, R. Grimaud, R. Lobinski, Sensitive Detection of Selenoproteins in Gel Electrophoresis by High Repetition Rate Femtosecond Laser Ablation-Inductively Coupled Plasma Mass Spectrometry. *Anal. Chem.* **79**, 6874–6880 (2007).
330. L. V. Schaffer, R. J. Millikin, R. M. Miller, L. C. Anderson, R. T. Fellers, Y. Ge, N. L. Kelleher, R. D. LeDuc, X. Liu, S. H. Payne, L. Sun, P. M. Thomas, T. Tucholski, Z. Wang, S. Wu, Z. Wu, D. Yu, M. R. Shortreed, L. M. Smith, Identification and Quantification of Proteoforms by Mass Spectrometry. *Proteomics.* **19**, e1800361 (2019).
331. P. L. Ross, Y. N. Huang, J. N. Marchese, B. Williamson, K. Parker, S. Hattan, N. Khainovski, S. Pillai, S. Dey, S. Daniels, S. Purkayastha, P. Juhasz, S. Martin, M. Bartlet-Jones, F. He, A. Jacobson, D. J. Pappin, Multiplexed protein quantitation in *Saccharomyces cerevisiae* using amine-reactive isobaric tagging reagents. *Mol. Cell. Proteomics MCP.* **3**, 1154–1169 (2004).
332. R. Yu, J. Zhang, Y. Zang, L. Zeng, W. Zuo, Y. Bai, Y. Liu, K. Sun, Y. Liu, <p>i>iTRAQ-based quantitative protein expression profiling of biomarkers in childhood B-cell and T-cell acute lymphoblastic leukemia</p>. *Cancer Manag. Res.* **11**, 7047–7063 (2019).
333. P. Kaur, N. M. Rizk, S. Ibrahim, N. Younes, A. Uppal, K. Dennis, T. Karve, K. Blakeslee, J. Kwagyan, M. Zirrie, H. W. Ransom, A. K. Cheema, iTRAQ-Based Quantitative Protein Expression Profiling and MRM Verification of Markers in Type 2 Diabetes. *J. Proteome Res.* **11**, 5527–5539 (2012).
334. Z. Ren, L. Bai, L. Shen, Z. Luo, Z. Zhou, Z. Zuo, X. Ma, J. Deng, Y. Wang, S. Xu, Y. Luo, S. Cao, S. Yu, Comparative iTRAQ Proteomics Reveals Multiple Effects of Selenium Yeast on Dairy Cows in Parturition. *Biol. Trace Elem. Res.* **197**, 464–474 (2020).

335. D. T. Hill, A. A. Isab, D. E. Griswold, M. J. DiMartino, E. D. Matz, A. L. Figueroa, J. E. Wawro, C. DeBrosse, W. M. Reiff, R. C. Elder, B. Jones, J. W. Webb, C. F. Shaw, Seleno-Auranofin (Et<sub>3</sub>PAuSe-tagI): Synthesis, Spectroscopic (EXAFS, 197Au Mössbauer, 31P, 1H, 13C, and 77Se NMR, ESI-MS) Characterization, Biological Activity, and Rapid Serum Albumin-Induced Triethylphosphine Oxide Generation. *Inorg. Chem.* **49**, 7663–7675 (2010).
336. L. R. A. James, Z.-Q. Xu, R. Sluyter, E. L. Hawksworth, C. Kelso, B. Lai, D. J. Paterson, M. D. de Jonge, N. E. Dixon, J. L. Beck, S. F. Ralph, C. T. Dillon, An investigation into the interactions of gold nanoparticles and anti-arthritis drugs with macrophages, and their reactivity towards thioredoxin reductase. *J. Inorg. Biochem.* **142**, 28–38 (2015).
337. Y.-C. Lo, T.-P. Ko, W.-C. Su, T.-L. Su, A. H.-J. Wang, Terpyridine–platinum(II) complexes are effective inhibitors of mammalian topoisomerases and human thioredoxin reductase 1. *J. Inorg. Biochem.* **103**, 1082–1092 (2009).
338. T. Shoeib, D. W. Atkinson, B. L. Sharp, Structural analysis of the anti-arthritis drug Auranofin: Its complexes with cysteine, selenocysteine and their fragmentation products. *Inorganica Chim. Acta.* **363**, 184–192 (2010).
339. L. Massai, C. Zoppi, D. Cirri, A. Pratesi, L. Messori, Reactions of Medicinal Gold(III) Compounds With Proteins and Peptides Explored by Electrospray Ionization Mass Spectrometry and Complementary Biophysical Methods. *Front. Chem.* **8**, 966 (2020).
340. E. Cordeau, C. Arnaudguilhem, B. Bouyssiere, A. Hagege, J. Martinez, G. Subra, S. Cantel, C. Enjalbal, Investigation of Elemental Mass Spectrometry in Pharmacology for Peptide Quantitation at Femtomolar Levels. *PLOS ONE.* **11**, e0157943 (2016).
341. C. Cheignon, E. Cordeau, N. Prache, S. Cantel, J. Martinez, G. Subra, C. Arnaudguilhem, B. Bouyssiere, C. Enjalbal, Receptor–Ligand Interaction Measured by Inductively Coupled Plasma Mass Spectrometry and Selenium Labeling. *J. Med. Chem.* **61**, 10173–10184 (2018).
342. M.-C. Hennion, Solid-phase extraction: method development, sorbents, and coupling with liquid chromatography. *J. Chromatogr. A.* **856**, 3–54 (1999).
343. F. Augusto, L. W. Hantao, N. G. S. Mogollón, S. C. G. N. Braga, New materials and trends in sorbents for solid-phase extraction. *TrAC Trends Anal. Chem.* **43**, 14–23 (2013).
344. B. Buszewski, M. Szultka, Past, Present, and Future of Solid Phase Extraction: A Review. *Crit. Rev. Anal. Chem.* **42**, 198–213 (2012).
345. J. Raeke, O. J. Lechtenfeld, M. Wagner, P. Herzprung, T. Reemtsma, Selectivity of solid phase extraction of freshwater dissolved organic matter and its effect on ultrahigh resolution mass spectra. *Environ. Sci. Process. Impacts.* **18**, 918–927 (2016).
346. C. M. Petersen, Alpha 2-macroglobulin and pregnancy zone protein. Serum levels, alpha 2-macroglobulin receptors, cellular synthesis and aspects of function in relation to immunology. *Dan. Med. Bull.* **40**, 409–446 (1993).
347. S. Yoshino, K. Fujimoto, T. Takada, S. Kawamura, J. Ogawa, Y. Kamata, Y. Koderu, M. Shichiri, Molecular form and concentration of serum  $\alpha$ 2-macroglobulin in diabetes. *Sci. Rep.* **9**, 12927 (2019).

348. Z. Wang, T. Rejtar, Z. S. Zhou, B. L. Karger, Desulfurization of cysteine-containing peptides resulting from sample preparation for protein characterization by mass spectrometry. *Rapid Commun. Mass Spectrom.* **24**, 267–275 (2010).
349. P. Bottari, R. Aebersold, F. Turecek, M. H. Gelb, Design and Synthesis of Visible Isotope-Coded Affinity Tags for the Absolute Quantification of Specific Proteins in Complex Mixtures. *Bioconjug. Chem.* **15**, 380–388 (2004).



## List of figures

|   |    |
|---|----|
| Figure 1 Structures and oxidation numbers of sulfur and selenium compounds resulting from the two electron oxidation reaction (9).....  | 26 |
| Figure 2 $pK_a$ values of selenols.....   | 27 |
| Figure 3 Chemical structures of methionine and cysteine and their Se counterparts: selenocysteine and selenomethionine.....   | 29 |
| Figure 4 Assimilation of inorganic selenium. The letters correspond to the metabolic pathways involved. ....  | 30 |
| Figure 5 Main selenometabolites in Se-rich yeast (courtesy of Joanna Szpunar).....  | 31 |
| Figure 6 :Comparison of $pK_a$ values of thiols and selenols.....   | 32 |
| Figure 7 Human selenocysteine transfer RNA (67).....  | 34 |
| Figure 8 Overview of selenocysteine biosynthesis and degradation (74).....  | 35 |
| Figure 9 Sequence of human TrxR1 A.) Canonical form of TrxR1 (non-major form in cells); B.) Major form of TrxR1 (isoform 5).....  | 38 |
| Figure 10 Putative number of SeCys residues in SelP in different organisms (81).....  | 40 |
| Figure 11 Sequence of human SELENOP (a) Amino-acid sequence of human SELENOP (138); (b) schematic representation of human SELENOP (on the basis of (135, 138) and Uniprot database). ....   | 40 |
| Figure 12 Chemical structure of cisplatin and the most common cisplatin derivatives.....  | 43 |
| Figure 13 Cisplatin behaviour in aqueous solution (149).....  | 44 |
| Figure 14 Auranofin and derivatives (a) Auranofin, b) $Au(Pt_3)_2$ , c) $Au(Pt_3)Cl$ , d) $Au(Pt_3)Br$ , e) $Au(Pt_3)I$ .....   | 45 |
| Figure 15 Chemical structure of non-platinum metal anti-cancer complexes.....   | 45 |
| Figure 16 Ligand-exchange equilibria of auranofin in chloroform (239).....  | 46 |
| Figure 17 Nucleophilic substitution of a sulfur ligand by selenium ligand in auranofin and further reactions of $Et_3P-Au-SePh$ (193).....  | 47 |
| Figure 18 Model peptide used as proxies of TrxR (a. Ott et al. (217), b. Pratesi et al. (222), c. Pratesi et al. (223)).....  | 50 |
| Figure 19 Immobilized metal affinity chromatography principle A. Metal ion are introduced to bind to the stationary phase, B. The protein of interest is introduced into the column, C. Protein histidine and metal chelate will interact forming a bond and retaining the protein on the column stationary phase, D. Using a pH gradient, the protein will be removed of the column..... | 54 |
| Figure 20 Separation mechanism by SEC columns (234).....  | 55 |
| Figure 21 Principle of ICP-MS (185).....  | 56 |
| Figure 22 Principle of electrospray ionization (from eu.idtdna.com).....  | 60 |
| Figure 23 Comparison of physical and analytical features for high-resolution, full mass range techniques in mass spectrometry.....  | 61 |
| Figure 24 Principle of Orbitrap (from Thermo Fisher Scientific).....  | 62 |
| Figure 25 Principle of matrix-assisted laser desorption ionisation (from creative-proteomics.com).....  | 63 |
| Figure 26 Principle of tandem mass spectrometry (from K.Murray).....  | 63 |
| Figure 27 Hyphenated techniques ICP-MS et ESI-MS specific information.....  | 65 |
| Figure 28 Areas of proteomics.....  | 66 |
| Figure 29 Bottom-up and Top-down proteomics principles (adapted from (267)).....  | 67 |
| Figure 30 Schematic interaction between SELENOP and IMAC stationary phase.....  | 71 |
| Figure 31 Schematic overview of the principle of HPLC configuration coupled with ICP-MS for SELENOP determination.....  | 73 |
| Figure 32 MALDI-MS spectra obtained for a native TrxR1 standard (black trace) and an auranofin labelled TrxR1 standard (red trace) (220). ....  | 81 |

|  |     |
|--|-----|
| Figure 33 MALDI MS spectra of intact rat TrxR1, pre-reduced with NADPH, alone or after 1 h incubation with auranofin, at 10:1 gold to protein molar ratio, and removal of unbound gold (200)..   | 82  |
| Figure 34 ESI mass spectra, transformed to an absolute mass scale (298) Components A–M correspond to : (A) TrxR; (B) TrxR + Au; (C) TrxR + AuL; (D) TrxR + Au + AuL; (E) TrxR + 2Au; (F) TrxR + 2Au + AuL; (G) TrxR + 2AuL; (H) TrxR + 2Au + 2AuL; (I) TrxR + 3Au; where L represents PEt3. (298)  | 83  |
| Figure 35 SEC-ICP-MS analysis of TrxR treated with [Au(TU) <sub>2</sub> ]Cl (Arrow indicates the peptide fraction co-eluted with Se and Au(218).....   | 84  |
| Figure 36 MALDI mass spectrometry of TrxR1 reduced by NADPH and incubated with terpyridine-platinum complex, tpt mean TP–Pt(II) (337).....   | 86  |
| Figure 37 Peptide mass of TrxR-arsenic by MALDI mass spectrometry (294).....   | 87  |
| Figure 38 MS/MS spectrum of the molecular ion [peptide + Au] <sup>+</sup> generated by neutral loss of triethylphosphine from the adduct [peptide + Au(PEt <sub>3</sub> )] <sup>+</sup> peptide = AGCVGAGLIK (217).....  | 90  |
| Figure 39 ESI-MS spectrum of the synthetic dodecapeptide Ac-SGGDILQSGCUG-NH <sub>2</sub> incubated with auranofin, acquired in negative ion mode (223).....  | 91  |
| Figure 40 Electrospray ionization spectra of the dodecapeptide with Au <sub>2</sub> ph (339).....  | 91  |
| Figure 41 Chemical structure of a) vasopressin and b) selenovasopressin.....   | 94  |
| Figure 42 ICP-MS Agilent Technologies model 7700s.....   | 101 |
| Figure 43 ESI-MS Orbitrap LUMOS Fusion A) with UPLC and B) TriVersa Nanomate and nanoUPLC.....   | 103 |
| Figure 44 ESI-MS Orbitrap LUMOS Fusion with UPLC.....  | 104 |
| Figure 45 Dual-HPLC system coupled with ICP-MS A. DI-HPLC-ICP-MS, B. Split and capillary system used to connect the column with UV, ICP and dilution HPLC and fraction collector.....  | 106 |
| Figure 46 Schematic representation of the Dual-HPLC coupled with ICP-MS A. Separation HPLC with phase A and B, B. IMAC column loaded with serum, C. Fraction collection module, D. Split between column end, fraction collection and UV module, E. UV module, F. Dilution HPLC, G. Second split between UV end, Dilution HPLC and ICP-MS, H. ICP-MS..... | 106 |
| Figure 47 SPE system used for SELENOP.....   | 107 |
| Figure 48 Spectrophotometer SPECTROstarnano.....   | 108 |
| Figure 49 Chromatogram of the initial SELENOP purification method using fraction collection.....   | 114 |
| Figure 50 Online analysis of IMAC purification of SELENOP with initial gradient from 200-360min.....   | 114 |
| Figure 51 Comparative experiment of the effect of temperature in the binding of SELENOP with IMAC stationary phase (red curve 4°C, blue curve 20°C).....   | 115 |
| Figure 52 Chromatogram of IMAC purification (Phase IMAC Sepharose, Mobile phase (A :0.5M ammonium acetate, C: 0.5M ammonium acetate) Gradient described in red correspond to the percentage of C with UV 254nm.....  | 117 |
| Figure 53 Chromatogram of repurification of SELENOP (Phase Heparin, Mobile phase (D :0.1M ammonium acetate, E: 1.5M ammonium acetate) Gradient described in red correspond to the percentage of E with UV 254nm.....   | 118 |
| Figure 54 Effect of pH on the SELENOP retention by heparin (Blue curve pH 7, Red curve pH 5.8).....  | 120 |
| Figure 55 Chromatogram obtain using Superdex <sup>TM</sup> 75kDa PC3.2/300 GL with 0.1 M ammonium acetate pH 7 of SELENOP( blue) and Gpx( red) at respectively 77 ppb and 0.17 ppb of selenium. ....   | 124 |
| Figure 56 Chromatogram obtain using SEC Acquity UPLC BEH 125 Gold with 0.1 M ammonium acetate pH 7.....  | 125 |
| Figure 57 SDS-PAGE gel electrophoresis of two purification experiments using Blue Coomassie staining.....  | 125 |
| Figure 58 Peptide LPPAAUQISQQLIPTEASASUR with the site of post-translational modification. ....  | 126 |



|   |     |
|---|-----|
| Figure 59 A. LC-MS chromatogram of SELENOP digested with trypsin 1/50 with C18 column, B. XIC of SELENOP peptide, C. MS spectrum of peak at tR = 11.18 min, D. MS spectrum of peak at tR = 12.59 min, E. MS spectrum of peak at tR = 17.85 min, F. MS spectrum of peak at tR = 20.40 min, G. MS spectrum of peak at tR = 20.51 min..... | 127 |
| Figure 60 A. TIC, B. XIC, C. MS, D; peptide sequence and E. MS/MS spectrum of LPPAUQISQQLIPTEASASUR at m/z 1050.7748 (z=3).....   | 128 |
| Figure 61 A. LC-MS chromatogram of SELENOP digested with trypsin 1/50 with nano C18 column, B. XIC of SELENOP peptide, C. MS spectrum of peak at tR = 35.08 min (red), D. MS spectrum of peak at tR = 67.04 min (orange), E. MS spectrum of peak at tR = 76.73 min (green).....   | 129 |
| Figure 62 A. LC-MS chromatogram of $\alpha$ -2-macroglobulin digested with trypsin 1/50 with C18 column, B. XIC of $\alpha$ -2-macroglobulin peptide, C. MS spectrum of peak at tR = 20.84 min, D. MS spectrum of peak at tR = 22.98 min, E. MS spectrum of peak at tR = 23.63 min.....   | 131 |
| Figure 63 A. LC-MS chromatogram of $\alpha$ -2-macroglobulin digested with trypsin 1/50 with nanoC18 column, B. XIC of $\alpha$ -2-macroglobulin peptide, C. MS spectrum of peak at tR = 70.47 min, D. MS spectrum of peak at tR = 84.20 min, E. MS spectrum of peak at tR = 91.31 min .....  | 132 |
| Figure 64 Chromatogram of the SELENOP and auranofin co-elution after the injection of SELENOP on a column contaminated with traces of auranofin (green $^{197}\text{Au}$ , red $^{80}\text{Se}$ ).....  | 135 |
| Figure 65 Chromatogram of the interaction between SELENOP and auranofin after DTT and incubation during 1h at 37°C observed by SEC (red $^{80}\text{Se}$ , green $^{197}\text{Au}$ ).....   | 136 |
| Figure 66 Chromatogram of the interaction between SELENOP and cisplatin after DTT treatment and incubation during 1h at 37°C observed by SEC (red $^{80}\text{Se}$ , green $^{195}\text{Pt}$ ).....   | 136 |
| Figure 67 Theoretical isotopic profile of peptide containing S-Se moiety.....   | 138 |
| Figure 68 A. TIC, B. XIC, C. MS, D. peptide sequence and E. MS/MS spectrum of MWRSGLALALCLLPSGGTESQDQSSLCK at m/z 676.7367 (z=5).....   | 139 |
| Figure 69 A. TIC, B. XIC, C. MS, D. peptide sequence and E. MS/MS spectrum of LPPAAUQISQQLIPTEASASURUKNQAK at m/z 1368.8786 (z=3).....  | 141 |
| Figure 70 Theoretical isotopic profile of peptide containing S-Se-Pt moiety.....  | 143 |
| Figure 71 A. TIC, B. XIC, C. MS, D. peptide sequence and E. MS/MS spectrum of AYCEKCKGNCSTTLK at m/z 716.20437 (z=5) .....  | 144 |
| Figure 72 A. TIC, B. XIC, C. MS, D. peptide sequence and E. MS/MS spectrum of TUQCKENLPSLUSCQGLRAEENITESCQUR at m/z 948.68207 (z=5) .....   | 145 |
| Figure 73 Selenoprotein P peptide displaying a metallodrug (auranofin or cisplatin) adduct and the MS/MS fragmentation of the peptide used to determine the binding site.....   | 146 |
| Figure 74 LC-MS of unreacted AVP. (A) TIC, (B) MS spectrum of peak at tR= 3.73 min .....  | 148 |
| Figure 75 LC-MS of unreacted [Se-Se]-AVP. (A) TIC, (B) MS spectrum of peak at tR= 3.74 min .....  | 149 |
| Figure 76 MS isotopic pattern of the unreacted [Se-Se]-AVP for mono- (m/z =1180.3310) and di- (m/z=590.6702) charged ion.....   | 150 |
| Figure 77 LC-MS of reduced [Se-Se]-AVP. (A) TIC. (B) MS spectrum of peak at tR = 4.16 min. (C) MS spectrum of peak at tR = 4.20 min.....  | 151 |
| Figure 78 LC-MS of reduced [Se-Se]-AVP. (A) MS spectrum of peak at tR = 4.16 min. (B) MS spectrum of peak at tR = 4.20 min .....  | 152 |
| Figure 79 MS/MS of reduced [Se-Se]-AVP at m/z= 1085 (z=1). Principal fragments at HCD = 30. 153   |     |
| Figure 80 MS/MS of reduced [Se-Se]-AVP at m/z=1101.3960 (z=1). Principal fragments at HCD = 30 .....  | 154 |
| Figure 81 MS/MS of reduced [Se-Se]-AVP at m/z=1101.3960 (z=1). Principal fragments at HCD = 35 .....  | 155 |
| Figure 82 LC-MS of [Se-Se]-AVP incubated overnight at 70 °C. (A) TIC. (B) MS spectrum of peak at tR = 3.71 minutes. (C) MS spectrum of peak at tR = 4.02 minutes. (D) MS spectrum of peak at tR = 4.13 minutes.....   | 156 |

*Figure 83 LC-MS of reduced AVP incubated with AF overnight at 37 °C. (A) TIC. (B) MS spectrum of peak at  $t_R = 3.72$  minutes. (C) MS spectrum of peak at  $t_R = 3.97$  minutes. ....157*

*Figure 84 LC-MS of reduced AVP incubated with  $Et_3PAuCl$  overnight at 37 °C. (A) TIC. (B) MS spectrum of peak at  $t_R = 3.72$  minutes. (C) MS spectrum of peak at  $t_R = 3.97$  minutes. (D) MS spectrum of peak at  $t_R = 4.35$  minutes .....158*

*Figure 85 LC-MS of AVP incubated with  $Et_3PAuCl$  at 70 °C (a) and 37 °C (b). XIC of ions  $m/z$  1084.44 (AVP,  $t_R=3.70$ ) and 1367.49 (peptide- $AuPEt_3$ ,  $t_R=4.56$ ).....160*

*Figure 86 LC-MS of [Se-Se]-AVP incubated with  $Et_3PAuCl$  at 70 °C (a) and 37 °C (b). XIC of ions  $m/z$  1180.33 (unreacted peptide,  $t_R=3.70$ ) and 1415.44 (peptide- $AuPEt_3$ ,  $t_R=4.62$ ) .....161*

*Figure 87 MS/MS of AVP incubated with  $Et_3PAuI$  at  $m/z$  841.2799 ( $z=2$ ). Principal fragments at HCD = 20.....162*

*Figure 88 MS/MS of [Se-Se]-AVP incubated with  $Et_3PAuI$  at  $m/z$  865.2541 ( $z=2$ ). Principal fragments at HCD = 20 .....163*



## List of Tables

|  |     |
|--|-----|
| <i>Table 1 Chemical and physical properties of selenium.</i>   | 25  |
| <i>Table 2 Isotopic abundance of selenium.</i>   | 26  |
| <i>Table 3 Humans selenoproteins</i>   | 36  |
| <i>Table 4 Summary of studies on the interactions between full length thioredoxin reductase and (potential) gold-based metallodrugs.</i>   | 48  |
| <i>Table 5 Summary of studies on the interactions between thioredoxin reductase proxies and (potential) gold-based metallodrugs.</i>   | 50  |
| <i>Table 6 Advantages and limitation of the various mass analysers</i>   | 57  |
| <i>Table 7 Spectral interferences and detection limit of Se.</i>   | 58  |
| <i>Table 8 List of selenopeptides used for the SELENOP mass spectrometry identification on the basis of a partial sequence</i>   | 74  |
| <i>Table 9 Commercial reagent used.</i>  | 97  |
| <i>Table 10 : Chemicals used</i>   | 97  |
| <i>Table 11 : Chemicals used (following)</i>   | 99  |
| <i>Table 12 HPLC Column operating conditions</i>   | 102 |
| <i>Table 13 ICP-MS operating conditions</i>  | 103 |
| <i>Table 14 ESI-MS LUMOS operating parameters</i>  | 103 |
| <i>Table 15 ESI-MS Q Exactive operating parameters</i>   | 104 |
| <i>Table 16 Parameters used to increase the efficiency and recovery of IMAC chromatography</i>   | 119 |
| <i>Table 17 Ultracentrifugation filter use for cut-off procedure.</i>  | 121 |
| <i>Table 18 Column used to obtain an analytical peak of SELENOP</i>  | 123 |
| <i>Table 19 Observed MS products obtain by LC-ESI-MS analysis in positive mode of SELENOP</i>  | 130 |
| <i>Table 20 Observed MS products obtain by LC-ESI-MS analysis in positive mode of <math>\alpha</math>-2-macroglobulin</i>  | 130 |
| <i>Table 21 Protein content obtained using commercial kit DTCm Protein assay kit (* concentration of selenium was calculated considering that MW of SELENOP = 43174 and that SELENOP is containing 10 SeCys)</i>                 | 133 |
| <i>Table 22 Selenium content obtained using ICP-MS and by following <math>^{76}\text{Se}</math>, <math>^{77}\text{Se}</math>, <math>^{78}\text{Se}</math>, <math>^{80}\text{Se}</math>, <math>^{82}\text{Se}</math> isotope</i>  | 133 |
| <i>Table 23 Selenium recovery obtained using ICP-MS and by following <math>^{76}\text{Se}</math>, <math>^{77}\text{Se}</math>, <math>^{78}\text{Se}</math>, <math>^{80}\text{Se}</math>, <math>^{82}\text{Se}</math> isotope</i> | 134 |
| <i>Table 24 Observed MS of SELENOP peptides interacting with gold (Red data are not supported by MS/MS characterisation)</i>   | 137 |

---

*Table 25 Observed MS peptide obtain by LC-ESI-MS analysis in positive mode (Red data are data without correct MS/MS validation) .....140*

*Table 26 Observed MS peptide obtain by LC-ESI-MS analysis in positive mode .....142*



## *Scientific production*

### Articles :

#### Main subject:

- Lamarche, J.; Ronga, L.; Szpunar, J.; Lobinski, R. Characterization and Quantification of selenoprotein P: Challenges to Mass Spectrometry. *Int. J. Mol. Sci.* **2021**, *22*, 6283. DOI: 10.3390/ijms22126283 (Status: Accepted) (*Annexe 20*)
- Lamarche, J. ; Alcoceba Álvarez, E. ; Cordeau, E. ; Enjalbal, C. ; Massai, L. ; Messori, L. ; Lobinski, R. ; Ronga, L. Comparative reactivity of medicinal gold(I) compounds with the cyclic peptide vasopressin and its diselenide analogue. *Dalton Trans.* **2021** DOI:10.1039/D1DT03470G (Status: Accepted)
- Probing of selenols (-SeH) as metal-binding targets for trace metals by atomic and mass spectrometry, Review manuscript in preparation

#### Additional topics:

- Azzaz, J. ; Rieu, A. ; Aires, V. ; Delmas, D. ; Chluba, J. ; Winckler, P. ; Marie-Agnès Bringer, M.A. ; Lamarche, J. ; Vervandier-Fasseur, D. ; Dalle, F. ; Lapaquette, P. ; Guzzo, J. Resveratrol-Induced Xenophagy Promotes Intracellular Bacteria Clearance in Intestinal Epithelial Cells and Macrophages, *Front. Immunol.*, **2019**, *9*, 3149. DOI: 10.3389/fimmu.2018.03149 (Status: Accepted)
- Duskova, K.; Lamarche, J.; Amor, S.; Caron, C.; Queyriaux, N.; Gaschard, M.; Penouilh M.J.; de Robillard, G.; Delmas, D.; Devillers, C.H.; Granzhan, A.; Teulade-Fichou, M.P.; Chavarot-Kerlidou, M.; Therrien, B.; Britton, S.; Monchaud D.; Identification of Three-Way DNA Junction Ligands through Screening of Chemical Libraries and Validation by Complementary in Vitro Assays, *J Med Chem*, **2019**, *62* (9), 4456-4466 DOI: 10.1021/acs.jmedchem.8b01978 (Accepted)
- Guillon, J.; Denevault-Sabourin, C.; Chevret, E.; Brachet-Botineau, M.; Milano, V.; Guédin-Beaurepaire, A.; Moreau, S.; Ronga, L.; Savrimoutou, S., Rubio, S.; Ferrer, J.; Lamarche, J.; Mergny, J.; Viaud-Massuard, M.; Ranz, M.; Largy, E.; Gabelica, V.; Rosu, F.; Gouilleux, F.; Desplat, V. Design, synthesis, and antiproliferative effect of 2,9-bis[4-(pyridinylalkylaminomethyl)phenyl]-1,10-phenanthroline derivatives on human leukemic cells by targeting G-quadruplex, *Arch. Pharm.* **2021**, *354*, e2000450 DOI: 10.1002/ardp.202000450 (Status: Accepted)

#### Conference poster:

- Ouerdane L.; Lamarche J.; Ronga L.; Bierla K.; Szpunar J.; Lobinski R. An integrated LC-ICP-MS and LC-ESI-MS approach for the characterization of purified selenoprotein P, **2019**, European Winter Conference on Plasma Spectrometry, Pau, France (*Annex 21*)
- Lamarche J.; Ouerdane L.; Ronga L.; Bierla K.; Szpunar J.; Lobinski R. Characterization of human serum selenoprotein P by mass spectrometry, **2019**, Metallomics, Warsaw, Poland (*Annex 22*)



*ANNEX*

## *List of Annexes*

|  |     |
|--|-----|
| Annex 1 Figures and tables.....  | 203 |
| Annex 2 Article Characterization and quantification of selenoprotein P: challenges to mass spectrometry<br>.....             | 229 |
| Annex 3 Poster: An integrated LC-ICP-MS and LC-ESI-MS approach for the characterization of<br>purified selenoprotein P ..... | 255 |
| Annex 4 Poster Characterization of human serum selenoprotein P by mass spectrometry .....                                    | 259 |

*Annex 1 Figures and tables*





## *List figures of Annex 1*

|   |     |
|---|-----|
| Annex 1 Figure 1 XIC and MS Spectrum of CINQLLC.....  | 207 |
| Annex 1 Figure 2 XIC and MS Spectrum of PYVEEAIKIAYCEKK.....  | 208 |
| Annex 1 Figure 3 XIC and MS Spectrum of NQLLCKLPTDSELAPR.....   | 209 |
| Annex 1 Figure 4 XIC and MS Spectrum of MWRSGLLALALCLLPSGGT.....  | 210 |
| Annex 1 Figure 5 XIC and MS Spectrum of TTLKDEDFCK.....   | 211 |
| Annex 1 Figure 6 XIC and MS Spectrum of TTLKDEDFCKR.....  | 212 |
| Annex 1 Figure 7 XIC and MS Spectrum of PMLNSNGSVTVVALLQASUYLCILQASK.....   | 213 |
| Annex 1 Figure 8 XIC and MS Spectrum of LQASUYLCILQASKLEDLRVK.....  | 214 |
| Annex 1 Figure 9 XIC and MS Spectrum of TGSAITUQCKENLPSLCSUQGLRA.....   | 215 |
| Annex 1 Figure 10 LC-MS of reduced AVP. (A) TIC. (B) MS spectrum of peak at $t_R = 3.67$ minutes.<br>.....  | 219 |
| Annex 1 Figure 11 LC-MS of AVP incubated with $Et_3PAuCl$ overnight at $70\text{ }^\circ C$ . (A) TIC. (B) MS<br>spectrum of peak at $t_R = 3.7$ minutes. (C) MS spectrum of peak at $t_R = 4.56$ minutes. (D) MS spectrum<br>of peak at $t_R = 5.56$ minutes. The dark part corresponds to the elution of $Et_3PAuCl$ .....                | 220 |
| Annex 1 Figure 12 LC-MS of AVP incubated with $Et_3PAuBr$ overnight at $70\text{ }^\circ C$ . (A) TIC. (B) MS<br>spectrum of peak at $t_R = 3.69$ minutes. (C) MS spectrum of peak at $t_R = 4.55$ minutes. (D) MS spectrum<br>of peak at $t_R = 5.53$ minutes. The dark part corresponds to the elution of $Et_3PAuBr$ . .....             | 221 |
| Annex 1 Figure 13 LC-MS of AVP incubated with $Et_3PAuI$ overnight at $70\text{ }^\circ C$ . (A) TIC. (B) MS<br>spectrum of peak at $t_R = 3.69$ minutes. (C) MS spectrum of peak at $t_R = 3.96$ minutes. (D) MS spectrum<br>of peak at $t_R = 4.56$ minutes. The dark part corresponds to the elution of $Et_3PAuI$ . .....               | 222 |
| Annex 1 Figure 14 LC-MS of AVP incubated with $[Au(PEt_3)_2]Cl$ overnight at $70\text{ }^\circ C$ . (A) TIC. (B) MS<br>spectrum of peak at $t_R = 3.96$ minutes. (C) MS spectrum of peak at $t_R = 4.47$ minutes. (D) MS spectrum<br>of peak at $t_R = 4.60$ minutes. The dark part corresponds to the elution of $[Au(PEt_3)_2]Cl$ . ..... | 223 |
| Annex 1 Figure 15 LC-MS of [Se-Se]-AVP incubated with $Et_3PAuCl$ overnight at $70\text{ }^\circ C$ . (A) TIC. (B)<br>MS spectrum of peak at $t_R = 4.62$ minutes. (C) MS spectrum of peak at $t_R = 5.55$ minutes. The dark<br>part corresponds to the elution of $Et_3PAuCl$ . .....  | 224 |
| Annex 1 Figure 16 LC-MS of [Se-Se]-AVP incubated with $Et_3PAuBr$ overnight at $70\text{ }^\circ C$ . (A) TIC. (B)<br>MS spectrum of peak at $t_R = 4.62$ minutes. (C) MS spectrum of peak at $t_R = 5.54$ minutes. The dark<br>part corresponds to the elution of $Et_3PAuBr$ .....  | 225 |
| Annex 1 Figure 17 LC-MS of [Se-Se]-AVP incubated with $Et_3PAuI$ overnight at $70\text{ }^\circ C$ . (A) TIC. (B)<br>MS spectrum of peak at $t_R = 4.62$ minutes. (C) MS spectrum of peak at $t_R = 5.54$ minutes. The dark part<br>corresponds to the elution of $Et_3PAuI$ . .....  | 226 |
| Annex 1 Figure 18 LC-MS of [Se-Se]-AVP incubated with $[Au(PEt_3)_2]Cl$ overnight at $70\text{ }^\circ C$ . (A) TIC.<br>(B) MS spectrum of peak at $t_R = 4.58$ minutes. (C) MS spectrum of peak at $t_R = 5.52$ minutes. The dark<br>part corresponds to the elution of $[Au(PEt_3)_2]Cl$ .....  | 227 |

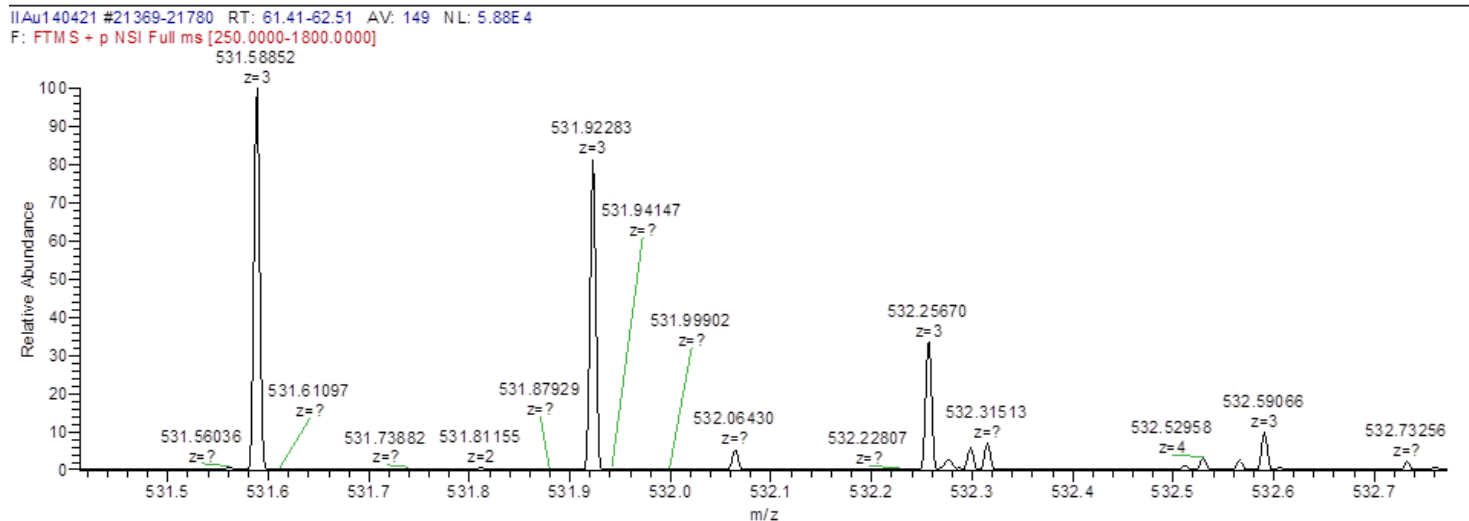
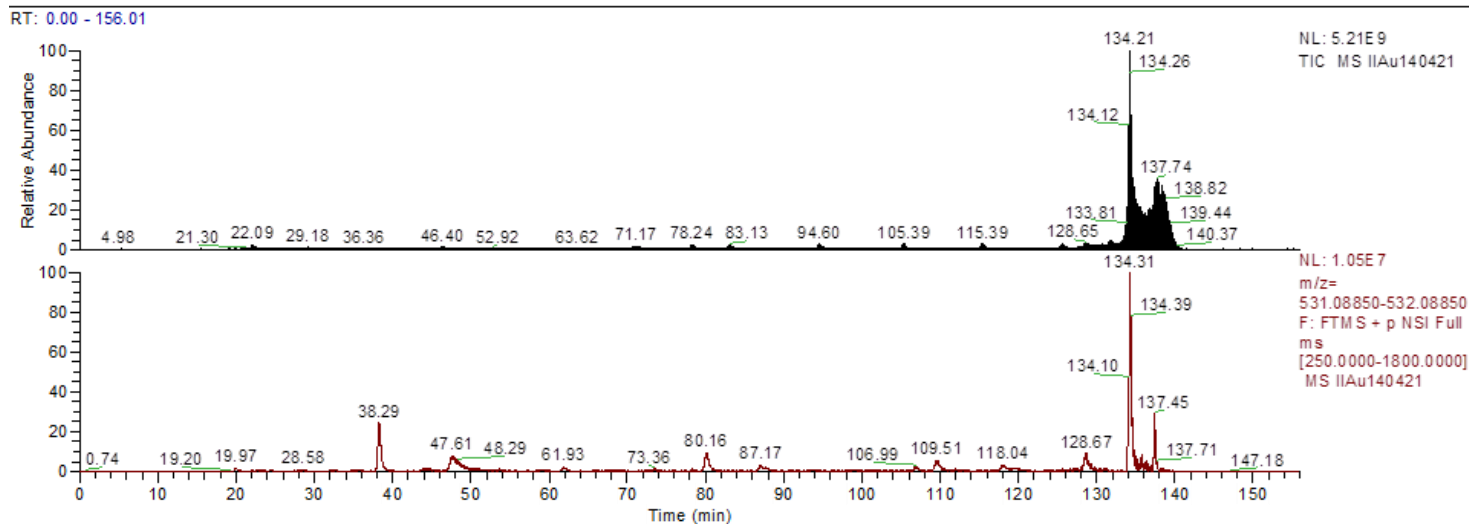
---

*List of tables of Annex 1*

Annex 1 Table 1 Observed MS products ..... 216

D:\Jeremy\...spectre okIIAu140421

06/19/21 14:38:44

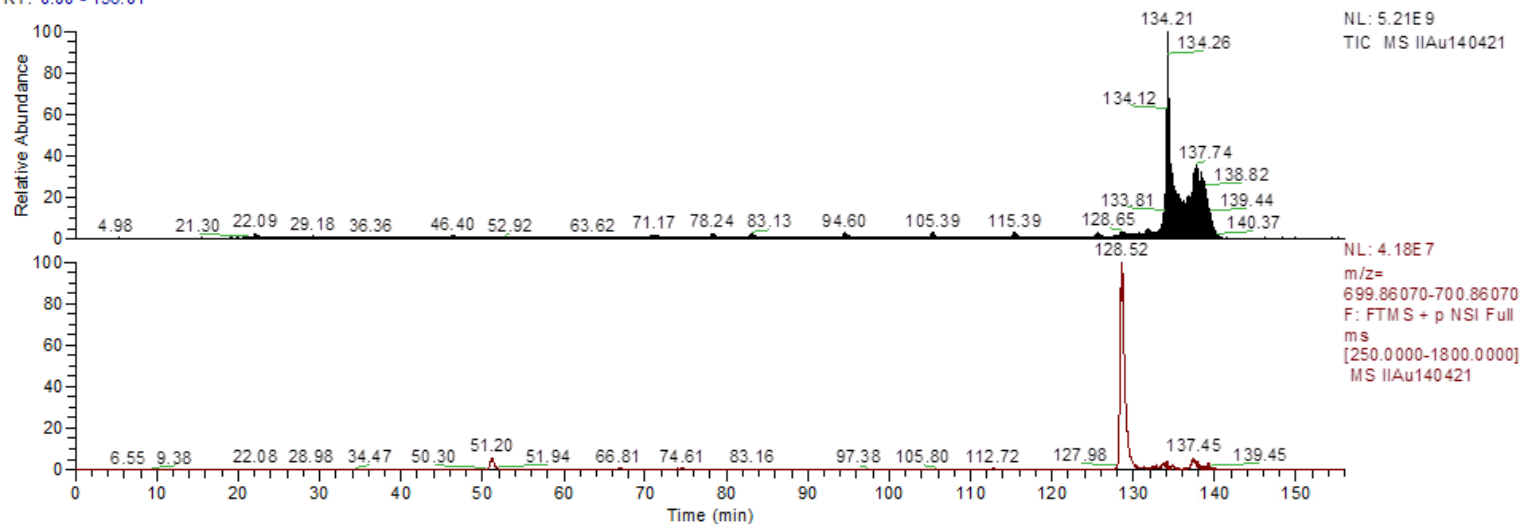


Annex 1 Figure 1 XIC and MS Spectrum of CINQLLC

D:\Jeremy\...spectre okIIAu140421

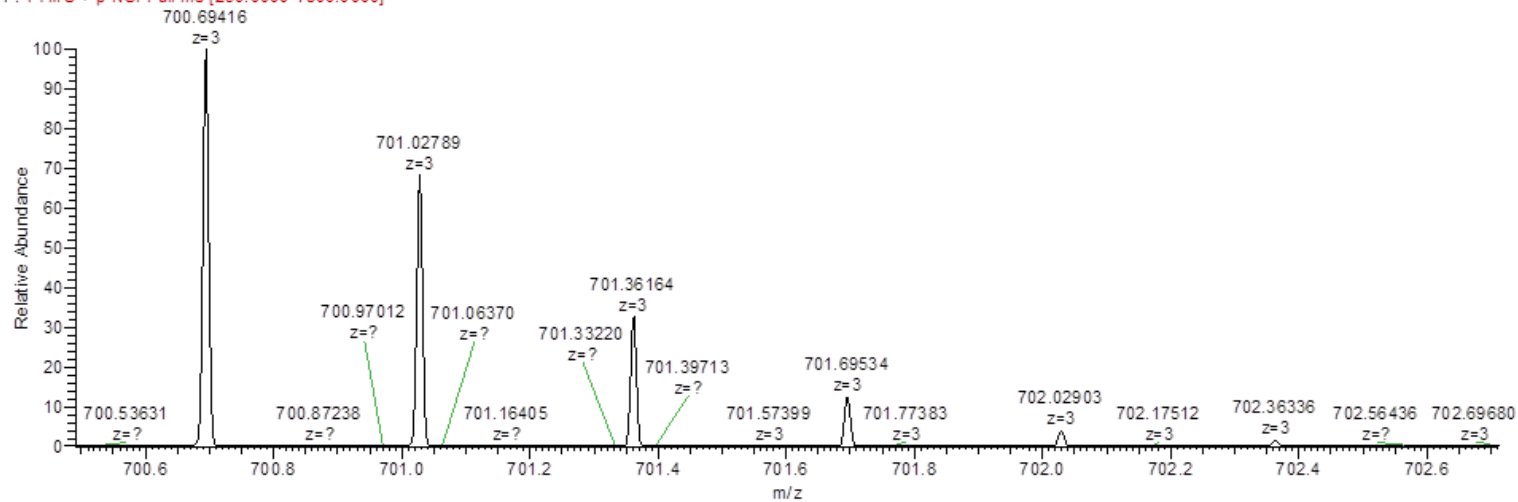
06/19/21 14:38:44

RT: 0.00 - 156.01



IIAu140421 #47815-48472 RT: 128.25-129.36 AV: 101 NL: 1.10E7

F: FTMS + p NSI Full ms [250.0000-1800.0000]

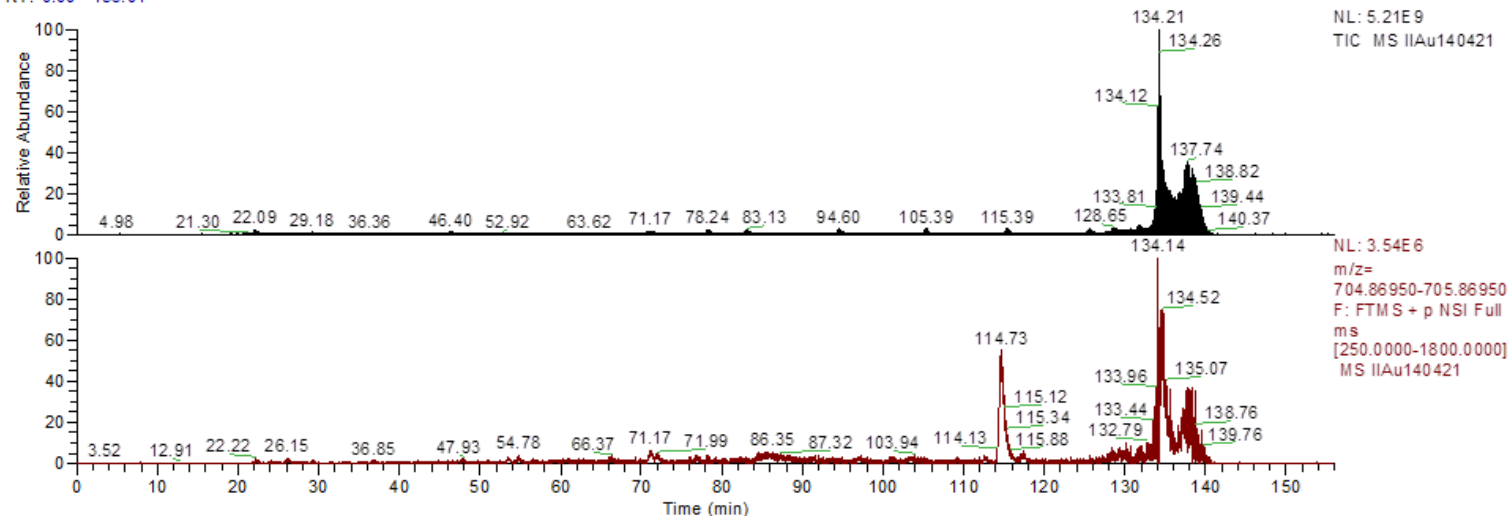


Annex 1 Figure 2 XIC and MS Spectrum of PYVEEAIKIAYCEKK

D:\Jeremy\...spectre okIIAu140421

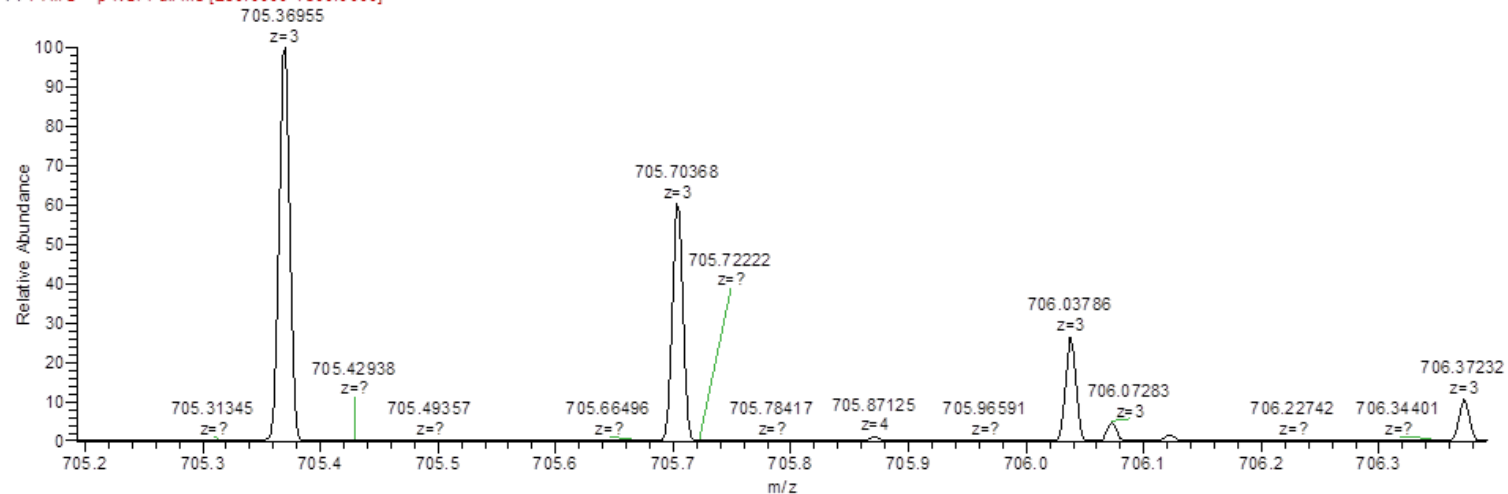
06/19/21 14:38:44

RT: 0.00 - 156.01



IIAu140421 #41981-42609 RT: 114.15-115.59 AV: 182 NL: 3.44E5

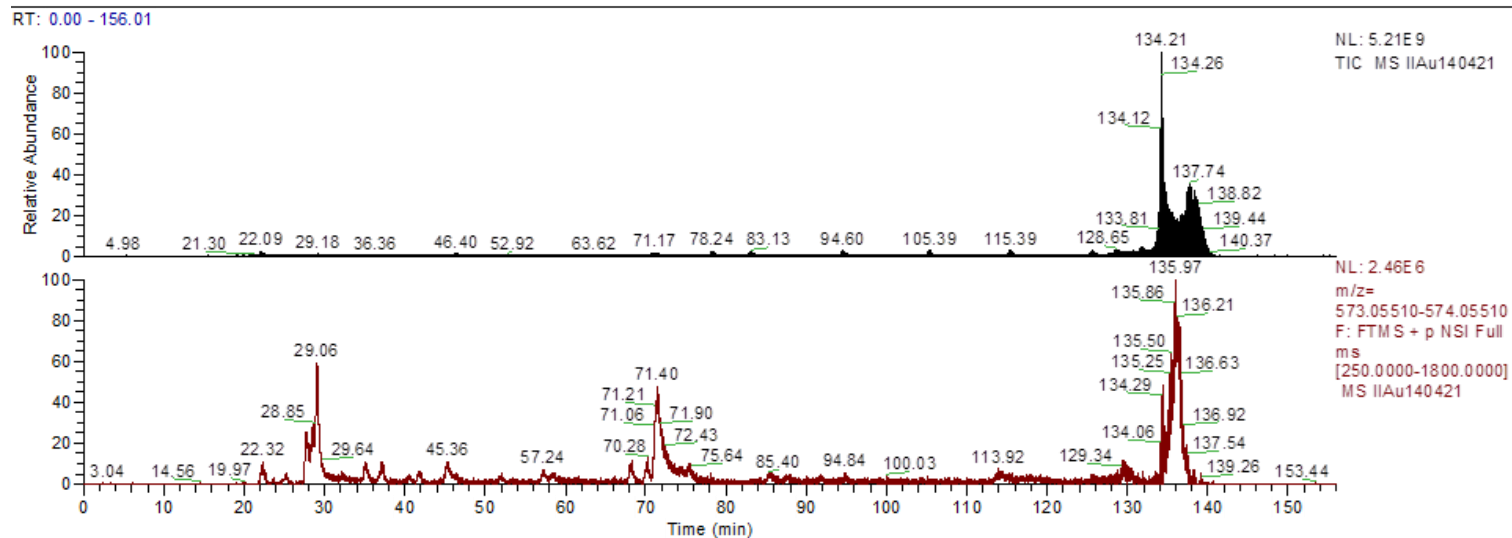
F: FTMS + p NSI Full ms [250.0000-1800.0000]



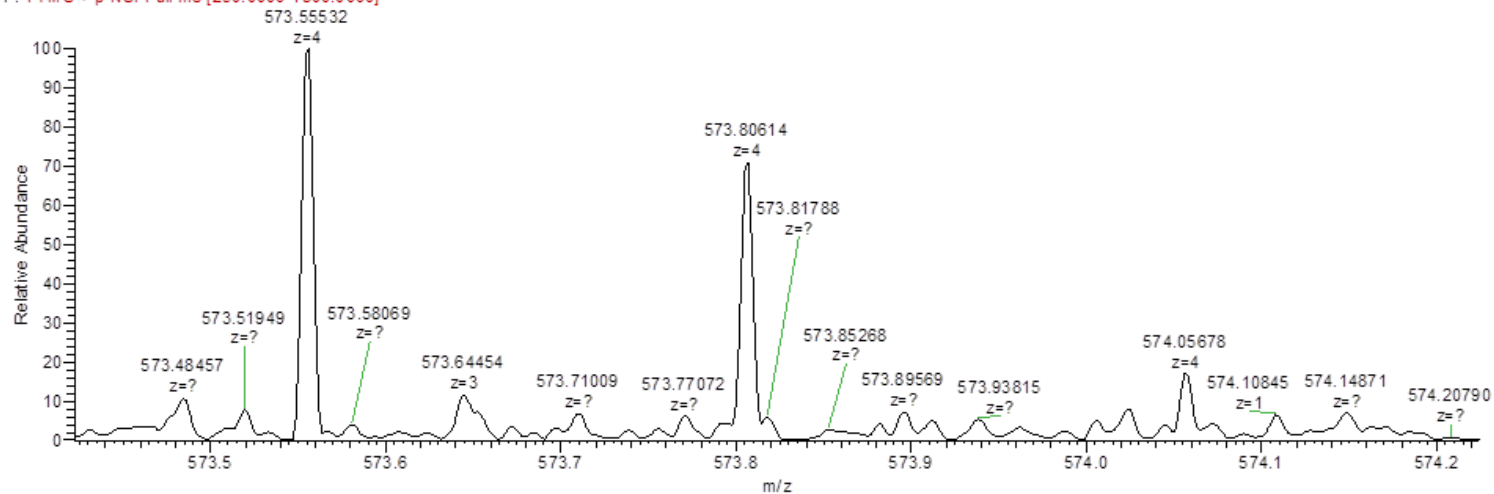
Annex 1 Figure 3 XIC and MS Spectrum of NQLLCKLPTDSELAPR

D:\Jeremy\...spectre okIIAu140421

06/19/21 14:38:44



II Au140421 #48071-49541 RT: 128.70-131.13 AV: 213 NL: 1.55E4  
F: FTMS + p NSI Full ms [250.0000-1800.0000]

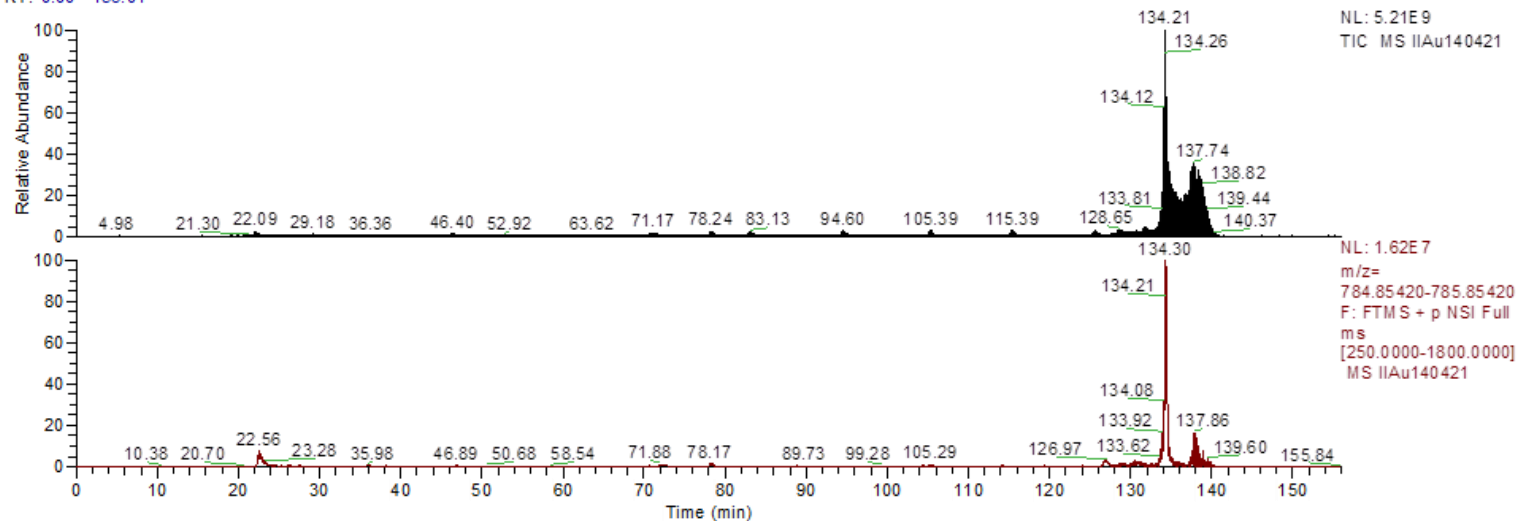


Annex 1 Figure 4 XIC and MS Spectrum of MWRSGLALALCLLPSSGGT

D:\Jeremy\...spectre okIIAu140421

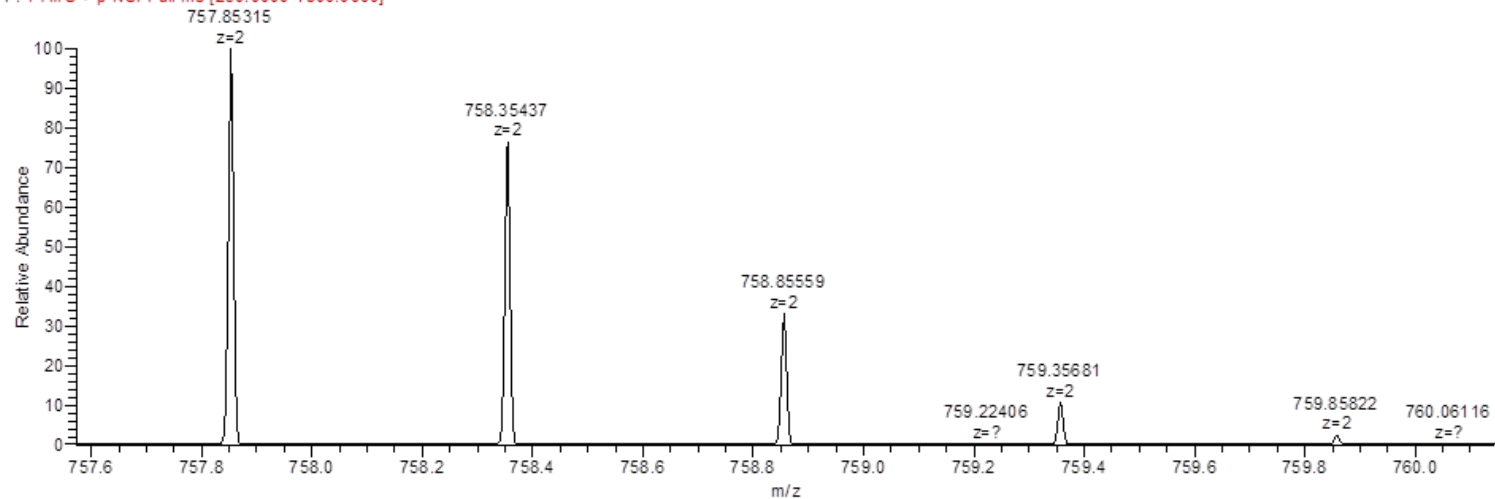
06/19/21 14:38:44

RT: 0.00 - 156.01



IIAu140421 #28102 RT: 78.51 AV: 1 NL: 1.93E7

F: FTMS + p NSI Full ms [250.0000-1800.0000]



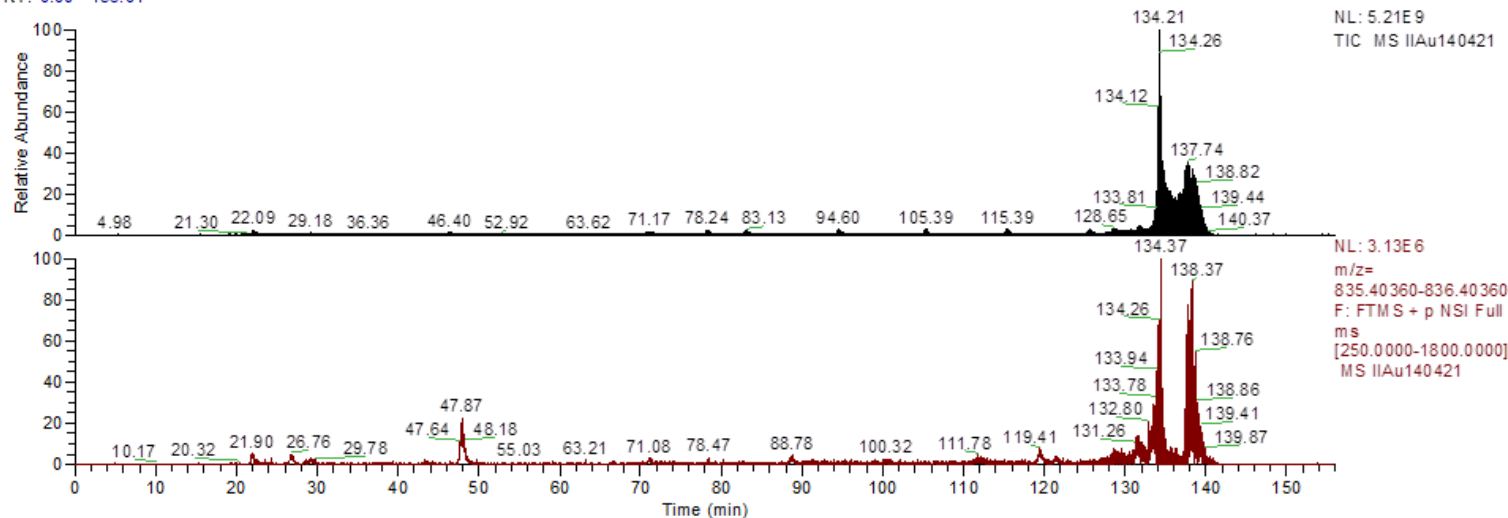
Annex 1 Figure 5 XIC and MS Spectrum of TTLKDEDFCK



D:\Jeremy\...spectre okIIAu140421

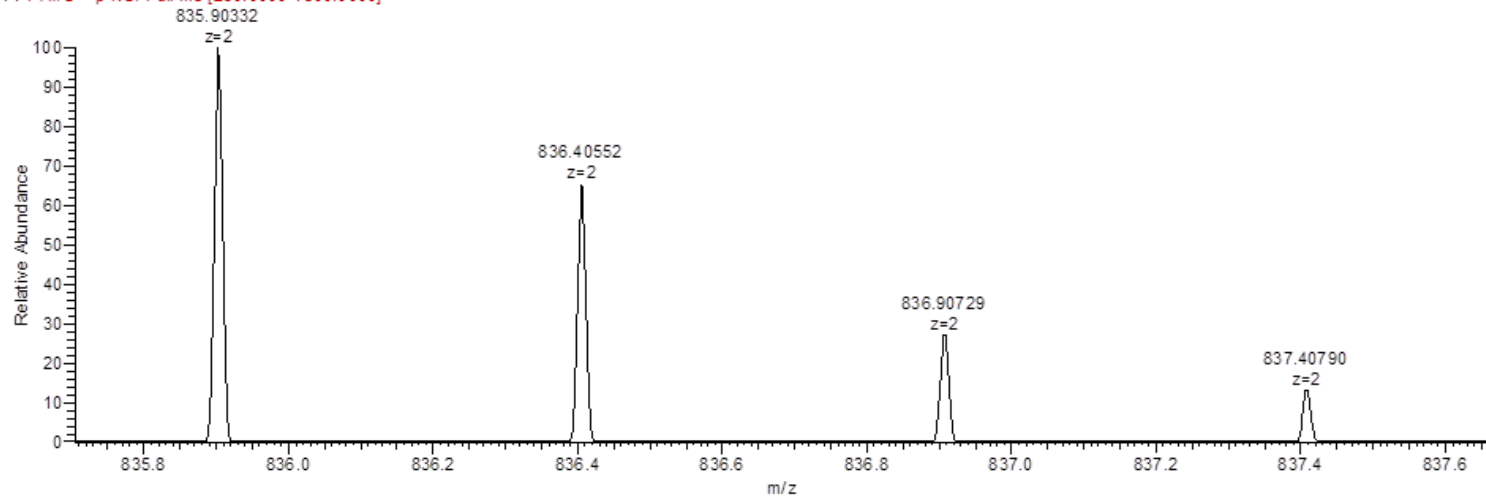
06/19/21 14:38:44

RT: 0.00 - 156.01



IIAu140421 #16117 RT: 47.53 AV: 1 NL: 1.38E5

F: FTMS + p NSI Full ms [250.0000-1800.0000]

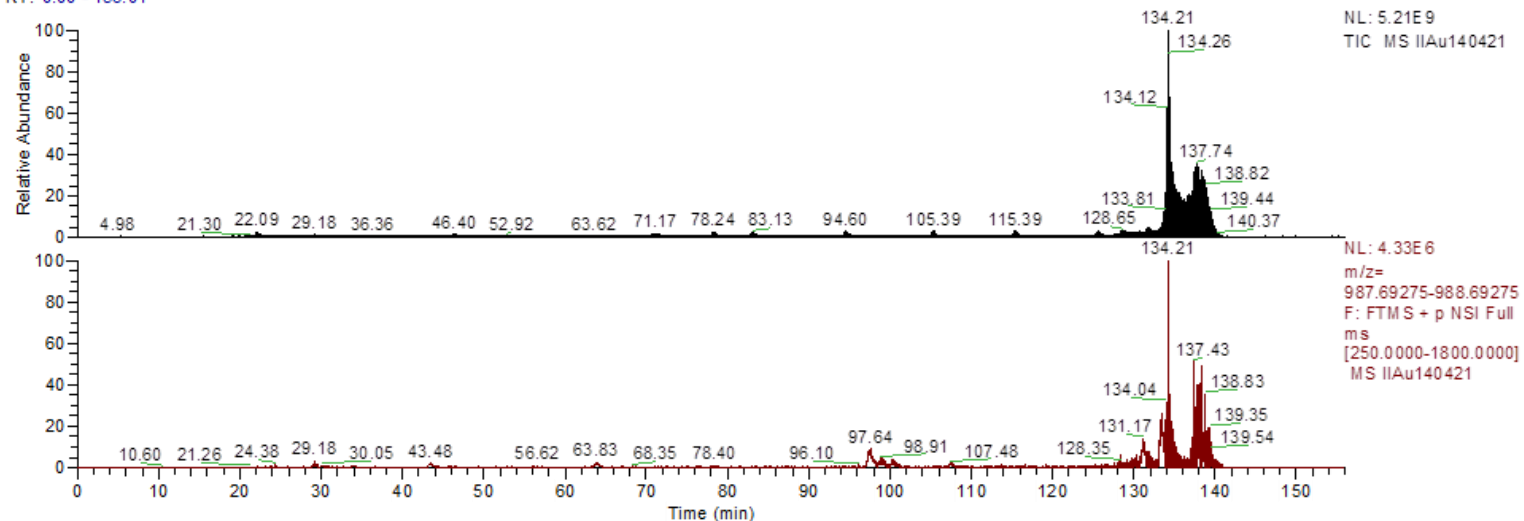


Annex 1 Figure 6 XIC and MS Spectrum of TTLKDEDFCKR

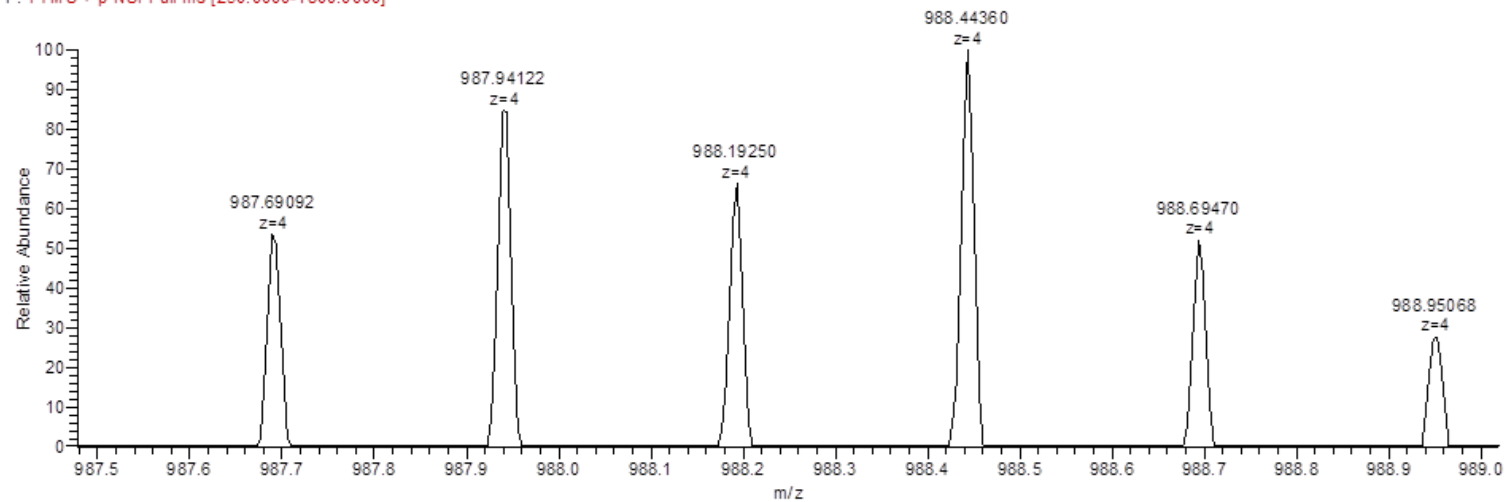
D:\Jeremy\...spectre okIIAu140421

06/19/21 14:38:44

RT: 0.00 - 156.01



IIAu140421 #36117 RT: 98.78 AV: 1 NL: 5.15E4  
F: FTMS + p NSI Full ms [250.0000-1800.0000]

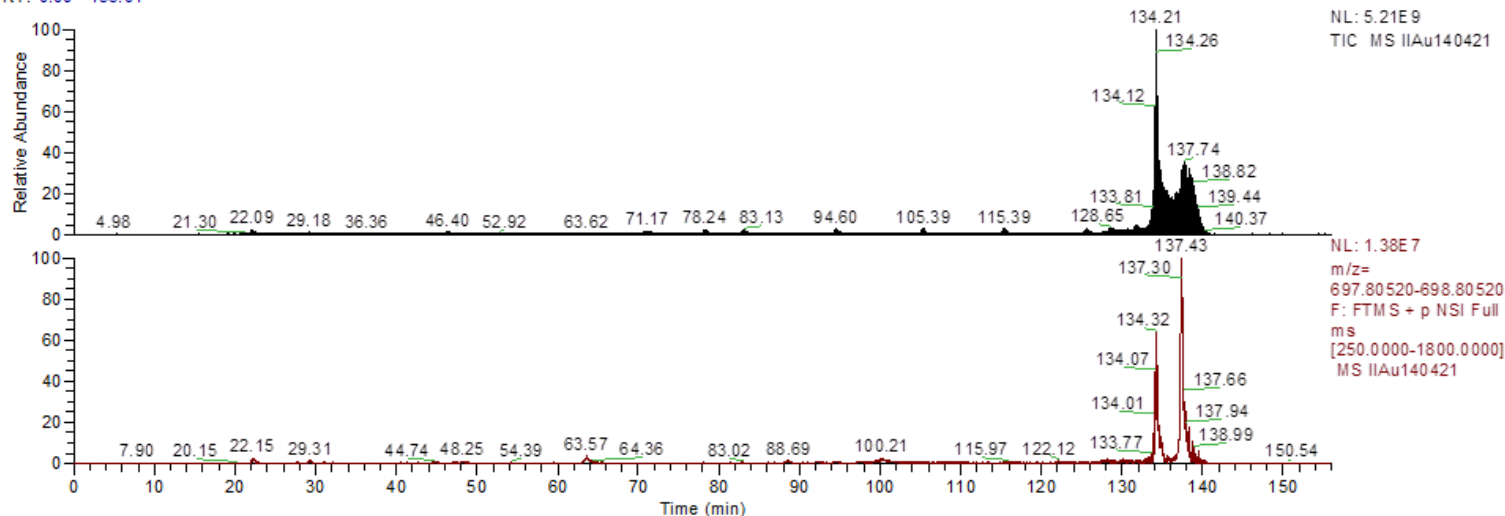


Annex 1 Figure 7 XIC and MS Spectrum of PMLNSNGSVTVVALLQASUYLCILQASK

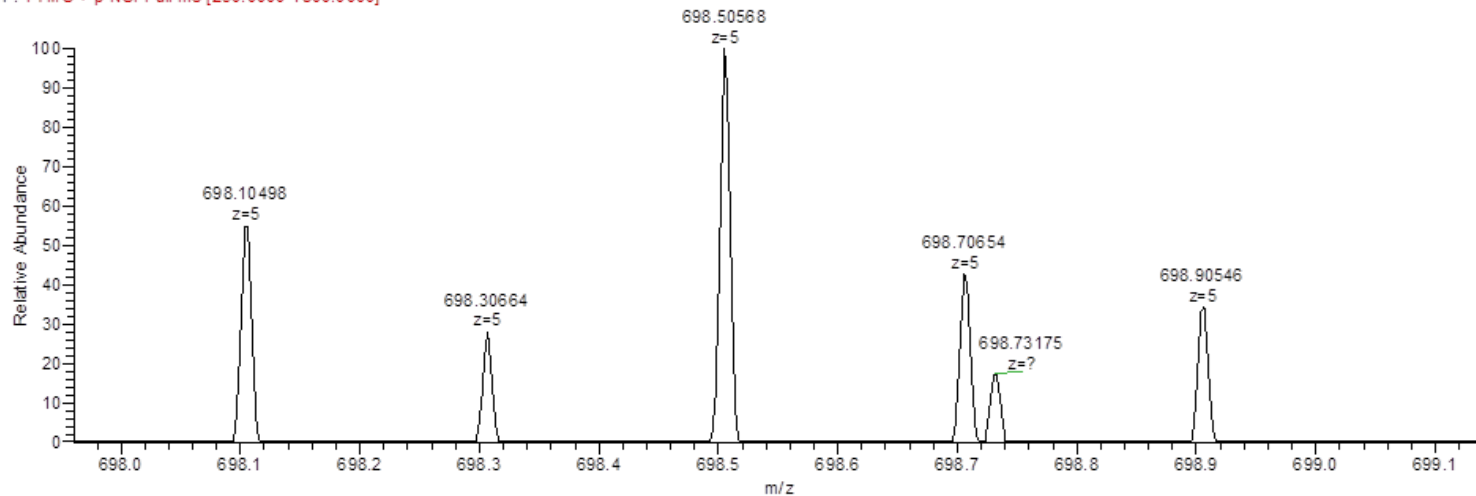
D:\Jeremy\...spectre okIIAu140421

06/19/21 14:38:44

RT: 0.00 - 156.01



IIAu140421 #16352 RT: 48.08 AV: 1 NL: 5.47E4  
 F: FTM S + p NSI Full ms [250.0000-1800.0000]

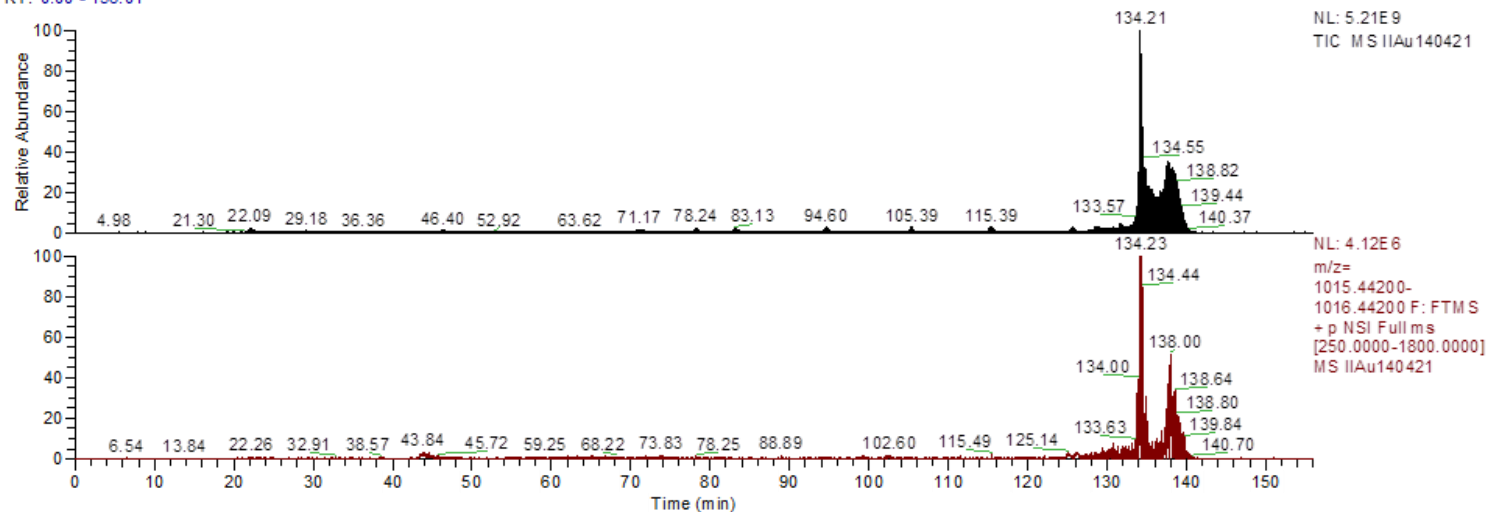


Annex 1 Figure 8 XIC and MS Spectrum of LQASUYLCILQASKLEDLRVK

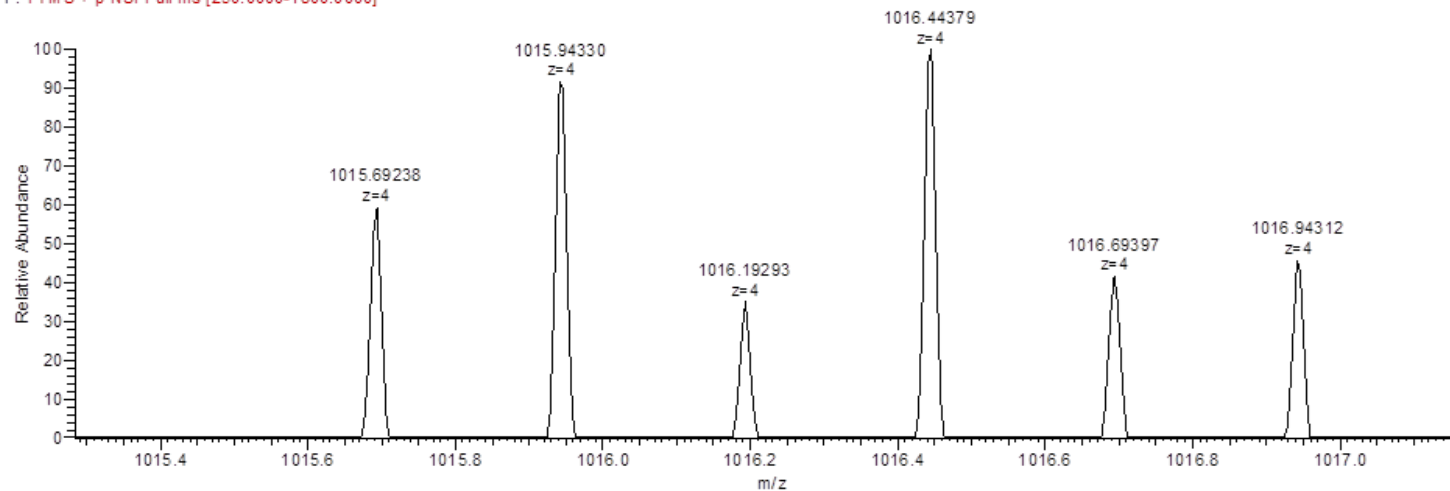
D:\Jeremy\...spectre oKIIAu140421

06/19/21 14:38:44

RT: 0.00 - 156.01

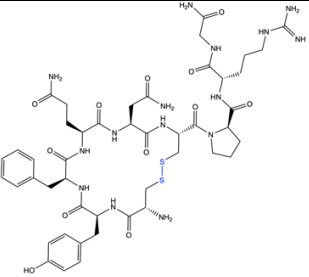
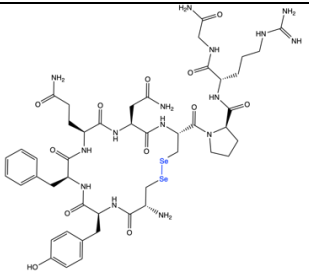
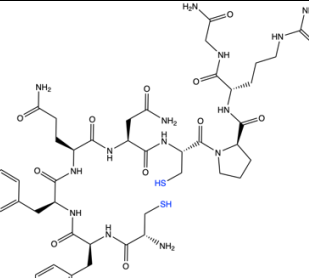


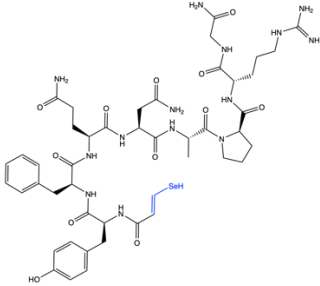
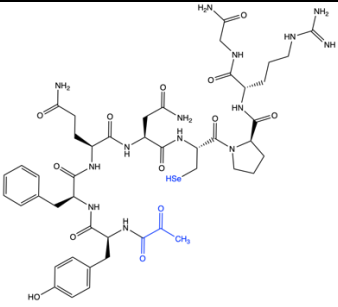
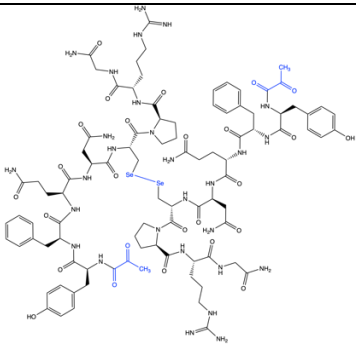
IIAu140421 #14572 RT: 43.79 AV: 1 NL: 4.32E4  
F: FTM S + p NSI Full ms [250.0000-1800.0000]

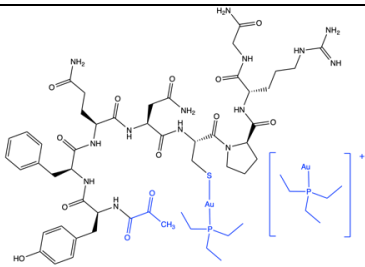
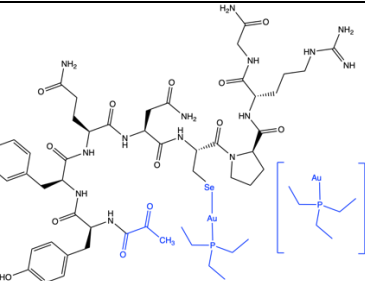


Annex 1 Figure 9 XIC and MS Spectrum of TGSAITUQCKENLPSLCSUQGLRA

Annex 1 Table 1 Observed MS products

| Entry, n° | Peptide code | Chemical structure   | Formula                        | Theoretical mass | Experimental mass | Observed ions, m/z              |
|-----------|--------------|--|--------------------------------|------------------|-------------------|---------------------------------|
| 1         | AVP          |    | $C_{46}H_{65}N_{15}O_{12}S_2$  | 1083.438         | 1083.440          | 1084.440 (z=1)<br>542.724 (z=2) |
| 2         | [Se-Se]-AVP  |   | $C_{46}H_{65}N_{15}O_{12}Se_2$ | 1179.326         | 1179.330          | 1180.330 (z=1)<br>590.670 (z=2) |
| 3         | Reduced AVP  |  | $C_{46}H_{67}N_{15}O_{12}S_2$  | 1085.454         | 1085.457          | 1086.457 (z=1)<br>543.733 (z=2) |

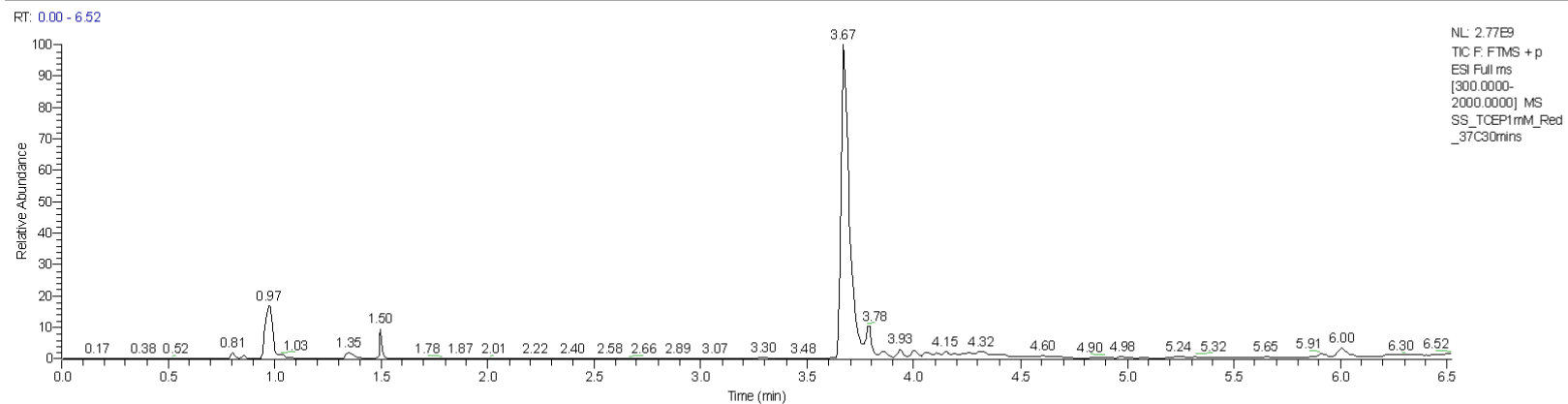
|   |                       |   |                                 |          |          |                                 |
|---|-----------------------|---|---------------------------------|----------|----------|---------------------------------|
| 4 | Reduced [Se-Se]-AVP 1 |  <p>The structure shows a single AVP molecule with a selenocysteine residue (SeH) highlighted in blue. The molecule consists of a cyclic peptide backbone with various side chains, including a phenyl group, a piperidine ring, and a hydroxyphenyl group.</p> | $C_{46}H_{64}N_{14}O_{12}Se$    | 1084.399 | 1084.406 | 1085.406 (z=1)<br>543.206 (z=2) |
| 5 | Reduced [Se-Se]-AVP 2 |  <p>The structure is similar to AVP 1 but features an acetyl group (CH<sub>3</sub>) on the selenocysteine residue, highlighted in blue.</p>   | $C_{46}H_{64}N_{14}O_{13}Se$    | 1100.394 | 1100.400 | 1101.400 (z=1)                  |
| 6 | [Se-Se]-AVP dimer     |  <p>The structure shows two AVP molecules linked together by a diselenide bridge (Se-Se) between their respective selenocysteine residues, which are highlighted in blue.</p>  | $C_{92}H_{126}N_{28}O_{26}Se_2$ | 2198.77  | 2198.78  | 1100.389 (z=2)<br>733.927 (z=3) |

|   |                                   |  |   |          |          |               |
|---|-----------------------------------|--|---|----------|----------|---------------|
| 7 | AVP-Au(PEt <sub>3</sub> )         |  | C <sub>58</sub> H <sub>93</sub> Au <sub>2</sub> N <sub>14</sub> O <sub>13</sub> P <sub>2</sub> S  | 1681.557 | 1681.558 | 841.279 (z=2) |
| 8 | [Se-Se]-AVP-Au(PEt <sub>3</sub> ) |  | C <sub>58</sub> H <sub>93</sub> Au <sub>2</sub> N <sub>14</sub> O <sub>13</sub> P <sub>2</sub> Se | 1729.501 | 1729.502 | 865.251 (z=2) |

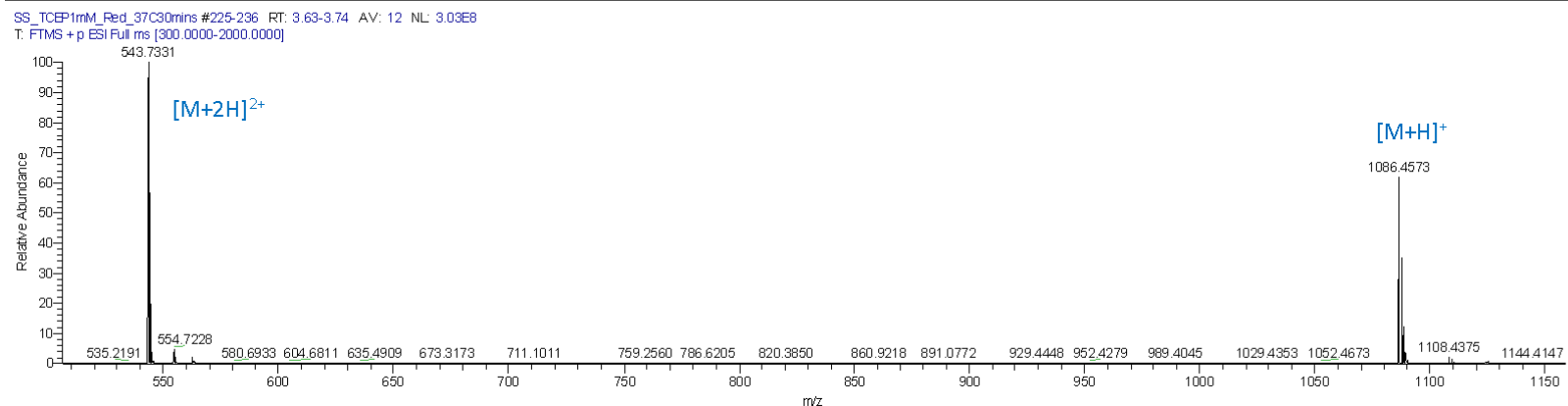
### Reduced AVP

D:\Master\...SS\_TCEP1mM\_Red\_37C30mins

05/05/21 12:07:12



**A**



**B**

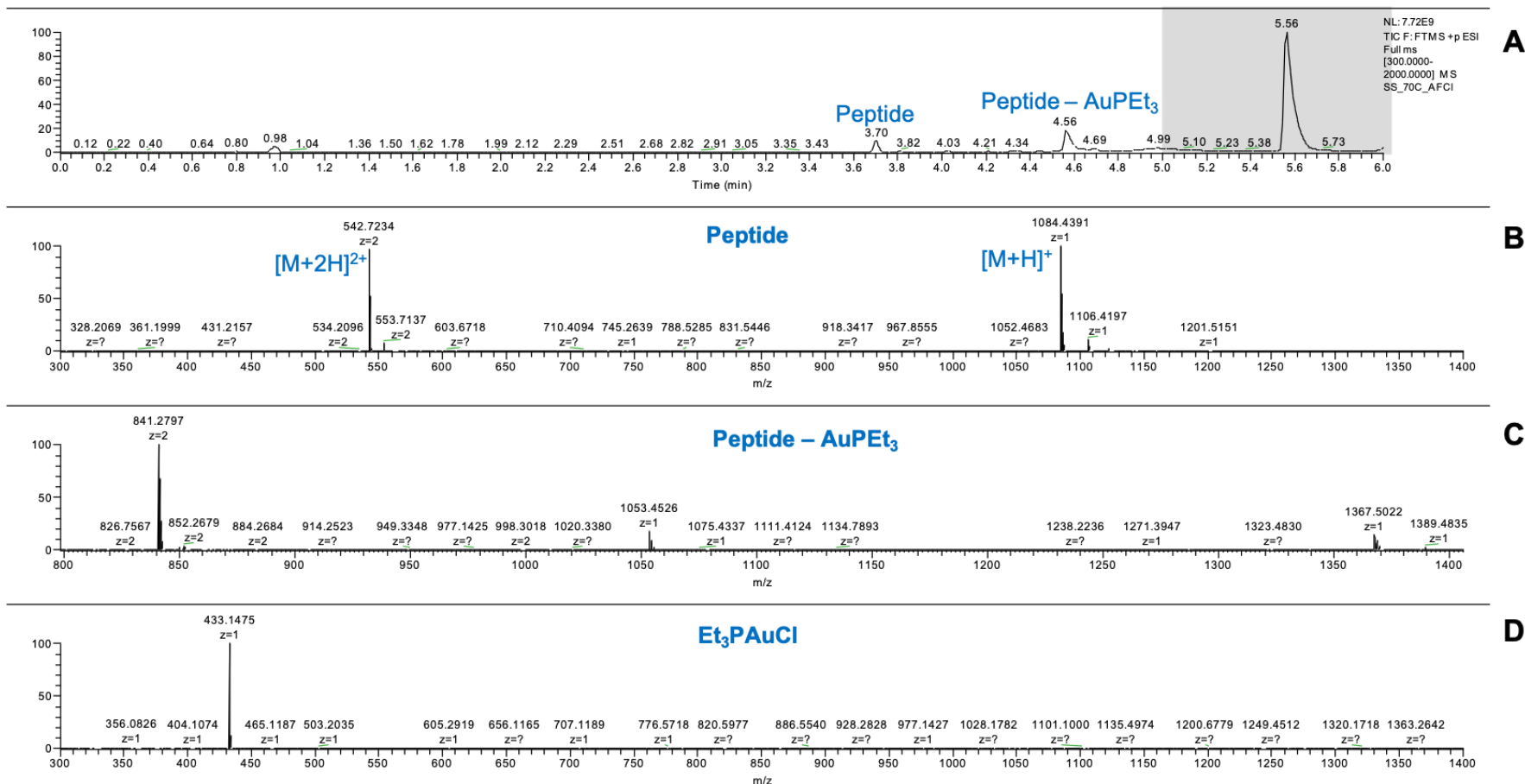
Annex 1 Figure 10 LC-MS of reduced AVP. (A) TIC. (B) MS spectrum of peak at  $t_R = 3.67$  minutes.



### AVP after incubation with Et<sub>3</sub>PAuCl at 70°C

D:\Master\...May\07052021\SS\_70C\_AFCI

05/07/21 10:33:40

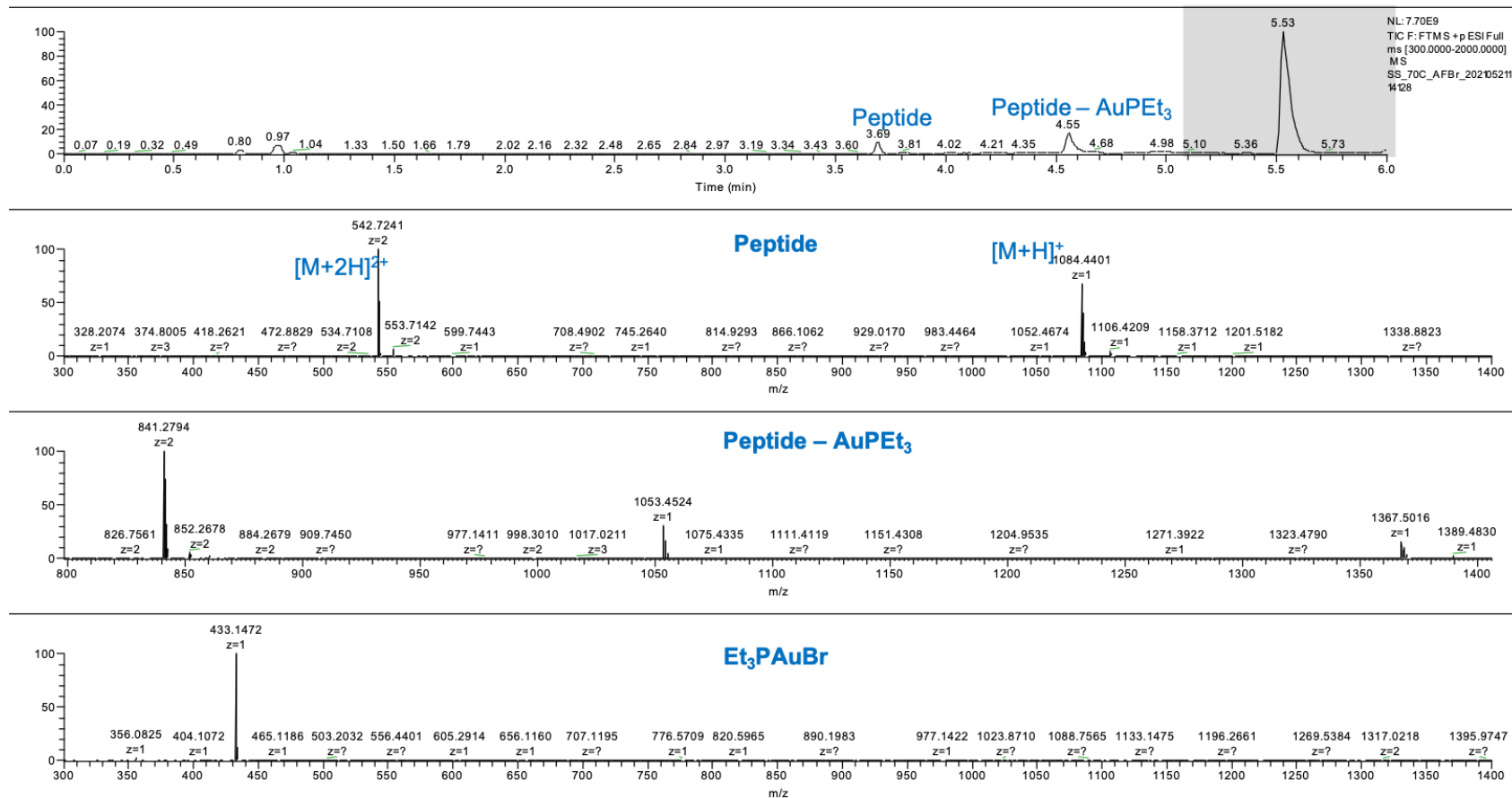


Annex 1 Figure 11 LC-MS of AVP incubated with Et<sub>3</sub>PAuCl overnight at 70 °C. (A) TIC. (B) MS spectrum of peak at t<sub>R</sub> = 3.7 minutes. (C) MS spectrum of peak at t<sub>R</sub> = 4.56 minutes. (D) MS spectrum of peak at t<sub>R</sub> = 5.56 minutes. The dark part corresponds to the elution of Et<sub>3</sub>PAuCl.

### AVP after incubation with Et<sub>3</sub>PAuBr at 70°C

D:\Master\...ISS\_70C\_AFBr\_20210521114128

05/21/21 11:42:39

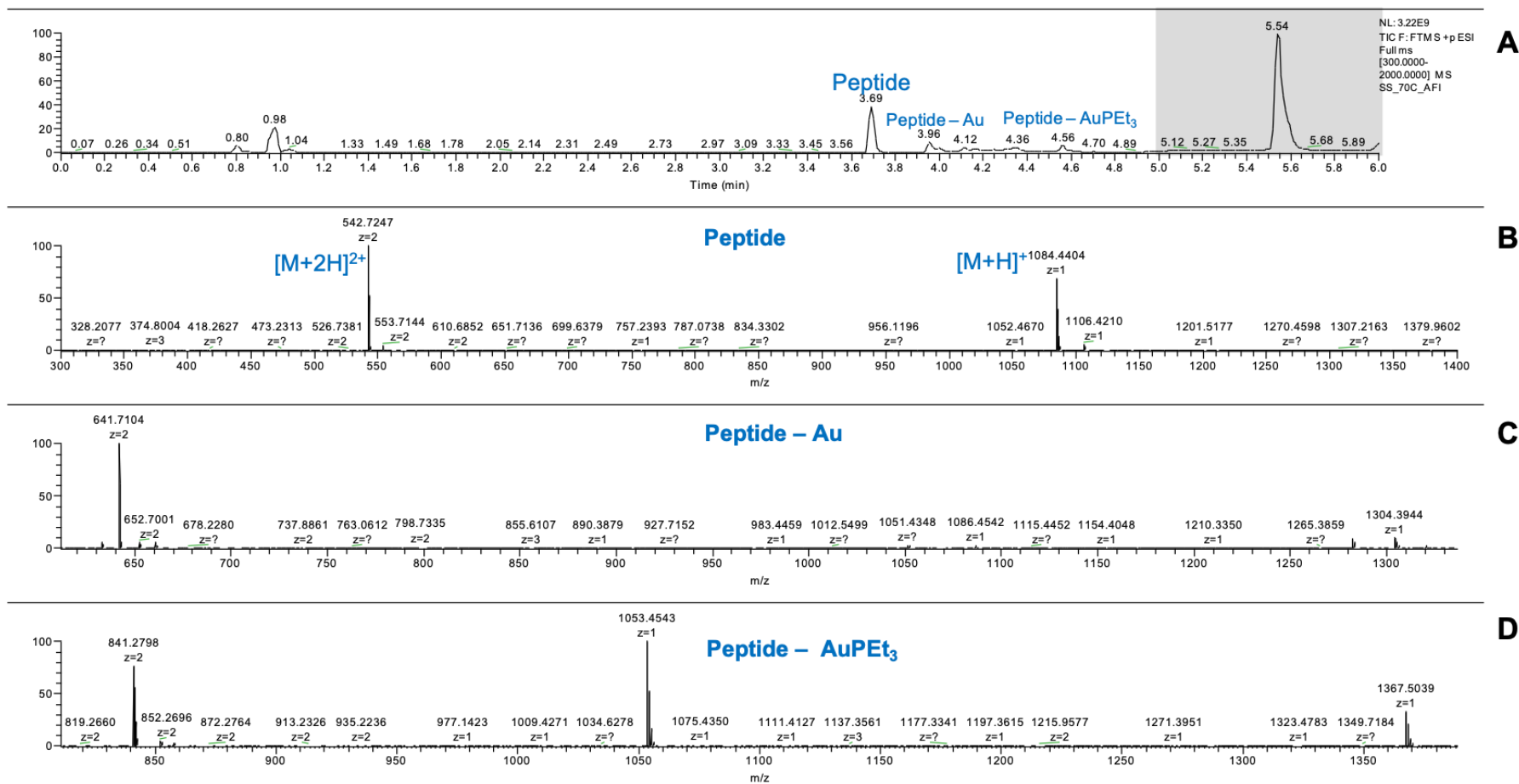


Annex 1 Figure 12 LC-MS of AVP incubated with Et<sub>3</sub>PAuBr overnight at 70 °C. (A) TIC. (B) MS spectrum of peak at  $t_R = 3.69$  minutes. (C) MS spectrum of peak at  $t_R = 4.55$  minutes. (D) MS spectrum of peak at  $t_R = 5.53$  minutes. The dark part corresponds to the elution of Et<sub>3</sub>PAuBr.

### AVP after incubation with Et<sub>3</sub>PAuI at 70°C

D:\Master...May21052021\SS\_70C\_AFI

05/21/21 12:05:07

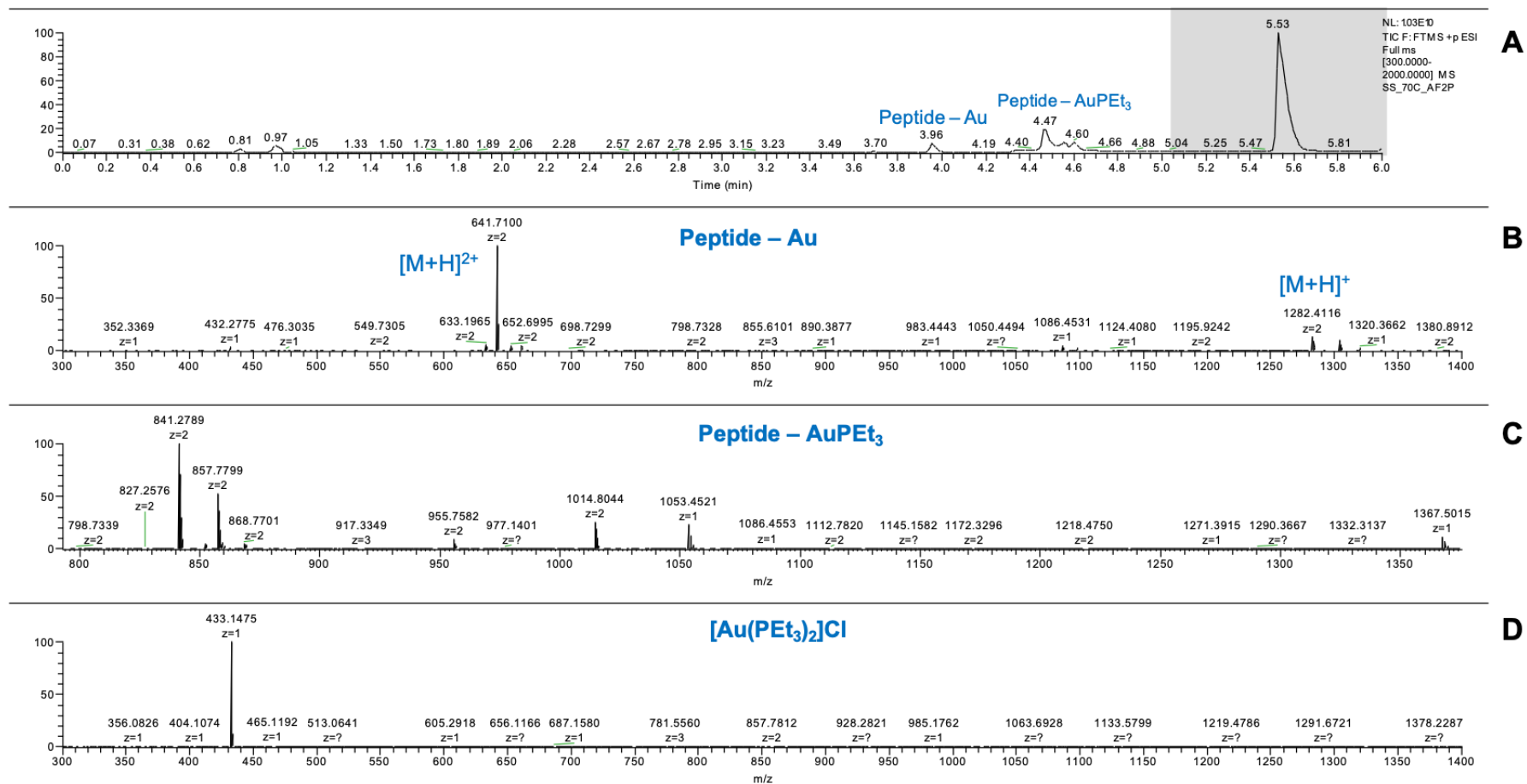


Annex 1 Figure 13 LC-MS of AVP incubated with Et<sub>3</sub>PAuI overnight at 70 °C. (A) TIC. (B) MS spectrum of peak at t<sub>R</sub> = 3.69 minutes. (C) MS spectrum of peak at t<sub>R</sub> = 3.96 minutes. (D) MS spectrum of peak at t<sub>R</sub> = 4.56 minutes. The dark part corresponds to the elution of Et<sub>3</sub>PAuI.

## AVP after incubation with $[Au(PEt_3)_2]Cl$ at 70°C

D:\Másterl...May21052021\SS\_70C\_AF2P

05/21/21 12:27:35



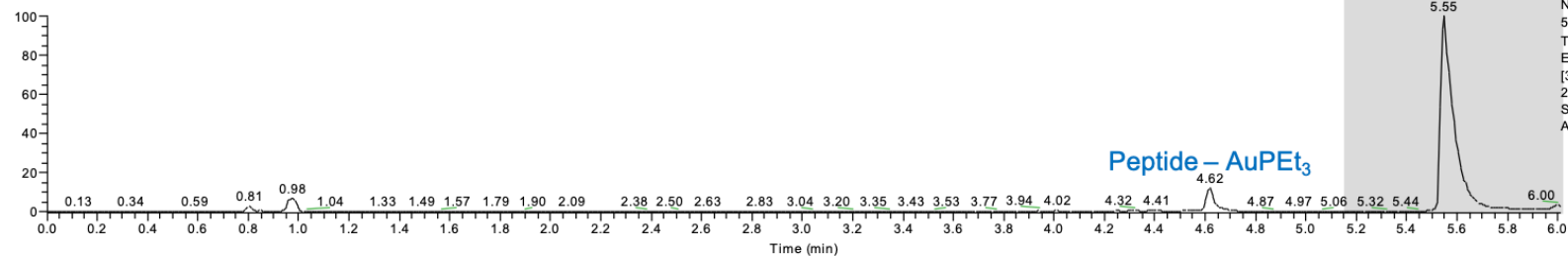
Annex 1 Figure 14 LC-MS of AVP incubated with  $[Au(PEt_3)_2]Cl$  overnight at 70 °C. (A) TIC. (B) MS spectrum of peak at  $t_R = 3.96$  minutes. (C) MS spectrum of peak at  $t_R = 4.47$  minutes. (D) MS spectrum of peak at  $t_R = 4.60$  minutes. The dark part corresponds to the elution of  $[Au(PEt_3)_2]Cl$ .

### [Se-Se]-AVP after incubation with Et<sub>3</sub>PAuCl at 70°C

D:\Master\...05052021\SeSe+AFCI\_NoDTT

05/05/21 10:52:48

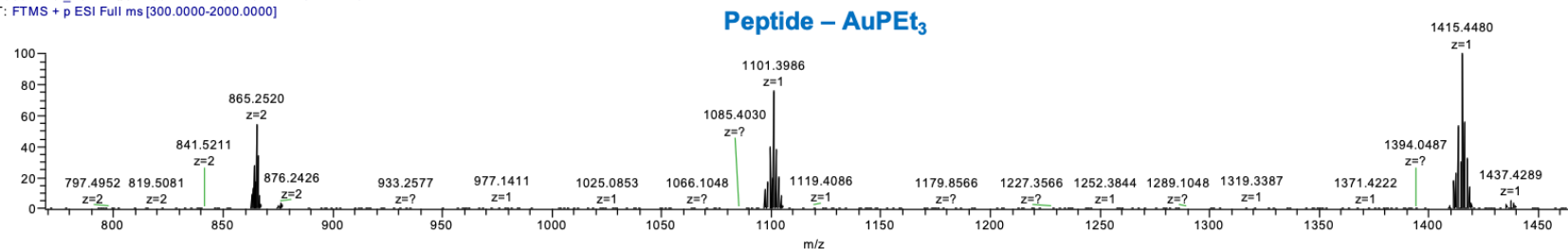
RT: 0.00 - 6.01



NL:  
5.40E9  
TIC F: FTMS + p  
ESI Full ms  
[300.0000-  
2000.0000] MS  
SeSe+  
AFCI\_NoDTT

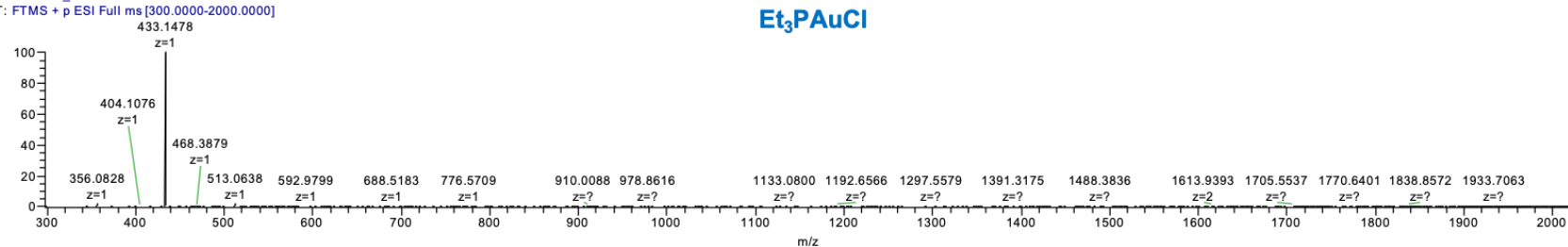
**A**

SeSe+AFCI\_NoDTT #347-352 RT: 4.59-4.64 AV: 6 NL: 1.97E7  
T: FTMS + p ESI Full ms [300.0000-2000.0000]



**B**

SeSe+AFCI\_NoDTT #436-450 RT: 5.53-5.66 AV: 15 NL: 1.75E9  
T: FTMS + p ESI Full ms [300.0000-2000.0000]



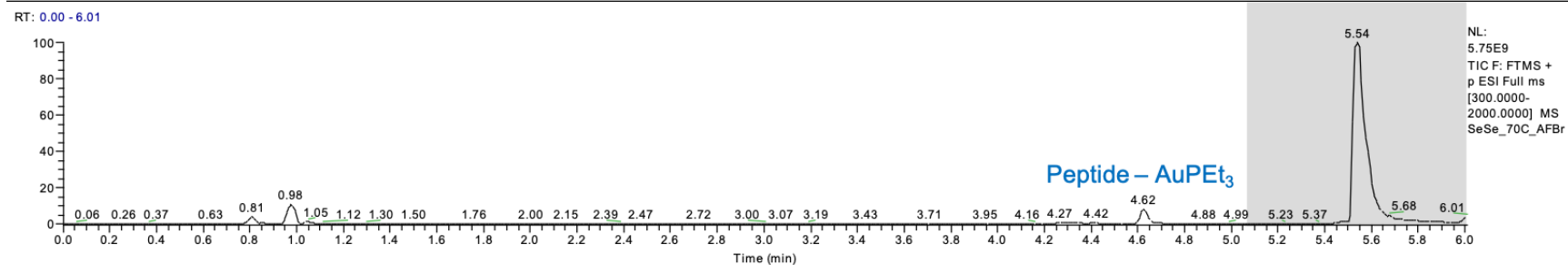
**C**

Annex 1 Figure 15 LC-MS of [Se-Se]-AVP incubated with Et<sub>3</sub>PAuCl overnight at 70 °C. (A) TIC. (B) MS spectrum of peak at tR = 4.62 minutes. (C) MS spectrum of peak at tR = 5.55 minutes. The dark part corresponds to the elution of Et<sub>3</sub>PAuCl.

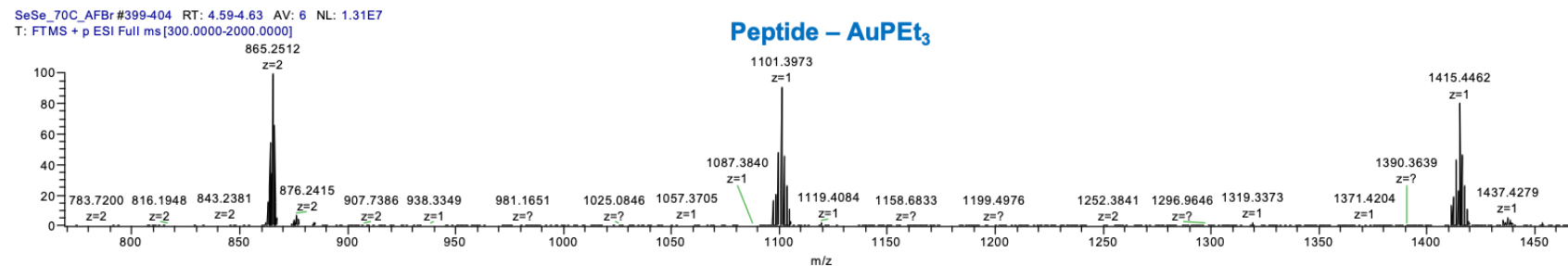
## [Se-Se]-AVP after incubation with Et<sub>3</sub>PAuBr at 70°C

D:\Máster\...May\21052021\SeSe\_70C\_AFB

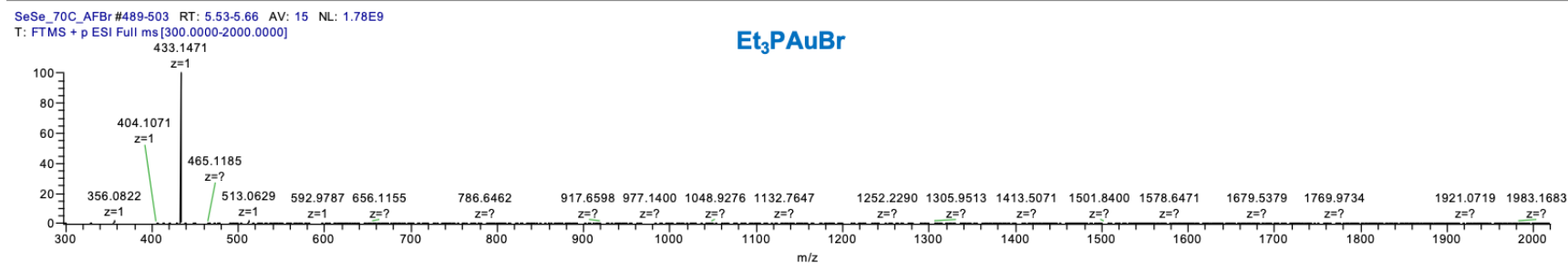
05/21/21 11:53:53



**A**



**B**



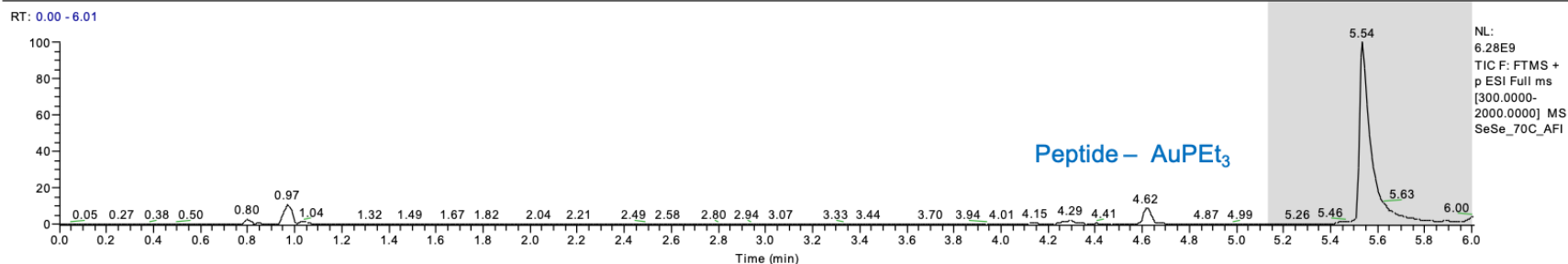
**C**

Annex 1 Figure 16 LC-MS of [Se-Se]-AVP incubated with Et<sub>3</sub>PAuBr overnight at 70 °C. (A) TIC. (B) MS spectrum of peak at tR = 4.62 minutes. (C) MS spectrum of peak at tR = 5.54 minutes. The dark part corresponds to the elution of Et<sub>3</sub>PAuBr.

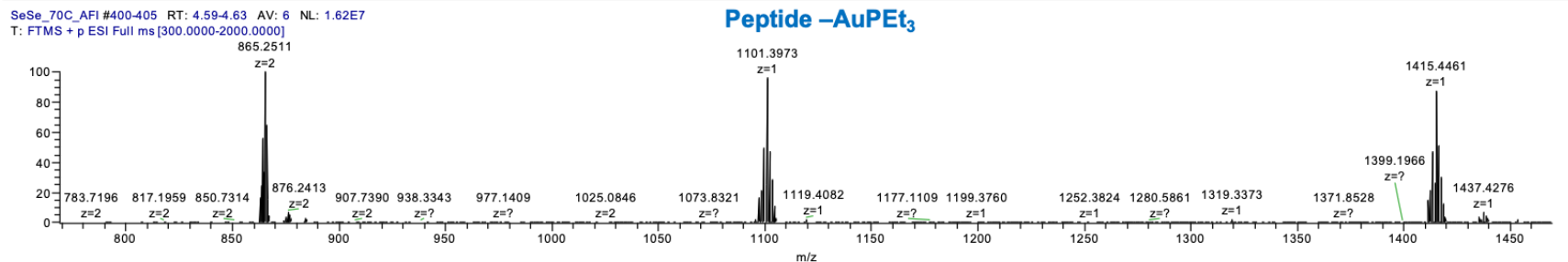
### [Se-Se]-AVP after incubation with Et<sub>3</sub>PAul at 70°C

D:\Másterl...\May\21052021\SeSe\_70C\_AFI

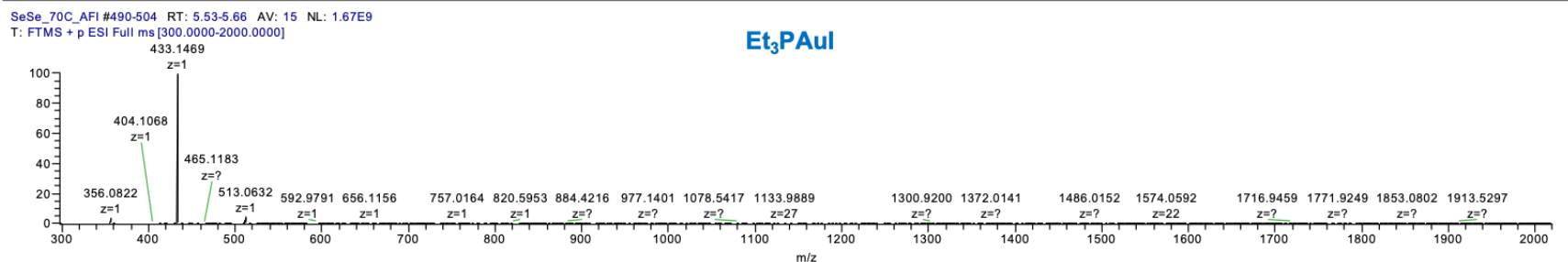
05/21/21 12:16:21



**A**



**B**



**C**

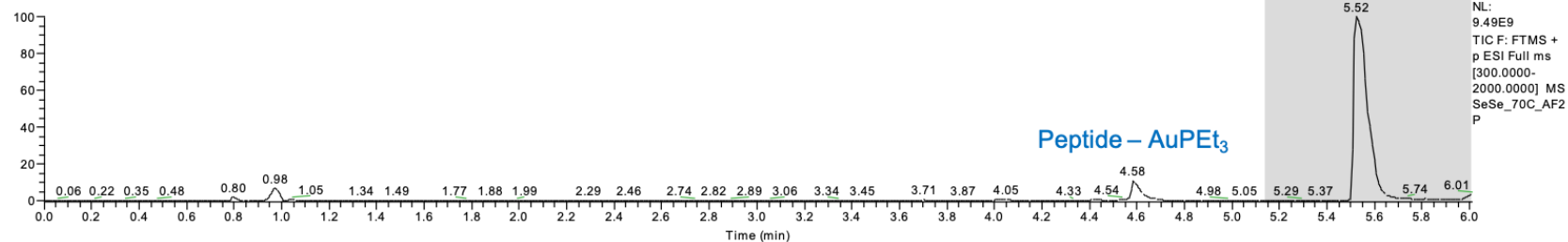
Annex 1 Figure 17 LC-MS of [Se-Se]-AVP incubated with Et<sub>3</sub>PAul overnight at 70 °C. (A) TIC. (B) MS spectrum of peak at *t<sub>R</sub>* = 4.62 minutes. (C) MS spectrum of peak at *t<sub>R</sub>* = 5.54 minutes. The dark part corresponds to the elution of Et<sub>3</sub>PAul.

## [Se-Se]-AVP after incubation with [Au(PET<sub>3</sub>)<sub>2</sub>]Cl at 70°C

D:\Master\...May21052021\SeSe\_70C\_AF2P

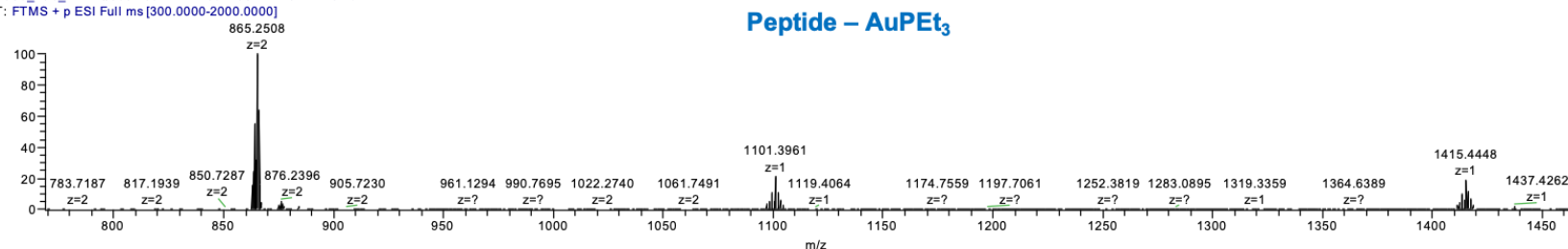
05/21/21 12:38:49

RT: 0.00 - 6.01



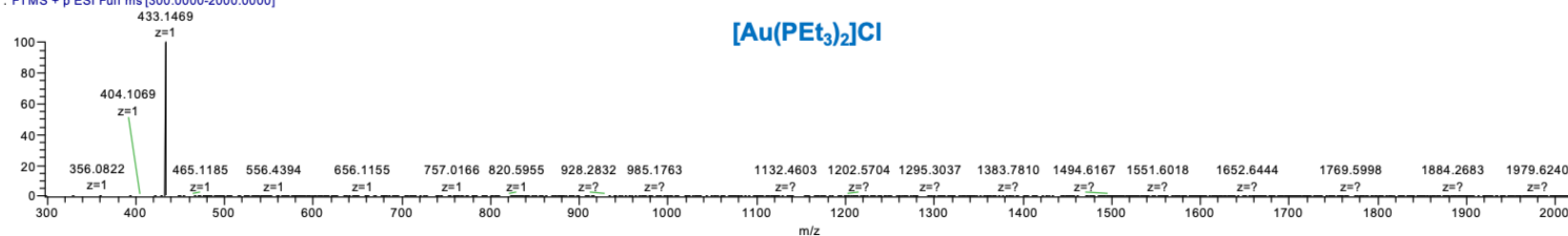
**A**

SeSe\_70C\_AF2P #396-400 RT: 4.59-4.63 AV: 5 NL: 6.78E7  
T: FTMS + p ESI Full ms [300.0000-2000.0000]



**B**

SeSe\_70C\_AF2P #491-504 RT: 5.53-5.66 AV: 14 NL: 2.73E9  
T: FTMS + p ESI Full ms [300.0000-2000.0000]



**C**

Annex 1 Figure 18 LC-MS of [Se-Se]-AVP incubated with [Au(PET<sub>3</sub>)<sub>2</sub>]Cl overnight at 70 °C. (A) TIC. (B) MS spectrum of peak at *t<sub>R</sub>* = 4.58 minutes. (C) MS spectrum of peak at *t<sub>R</sub>* = 5.52 minutes. The dark part corresponds to the elution of [Au(PET<sub>3</sub>)<sub>2</sub>]Cl





*Annex 2 Article Characterization and quantification of  
selenoprotein P: challenges to mass spectrometry*





Review

## Characterization and Quantification of Selenoprotein P: Challenges to Mass Spectrometry

Jérémy Lamarche <sup>1,\*</sup> , Luisa Ronga <sup>1</sup>, Joanna Szpunar <sup>1</sup> and Ryszard Lobinski <sup>1,2,3</sup>

- <sup>1</sup> IPREM UMR5254, E2S UPPA, Institut des Sciences Analytiques et de Physico-Chimie Pour l'Environnement et les Matériaux, CNRS, Université de Pau et des Pays de l'Adour, Hélioparc, 64053 Pau, France; luisa.ronga@univ-pau.fr (L.R.); joanna.szpunar@univ-pau.fr (J.S.); ryszard.lobinski@univ-pau.fr (R.L.)  
<sup>2</sup> World-Class Research Center "Digital Biodesign and Personalized Healthcare", IM Sechenov First Moscow State Medical University (Sechenov University), 119435 Moscow, Russia  
<sup>3</sup> Chair of Analytical Chemistry, Warsaw University of Technology, Noakowskiego 3, 00-664 Warsaw, Poland  
 \* Correspondence: jeremy.lamarche@univ-pau.fr

**Abstract:** Selenoprotein P (SELENOP) is an emerging marker of the nutritional status of selenium and of various diseases, however, its chemical characteristics still need to be investigated and methods for its accurate quantitation improved. SELENOP is unique among selenoproteins, as it contains multiple genetically encoded SeCys residues, whereas all the other characterized selenoproteins contain just one. SELENOP occurs in the form of multiple isoforms, truncated species and post-translationally modified variants which are relatively poorly characterized. The accurate quantification of SELENOP is contingent on the availability of specific primary standards and reference methods. Before a recombinant SELENOP becomes available to be used as a primary standard, careful investigation of the characteristics of the SELENOP measured by electrospray MS and strict control of the recoveries at the various steps of the analytical procedures are strongly recommended. This review critically discusses the state-of-the-art of analytical approaches to the characterization and quantification of SELENOP. While immunoassays remain the standard for the determination of human and animal health status, because of their speed and simplicity, mass spectrometry techniques offer many attractive and complementary features that are highlighted and critically evaluated.

**Keywords:** selenoprotein P; mass spectrometry; metrology; selenium; cancer; biomarker; selenocysteine



**Citation:** Lamarche, J.; Ronga, L.; Szpunar, J.; Lobinski, R. Characterization and Quantification of Selenoprotein P: Challenges to Mass Spectrometry. *Int. J. Mol. Sci.* **2021**, *22*, 6283. <https://doi.org/10.3390/ijms22126283>

Academic Editor: Antonella Roveri

Received: 4 May 2021

Accepted: 7 June 2021

Published: 11 June 2021

**Publisher's Note:** MDPI stays neutral with regard to jurisdictional claims in published maps and institutional affiliations.



Copyright: © 2021 by the authors. Licensee MDPI, Basel, Switzerland. This article is an open access article distributed under the terms and conditions of the Creative Commons Attribution (CC BY) license (<https://creativecommons.org/licenses/by/4.0/>).

### 1. Introduction

Selenium, originally known for its toxicity, was subsequently recognized as an essential trace element [1] and has been increasingly marketed as a life-style drug [2]. The importance of Se is related to its antioxidant properties, its role in the endocrine and immune system, as well as its involvement in the protection against certain diseases, such as cancer, diabetes, cardiovascular or immune system disorders [3]. The narrow range of the optimum selenium concentration in biological fluids, the multiplicity of its chemical forms and the diversity of its biological activities are driving interest for precise molecular markers of its status in various organisms.

The activity of Se is mainly mediated by selenoproteins. They contain in their sequence at least one selenocysteine (SeCys, U), which is genetically encoded and often referred to as the 21st amino-acid [4]. In the presence of a specific stemloop RNA sequence element (SECIS), the UGA codon, normally acting as a stop codon to terminate translation, codes for the insertion of SeCys into a polypeptide chain [2,5]. The pioneering works of Gladyshev group [6,7] started the development of algorithms predicting the existence of many selenoproteins in different biological species [8,9]. The number of selenoproteins that can be expressed in different organisms varies, ranging from 1 in certain insects, to 9 in common spider, 25 in humans [10], and 32 in oysters [11]. In vertebrates, the mRNA

encoding SELENOP is distinct from that encoding other selenoproteins, in that it contains two SECIS elements instead of one [12].

Selenoprotein P is unique amongst all the characterized selenoproteins in that it contains multiple SeCys residues, whereas all other selenoproteins contain only one SeCys. The number of SeCys residues in SELENOP from different organisms varies (Figure 1), amounting to 10 for humans, 46 in oysters [11] and 132 in one-species bivalves [13].

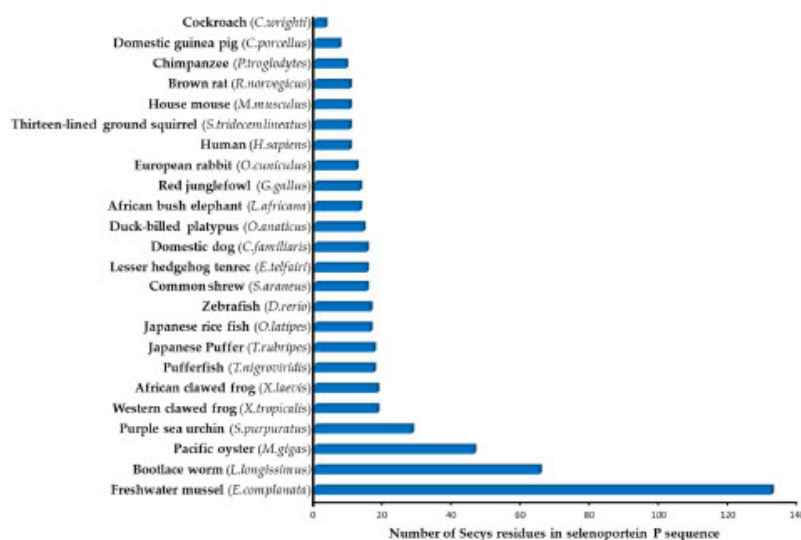


Figure 1. Putative number of SeCys residues in SELENOP in different organisms (according to [11,12,14]).

SELENOP was first reported in 1973 by Burk et al. [15] and Rotruck et al. [16]. Mc-Connell et al. [17] and Motsenbocker et al. [18] found that SELENOP was synthesized in the liver of rats and secreted into the plasma. A few years later, the existence of SELENOP was confirmed in humans, where it is considered as a valuable marker for nutritional selenium status [19]. In 2016, Gladyshev et al. proposed a non-ambiguous notation for all selenoproteins using the root symbol SELENO followed by a letter, leading to the creation of the abbreviation SELENOP for selenoprotein P, replacing the previously used as abbreviations such as SeP, SEEP1, SeIP [20]. Expression, functions and role of SELENOP in mammals were reviewed [21].

As a biomarker, SELENOP can discriminate between the specific and nonspecific (and therefore non-significant) incorporation of Se in proteins [22,23]. It responds to Se supplementation over a wider range of intakes than GPx3 [24]. In marginally supplied individuals, low serum Se was found to be mirrored by the circulating SELENOP concentration, but not by the GPx3 activity [25]. In studies of populations with relatively low selenium intakes, SELENOP was found to respond to different dietary selenium forms [26]. Serum SELENOP concentration can be more than a biomarker of Se status: it was proposed to be used for the diagnosis and assessment of treatment efficacy and long-term prognosis in patients with pulmonary arterial hypertension [27] and hypertension [28]. Recently, the mortality risk from COVID-19 was shown to be associated with selenium deficiency, and more specifically with SELENOP deficiency, causing a dysregulation of the redox homeostasis in pathological conditions which resulted in an excessive reactive oxygen species (ROS) generation [29,30].

During the last 40 years, many functions have been attributed to SELENOP including its involvement in the storage of selenium in the brain, testis [23,31] and kidney [32],

defence against oxidative stress [33], loss of fertility [23], polycystic ovary syndrome [34] or regulation of heavy metals concentration [35,36]. SELENOP was reported to play a role in the potential development of various forms of cancer [37–40] and to be associated with neurodegenerative diseases such as Alzheimer's [39,41–43]. SELENOP was evoked as a therapeutic target for type 2 diabetes [41,44–46] because of its role in the regulation of glucose metabolism and insulin sensitivity. Recent advances in the understanding of the role of SELENOP and its potential medical/pharmaceutical implications were reviewed [47].

In order to fully elucidate the mode of action and the importance of SELENOP in the different pathological pathways, a complete structural characterization, quantitative determination and localization of SELENOP in the tissues are needed [48]. Mass spectrometry techniques are uniquely placed to address these ongoing challenges. The goal of this review is to critically discuss the current state-of-the-art analytical methods for the characterization and determination of SELENOP, identify the open questions and indicate how they can be answered.

## 2. Selenoprotein P Characteristics

To date, the three-dimensional structure of SELENOP has not been solved. A possible reason for this is the difficulty in the exogenous over-expression of SELENOP in bacteria or in cultured cells, because of the presence of multiple Sec residues in the polypeptide [47]. Studies using recombinant SELENOP have been rare [49]. Consequently, the SELENOP characterization was carried out on protein expressed endogenously by cell lines or purified from plasma and serum.

The matured predominant isoform of human SELENOP consists of 359 amino acids (AA) after cleavage of the predicted signal peptide (AA 1–21) [47] (Figure 2a). The selenium content (as SeCys) of SELENOP is distributed into two parts [21,47]. The N-terminal domain contains one selenocysteine at the 40th amino-acid in a U-x-x-C redox motif. The shorter C-terminal domain contains multiples selenocysteine, up to 9 in total for rats, mice, and humans [50,51]. The N-terminal domain is responsible for the enzymatic activity of this protein, while the C-terminal domain acts as the Se supplier [52] (Figure 2b).

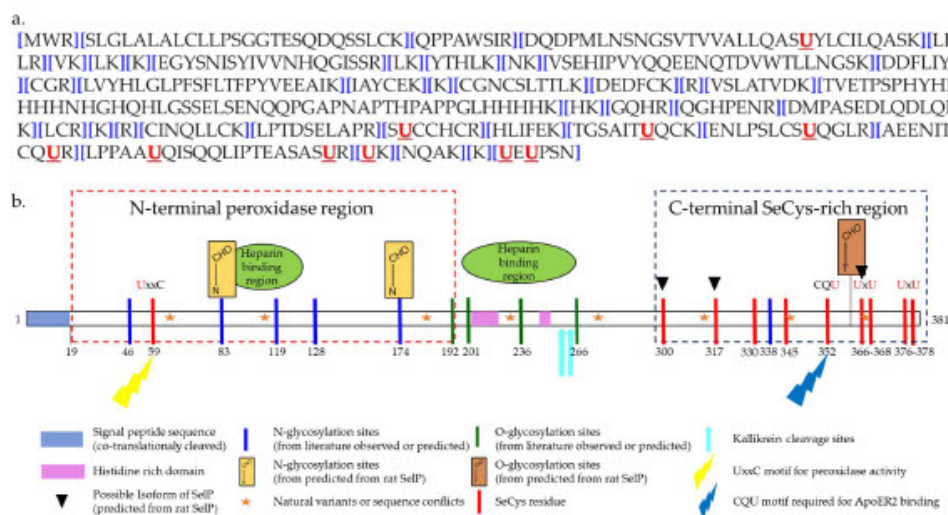


Figure 2. Sequence of human SELENOP. (a) Amino-acid sequence of human SELENOP [53]; (b) schematic representation of human SELENOP (on the basis of [47,53] and Uniprot database).



SELENOP is not a homogenous protein. As a consequence of the SeCys gene expression by stop codon recoding, multiple forms of the SELENOP of different molecular weight exist in terms of relation to genotype, differential splicing, premature interrupted translation at one of the UGA codons, limited post-translational proteolysis or partial replacement of SeCys by Cys [47,54–57]. To date, four isoforms have been identified in rat plasma. Beside the full-length isoform with 10 selenocysteine residues, shorter isoforms terminating at the 2nd, 3rd, and 7th selenocysteine [56], with 1, 2 and 6 selenocysteines, respectively, were reported [58]. Interestingly, in a study involving ca. 2000 subjects, the average determined number of Se atoms per SELENOP molecule (5.4) was considerably below the predicted number of 10 Se atoms [59].

In the native form, SELENOP contains selenenylsulfide and disulfide bridges. It possesses three N-glycosylation sites at the N-terminus and one O-glycosylation site at the C-terminus [60] and thus, can be referred to as glycoprotein. One highly glycosylated form is secreted by the liver [61]. Selenium-supplemented HepG2 hepatoma cells secrete N-glycosylated SELENOP as well [62]. The post-translational modifications are thought to confer a particular structural behavior to SELENOP and to protect selenium by reducing its reactivity [10].

### 3. Isolation of Selenoprotein P from Biological Samples Prior to Mass Spectrometry (MS) Characterization

SELENOP is typically present in serum at a level of ca. 50 ng/mL. Its concentrations in cultured cells, breast milk, or tissues are an order of magnitude lower. The abundance of SELENOP in human serum exceeds that of plasma glutathione peroxidase (GPx) and selenized albumin (SeAlb) [31].

Taking into account the presence of a multitude of proteins in a 1000-fold excess, any characterization of SELENOP by mass spectrometry should be preceded by its isolation and enrichment. The methods are usually based on the immunoaffinity precipitation or chromatography (mono- and/or poly-clonal antibodies) [52,58,63–66] or chemical affinity (heparine [56,67,68] or immobilized transition metals [49,69]).

#### 3.1. Immunoaffinity Precipitation and Chromatography

The use of immunoaffinity has been largely explored for isolation of SELENOP, but this strategy is critically dependent on the quality and selectivity of antibodies. The cross-activity of one antibody with an antigen from different species is not granted and must be tested. Moreover, the activity of the antibody is highly variable for the serum of one animal to the other and must also be systematically tested.

The first purification of SELENOP by immunoprecipitation was performed from rat serum, using monoclonal antibodies [63]. Subsequently, Akesson et al. [58] used the rat monoclonal antibodies for purification of human SELENOP. Other groups reported the preparation [64,70] or use [71] of monoclonal antibody raised against rat SELENOP [64]. No cross-reactivity with plasma from five animal species [58] was observed. Commercially available antibodies against murine SELENOP do not cross react with the human orthologue [69]. Recombinant rat SELENOP was efficiently immunoprecipitated by a commercial penta-histidine antibody but not by the tetrahistidine one [49].

Considerable developments in the field of SELENOP antibodies have taken place in the recent years driven by the need for the development of ELISA kits (see below). They are based on the use of antibodies prepared by using recombinant mutant SELENOP as immunogen. These expressed SELENOP mutants are characterized by the absence of SeCys which are all replaced by Cys [72] or Ser [73]. A recombinant SELENOP commonly used as immunogen for commercial antibody development encompasses the 60-299 SELENOP sequence without SeCys residues [74]. Alternatively, SELENOP purified from human serum was employed as immunogen [52,70,75].

The antibody-based methods for purification and measurement of SELENOP may not allow the distinction among the isoforms [56]. Indeed, antibodies are usually directed towards one of its domains (N or C). Consequently, they capture not only full-length

SELENOP but also its N- or C-terminal side domain fragments. In vivo, SELENOP is cleaved by plasma kallikrein which generates N-terminal and C-terminal fragments of SELENOP [75]. The combined use of antibodies specific for N- or C-terminal SELENOP side domain fragments allows the differentiation between the full-length SELENOP from total SELENOP (truncated and full length) [52,54,66].

Technically speaking, immunoprecipitation of SELENOP can be conveniently performed with commercial antibodies conjugated to polystyrene superparamagnetic beads [65]. GPx3 is co-immunoprecipitated with SELENOP, resulting in incomplete separations which is likely to be due to the similarity in the structure of the N-terminal part of SELENOP and GPx3 [65]. This point has not been addressed by recent studies where combined antibodies specific for the different SELENOP *termini* were employed.

### 3.2. Heparin Affinity Methods

Two histidine-rich stretches containing up to 10 sequential basic amino acids are present in the 185–198 and 225–234 amino-acid sequences in rats [67]. The rat and human SELENOP sequences encode two His-rich regions: the first region consists of 8 (rat) or 9 (human) histidines out of 14 residues, and the second, a stretch of 7 (rat) or 4 (human) consecutive histidines [76]. The presence of these stretches confers to SELENOP a feature of binding to heparin [67].

SELENOP binds to heparin as a function of pH. The binding is facilitated by an increase in protonation of histidine residues. Therefore, SELENOP will bind to heparin under acidic conditions but remains unbound at physiological pH [21]. The pKa of histidine (7.0) explains the release of SELENOP from heparin at alkaline conditions [67].

Heitland et al. were able to isolate SELENOP using heparin column from other serum proteins with a total recovery of selenium (96%) [68]. A recovery above 90% was reported [77]. Problems linked to nonspecific adsorption of plasma-extracellular glutathione peroxidase (GPx) and albumin on the heparin affinity column were evoked [77].

Purified SELENOP can be separated in three peaks using heparin chromatography suggesting its capability to discriminate amongst the isoforms [56].

### 3.3. Immobilized Metal Affinity Methods (IMAC)

These histidine-rich regions in conjunction with the Cys and SeCys content, are likely responsible for the coordination to heavy metals such as, e.g., mercury [76]. The presence of such motifs makes it possible to retain SELENOP on an IMAC-sepharose column loaded with cobalt [69]. Co<sup>2+</sup> was found superior to Cu<sup>2+</sup>, Ni<sup>2+</sup>, Zn<sup>2+</sup>, and Cd<sup>2+</sup> for metal affinity LC [69].

The Ni-agarose chromatography was performed using Ni-NTA spin columns and turned out to be efficient for the isolation of SELENOP, prior to SDS PAGE and Western blotting analysis [49].

### 3.4. Sequential Purifications

In order to increase the purity of the isolated SELENOP, the above discussed steps can be employed in a sequence. Akesson et al. reached a 1000-fold purification of SELENOP by combining immunoaffinity LC and heparin [58]. The immunoaffinity purified protein was further separated into several forms using heparin-sepharose column [64].

Daegen et al. separated plasma into three components (GPx, SELENOP, and Alb) using heparin-sepharose and blue 2-sepharose (to remove SeAlb) [78]. A combination of IMAC and heparin offered a 15,000-fold enrichment of SELENOP [69]. Isolation of electrophoretically pure SELENOP was reported to be achieved in three steps: heparin agarose, ultrafiltration concentration, anion-exchange, Ni-NTA-agarose [61]. The combination of heparin-sepharose CL-GB, Q Sepharose F and Ni-NTA agarose chromatography, followed by desalting by gel filtration, allowed a 13,000-fold purification of SELENOP with an overall yield of 16% [79]. The low yield of sequential purification is often due to the multiplication of steps inducing loss of protein. In recent studies, the use of heparin was



shown to be the most efficient for SELENOP purification with a yield of 96% [68], however this method does not concentrate the protein.

#### 4. Detection and Characterization of SELENOP by Soft Ionization Mass Spectrometry

The isolated SELENOP can be formally identified without mass spectrometry by the N-terminal amino-acid sequence (or microsequencing) [79]. However, the advantage of MS in terms of sensitivity and speed cannot be overestimated. So far, to our knowledge, there have been no mass spectra published for the intact full-length SELENOP and their truncated isoforms. Most of the published MS data concern the analysis of peptides, obtained after tryptic digestion, by matrix-assisted laser desorption ionization (MALDI) or electrospray ionization MS. The latter allows the determination of the peptide sequence upon collision induced fragmentation (MS/MS). The list of the reported peptides allowing the 100% sequence specificity and their correspondence to full-length or truncated isoforms is given in (Table 1).

A number of bioinformatic tools have been developed for the detection of selenoproteins in high throughput MS schemes [9,80]. Several enzymes (such as trypsin or endoproteinase) can be used to lyse the proteins and to obtain different SELENOP characteristic peptides. The inconvenience of bottom-up proteomics approaches is that it is not always possible to identify isoforms from which the peptides are derived. Their advantage is the capability to deal with the post-translational modification.

The major challenges in mass spectrometry analysis include the ability to be able to distinguish between isoforms, to complete the characterization of truncated forms and to develop analytical methods for their quantification. The potential of top-down proteomics for this purpose is very promising [81].

##### 4.1. MALDI-MS

MALDI-MS allowed the discovery in rat plasma of three SELENOP isoforms that have identical N-termini, and differ in the length of the amino-acid chain [56]. The full-length SELENOP and the isoforms were separated by SDS PAGE. They were reduced, alkylated, deglycosylated and digested with trypsin. Additional peptides could be identified by digestion with Glu-C of the SeIP isolated by heparin, without the need for its subsequent purification by SDS PAGE. Mass spectrometry could identify the C-termini of the isoforms according to the prediction (at the 2nd, 3rd and 7th selenocysteine residue) [56].

MALDI-MS was also used to identify the sites of glycosylation of the full-length SELENOP [60]. The procedure was based on a treatment with PNGase F, which cleaves off asparagine-linked carbohydrates and converts the residue asparagine to aspartic acid. Of the five potential glycosylation sites, three located at residues 64, 155 and 169 were occupied, and two at residues 351 and 356 were not occupied. Threonine 346 was variably O-glycosylated. Full-length SELENOP was found to be both N- and O-glycosylated [60].

MALDI-MS was also essential in the identification of Se-S and disulfide linkage sites [60]. The strategy of sample preparation for the determination of the oxidation state of the cysteine residues consisted of the alkylation of all free cysteines and selenocysteines in the short form of SELENOP with iodoacetamide, digestion with endoproteinase, and deglycosylation [60]. A selenide-sulfide bond was found in the shortened isoform to be analogous to the selenol-thiol pair considered to be redox-active [60]. Two selenylsulfide bonds were identified by MALDI-MS in a peptide isolated from a tryptic digest of rat SELENOP [82].

##### 4.2. Electrospray MS

The basic advantage of electrospray ionization (ESI) MS over MALDI is the possibility to sequence peptides in LC-MS/MS on the basis of the  $m/z$  of their  $b$  and  $y$  fragments. ESI MS was used to verify the sequences of the putative glycosylated peptides in rat SELENOP [60] and the confirmation of the existence of disulfide linkages [60,82].

High pressure liquid chromatography (HPLC)-MS/MS was a convenient technique for the identification of SELENOpeptides in a tryptic digest of purified SELENOP. It allowed the formal confirmation of SELENOP presence in human breast milk [83]. A sequence with a coverage of 80% of the theoretical one was reported on the basis of the tryptic digest analysis, and two SELENOpeptides were formally identified [83].

SELENOP, being a low-abundant protein in serum, was not detected by a regular shotgun proteomics approach [84]. The analysis of the fraction purified by heparin allowed the detection of three unique SELENOP peptides identified by only one post-translational modification for each, and a sequence coverage of 41.5% [84]. The purification of SELENOP by SDS PAGE and blotting, which was followed by tryptic digestion and HPLC-MS/MS, allowed the identification of 7 SELP peptides totalling 115 post-translational modifications (none of which contained selenium) in the 49 kDa SELENOP band in the blot, accounting for a sequence coverage factor of 17.7%. Selenium contained peptides missed by the regular shotgun proteomics procedure. The identification of two SELENOpeptides increased the sequence coverage to 24.4% [84]. Three isoforms of SELENOP were identified by this method [65].

Human SELP still needs a complete MS characterization covering all the SELENOpeptides. The recent data obtained are summarized in Table 1.

The developments in soft ionization mass spectrometry open new perspectives in the detection of SELENOP in broad scope proteomic studies. The method is based on nano-flow liquid chromatography (LC) with electrospray MS/MS detection and data-independent acquisition MS [85]. For instance, label-free proteomics showed selenoprotein P as the most abundant proteins in milk of cows, more precisely, in cows producing milk with A2A2-β-casein variants [86]. The protocols can be quantitative by using isobaric tagging for relative and absolute Quantification (iTRAQ) [80,87–89].

**Table 1.** List of SELENOpeptides used for the SELENOP mass spectrometry identification on the basis of a partial sequence (peptides with the same sequence are highlighted in colors).

| Matrix            | SELENOP Specific Sequence with Sec Detected   | Identified Isoform  | Ref. |
|-------------------|---|---|------|
| Rat plasma        | <sup>28</sup> GTVTVVALLQASUYLCLLQASRL <sup>51</sup><br><sup>239</sup> QGHLESUDMGASEGLQLSLAQR <sup>260</sup><br><sup>252</sup> GLQLSLAQRKLRRCINQLLCKLSE <sup>278</sup><br><sup>298</sup> SGSAITUQCAENLPSLCSUQGLFAEEK <sup>324</sup><br><sup>333</sup> SPPAAUHSQHVSPTASPNUSUNNK <sup>367</sup><br><sup>348</sup> ASPNUSUNNKTKKUKUNLN <sup>366</sup> | 4 Isoforms:<br>50 kDa (full length)<br>49 kDa (terminated at 351)<br>38 kDa (terminated at 262)<br>36 kDa (terminated at 244) | [56] |
| Rat plasma        | <sup>28</sup> GTVTVVALLQASUYLCLLQASR <sup>49</sup><br><sup>328</sup> SCQCRSPPAAUHSQHVSPT <sup>347</sup>   | 1 Isoform terminated at 244   | [60] |
| Rat plasma        | <sup>298</sup> SGSAITUQCAENLPSLCSUQGLFAEEK <sup>324</sup>   | <i>n.d.</i>   | [82] |
| Human plasma      | <sup>322</sup> ENLPSLCUQGLR <sup>334</sup><br><sup>335</sup> AEEENITESCQR <sup>346</sup>  | <i>n.d.</i>   | [84] |
| Human plasma      | <sup>312</sup> TGSAITUQCK <sup>321</sup><br><sup>322</sup> ENLPSLCSUQGLR <sup>334</sup><br><sup>335</sup> AEEENITESCQR <sup>346</sup>   | 3 Isoforms:<br>45 kDa (terminated at 299)<br>49 kDa ( <i>n.d.</i> )<br>57 kDa ( <i>n.d.</i> )                                 | [65] |
| Human breast milk | <sup>312</sup> TGSAITUQCKENLPSLCSUQGLR <sup>334</sup><br><sup>370</sup> NQAKKUEUPSN <sup>382</sup>  | <i>n.d.</i>   | [83] |
| Human serum       | <sup>299</sup> SUCCHCR <sup>305</sup><br><sup>311</sup> TGSAITUQCK <sup>321</sup><br><sup>322</sup> ENLPSLCSUQGLR <sup>334</sup><br><sup>335</sup> AEEENITESCQR <sup>346</sup><br><sup>347</sup> LPPAAUQISQQLIPTEASASUR <sup>368</sup><br><sup>368</sup> UKNQAK <sup>374</sup><br><sup>375</sup> KUEUPSN <sup>381</sup>                           | <i>n.d.</i>   | [90] |
| Human serum       | <sup>38</sup> DQDPMLNSNGSVTVVALLQASUYLCILQASK <sup>68</sup><br><sup>311</sup> TGSAITUQCK <sup>321</sup><br><sup>322</sup> ENLPSLCSUQGLR <sup>334</sup><br><sup>335</sup> AEEENITESCQR <sup>346</sup><br><sup>347</sup> LPPAAUQISQQLIPTEASASUR <sup>368</sup>  | <i>n.d.</i>   | [91] |

*n.d.*: no data.

## 5. Quantification of SELENOP

### 5.1. Immunoassays

Originally, radioimmunoassays based on the in-vitro synthesized or partially purified labeled SELENOP preparations were proposed by [19,63,92,93]. Nevertheless, due to the cumbersome procedures and restrictive regulations concerning the use of radioactive materials, these assays were only used in very few studies and were not widely adopted by the larger community.

ELISA (enzyme-linked immunosorbent assay) for SELENOP was first developed as early as 2010 [24], but the early ELISA assays were time consuming and inconvenient for clinical use. However, the approach is rapidly gaining popularity for the absolute quantification of SeIP in plasma samples [59,94]. Several kits are commercially available [73,74,95–97]. The results depend largely on the kit used and caution and criticism are required when comparing data obtained with the different kits [98].

The accuracy of the results depends on the epitope identified by the antibody and its selectivity (activity towards the other proteins). If an antibody recognizes just, for example, the N-terminal, the assays will capture not only full-length SELENOP but also the SELENOP-N-terminal fragment [52]. An assay using colloidal gold particles coated with two types of anti-SELENOP monoclonal antibodies, one recognizing the N-terminal side domain and the other recognizing the C-terminal, was developed for measuring full-length selenoprotein P in human serum [52].

The in-plate variation, within-laboratory variation, and between laboratory variation are all typically below 15% with a limit of quantification of 10 ng/mL [59]. The accuracy of ELISA (difference with the SRM value) was assessed to be 2.9% [59]. Because of the limited presence of mass spectrometry technology in the clinical environment, immunoassays are the most widely used technique for human and animal health status.

### 5.2. Liquid Chromatography—Inductively Coupled Plasma—Mass Spectrometry(ICP-MS)

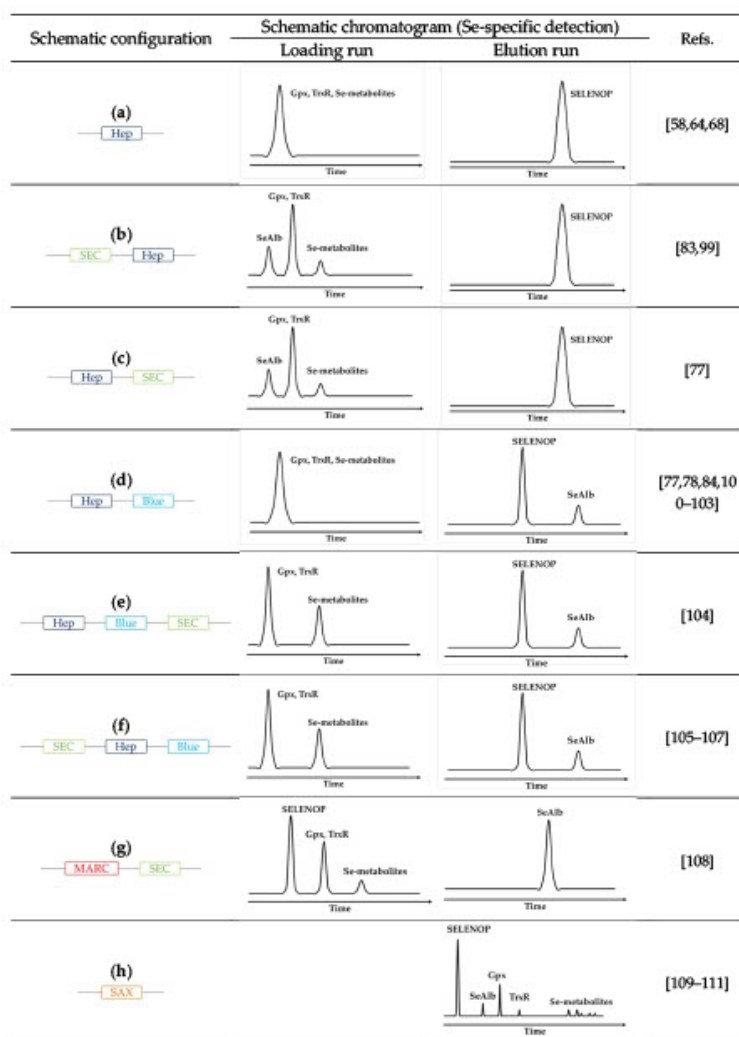
SELENOProtein P can be quantified by measuring the Se response provided that the protein is separated from the other Se-containing species by HPLC. The initial use of hydride generation atomic absorption or fluorescence spectrometry was replaced by ICP-MS because of its higher sensitivity, isotopic specificity and simplicity avoiding the need for post-column chemical conversion of SELENOP to Se or to selenium hydride. Because of the high relative abundance of SELENOP, the challenge of separation is practically limited to SELENOP from selenoalbumin, GPx3, and selenometabolite fraction.

The principle of the methods is based on downscaling and on-line arrangement in different configurations of the three principal techniques discussed above: size-exclusion LC for the separation according to the molecular weight, heparin LC for the selective retention of SELENOP, and Blue-Sepharose column for the selective retention of SeAlb. As a result, the SELENOP signal is obtained in the form of a chromatographic peak, other species may sometimes be separated by SEC. The principle of the proposed arrangements and the type of signal used for quantification is schematically shown in (Figure 3).

The most widely used principle for the on-line isolation of SELENOP consists of the retention of SELENOP by affinity using a heparin column while all other selenium species are eluted and detected as a peak in the loading run [68]. The subsequent elution run produces a peak corresponding to SeIP (Figure 3a). The incorporation of a SEC (heparine) column on-line, either preceding [83,99] (Figure 3b) or following [77] (Figure 3c), allows the discrimination of the selenium species eluting in the loading run into HMW Se-containing proteins (Se-albumin and GPx) and LMW metabolite fraction.

A more sophisticated version of the system includes a switching valve and a circuit containing a column with an affinity for albumin, allowing for the specific recovery of SeAlb during the loading run for its subsequent quantification (Figure 3d) [84,100–103]. It can be refined by the integration of a SEC column into the system (Figure 3e–f) [104–107].





**Figure 3.** Schematic overview of the principle of HPLC configuration coupled with ICP-MS for SELENOP determination (a) schematic chromatogram of affinity column heparin coupled with ICP-MS (Se-specific detection) [58,64,68], (b) schematic chromatogram of a size exclusion column followed by an affinity column Heparin coupled with ICP-MS (Se-specific detection) [83,99], (c) schematic chromatogram of affinity column heparin followed by a size exclusion column coupled with ICP-MS (Se-specific detection) [77], (d) schematic chromatogram of multi-affinity columns heparin followed by blue-sepharose coupled with ICP-MS (Se-specific detection) [77,78,84,100-103], (e) schematic chromatogram of multi-affinity columns heparin followed by blue-sepharose and a size exclusion column coupled with ICP-MS (Se-specific detection) [104], (f) schematic chromatogram of a size exclusion column followed by multi-affinity columns heparin and blue-sepharose coupled with ICP-MS (Se-specific detection) [105-107], (g) schematic chromatogram of multi-affinity removal column followed by size exclusion column coupled with ICP-MS (Se-specific detection) [108], (h) schematic chromatogram of a strong anion-exchange column coupled with ICP-MS (Se-specific detection) [109-111], (Hep: HiTrap Heparin affinity column, SEC: Size-exclusion chromatography, Blue: HiTrap Blue affinity column, MARC: Multi-affinity removal column, SAX: Strong anion-exchange column).

Size-exclusion LC alone does not offer a sufficient resolution nor preconcentration to separate SELENOP from SeIAlb [112,113]. However, when coupled in-tandem with a SeIAlb method, SELENOP appears as a peak partially separated from GPx3 and separated from LMW selenometabolite fraction (Figure 3g) [108].

Alternatively, as SeI<sub>P</sub> is the only selenoium species in serum and cerebrospinal fluid not retained on the anion-exchange column; anion-exchange HPLC (Figure 3h) was used to separate it from other species [109–111].

#### 5.2.1. Selectivity and Sensitivity ICP-MS Detection

ICP-MS allows a specific detection of the individual selenium isotopes. Selenoprotein P can be therefore quantified via its selenium content once it has been separated from the other selenium-containing species. Even if the sensitivity of ICP-MS for selenium is inferior to that for most metals because of its higher first ionization potential (9.75 eV), higher proneness to matrix suppression, and the split of ions available among six isotopes, it is fully compatible with the requirements for SELENOP detection in HPLC.

The main problem is the choice of the least interfered isotope as all the Se isotopes can be interfered by polyatomic ions: Ar<sub>2</sub> dimers or Ar combinations with Br, S, or Br. A possible interference is <sup>156</sup>Gd in serum of patients having received Gd contrast agents were also evoked [68]. The interfering elements can be separated by HPLC [102] and are usually not a problem which favors the choice of <sup>77</sup>Se (7.63% abundance) or <sup>82</sup>Se (8.73%). The interference on <sup>78</sup>Se<sup>+</sup> can be effectively eliminated by the use of a H<sub>2</sub> pressurized collision cell [114]. The use of the most abundant <sup>80</sup>Se (49.6%) requires the removal of the Ar<sub>2</sub><sup>+</sup> ions which can be achieved by using a collision cell installed between two quadrupoles as it is the case in the ICP-MS/MS instruments [114]. The latter also allows the non-interfered detection of the <sup>80</sup>Se<sup>16</sup>O<sup>+</sup> ion produced by the oxidation of Se in the reaction cell [114].

#### 5.2.2. Calibration and Quantification

A major problem in the quantification of SELENOP is the non-availability of an authentic SELENOP standard as it is currently practically impossible to obtain recombinant SELENOP in reasonable purity and quantity. Calibration is therefore carried out using a proxy such as selenite, selenomethionine, a peptide characteristic of SELENOP, or recombinant homologue of SELENOP in which the Sec residues were replaced by Cys.

The standards used for calibration are usually isotopically labeled. However, the term “isotope dilution analysis (IDA)” frequently used in the context of quantification of SELENOP by HPLC-ICP-MS does not bear the original meaning of absolute (traceable to SI units) quantification. As there is not isotopically labeled SELENOP available, the analyte (SELENOP) and the spike used are not in the same chemical form.

The principal quantification strategies of SELENOP using calibration by isotope dilution are based on:

1. the measurement, in an HPLC peak, of the intensity ratio between the natural selenium isotope from the SELENOP after HPLC separation of the latter and the enriched Se (<sup>77</sup>Se, <sup>74</sup>Se) added post-column as SeMet or selenite (“spike”). The method is referred to as species-unspecific isotope dilution [83,84,101,104,105,107].
2. the measurement, in an HPLC peak, of the intensity ratio between Se in selenomethionine obtained by the complete proteolysis of the selenoprotein and the isotopically enriched <sup>77</sup>SeMet standard (“spike”). The method can be referred as species-specific isotope dilution on the amino-acid level. The proof of principle was demonstrated by Ruiz Encinar et al. [115] and the approach was applied to the SELENOP quantification by Jitaru et al. [116].
3. the measurement, in an HPLC peak, of the intensity ratio between the Se in a Se-containing peptide obtained from a selenoprotein by tryptic digestion and the isotopically enriched Se (<sup>77</sup>Se, <sup>74</sup>Se) in the identical synthetic peptide. The addition of peptide spikes to the plasma samples was followed by tryptic digestion, alkylation, and isotope ration determination using HPLC-ICP-MS. The principle of the method

was demonstrated by Polatajko et al. [117]. The method was first applied to the quantification of SELENOP by Ballihaut et al. [84]. Deitrich et al. [53] proposed the use of two synthetic peptides (isotopically enriched,  $Se^{76}$ ) derived from SELENOP for its quantification by IDA-ICP-MS/MS. The disadvantage is the introduction of additional uncertainty due to the necessity of control of the efficiency of the enzymatic digestion the use of SELENOpeptides [105].

4. the use of a proxy protein as standard. The closest proxy protein has been for the moment a full-length human recombinant SELENOP in which the original 10 SeCys residues (Sec) were replaced by 10 cysteines (Cys). This replacement was achieved by point mutations of nucleotide triplets coding Sec to triplets coding Cys in the coding sequence for selenoprotein present in the expression vector used as a template for *E.coli* protein synthesis [100]. Selenium was introduced in the polypeptide chain during cell-free protein *E.coli* synthesis in the form of SeMet or  $^{76}Se$ -Met for the preparation of the SEPP1 standard and an isotopically labeled spike for isotope dilution analysis [118,119]. The standard and spike were purified by SDS PAGE [100]. However imperfect the assumption of the similarity of the behavior of the standard and the spike might be, the use of such an isotopically enriched spike allowed the quantification by standard addition and isotope dilution analysis by ICP-MS after the purification of SELENOP by affinity chromatography.

### 5.3. Gel-Electrophoresis-Based Methods

Isoelectric focusing (IEF) and sodium dodecyl sulphate-polyacrylamide gel-electrophoresis (SDS-PAGE) allow for the separation of full-length and truncated SELENOP forms. The quantification of SELENOP and its isoforms in the produced band(s) can be achieved by the detection of selenium (either radioactive or not) or directly by the detection of the protein (recognized by a specific antibody).

The mature SELENOP has a molecular mass of 41 kDa but migrates as multiple bands, of approximately 50–60 kDa in SDS PAGE, probably due to variations in glycosylation (conserved 2 N-linked—and one O-linked glycosylation) [47]. Deglycosylation shifts the migration band from 57 kDa to 43 kDa [93]. A small difference can be seen in mobility (69 kDa under nonreducing conditions) and 66 kDa under reducing conditions [79].

#### 5.3.1. $^{75}Se$ Detection

The migration of  $^{75}Se$  radioactivity in the gel played a fundamental role in the early works, allowing for the discovery and rough characterization of SELENOP [17,18]. The comparison of the radioactivity in the band with that of a standard is a straightforward method of quantification. An additional advantage is a convenient evaluation of SELENOP recovery from the gel. The inconvenience is the need for handling gamma-radioactivity which requires dedicated laboratories. Note that the technique requires that the quantified  $^{75}Se$  is present in the radioactive form. Whereas it is an elegant quantification technique in animal studies, it is not an option for human SELENOP.

#### 5.3.2. Western Blotting Detection

The principle of the method consists of the separation of SELENOP by SDS PAGE and its transfer onto a PVDF membrane. The membranes are subsequently incubated with primary and secondary antibodies and developed with enhanced chemiluminescence. Standard curves were constructed using a dilute NIST1950 reference material [49,96].

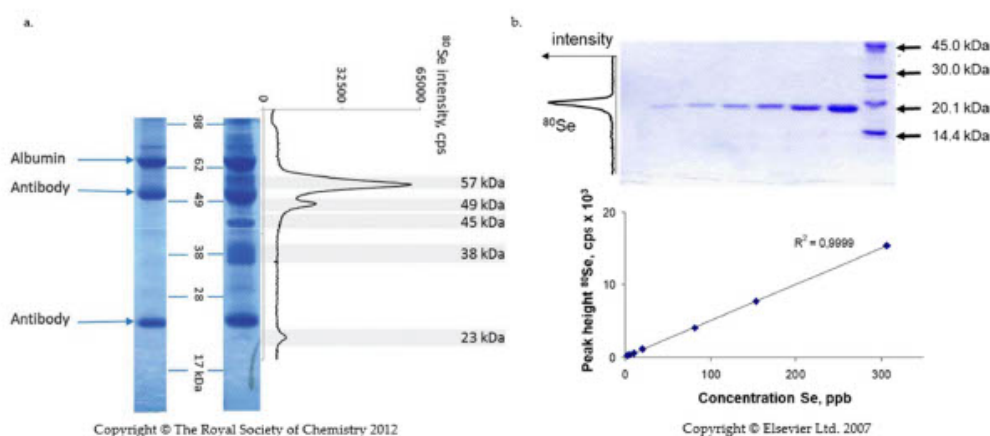
The method is particularly attractive in combination with immunoprecipitation [55,65] allowing the isolation and pre-concentration of SELENOP from complex samples.

The selectivity of the method depends less critically on the quality of antibodies than in the case of ELISA as SDS PAGE offers an additional separation step. The method does not account for losses at the different stages of the procedure, but many of these losses are compensated by the calibration with a standard reference material. Western blotting is robust but is not traceable to the SELENOP sequence.



### 5.3.3. Laser Ablation-ICP MS Detection

The detection consists of the evaporation of SELENOP present in the band separated by isoelectric focusing (IEF) or SDS PAGE using a laser beam followed by the quantification of selenium in the produced aerosol by ICP-MS. This method was first proposed by Fan et al. [120] and later developed for the quantification of selenium proteins by Ballihaut et al. [121,122] and Bianga et al. [123]. The analytical signal resembles a chromatogram (Figure 4).



**Figure 4.** Quantification of SELENOP by laser ablation ICP MS. (a) SDS-PAGE of immunoprecipitated SELENOP from serum. Left lane: albumin standard and antibodies bands; Right lane: sample lane; graph:  $^{80}\text{Se}$  intensity as a function of position in the gel [65]; (b) Construction of a calibration curve in SDS PAGE—laser ablation ICP MS with GPx [121]. The calibration curve is a linear function of the quantity of protein in the gel. G. Ballihaut, L.E. Kilpatrick, E.L. Kilpatrick, W.C. Davis, Multiple forms of selenoprotein P in candidate human plasma standard reference material, Metallomics, 2012, 4, 6, 533-538, with permission of Oxford University Press; Reprinted from TrAC Trend in Analytical Chemistry, 26, 3, 2007, G. Ballihaut, C. Pécheyrat, S. Monicou, H. Preud'homme, R. Grimaud, R. Lobinski, G. Ballihaut, R. Grimaud, R. Lobinski, Multimode detection (LA-ICP-MS, MALDI-MS and nanoHPLC-ESI-MS<sup>2</sup>) in 1D and 2D gel-electrophoresis for selenium-containing proteins, 183-190, Copyright (2007), with permission from Elsevier.

The identity and purity of the band can be verified by tryptic digestion and ESI MS/MS analysis of the non-ablated part of the gel. Calibration is carried out in a parallel lane using a well-characterized Se-containing protein with a known Se concentration, such as a fully selenized calmoduline [122] or glutathion peroxidase [121].

The LA-ICP-MS detection limits were reported to be 10 times lower for GPx than those of Western blot analyses [124]. However, because LA-ICP-MS is sensitive to selenium and the number of Se atoms in SELENOP is ten times bigger than in GPx, similar detection limits to those of Western blot are expected for SELENOP. Indeed, in well optimized conditions, the reported sensitivity was close to that of radioactivity detection [125]. Note that the advent of triple quadrupole ICP-MS offers a considerable margin for improvement of the detection limits as the most abundant  $^{80}\text{Se}$  can be chosen for detection [124]. LA-ICP-MS offers a dynamic range of five orders of magnitude which largely surpasses that of Western blotting detection (two orders of magnitude) and of ELISA (one order of magnitude) which is important for the analysis of unknown sample.

### 5.4. Isobaric Tagging for Relative and Absolute Quantification (i-TRAQ)

The use of LC-MS/MS as a way to quantify SELENOP was developed with the advent of new techniques such as label-free quantification (LFQ), and tandem mass tag [126].

The iTRAQ (isobaric tagging for relative and absolute quantification) method is based on the covalent labeling of the N-terminus and side chain amines of peptides from protein digestions with tags of varying mass. The samples are then pooled and liquid chromatography tandem mass spectrometry (MS/MS). A database search using the fragmentation data allows for the identification of the labeled peptides and hence the corresponding proteins. The fragmentation of the attached tag generates a low-molecular-mass reporter ion that can be used to relatively quantify the peptides and the proteins from which they originated [127].

To enhance the detection and identification of medium- and low-abundance proteins (such as SELENOP), different immuno-depletion methods are usually used. Since lipids interfere with iTRAQ labeling (as well as detection of peptides by mass spectrometry), the serum samples have to be delipidated before the analysis [80].

SELENOP has been reported in iTRAQ-based multiplex quantitative proteomics investigations searching for biomarkers of disease [80,87–89,128,129] or of Se-exposure [130].

#### 5.5. Quality Control and Assurance

As discussed above, several assays for the quantification of human SELENOP have been described. The reported serum concentrations of SELENOP differ considerably between assays, areas and type of diseases, as well as the laboratories. It is unclear whether the reason for this is biological variations or inadequacy of the analytical methodology [47]. Therefore, there is an urgent need for a better understanding of the sources of error in SELENOP analyses.

The SELENOP instability in the sample can be a source of error regardless of the analytical technique used. SELENOP was reported to be stable in serum over prolonged periods of time and upon repeated freezing [68,94] but other researchers found it to decompose quickly and lose selenium [110]. SELENOP proteolysis upon storage and its interactions with abundant or specific plasma proteins may occur [23]. In order to reduce the risk of autolysis, diisopropyl fluorophosphate was recommended to be added to each pooled fraction to avoid the proteolytic cleavage of SELENOP [79]. The question of the stability of semi-purified SELENOP has not been widely discussed but the matrix removal is likely to affect the stability of the protein.

Each of the techniques proposed has its own sources of error. Antibody-based enzyme immunoassays suffer from a difficult-to-control selectivity and high standard deviations. The validation of most commercial assays for SELENOP had been missing until 2015 [72] leading to inconsistencies and poor data comparability. The SELENOP quantification is closely linked to the choice of the kit and the quality of the antibody employed. A recent comparison of the commercially available kits for the determination of SELENOP levels in 21 human serum samples showed that only one out of the three commercial kits tested showed a good correlation with the method developed in-house [98].

In chromatographic methods, the peak assignment is based on the retention hypothesis which assumes the specificity of the separation to SELENOP. The molecular confirmation of the identity of the SELENOP determined (full length, truncated, post-translationally modified) is often lacking. The SELENOP recovery in the separation procedures is seldom reported. However, the traceability for the Se mass balance (100% column recovery), the unambiguous identification of the SELENOP eluted, and the verification of the fraction purity are the *sine qua non* conditions to assign the accurate value to the SELENOP concentration [84].

On the level of quantification by ICP-MS, calibration by unspecific or semi-specific isotope dilution does not account for any losses or transformations occurring during sample preparation or species separation. The assumption of the identical response of the selenite and Se present in SELENOP may not be true under some conditions. The precision of the isotope ratio measurement is a considerable source of measurement uncertainty at levels close to the detection limits [53] which requires improvements in terms of sensitivity.



The accurate quantification is contingent on the availability of specific certified reference materials (CRMs), pure primary standards and reference methods. Interlaboratory assays have been scarce and limited to a single type approach, e.g., to ELISA [98]. A comparison of Western blotting with ELISA [96] showed that the results from both methods were in agreement and indicated an unchanged pattern of immunoreactive protein isoforms.

A great step towards quality assurance is the increasing number of works reporting the SELENOP concentration values in the CRMs available on the market. The data reported by several authors are summarized in Table 2 which shows a good coherence of the results obtained by ICP-MS approaches. However, no comparison of this data obtained with immunological methods has been available, most of these methods actually use the CRM as calibration standard [59].

**Table 2.** SELENOP concentration values reported for the analysis of standard reference materials by HPLC-ICP-MS.

| Certified Reference Material | Calibration (Calibrant)                             | SELENOP Average Concentration (ng/mL as Se) | Ref.  |
|------------------------------|---|---|-------|
| SRM 1950                     | On-line post-column IDA ( $^{77}\text{Se}$ )        | 105 ± 3.8                                   | [84]  |
|                              | IDA ( $^{76}\text{Se}$ enriched peptides)           | 60.6 ± 3.2                                  | [53]  |
|                              | On-line post-column IDA ( $^{77}\text{Se}$ )        | 61.1 ± 7.4                                  | [100] |
|                              | External (SeIP)                                     | 52 ± 1.6                                    | [68]  |
| BCR 637                      | External (selenite)                                 | 51 ± 1                                      | [102] |
|                              | On-line post-column IDA ( $^{77}\text{Se}$ )        | 52 ± 5                                      | [104] |
|                              | On-line post-column IDA ( $^{77}\text{Se}$ )        | 81 ± 7                                      | [84]  |
|                              | On-line post-column IDA ( $^{77}\text{Se}$ )        | 52.7 ± 4.3                                  | [100] |
|                              | IDA ( $^{76}\text{Se}$ enriched peptides)           | 56.2 ± 1.7                                  | [53]  |
|                              | On-line post-column IDA ( $^{74}\text{Se}$ )        | 61 ± 4.3                                    | [105] |
| BCR 638                      | On-line post-column IDA-ICP-MS ( $^{77}\text{Se}$ ) | 65 ± 5                                      | [131] |
|                              | External (selenite)                                 | 57 ± 2                                      |       |
|                              | External (selenite)                                 | 59 ± 1                                      | [104] |
|                              | On-line post-column IDA ( $^{77}\text{Se}$ )        | 54 ± 12                                     |       |
| BCR 639                      | External (selenite)                                 | 56 ± 1                                      | [102] |
|                              | On-line post-column IDA ( $^{77}\text{Se}$ )        | 52 ± 3                                      | [104] |

## 6. Imaging

In the absence of imaging studies using mass spectrometry, the imaging of SELENOP in tissues can be carried out using either chemical fluorescent probes targeting free SeCys residues or by immunohistochemistry using SELENOP directed antibodies.

The use of the strong nucleophilic properties of selenols to simulate the cleavage of Se-Se and Se-S bonds is a widely used mechanism for designing the fluorescent probes for the detection of bioselenols validated for thioredoxine reductase. Currently, few selenol specific fluorescent probes are commercially available for medical diagnosis or SELENOP detection, and it is difficult to distinguish various functional selenoproteins by detecting selenol [132].

Antibodies can be used for selective imaging of SELENOP in tissue slices. The methods include: immunoperoxidase staining, immunofluorescence, and immunohistochemical analysis in paraffin-embedded samples. Immunohistochemical localization of SELENOP revealed its presence in liver and brain bound to capillary endothelial cell walls [49].

## 7. Applications and Reference Values

Table 3 summarizes the results of clinical studies in a variety of areas reporting SELENOP concentration in serum samples of healthy individuals and patients affected by

specific diseases, measured by different molecular (immunoassays) or elemental methods (ICP). The variations in the data obtained by different techniques and laboratories are significant. In practice, clinical conclusions can be drawn solely on the basis of data obtained in the same laboratory.

Most of the studies have been limited to serum. A recent study of breast milk from five healthy mothers reported a SELENOP concentration of  $20.1 \pm 1.0$  ng/mL (as Se) by HPLC-ICP-MS [83]. An early study of the cerebrospinal fluid of 24 neurologically healthy subjects by HPLC-ICP-MS resulted in a mean concentration of 0.47 ng/mL, a factor of 10 lower than the corresponding concentration in serum [110]. Recently, a study of 75 Parkinson's disease patients reported a mean value of 1.92 ng SELENOP (as Se) /mL in comparison with 2.02 ng/mL found in the population of 68 control subjects.

The isotopic selectivity of ICP-MS and the fact that selenium has multiple isotopes offers a possibility to use stable isotopic tracers to follow the incorporation of Se coming from different food sources into selenoproteins, including SELENOP. The intravenously injected  $^{82}\text{Se}$ -enriched SeMet into mice under different nutritional statuses (Se-adequate and Se-deficient) before the isotope-specific measurements of the expressed selenoproteins were taken, allowed studies to discriminate part of the exogenous  $^{82}\text{Se}$  incorporated into SELENOP [113].

Table 3. Overview of SELENOP concentrations in blood sample studies involving several subjects. The values that can be consider as control are highlighted in grey.

| Patients' Characteristics (Number)           | Country | SELENOP Average (Range), ng Se/mL | Technique Used for Quantification  | Ref.  |
|--|---------|-----------------------------------|------------------------------------|-------|
| Healthy (73)                                 |         | 96.9 ± 20.1 *                     |                                    |       |
| Hypercholesterolaemic before treatment (7)   | Japan   | 104 ± 20.1 *                      | ELISA (in-house kit)               | [70]  |
| Hypercholesterolaemic after treatment (7)    |         | 42.1 ± 23.8 *                     |                                    |       |
| Healthy (5)                                  | Spain   | 54.8 ± 3.99                       | HPLC-ICP-MS (post-column IDA)      | [101] |
| Haemodialysis (5)                            |         | 35.2 ± 2.66                       |                                    |       |
| Healthy (20)                                 | Japan   | 62.2 ± 14.6 *                     | AAS                                | [133] |
| Ulcerative colitis (34)                      |         | 54.8 ± 18.3 *                     |                                    |       |
| Crohn's Disease with elemental diet (17)     | Japan   | 25.6 ± 7.32 *                     | AAS                                | [133] |
| Crohn's Disease with non-elemental diet (20) |         | 32.9 ± 9.14 *                     |                                    |       |
| Healthy (318)                                | Germany | 98.4 ± n.a.                       | ILMA (in-house kit)                | [94]  |
| Healthy (399)                                | Greece  | 49 ± 15                           | HPLC-ICP-MS (post-column IDA)      | [104] |
| Healthy (15)                                 | Italy   | 56 ± 8                            | HPLC-ICP-MS (external calibration) | [103] |
| Type 2 diabetes (40)                         |         | 58 ± 9                            |                                    |       |
| Healthy (20)                                 | Korea   | 6.62 (4.62–12.7) ± n.a. *         | ELISA kit USCN Life Science        | [97]  |
| Type 2 diabete (40)                          |         | 18.9 (9.07–39.3) ± n.a. *         |                                    |       |
| Prediabete (40)                              |         | 15.9 (9.44–28.9) ± n.a. *         |                                    |       |
| Neurologically healthy (24)                  | Germany | 1.55–50.6 ± 0.03                  | HPLC-ICP-MS (external calibration) | [110] |
| Control (966)                                | Europe  | 78.6 (53–112) ± 16.9 *            | ILMA Selenotest™, ICI GmbH         | [38]  |
| Patient with colon cancer (598)              |         | 75 (49.4–110) ± 16.9 *            |                                    |       |
| Patient with rectal cancer (368)             |         | 76.8 (53–110) ± 16.9 *            |                                    |       |
| Healthy mother (83)                          | Spain   | 42.49 ± 9.49 (ICP-MS)             | HPLC-ICP-MS (post-column IDA)      | [107] |
| Healthy baby (83)                            |         | 6.99 ± 2.26 (ELISA) *             |                                    |       |
|  |         | 28.06 ± 7.69 (ICP-MS)             |                                    |       |
|  |         | 0.35 ± 0.18 (ELISA) *             | Elisa kit USCN Business Co         |       |

Table 3. Cont.

| Patients' Characteristics (Number)   | Country | SELENOP Average (Range), ng Se/mL   | Technique Used for Quantification                                 | Ref.  |
|--|---------|---|---|-------|
| Healthy (29)<br>Overweight/obese individuals (34)                          | China   | 265 ± 234 *<br>957 ± 715 *  | ELISA kit USCN Life Science                                       | [95]  |
| Healthy (76)   | Japan   | 45.9 ± 9.51 *   | Sol particle homogeneous immunoassay (SPIA)                       | [66]  |
| Occupationally non-exposed (50) after coronary angiography (controls) (20) | Germany | 31.1–59.2 ± (2.18–4.14)   | HPLC-ICP-MS (external calibration)                                | [68]  |
| pulmonary arterial hypertension patients (65)                              | Japan   | 44.4 ± 4.94 *<br>56.1 ± 10.4 *  | sol particle homogeneous immunoassay (SPIA)                       | [27]  |
| Control (around 2000)<br>Patient before selenium treatment (55)            | Sweden  | 80.5 ± n.a. *   | ELISA Kit selenOtest™, SelenOmed GmbH (validated by Western blot) | [96]  |
| Patient treated with 0.5 mg selenite/m <sup>2</sup>                        |         | 62.2 ± n.a. *   |   |       |
| Patient treated with 1–33.4 mg selenite/m <sup>2</sup>                     |         | >183 ± n.a. *   |   |       |
| Control group (37) infarct-related cardiogenic shock day 1 (147)           | Germany | 67.7 ± n.a. *   | ELISA kit Cloud Clone   | [134] |
| infarct-related cardiogenic shock day 3 (147)                              |         | 112 ± n.a. *<br>411 ± n.a. *  |   |       |
| Healthy (39)<br>Lung cancer (48)   | Spain   | 76.74 ± 3.72<br>82.04 ± 4.41  | HPLC-ICP-MS (SUID)  | [105] |
| Control group (966 EPIC study)<br>Liver transplanted patient alive (63)    | Germany | 78.6 (53–112) ± 16.9 *  | ELISA Kit selenOtest™, selenOmed GmbH                             | [135] |
| Liver transplanted patient deceased (16)                                   |         | 37.9 (11.7–85.2) ± 12.8 *<br>36.2 (18.5–60.7) ± 11 *                              |   |       |
| Controls group (1160)<br>Advanced prostate cancer patient (1160)           | Denmark | 101 (64–146) ± n.a. *   | CE-certified SELENOP-ELISA  | [136] |
| High-grade prostate cancer patient (1160)                                  |         | 98.8 (62.2–146) ± n.a. *  |   |       |
| Advanced-stage prostate cancer patient (281)                               |         | 101 (65.8–146) ± n.a. *<br>98.8 (58.5–148) ± n.a. *                               |   |       |
| Type 2 diabetes patients (176)   | China   | 33.2 ± 8.93 *   | ELISA kit Cloud Clone   | [42]  |
| Healthy mother (20)<br>Healthy baby (20)                                   | Spain   | 57.1 ± 8.7 (ICP)<br>22.1 ± 10.6 (ELISA)<br>33.6 ± 4.2 (ICP)<br>11.8 ± 2.8 (ELISA) | HPLC-ICP-MS (SUID)<br>SELENOP-ELISA Kit                           | [137] |

\* Values have been recalculated to be expressed as concentration of Se (ng/mL) in SELENOP, assuming that SELENOP contains 10 atoms of Se in its sequence and its molecular weight of 43,174 g·mol<sup>-1</sup>. n.a. = non-available.

## 8. Conclusions

SELENOP holds promise to be a valuable biomarker of selenium status, but its chemical characteristics still need to be investigated and methods for its accurate quantitation improved.

Immunoassays remain the standard for the determination of human and animal health status, because of their speed, simplicity and limited presence of mass spectrometry technology in the clinical environment. The validation of assays has been considerably improving and interlaboratory comparisons undertaken in order to prevent erroneous data and incorrect interpretations. In particular, critical comparisons of data obtained using methods based on a different principle: immunoassays and mass spectrometry are necessary. Before recombinant SELENOP becomes available to be used as a primary standard for isotope dilution quantifications, careful investigation of the characteristics of the SELENOP measured by electrospray MS and strict control of the recoveries at the various steps of the analytical procedures are strongly recommended.

The molecular characterization of SELENOP isolated from different species is required to address the questions of truncated isoforms; those varying in terms of amino-acid composition and sequence, as well as in terms of post-translational modifications require more in-depth studies which would definitely profit from the approaches of top-down proteomics. To date, the results yielded by the classical protein analysis, peptide mapping and microsequencing, remain fundamental to our knowledge about the isoforms. MALDI FT-ICR imaging is indispensable to verify the imaging data obtained by selenol probes and immunostaining of tissue slices.

While most studies into SELENOP's characterization have been carried out on rats, the exploration of the SELENOP expression in organisms theoretically capable of incorporating dozens of SeCys residues into a SELENOP sequence is a fascinating topic [11].

**Author Contributions:** Conceptualization, R.L.; writing—original draft preparation, J.L., L.R., J.S.; writing—review and editing, L.R., J.S., R.L.; funding acquisition, L.R. All authors have read and agreed to the published version of the manuscript.

**Funding:** J.L. acknowledges the PhD grant from the Nouvelle Aquitaine Region and the E2S-UPPA.

**Institutional Review Board Statement:** Not applicable.

**Informed Consent Statement:** Not applicable.

**Data Availability Statement:** Not applicable.

**Conflicts of Interest:** The authors declare no conflict of interest.

## Abbreviations

|        |   |
|--------|---|
| AA     | amino-acid                                    |
| AAS    | atomic absorption spectroscopy                |
| Alb    | albumin                                       |
| Blue   | HiTrap blue affinity column                   |
| CRM    | certified reference material                  |
| ELISA  | enzyme-linked immunosorbent assay             |
| ESI    | electrospray ionization                       |
| FT-ICR | fourier-transform ion cyclotron resonance     |
| Glu-C  | endoproteinase glu-c = glutamyl endopeptidase |
| Gpx    | glutathione peroxidase                        |
| Hep    | HiTrap heparin affinity column                |
| His    | histidine                                     |
| HMW    | high molecular weight                         |
| HPLC   | high pressure liquid chromatography           |
| ICP-MS | inductively coupled plasma- mass spectrometry |



|          |   |
|----------|---|
| IDA      | isotopic dilution analysis                                  |
| IEF      | isoelectric focusing  |
| ILMA     | immunoluminometric assay                                    |
| IMAC     | immobilized metal ion affinity chromatography               |
| iTRAQ    | isobaric tagging for relative and absolute quantification   |
| LA       | laser ablation  |
| LC       | liquid chromatography                                       |
| LFQ      | label-free quantification                                   |
| LMW      | low molecular weight  |
| MARC     | multi-affinity removal column                               |
| MALDI    | matrix-assisted laser desorption/ionization                 |
| MS       | mass spectrometry   |
| NTA      | nitrilotriacetic acid                                       |
| PNGaseF  | peptide: N-glycosidase F                                    |
| PVDF     | polyvinylidene fluoride                                     |
| SAX      | strong anion-exchange column                                |
| SDS-PAGE | sodium dodecyl sulphate- polyacrylamide gel-electrophoresis |
| SEC      | size-exclusion chromatography                               |
| SECIS    | selenocysteine insertion structure                          |
| SeCys    | selenocysteine  |
| SELENOP  | selenoprotein P   |
| SPIA     | sol particle homogeneous immunocassay                       |
| SUID     | species-unspecific isotopic dilution analysis               |

## References

- Hatfield, D.L.; Schweizer, U.; Tsuji, P.A.; Gladyshev, V.N. (Eds.) *Selenium: Its Molecular Biology and Role in Human Health*; Springer Science & Business Media: Berlin/Heidelberg, Germany, 2016.
- Gromer, S.; Eubel, J.K.; Lee, B.L.; Jacob, J. Human selenoproteins at a glance. *Cdl. Mol. Life Sci.* **2005**, *62*, 2414–2437. [[CrossRef](#)] [[PubMed](#)]
- Roman, M.; Jitaru, P.; Barbante, C. Selenium biochemistry and its role for human health. *Metallomics* **2014**, *6*, 25–54. [[CrossRef](#)]
- Böck, A.; Forchhammer, K.; Heider, J.; Leinfelder, W.; Sawers, G.; Vepřek, B.; Zinoni, F. Selenocysteine: The 21st amino acid. *Md. Microbiol.* **1991**, *5*, 515–520. [[CrossRef](#)] [[PubMed](#)]
- Shetty, S.; Copeland, P.R. Molecular mechanism of selenoprotein P synthesis. *Biochim. Biophys. Acta Gen. Subj.* **2018**, *1862*, 2506–2510. [[CrossRef](#)] [[PubMed](#)]
- Kryukov, G.V.; Castellano, S.; Novoselov, S.V.; Lobanov, A.V.; Zehab, O.; Guigó, R.; Gladyshev, V.N. Characterization of mammalian selenoproteomes. *Science* **2003**, *300*, 1439–1443. [[CrossRef](#)]
- Zhang, Y.; Gladyshev, V.N. An algorithm for identification of bacterial selenocysteine insertion sequence elements and selenoprotein genes. *Bioinformatics* **2005**, *21*, 2580–2589. [[CrossRef](#)] [[PubMed](#)]
- Santesmasses, D.; Mariotti, M.; Gladyshev, V.N. Bioinformatics of selenoproteins. *Antioxid. Redox Signal.* **2020**, *33*, 525–536. [[CrossRef](#)]
- Zhang, Y.; Zheng, J. Bioinformatics of metalloproteins and metalloproteomes. *Molecular* **2020**, *25*, 3366. [[CrossRef](#)] [[PubMed](#)]
- Labunskyy, V.; Hatfield, D.L.; Gladyshev, V.N. Selenoproteins: Molecular pathways and physiological roles. *Physiol. Rev.* **2014**, *94*, 739–777. [[CrossRef](#)] [[PubMed](#)]
- Bacalacos, J.; Santesmasses, D.; Mariotti, M.; Bierla, K.; Vetic, M.B.; Lynch, S.; McAllen, R.; Mackrill, J.J.; Loughran, G.; Guigó, R.; et al. Processive recoding and metazoan evolution of selenoprotein P: Up to UGAs in molluscs. *J. Mol. Biol.* **2019**, *431*, 4381–4407. [[CrossRef](#)] [[PubMed](#)]
- Bacalacos, J.; Mackrill, J.J. Why Multiples of 21? Why does Selenoprotein P Contain Multiple Selenocysteine Residues? *Curr. Nutraceuticals* **2020**, *1*, 42–53. [[CrossRef](#)]
- Jiang, L.; Liu, Q. SelGenAmic: An algorithm for selenoprotein gene assembly. *Adv. Struct. Sqf. Stud.* **2017**, *1661*, 29–39. [[CrossRef](#)]
- Lobanov, A.V.; Hatfield, D.L.; Gladyshev, V.N. Reduced reliance on the trace element selenium during evolution of mammals. *Genome Biol.* **2008**, *9*, 1–11. [[CrossRef](#)] [[PubMed](#)]
- Burk, R.F. Effect of dietary selenium level on 75se binding to rat plasma proteins. *Exp. Biol. Med.* **1973**, *143*, 719–722. [[CrossRef](#)]
- Rotruck, J.T.; Pope, A.L.; Ganther, H.E.; Swanson, A.B.; Hafeman, D.G.; Hoekstra, W.G. Selenium: Biochemical role as a component of glutathione peroxidase. *Science* **1973**, *179*, 588–590. [[CrossRef](#)]
- McConnell, K.P.; Burton, R.M.; Kute, T.; Higgins, P.J. Selenoproteins from rat testis cytosol. *Biochim. Biophys. Acta Gen. Subj.* **1979**, *588*, 113–119. [[CrossRef](#)]
- Motsenbocker, M.A.; Tappel, A.L. A selenocysteine-containing selenium-transport protein in rat plasma. *Biochim. Biophys. Acta Gen. Subj.* **1982**, *719*, 147–153. [[CrossRef](#)]

19. Persson-Moschos, M.; Huang, W.; Srikumar, T.S.; Åkesson, B.; Lindeberg, S. Selenoprotein P in serum as a biochemical marker of selenium status. *Analyst* **1995**, *120*, 833–836. [[CrossRef](#)]
20. Gladyshev, V.N.; Arnér, E.; Berry, M.J.; Briggli-Flohé, R.; Bruford, E.; Burk, R.F.; Carlson, B.A.; Castellano, S.; Chavatte, L.; Conrad, M.; et al. Selenoprotein gene nomenclature. *J. Biol. Chem.* **2016**, *291*, 24036–24040. [[CrossRef](#)]
21. Burk, R.F.; Hill, K.E. Selenoprotein P—Expression, functions, and roles in mammals. *Biochim. Biophys. Acta Gen. Subj.* **2009**, *1790*, 1441–1447. [[CrossRef](#)]
22. Combs, G.F., Jr. Biomarkers of selenium status. *Nutrients* **2015**, *7*, 2209–2236. [[CrossRef](#)]
23. Michaelis, M.; Gralla, O.; Behrends, T.; Scharpf, M.; Endermann, T.; Rijntjes, E.; Pietschmann, N.; Hollenbach, B.; Schomburg, L. Selenoprotein P in seminal fluid is a novel biomarker of sperm quality. *Biochem. Biophys. Res. Commun.* **2014**, *443*, 905–910. [[CrossRef](#)] [[PubMed](#)]
24. Xia, Y.E.; Hill, K.; Li, P.; Xu, J.; Zhou, D.; Motley, A.K.; Wang, L.; Byrne, D.W.; Burk, R.F. Optimization of selenoprotein P and other plasma selenium biomarkers for the assessment of the selenium nutritional requirement: A placebo-controlled, double-blind study of selenomethionine supplementation in selenium-deficient Chinese subjects. *Am. J. Clin. Nutr.* **2010**, *92*, 525–531. [[CrossRef](#)] [[PubMed](#)]
25. Hoeflich, J.; Hollenbach, B.; Behrends, T.; Hoeg, A.; Stosnach, H.; Schomburg, L. The choice of biomarkers determines the selenium status in young German vegans and vegetarians. *Br. J. Nutr.* **2010**, *104*, 1601–1604. [[CrossRef](#)] [[PubMed](#)]
26. Hurst, R.; Armah, C.N.; Dainty, J.R.; Hart, D.J.; Teucher, B.; Goldson, A.J.; Broadley, M.R.; Motley, A.K.; Fairweather-Tait, S.J. Establishing optimal selenium status: Results of a randomized, double-blind, placebo-controlled trial. *Am. J. Clin. Nutr.* **2010**, *91*, 923–931. [[CrossRef](#)]
27. Kikuchi, N.; Satoh, K.; Satoh, T.; Yaoita, N.; Siddique, M.A.H.; Omura, J.; Kurosawa, R.; Nogi, M.; Sunamura, S.; Miyata, S.; et al. Diagnostic and prognostic significance of serum levels of SeP (Selenoprotein P) in patients with pulmonary hypertension. *Arterioscler. Thromb. Vasc. Biol.* **2019**, *39*, 2553–2562. [[CrossRef](#)]
28. Vu, D.L.; Saurav, K.; Mylenko, M.; Ranglová, K.; Kuta, J.; Ewe, D.; Masojádek, J.; Hrouzek, P. In vitro bioaccessibility of selenoamino acids from selenium (Se)-enriched *Chlorella vulgaris* biomass in comparison to selenized yeast; a Se-enriched food supplement; and Se-rich foods. *Food Chem.* **2019**, *279*, 12–19. [[CrossRef](#)]
29. Heller, R.A.; Sun, Q.; Hackler, J.; Seelig, J.; Seibert, L.; Cherkezov, A.; Mirich, W.B.; Seemann, P.; Diegmann, J.; Pilz, M.; et al. Prediction of survival odds in COVID-19 by zinc, age and selenoprotein P as composite biomarker. *Redox Biol.* **2021**, *38*, 101764. [[CrossRef](#)]
30. Moghaddam, A.; Heller, R.A.; Sun, Q.; Seelig, J.; Cherkezov, A.; Seibert, L.; Hackler, J.; Seemann, P.; Diegmann, J.; Pilz, M.; et al. Selenium deficiency is associated with mortality risk from COVID-19. *Nutrition* **2020**, *12*, 2098. [[CrossRef](#)]
31. Reeves, M.A.; Hoffmann, P.R. The human selenoproteome: Recent insights into functions and regulation. *Cdl. Md. Life Sci.* **2009**, *66*, 2457–2478. [[CrossRef](#)]
32. Burk, R.F.; Hill, K.E.; Read, R.; Bellew, T. Response of rat selenoprotein P to selenium administration and fate of its selenium. *Am. J. Physiol. Metab.* **1991**, *261*, E26–E30. [[CrossRef](#)]
33. Eckers, J.C.; Kalen, A.L.; Xiao, W.; Sarsour, E.H.; Goswami, P.C. Selenoprotein p inhibits radiation-induced late reactive oxygen species accumulation and normal cell injury. *Int. J. Radiat. Oncol.* **2013**, *87*, 619–625. [[CrossRef](#)] [[PubMed](#)]
34. Temur, M.; Taggöz, F.N.; Ertürk, N.K. Elevated circulating Selenoprotein P levels in patients with polycystic ovary syndrome. *J. Obstet. Gynaecol.* **2021**, *2021*, 1–5. [[CrossRef](#)]
35. Fujii, M.; Saijoh, K.; Sumino, K. Regulation of selenoprotein P mRNA expression in comparison with metallothionein and osteonectin mRNAs following cadmium and dexamethasone administration. *Kobe J. Med Sci.* **1997**, *43*, 13–23.
36. Yoneda, S.; Suzuki, K.T. Equimolar Hg-Se complex binds to Selenoprotein P. *Biochem. Biophys. Res. Commun.* **1997**, *231*, 7–11. [[CrossRef](#)] [[PubMed](#)]
37. Barrett, C.W.; Reddy, V.K.; Short, S.; Motley, A.K.; Lintel, M.K.; Bradley, A.M.; Freeman, T.; Vallance, J.; Ning, W.; Parang, B.; et al. Selenoprotein P influences colitis-induced tumorigenesis by mediating stemness and oxidative damage. *J. Clin. Investig.* **2015**, *125*, 2646–2660. [[CrossRef](#)] [[PubMed](#)]
38. Hughes, D.J.; Fedirko, V.; Jenab, M.; Schomburg, L.; Méplan, C.; Freisling, H.; Bueno-De-Mesquita, H.; Hybsier, S.; Becker, N.-P.; Czuban, M.; et al. Selenium status is associated with colorectal cancer risk in the European prospective investigation of cancer and nutrition cohort. *Int. J. Cancer* **2014**, *136*, 1149–1161. [[CrossRef](#)]
39. Köhrle, J. Selenium in endocrinology—Selenoprotein-related diseases, population studies, and epidemiological evidence. *Endocrinology* **2021**, *162*. [[CrossRef](#)]
40. Takata, Y.; Xiang, Y.-B.; Burk, R.F.; Li, H.; Hill, K.; Cai, H.; Gao, J.; Zheng, W.; Shu, X.-O.; Cai, Q. Plasma selenoprotein P concentration and lung cancer risk: Results from a case-control study nested within the Shanghai men's health study. *Carcinogenesis* **2018**, *39*, 1352–1358. [[CrossRef](#)]
41. Rayman, M.P. Selenium and human health. *Lancet* **2012**, *379*, 1256–1268. [[CrossRef](#)]
42. Xi, J.; Zhang, Q.; Wang, J.; Guo, R.; Wang, L. Factors influencing selenium concentration in community-dwelling patients with type 2 diabetes mellitus. *Biol. Trace Elem. Res.* **2020**, *199*, 1–7. [[CrossRef](#)]
43. Zhang, Z.-H.; Song, G.-L. Roles of selenoproteins in brain function and the potential mechanism of selenium in Alzheimer's disease. *Front. Neurosci.* **2021**, *15*, 215. [[CrossRef](#)]



44. Misu, H.; Takamura, T.; Takayama, H.; Hayashi, H.; Nagata, N.; Kurita, S.; Ishikura, K.; Ando, H.; Takeshita, Y.; Ota, T.; et al. A liver-derived secretory protein, Selenoprotein P, causes insulin resistance. *Cell Metab.* **2010**, *12*, 483–495. [[CrossRef](#)]
45. Saito, Y. Selenoprotein P as a significant regulator of pancreatic  $\beta$  cell function. *J. Biochem.* **2019**, *167*, 119–124. [[CrossRef](#)]
46. Huang, Y.-C.; Wu, T.-L.; Zeng, H.; Cheng, W.-H. Dietary selenium requirement for the prevention of glucose intolerance and insulin resistance in middle-aged mice. *J. Nutr.* **2021**. [[CrossRef](#)]
47. Tsutsumi, R.; Saito, Y. Selenoprotein P: P for plasma, prognosis, prophylaxis, and more. *Biol. Pharm. Bull.* **2020**, *43*, 366–374. [[CrossRef](#)]
48. Cardoso, B.R.; Garico, K.; Roberts, B.R. Expanding beyond ICP-MS to better understand selenium biochemistry. *Metallomics* **2019**, *11*, 1974–1983. [[CrossRef](#)]
49. Tujebajeva, R.M.; Copeland, P.R.; Xu, X.; Carlson, B.A.; Harney, J.W.; Driscoll, D.M.; Hatfield, D.L.; Berry, M.J. Decoding apparatus for eukaryotic selenocysteine insertion. *EMBO Rep.* **2000**, *1*, 158–163. [[CrossRef](#)]
50. Hill, K.; Lloyd, R.; Yang, J.; Read, R.; Burk, R. The cDNA for rat selenoprotein P contains TGA codons in the open reading frame. *J. Biol. Chem.* **1991**, *266*, 10050–10053. [[CrossRef](#)]
51. Burk, R.F.; Hill, K.E. Some properties of selenoprotein P. *Biol. Trace Elem. Res.* **1992**, *33*, 151–153. [[CrossRef](#)]
52. Tanaka, M.; Saito, Y.; Misu, H.; Kato, S.; Kita, Y.; Takeshita, Y.; Kanamori, T.; Nagano, T.; Nakagen, M.; Urabe, T.; et al. Development of a Sol particle homogeneous immunoassay for measuring full-length Selenoprotein P in human serum. *J. Clin. Lab. Anal.* **2014**, *30*, 114–122. [[CrossRef](#)]
53. Ward-Deitrich, C.; Cuello-Núñez, S.; Kmíotek, D.; Torma, F.A.; Busto, M.D.C.; Fiscaro, P.; Goenaga-Infante, H. Accurate quantification of Selenoprotein P (SEPP1) in plasma using isotopically enriched seleno-peptides and species-specific isotope dilution with HPLC coupled to ICP-MS/MS. *Anal. Chem.* **2016**, *88*, 6357–6365. [[CrossRef](#)]
54. Saito, Y.; Sato, N.; Hirashima, M.; Takebe, G.; Nagasawa, S.; Takahashi, K. Domain structure of bi-functional selenoprotein P. *Biochem. J.* **2004**, *381*, 841–846. [[CrossRef](#)]
55. Turanov, A.A.; Everley, R.A.; Hybsier, S.; Renko, K.; Schomburg, L.; Gygi, S.P.; Hatfield, D.L.; Gladyshev, V.N. Regulation of selenocysteine content of human Selenoprotein P by dietary selenium and insertion of cysteine in place of selenocysteine. *PLoS ONE* **2015**, *10*, e0140353. [[CrossRef](#)]
56. Ma, S.; Hill, K.E.; Caprioli, R.M.; Burk, R.F. Mass spectrometric characterization of full-length rat selenoprotein P and three isoforms shortened at the C terminus. Evidence that three UGA codons in the mRNA open reading frame have alternative functions of specifying selenocysteine insertion or translation termination. *J. Biol. Chem.* **2002**, *277*, 12749–12754.
57. Méplan, C.; Nicol, F.; Burtle, B.T.; Crosley, L.K.; Arthur, J.R.; Mathers, J.C.; Hesketh, J.E. Relative abundance of Selenoprotein P isoforms in human plasma depends on genotype, se intake, and cancer status. *Antioxid. Redox Signal.* **2009**, *11*, 2631–2640. [[CrossRef](#)]
58. Åkesson, B.; Bellew, T.; Burk, R.F. Purification of selenoprotein P from human plasma. *Biochim. Biophys. Acta Protein Struct. Md. Enzym.* **1994**, *1204*, 243–249. [[CrossRef](#)]
59. Hybsier, S.; Schulz, T.; Wu, Z.; Demuth, I.; Minich, W.B.; Renko, K.; Rijntjes, E.; Köhrle, J.; Strasburger, C.J.; Steinhagen-Thiessen, E.; et al. Sex-specific and inter-individual differences in biomarkers of selenium status identified by a calibrated ELISA for selenoprotein P. *Redox Biol.* **2017**, *11*, 403–414. [[CrossRef](#)]
60. Ma, S.; Hill, K.E.; Burk, R.F.; Caprioli, R.M. Mass spectrometric identification of N- and O-glycosylation sites of full-length rat Selenoprotein P and determination of selenide–sulfide and disulfide linkages in the shortest isoform. *Biochemistry* **2003**, *42*, 9703–9711. [[CrossRef](#)]
61. Mostert, V.; Lombeck, I.; Abel, J. A novel method for the purification of selenoprotein P from human plasma. *Arch. Biochem. Biophys.* **1998**, *357*, 326–330. [[CrossRef](#)]
62. Steinbrüenner, H.; Alili, L.; Stuhlmann, D.; Sies, H.; Brenneisen, P. Post-translational processing of selenoprotein P: Implications of glycosylation for its utilisation by target cells. *Biol. Chem.* **2007**, *388*, 1043–1051. [[CrossRef](#)]
63. Yang, J.-G.; Morrison-Plummer, J.; Burk, R.F. Purification and quantitation of a rat plasma selenoprotein distinct from glutathione peroxidase using monoclonal antibodies. *J. Biol. Chem.* **1987**, *262*, 13372–13375. [[CrossRef](#)]
64. Himeno, S.; Chittum, H.S.; Burk, R.F. Isoforms of selenoprotein P in rat plasma. Evidence for a full-length form and another form that terminates at the second UGA in the open reading frame. *J. Biol. Chem.* **1996**, *271*, 15769–15775. [[CrossRef](#)]
65. Ballihaut, G.; Kilpatrick, L.E.; Kilpatrick, E.L.; Davis, W.C. Multiple forms of selenoprotein P in a candidate human plasma standard reference material. *Metallomics* **2012**, *4*, 533–538. [[CrossRef](#)]
66. Oo, S.M.; Misu, H.; Saito, Y.; Tanaka, M.; Kato, S.; Kita, Y.; Takayama, H.; Takeshita, Y.; Kanamori, T.; Nagano, T.; et al. Serum selenoprotein P, but not selenium, predicts future hyperglycemia in a general Japanese population. *Sci. Rep.* **2018**, *8*, 1–10. [[CrossRef](#)]
67. Hondal, R.J.; Ma, S.; Caprioli, R.M.; Hill, K.E.; Burk, R.F. Heparin-binding histidine and lysine residues of rat selenoprotein P. *J. Biol. Chem.* **2001**, *276*, 15823–15831. [[CrossRef](#)]
68. Heitland, P.; Köster, H.D. Biomonitoring of selenoprotein P in human serum by fast affinity chromatography coupled to ICP-MS. *Int. J. Hyg. Environ. Health* **2018**, *221*, 564–568. [[CrossRef](#)]
69. Sidenius, U.; Farver, O.; Jøns, O.; Gammelgaard, B. Comparison of different transition metal ions for immobilized metal affinity chromatography of selenoprotein P from human plasma. *J. Chromatogr. B Biomed. Sci. Appl.* **1999**, *735*, 85–91. [[CrossRef](#)]

70. Saito, Y.; Watanabe, Y.; Saito, E.; Honjoh, T.; Takahashi, K. Production and application of monoclonal antibodies to human selenoprotein P. *J. Health Sci.* **2001**, *47*, 346–352. [[CrossRef](#)]
71. Olson, G.E.; Winfrey, V.P.; NagDas, S.K.; Hill, K.E.; Burk, R.F. Apolipoprotein E receptor-(ApoER2) mediates selenium uptake from selenoprotein P by the mouse testis. *J. Biol. Chem.* **2007**, *282*, 12290–12297. [[CrossRef](#)] [[PubMed](#)]
72. Hybsier, S.; Wu, Z.; Schulz, T.; Strasburger, C.; Köhrle, J.; Minich, W.; Schomburg, L. Establishment and characterization of a new ELISA for selenoprotein P. *Perspect. Sci.* **2015**, *3*, 23–24. [[CrossRef](#)]
73. Altinova, A.E.; Iyidir, O.T.; Ozkan, C.; Ors, D.; Öztürk, M.; Gulbahar, O.; Bozkurt, N.; Törtüner, F.B.; Akturk, M.; Cakir, N.; et al. Selenoprotein P is not elevated in gestational diabetes mellitus. *Gynecol. Endocrinol.* **2015**, *31*, 874–876. [[CrossRef](#)]
74. Baran, A.; Nowowiejska, J.; Krabel, J.A.; Kaminski, T.W.; Maciaszek, M.; Flisiak, I. Higher serum selenoprotein P Level as a novel inductor of metabolic complications in psoriasis. *Int. J. Mol. Sci.* **2020**, *21*, 4594. [[CrossRef](#)] [[PubMed](#)]
75. Wang, Y.; Zou, Y.; Wang, T.; Han, S.; Liu, X.; Zhang, Y.; Su, S.; Zhou, H.; Zhang, X.; Liang, H. A spatial study on serum selenoprotein P and Keshan disease in Heilongjiang Province, China. *J. Trace Elem. Med. Biol.* **2021**, *65*, 126728. [[CrossRef](#)] [[PubMed](#)]
76. Suzuki, K.T.; Sasakura, C.; Yoneda, S. Binding sites for the (Hg-Se) complex on selenoprotein P. *Biochim. Biophys. Acta Protein Struct. Mol. Enzym.* **1998**, *1429*, 102–112. [[CrossRef](#)]
77. Suzuki, Y.; Sakai, T.; Furuta, N. Isolation of selenoprotein-P and determination of Se concentration incorporated in proteins in human and mouse plasma by tandem heparin affinity and size-exclusion column HPLC-ICPMS. *Anal. Sci.* **2012**, *28*, 221. [[CrossRef](#)] [[PubMed](#)]
78. Deagen, J.; Butler, J.; Zachara, B.; Whanger, P. Determination of the distribution of selenium between glutathione peroxidase, selenoprotein P, and albumin in plasma. *Anal. Biochem.* **1993**, *208*, 176–181. [[CrossRef](#)]
79. Saito, Y.; Hayashi, T.; Tanaka, A.; Watanabe, Y.; Suzuki, M.; Saito, E.; Takahashi, K. Selenoprotein P in human plasma as an extracellular phospholipid hydroperoxide glutathione peroxidase. Isolation and enzymatic characterization of human selenoprotein p. *J. Biol. Chem.* **1999**, *274*, 2866–2871. [[CrossRef](#)]
80. Jing, L.; Parker, C.E.; Seo, D.; Hines, M.W.; Dicheva, N.; Yu, Y.; Schwirn, D.; Ginsburg, G.S.; Chen, X. Discovery of biomarker candidates for coronary artery disease from an APOE-knock out mouse model using iTRAQ-based multiplex quantitative proteomics. *Proteomics* **2011**, *11*, 2763–2776. [[CrossRef](#)] [[PubMed](#)]
81. Smith, L.M.; Kelleher, N.L. Proteoforms as the next proteomics currency. *Science* **2018**, *359*, 1106–1107. [[CrossRef](#)]
82. Ma, S.; Hill, K.E.; Burk, R.F.; Caprioli, R.M. Mass spectrometric determination of selenylsulfide linkages in rat selenoprotein P. *J. Mass Spectrom.* **2005**, *40*, 400–404. [[CrossRef](#)]
83. Arias-Borrego, A.; Callejón-Leblic, M.B.; Rodríguez-Moro, G.; Velasco, I.; Gómez-Ariza, J.; García-Barrera, T. A novel HPLC column switching method coupled to ICP-MS/QTOF for the first determination of selenoprotein P (SELENOP) in human breast milk. *Food Chem.* **2020**, *321*, 126692. [[CrossRef](#)]
84. Ballihaut, G.; Kilpatrick, L.E.; Davis, W.C. Detection, identification, and quantification of selenoproteins in a candidate human plasma standard reference material. *Anal. Chem.* **2011**, *83*, 8667–8674. [[CrossRef](#)] [[PubMed](#)]
85. Brudeker, R.; Muntel, J.; Müller, S.; Bernhardt, O.M.; Gandhi, T.; Cominetti, O.; Macron, C.; Carayol, J.; Rinner, O.; Astrup, A.; et al. Analysis of plasma samples by capillary-flow data-independent acquisition profiles proteomics of weight loss and maintenance. *Mol. Cell. Proteom.* **2019**, *18*, 1242–1254. [[CrossRef](#)]
86. Wang, X.; Yu, Z.; Zhao, X.; Han, R.; Huang, D.; Yang, Y.; Cheng, G. Comparative proteomic characterization of bovine milk containing  $\beta$ -casein variants A1A and A2A, and their heterozygote A1A2. *J. Sci. Food Agric.* **2020**, *101*, 718–725. [[CrossRef](#)]
87. Cole, R.N.; Ruczinski, I.; Schulze, K.; Christian, P.; Herbrich, S.; Wu, L.; Devine, L.R.; O'Meally, R.N.; Shrestha, S.; Boronina, T.N.; et al. The plasma proteome identifies expected and novel proteins correlated with micronutrient status in undernourished Nepalese children. *J. Nutr.* **2013**, *143*, 1540–1548. [[CrossRef](#)] [[PubMed](#)]
88. Shen, X.; Huo, B.; Wu, T.; Song, C.; Chi, Y. iTRAQ-based proteomic analysis to identify molecular mechanisms of the selenium deficiency response in the Przewalski's gazelle. *J. Proteom.* **2019**, *203*, 103389. [[CrossRef](#)] [[PubMed](#)]
89. Yan, B.; Chen, B.; Min, S.; Gao, Y.; Zhang, Y.; Xu, P.; Li, C.; Chen, J.; Luo, G.; Liu, C. iTRAQ-based comparative serum proteomic analysis of prostate cancer patients with or without bone metastasis. *J. Cancer* **2019**, *10*, 4165–4177. [[CrossRef](#)]
90. Ouerdane, L.; Gil-Casal, S.; Lobinski, R.; Szpunar, J. Purification of selenoprotein P from human blood using IMAC-Co and heparin columns followed by its characterization by LC ICP-MS and LC ESI-LTQ Orbitrap MS. In Proceedings of the Winter Conference on Plasma Spectrochemistry, Zaragoza, Spain, 30 January–4 February 2011.
91. Lamarche, J.; Bierla, K.; Lobinski, R. Unpublished data. 2021.
92. Hill, K.E.; Xia, Y.; Åkesson, B.; Boeglin, M.E.; Burk, R.F. Selenoprotein P concentration in plasma is an index of selenium status in selenium-deficient and selenium-supplemented Chinese subjects. *J. Nutr.* **1996**, *126*, 138–145. [[CrossRef](#)]
93. Read, R.; Bellew, T.; Yang, J.G.; E Hill, K.; Palmer, I.S.; Burk, R.F. Selenium and amino acid composition of selenoprotein P, the major selenoprotein in rat serum. *J. Biol. Chem.* **1990**, *265*, 17899–17905. [[CrossRef](#)]
94. Hollenbach, B.; Morgenthaler, N.G.; Struck, J.; Alonso, C.; Bergmann, A.; Köhrle, J.; Schomburg, L. New assay for the measurement of selenoprotein P as a sepsis biomarker from serum. *J. Trace Elem. Med. Biol.* **2008**, *22*, 24–32. [[CrossRef](#)]
95. Chen, M.; Liu, B.; Wilkinson, D.; Hutchison, A.T.; Thompson, C.H.; Wittert, G.; Heilbronn, L.K. Selenoprotein P is elevated in individuals with obesity, but is not independently associated with insulin resistance. *Obes. Res. Clin. Pract.* **2017**, *11*, 227–232. [[CrossRef](#)]



96. Brodin, O.; Hackler, J.; Misra, S.; Wendt, S.; Sun, Q.; Laaf, E.; Stoppe, C.; Björnstedt, M.; Schomburg, L. Selenoprotein P as biomarker of selenium status in clinical trials with therapeutic dosages of selenite. *Nutrients* **2020**, *12*, 1067. [[CrossRef](#)]
97. Yang, S.J.; Hwang, S.Y.; Choi, H.Y.; Yoo, H.J.; Seo, J.A.; Kim, S.G.; Kim, N.H.; Baik, S.H.; Choi, D.S.; Choi, K.M. Serum selenoprotein P levels in patients with type diabetes and prediabetes: Implications for insulin resistance, inflammation, and atherosclerosis. *J. Clin. Endocrinol. Metab.* **2011**, *96*, E1325–E1329. [[CrossRef](#)]
98. Saito, Y.; Misu, H.; Takayama, H.; Takashima, S.-I.; Usui, S.; Takamura, M.; Kaneko, S.; Takamura, T.; Noguchi, N. Comparison of human selenoprotein P determinants in serum between our original methods and commercially available kits. *Biol. Pharm. Bull.* **2018**, *41*, 828–832. [[CrossRef](#)]
99. Shigeta, K.; Sato, K.; Furuta, N. Determination of selenoprotein P in submicrolitre samples of human plasma using micro-affinity chromatography coupled with low flow ICP-MS. *J. Anal. At. Spectrom.* **2007**, *22*, 911–916. [[CrossRef](#)]
100. Busto del Castillo, M.E.; Oster, C.; Cuello-Núñez, S.; Deitrich, C.L.; Raab, A.; Konopka, A.; Lehmann, W.D.; Goenaga-Infante, H.; Fiscaro, P. Accurate quantification of selenoproteins in human plasma/serum by isotope dilution ICP-MS: Focus on selenoprotein P. *J. Anal. At. Spectrom.* **2016**, *31*, 1904–1912. [[CrossRef](#)]
101. Hinojosa Reyes, L.; Marchante-Gayón, J.M.; García Alonso, J.I.; Sarz-Medel, A. Quantitative speciation of selenium in human serum by affinity chromatography coupled to post-column isotope dilution analysis ICP-MS. *J. Anal. At. Spectrom.* **2003**, *18*, 1210–1216. [[CrossRef](#)]
102. Jitaru, P.; Prete, M.; Cozzi, G.; Turetta, C.; Cairns, W.; Seraglia, R.; Traldi, P.; Cescon, P.; Barbante, C. Speciation analysis of selenoproteins in human serum by solid-phase extraction and affinity HPLC hyphenated to ICP-quadrupole MS. *J. Anal. At. Spectrom.* **2008**, *23*, 402–406. [[CrossRef](#)]
103. Roman, M.; Lapolla, A.; Jitaru, P.; Sechi, A.; Cosma, C.; Cozzi, G.; Cescon, P.; Barbante, C. Plasma selenoproteins concentrations in type diabetes mellitus—A pilot study. *Transl. Res.* **2010**, *156*, 242–250. [[CrossRef](#)]
104. Letsiou, S.; Lu, Y.; Nomikos, T.; Antonopoulou, S.; Panagiotakos, D.; Pitsavos, C.; Stefanadis, C.; Pergantis, S.A. High-throughput quantification of selenium in individual serum proteins from a healthy human population using HPLC on-line with isotope dilution inductively coupled plasma-MS. *Proteomics* **2010**, *10*, 3447–3457. [[CrossRef](#)]
105. Callejón-Leblic, M.B.; Rodríguez-Moro, G.; Arias-Borrego, A.; Pereira-Vega, A.; Gómez-Ariza, J.L.; García-Barrera, T. Absolute quantification of selenoproteins and selenometabolites in lung cancer human serum by column switching coupled to triple quadrupole inductively coupled plasma mass spectrometry. *J. Chromatogr. A* **2020**, *1619*, 460919. [[CrossRef](#)]
106. García-Sevillano, M.A.; García-Barrera, T.; Gómez-Ariza, J.L. Simultaneous speciation of selenoproteins and selenometabolites in plasma and serum by dual size exclusion-affinity chromatography with online isotope dilution inductively coupled plasma mass spectrometry. *Anal. Bioanal. Chem.* **2014**, *406*, 2719–2725. [[CrossRef](#)]
107. Santos, C.; García-Fuentes, E.; Callejón-Leblic, M.B.; García-Barrera, T.; Gómez-Ariza, J.L.; Rayman, M.P.; Velasco, I. Selenium, selenoproteins and selenometabolites in mothers and babies at the time of birth. *Br. J. Nutr.* **2017**, *117*, 1304–1311. [[CrossRef](#)] [[PubMed](#)]
108. Palacios, O.; Ruiz Encinar, J.; Schaumlöffel, D.; Lobinski, R. Fractionation of selenium-containing proteins in serum by multiaffinity liquid chromatography before size-exclusion chromatography-ICPMS. *Anal. Bioanal. Chem.* **2006**, *384*, 1276–1283. [[CrossRef](#)]
109. Maass, F.; Michalke, B.; Willkommen, D.; Schulte, C.; Tönges, L.; Boerger, M.; Zerr, I.; Bähr, M.; Lingor, P. Selenium speciation analysis in the cerebrospinal fluid of patients with Parkinson's disease. *J. Trace Elem. Med. Biol.* **2020**, *57*, 126412. [[CrossRef](#)]
110. Solovyev, N.; Berthele, A.; Michalke, B. Selenium speciation in paired serum and cerebrospinal fluid samples. *Anal. Bioanal. Chem.* **2013**, *405*, 1875–1884. [[CrossRef](#)]
111. Xu, M.; Yang, L.; Wang, Q. Quantification of selenium-tagged proteins in human plasma using species-unspecific isotope dilution ICP-DRC-qMS coupled on-line with anion exchange chromatography. *J. Anal. At. Spectrom.* **2008**, *23*, 1545–1549. [[CrossRef](#)]
112. Anan, Y.; Ogra, Y. Toxicological and pharmacological analysis of selenohomolanthionine in mice. *Toxicol. Res.* **2013**, *2*, 115–122. [[CrossRef](#)]
113. Suzuki, Y.; Hashiura, Y.; Sakai, T.; Yamamoto, T.; Matsukawa, T.; Shinohara, A.; Furuta, N. Selenium metabolism and excretion in mice after injection of 82Se-enriched selenomethionine. *Metallomics* **2013**, *5*, 445–452. [[CrossRef](#)]
114. Tanner, S.D.; Baranov, V.I.; Bandura, D.R. Reaction cells and collision cells for ICP-MS: A tutorial review. *Spectrochim. Acta Part B At. Spectrosc.* **2002**, *57*, 1361. [[CrossRef](#)]
115. Encinar, J.R.; Schaumlöffel, D.; Ogra, Y.; Lobinski, R. Determination of selenomethionine and selenocysteine in human serum using speciated isotope dilution-capillary HPLC-inductively coupled plasma collision cell mass spectrometry. *Anal. Chem.* **2004**, *76*, 6635–6642. [[CrossRef](#)]
116. Jitaru, P.; Goenaga-Infante, H.; Vaslin-Reimann, S.; Fiscaro, P. A systematic approach to the accurate quantification of selenium in serum selenoalbumin by HPLC-ICP-MS. *Anal. Chim. Acta* **2010**, *657*, 100–107. [[CrossRef](#)]
117. Polatajko, A.; Encinar, J.R.; Schaumlöffel, D.; Szpunar, J. Quantification of a selenium-containing protein in yeast extract via an accurate determination of a tryptic peptide by species-specific isotope dilution capillary HPLC-ICP MS. *Chem. Anal.* **2005**, *50*, 265–278.
118. Konopka, A.; Winter, D.; Konopka, W.; Busto, M.D.C.; Nunez, S.; Goenaga-Infante, H.; Fiscaro, P.; Lehmann, W.D. [Sec-to-Cys]selenoprotein—A novel type of recombinant, full-length selenoprotein standard for quantitative proteomics. *J. Anal. At. Spectrom.* **2016**, *31*, 1929–1938. [[CrossRef](#)]

119. Konopka, A.; Zinn, N.; Wild, C.; Lehmann, W.D. Preparation of heteroelement-incorporated and stable isotope-labeled protein standards for quantitative proteomics. *Adv. Struct. Saf. Stud.* **2014**, *1156*, 337–363. [[CrossRef](#)]
120. Fan, T.W.-M.; Pruszkowski, E.; Shuttleworth, S. Speciation of selenoproteins in Se-contaminated wildlife by gel electrophoresis and laser ablation-ICP-MS. *J. Anal. At. Spectrom.* **2002**, *17*, 1621–1623. [[CrossRef](#)]
121. Ballihaut, G.; Pécheyran, C.; Mounicou, S.; Præud'homme, H.; Grimaud, R.; Lobinski, R.; Ballihaut, G.; Grimaud, R. Multimode detection (LA-ICP-MS, MALDI-MS and nanoHPLC-ESI-MS) in 1D and 2D gel electrophoresis for selenium-containing proteins. *TrAC Trends Anal. Chem.* **2007**, *26*, 183–190. [[CrossRef](#)]
122. Ballihaut, G.; Tastet, L.; Pécheyran, C.; Bouyssière, B.; Donard, O.; Grimaud, R.; Lobinski, R. Biosynthesis, purification and analysis of selenomethionyl calmodulin by gel electrophoresis-laser ablation-ICP-MS and capillary HPLC-ICP-MS peptide mapping following in-gel tryptic digestion. *J. Anal. At. Spectrom.* **2005**, *20*, 493–499. [[CrossRef](#)]
123. Bianga, J.; Touat-Hamici, Z.; Bierla, K.; Mounicou, S.; Szpunar, J.; Chavatte, L.; Lobinski, R. Speciation analysis for trace levels of selenoproteins in cultured human cells. *J. Proteom.* **2014**, *108*, 316–324. [[CrossRef](#)] [[PubMed](#)]
124. Sonet, J.; Mounicou, S.; Chavatte, L. Nonradioactive isotopic labeling and tracing of selenoproteins in cultured cell lines. *Adv. Struct. Saf. Stud.* **2017**, *1661*, 193–203. [[CrossRef](#)]
125. Ballihaut, G.; Clavier, F.; Pécheyran, C.; Mounicou, S.; Grimaud, R.; Lobinski, R. Sensitive detection of selenoproteins in gel electrophoresis by high repetition rate femtosecond laser ablation-inductively coupled plasma mass spectrometry. *Anal. Chem.* **2007**, *79*, 6874–6880. [[CrossRef](#)]
126. Schaffer, L.V.; Millikin, R.J.; Miller, R.M.; Anderson, L.C.; Fellers, R.T.; Ge, Y.; Kelleher, N.L.; LeDuc, R.D.; Liu, X.; Payne, S.H.; et al. Identification and quantification of proteoforms by mass spectrometry. *Proteomics* **2019**, *19*, e1800361. [[CrossRef](#)] [[PubMed](#)]
127. Ross, P.L.; Huang, Y.N.; Marchese, J.N.; Williamson, B.; Parker, K.; Hattan, S.; Khainovski, N.; Pillai, S.; Dey, S.; Daniels, S.; et al. Multiplexed protein quantitation in *Saccharomyces cerevisiae* using amine-reactive isobaric tagging reagents. *Mol. Cell. Proteom.* **2004**, *3*, 1154–1169. [[CrossRef](#)] [[PubMed](#)]
128. Kaur, P.; Rizk, N.M.; Ibrahim, S.; Younes, N.; Uppal, A.; Dennis, K.; Karve, T.; Blakeslee, K.; Kwagyan, J.; Zirir, M.; et al. iTRAQ-based quantitative protein expression profiling and mrm verification of markers in type diabetes. *J. Proteome Res.* **2012**, *11*, 5527–5539. [[CrossRef](#)]
129. Yu, R.; Zhang, J.; Zang, Y.; Zeng, L.; Zuo, W.; Bai, Y.; Liu, Y.; Sun, K.; Liu, Y. iTRAQ-based quantitative protein expression profiling of biomarkers in childhood B-cell and T-cell acute lymphoblastic leukemia. *Cancer Manag. Res.* **2019**, *11*, 7047–7063. [[CrossRef](#)]
130. Ren, Z.-H.; Bai, L.-P.; Shen, L.-H.; Luo, Z.-Z.; Zhou, Z.-H.; Zuo, Z.-C.; Ma, X.-P.; Deng, J.-L.; Wang, Y.; Xu, S.-Y.; et al. Comparative iTRAQ proteomics reveals multiple effects of selenium yeast on dairy cows in parturition. *Biol. Trace Elem. Res.* **2020**, *197*, 464–474. [[CrossRef](#)]
131. Jitaru, P.; Cozzi, G.; Gambaro, A.; Cescon, P.; Barbante, C. Simultaneous speciation analysis of glutathione peroxidase, selenoprotein P and selenoalbumin in human serum by tandem anion exchange-affinity HPLC and on-line isotope dilution ICP-quadrupole MS. *Anal. Bioanal. Chem.* **2008**, *391*, 661–669. [[CrossRef](#)]
132. Liu, Y.; Feng, X.; Yu, Y.; Zhao, Q.; Tang, C.; Zhang, J. A review of bioselenol-specific fluorescent probes: Synthesis, properties, and imaging applications. *Anal. Chim. Acta* **2020**, *1110*, 141–150. [[CrossRef](#)]
133. Andoh, A.; Hirashima, M.; Maeda, H.; Hata, K.; Inatomi, O.; Tsujikawa, T.; Sasaki, M.; Takahashi, K.; Fujiyama, Y. Serum selenoprotein-P levels in patients with inflammatory bowel disease. *Nutrition* **2005**, *21*, 574–579. [[CrossRef](#)]
134. Büttner, P.; Obradovic, D.; Wunderlich, S.; Feistritz, H.-J.; Holzwirth, E.; Lauten, P.; Fuernau, G.; de Waha-Thiele, S.; Desch, S.; Thiele, H. Selenoprotein P in myocardial infarction with cardiogenic shock. *Shock* **2020**, *53*, 58–62. [[CrossRef](#)]
135. Gül-Klein, S.; Haxhira, D.; Seelig, J.; Kästner, A.; Hackler, J.; Sun, Q.; Heller, R.; Lachmann, N.; Pratschke, J.; Schmelzle, M.; et al. Serum selenium status as a diagnostic marker for the prognosis of liver transplantation. *Nutrition* **2021**, *13*, 619. [[CrossRef](#)]
136. Outzen, M.; Tjønneland, A.; Hughes, D.J.; Jenab, M.; Frederiksen, K.; Schomburg, L.; Morris, S.; Overvad, K.; Olsen, A. Toenail selenium, plasma selenoprotein P and risk of advanced prostate cancer: A nested case-control study. *Int. J. Cancer* **2021**, *148*, 876–883. [[CrossRef](#)]
137. Hoová, J.; López, I.V.; Soblechero, E.G.; Arias-Borrego, A.; García-Barrera, T. Digging deeper into the mother-offspring transfer of selenium through human breast milk. *J. Food Compos. Anal.* **2021**, *99*, 103870. [[CrossRef](#)]



*Annex 3 Poster: An integrated LC-ICP-MS and LC-ESI-MS  
approach for the characterization of purified selenoprotein P*








## An integrated LC-ICP MS and LC-ESI-MS approach for the characterization of purified selenoprotein P

Laurent Ouerdane, Jérémy Lamarche, Luisa Ronga, Katarzyna Bierla, Joanna Szpunar, Ryszard Łobiński

IPREM, Université de Pau et des Pays de l'Adour / CNRS UMR 5254, Pau, France



### Introduction

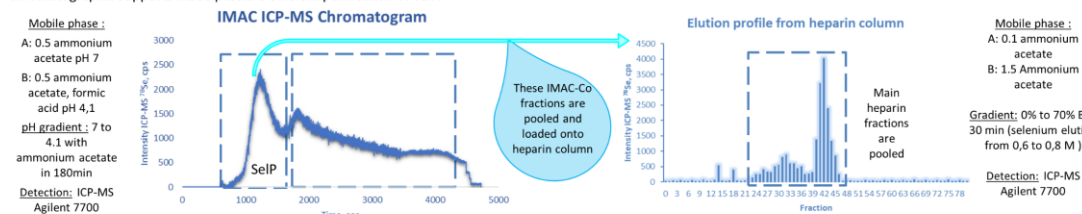
Selenium is an essential trace element known for its antioxidant activities. In mammals, selenium deficiency has been associated with muscular, neurological and immune disorders, and also with an increase in cancer incidence and mortality. The vital role of selenium has been widely recognized by selenium supplementation of the diet. The physiological role of selenium is principally awarded to its co-translational incorporation into selenoproteins as selenocysteine (SeCys), referred to as the 21st amino acid. Twenty-five selenoproteins have been identified and constitute the human selenoproteome. It has been recognized that most biological functions of selenium (Se) are mediated by specific proteins such as the selenoprotein P (SeP), which is the major selenoprotein in plasma (up to 10 SeCys in its sequence) responsible for transport and distribution of Se. Furthermore, SeP has also been associated with neurodegenerative diseases such as Alzheimer's and Type 2 diabetes.

Due to its low abundance and the complexity of its biological samples, the full characterization of SeP, its multiple isoforms and post-translational modifications (e.g. glycosylations, Se-S bridges) is critically dependent on the availability of protein pre-concentration techniques and adequate analytical methodology.

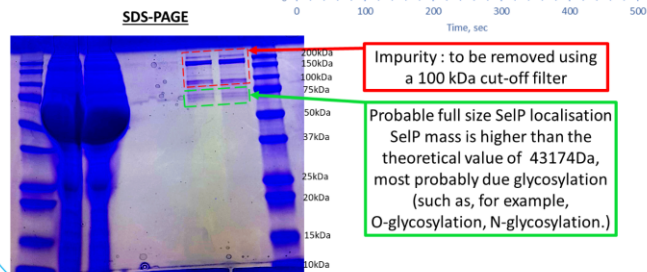
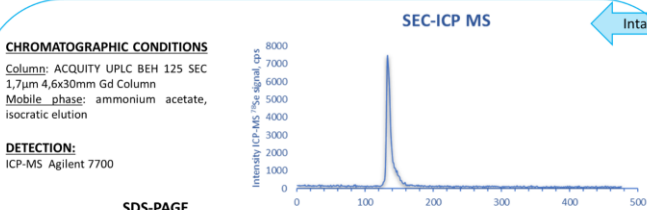
Here, we present a method for the purification of SeP from human blood serum (15 mL) by immobilized metal affinity chromatography using Co(II) (IMAC-Co) followed by heparin affinity chromatography; the quality of enrichment was verified by comparing UV and ICP-MS signals of eluting fractions. The interaction of histidine-rich regions of SeP with the chromatographic supports made possible efficient purification of SeP.

### Selenoprotein P purification by IMAC-Co & Heparin column

Selenoprotein P was purified from human blood serum (15 mL) by immobilized metal affinity chromatography using Co(II) (IMAC-Co) followed by heparin affinity chromatography; the quality of enrichment was verified by comparing UV and ICP-MS signals of eluting fractions. The interaction of histidine-rich regions of SeP with the chromatographic supports made possible efficient purification of SeP.



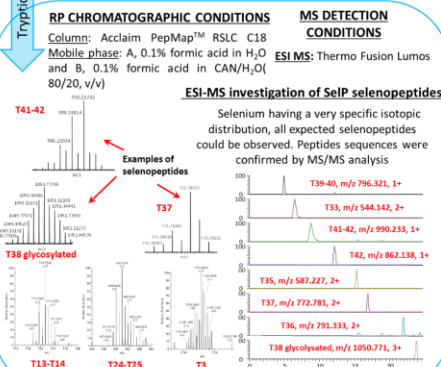
### Intact SeP characterization



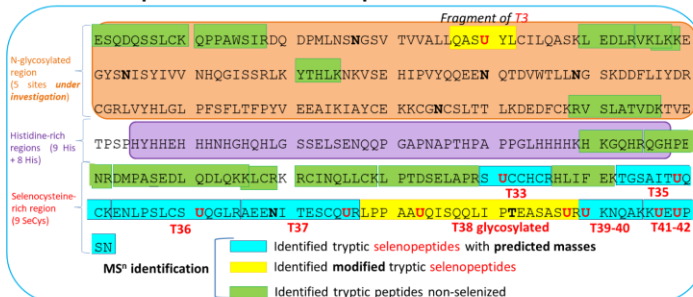
### Cut-off procedure

SeP was pre-concentrated after heparin column elution using a 10kDa cut-off filter; then part of SeP was digested with trypsin and the other part kept intact.

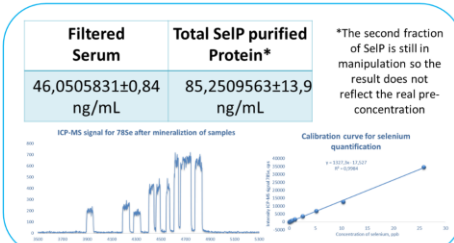
### Digested SeP characterization



### Expected amino acid sequence of human SeP



### Determination of the selenium concentration



### Acknowledgements

J. Lamarche thanks the Nouvelle Aquitaine Region and the UPPA for his PhD grant. The support of the FT-MS instrumental platform funded by the EQUIPEX MARSS project (11-EQPX-0027) is acknowledged.

### Conclusion

The study allowed successful re-evaluation of the results previously obtained by our team; all 10 selenocysteines of human selenoprotein P have been accounted by mass spectrometry. Using both ICP-MS and ESI-MS techniques we were able to characterize a number of SeP peptides containing selenocysteine and carry out quantitative control of selenium at all the purification steps.





*Annex 4 Poster Characterization of human serum  
selenoprotein P by mass spectrometry*



# Characterization of Human serum Selenoprotein P by mass spectrometry

Jérémy Lamarche, Laurent Ouerdane, Luisa Ronga, Katarzyna Bierla, Joanna Szpunar, Ryszard Łobiński  
 Institute of Analytical Sciences for the Environment and Materials (IPREM UMR 5254), CNRS-UPPA, Hélioparc, 2 av. Pr. Angot, 64053 Pau, France

**Introduction**

Selenium is known to be an essential trace element with antioxidant activity. In mammals selenium deficiency has been associated with several disorders, such as muscular, neurological and immune dysregulation, but also with an increase in cancer incidence and mortality. The vital role of selenium has been recognized worldwide and supplementary diets are commonly used in populations with insufficient selenium (Se) intake. The physiological role of selenium is mainly due to its co-translational incorporation into selenoproteins as selenocysteine (SeCys), referred to as the 21<sup>st</sup> amino acid. Most biological functions of Se in humans are mediated by specific proteins (the human proteome includes 25 selenoproteins). Selenoprotein P (SeP) is the major selenoprotein in plasma with up to 10 SeCys in its sequence and is known to control the transport and distribution of Se in the entire body. SeP is supposed to be involved in some diseases, such as, Alzheimer, Type 2 diabetes, and is associated with infertility. Because of the complexity of the human serum proteome, the low abundance of Selenoprotein P, the occurrence of its putative multiple isoforms and post-translational modifications (e.g., glycosylation, Se-S bridge). The characterization of SeP requires the protein selective pre-concentration and custom-designed optimization of analytical methodology.

The goal of this study is a comprehensive characterization of SeP in view of the development of analytical methods for its metrology, including its isoforms, in clinical research. We developed a method for the purification of SeP from human serum using two-dimensional affinity chromatography. The two chromatographic steps using immobilized metal (cobalt) affinity and heparin affinity chromatography allowed the purification of SeP with a selectivity exceeding 1000. The following characterization of purified SeP by nanoHPLC-ESI MS allowed accounting for all selenocysteine-containing tryptic SeP peptides and the elucidation of some glycosylations sites. It was followed by the identification of selenopeptides characteristic for truncated SeP forms and the selection of the most promising candidates for the quantitative analysis of SeP and its isoforms by high resolution Orbitrap mass spectrometry.

**Sample preparation**

Before performing the purification step the blood serum is filtered using Minisart plus Syringe filters 17829 0.45µm in order to remove particles and protein precipitate that can occur during freezing and thawing of the serum.

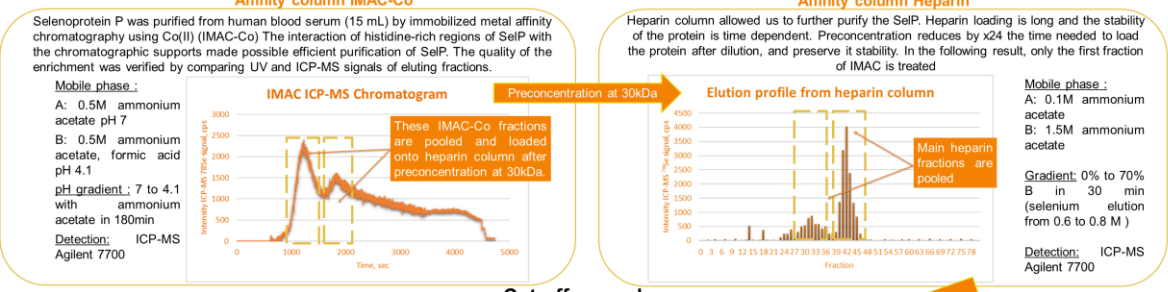
**Selenoprotein P purification by affinity column**

**Affinity column IMAC-Co**

Selenoprotein P was purified from human blood serum (15 mL) by immobilized metal affinity chromatography using Co(II) (IMAC-Co). The interaction of histidine-rich regions of SeP with the chromatographic supports made possible efficient purification of SeP. The quality of the enrichment was verified by comparing UV and ICP-MS signals of eluting fractions.

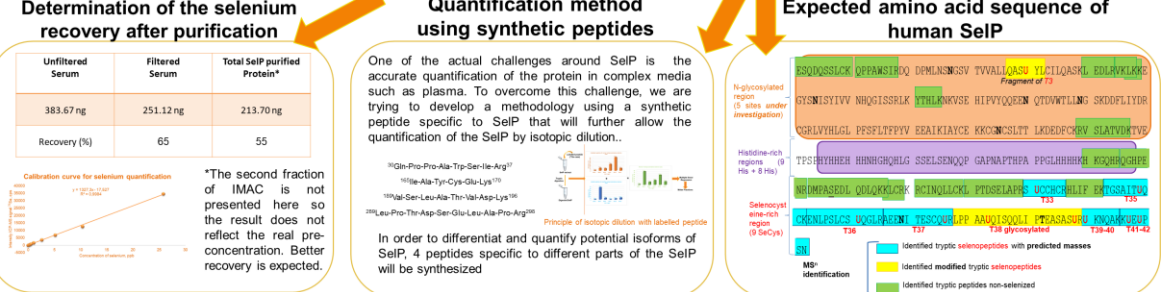
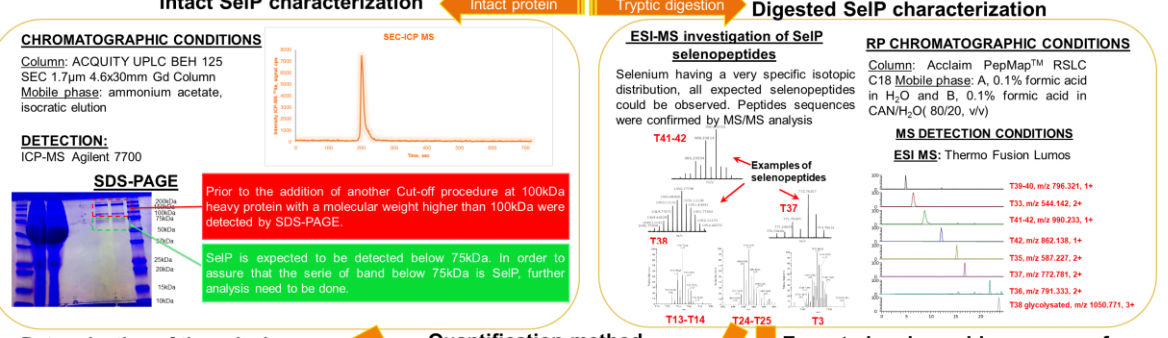
**Affinity column Heparin**

Heparin column allowed us to further purify the SeP. Heparin loading is long and the stability of the protein is time dependent. Preconcentration reduces by x24 the time needed to load the protein after dilution, and preserve its stability. In the following result, only the first fraction of IMAC is treated.



**Cut-off procedure**

SeP was preconcentrated after heparin column elution using a 10kDa and 100kDa cut-off filter, then part of SeP was digested with trypsin and the other part kept intact.



**Conclusion**

The study allowed a successful re-evaluation of the results previously obtained by our team; all the 10 selenocysteines of human selenoprotein P have been accounted by mass spectrometry. Using both ICP-MS and ESI-MS techniques we were able to characterize the number of SeP peptides containing selenocysteine and carry out quantitative control of selenium at all the purification steps. Further work will allow a reduction of the manipulation time, a development of an accurate quantification method of selenoprotein P, and the identification of several isoforms.

**Acknowledgements**

J. Lamarche thanks the Nouvelle Aquitaine Region and the UPPA for his PhD grant, the support of the FT-MS instrumental platform funded by the EQUIPEX MARSS project (11-EQPX-0027) is acknowledged and the expertise of Pr J.Guillon team in peptide synthesis for help in the creation of synthetic peptide.

ETUDE DES INTERACTIONS DE LA SELENOPROTEINE P ET DE LA VASSOPRESSINE DISELENIEE EN  
PRESENCE D'AURANOFINE ET DE CISPLATINE

Jérémy LAMARCHE – 16 décembre 2021

---



ETUDE DES INTERACTIONS DE LA SELENOPROTEINE P ET DE LA VASSOPRESSINE DISSELENIEE EN  
PRESENCE D'AURANOFINE ET DE CISPLATINE

Jérémy LAMARCHE – 16 décembre 2021

---





ECOLE DOCTORALE :  
Ecole doctorale sciences exactes et leurs applications ED 211

LABORATOIRE :  
Institut des sciences analytiques et de physico-chimie pour l'environnement et les matériaux  
(IPREM)

### RESUME :

Le sélénium est connu pour être un oligo-élément essentiel aux activités antioxydantes. Son rôle physiologique est principalement dû à son incorporation co-translationnelle dans les sélénoprotéines comme la sélénocystéine (SeCys), appelée 21<sup>e</sup> acide aminé. La sélénoprotéine P (SELENOP) est la principale sélénoprotéine plasmatique avec jusqu'à 10 SeCys dans sa séquence. En raison de la complexité chimique de la matrice sérique, de la faible abondance de la sélénoprotéine P et de l'occurrence de ses isoformes multiples putatives et des modifications post-translationnelles (par exemple, glycosylation, ponts Se-S et Se-Se), la caractérisation de la sélénoprotéine P nécessite la préconcentration sélective des protéines et l'optimisation personnalisée de la méthodologie analytique.

Contenant 10 résidus SeCys, SELENOP est une cible préférentielle potentielle pour les métallomédicaments (auranofine, cisplatine). Les interactions n'ont pas encore été étudiées au niveau moléculaire, malgré des preuves considérables que les séléniols libres sont des sites d'attente pour l'auranofine dans une autre sélénoprotéine, la thiorédoxine réductase. Le manque d'études sur la sélénoprotéine P est probablement dû au fait que la protéine ne peut pas être exprimée de manière hétérologue et doit être purifiée à partir du sérum où elle est présente à une concentration de ng/g (sous forme de Se).

Cette thèse présente le développement de la méthode de purification du SELENOP à partir de sérum humain par chromatographie d'affinité bidimensionnelle. Les deux étapes chromatographiques utilisant la chromatographie d'affinité sur métal immobilisé (cobalt) et d'affinité sur héparine ont permis la purification de SELENOP avec une excellente sélectivité. La caractérisation ultérieure du SELENOP purifié par nanoHPLC - électrospray ESI MS/MS a permis de rendre compte de presque tous les peptides tryptiques SELENOP contenant de la sélénocystéine et d'élucider certains sites de glycosylation. De plus, la récupération du sélénium incorporé dans SELENOP a été suivie quantitativement, pour la première fois, à chaque étape de la procédure de purification. La récupération de SELENOP était de 14 % après toutes les étapes de purification. Le sélénium présent dans SELENOP s'est avéré représenter 35 % du sélénium total dans le sérum.

La purification de SELENOP a permis la première étude de ses interactions avec l'auranofine, contenant Au(I) et contenant du cisplatine, Au(I) et Pt(II), respectivement. La formation d'adduits après incubation de SELENOP a été observée avec les deux métallomédicaments. Après digestion avec de la trypsine, des modifications Au et Pt ont été observées sur les peptides résultants. Dans le cas de l'auranofine et du cisplatine, deux peptides SELENOP se sont avérés former des adduits Au ou Pt par liaison Cy et SeCys (caractérisation MS/MS). Ces quatre peptides, spécifiques de SELENOP, présentaient des séquences différentes.

De plus, pour étudier comparativement les interactions des ponts Se-Se et S-S avec les métallomédicaments, la vasopressine et ses analogues diséléniures ont été utilisés comme peptides modèles. Leur réactivité avec l'auranofine et ses analogues stricts a été étudiée par LC-electrospray MS/MS. Des preuves ont été obtenues du clivage possible des ponts SS et Se-Se induit par Au(I) en l'absence d'agents réducteurs, contrairement aux études précédentes nécessitant une réduction préalable de la liaison Se-Se pour la faire réagir avec Au (I) composés. De plus, nous avons constaté qu'à haute température (70 °C), les atomes de soufre et de sélénium étaient métallés avec la liaison préférentielle de l'or au sélénium, la réaction n'ayant pas lieu dans des conditions physiologiques (37 °C).